Optimization Models For Understanding Migration Patterns of Juvenile Chinook Salmon

by

Richard A. Hinrichsen

A dissertation submitted in partial fulfillment
of the requirements for the degree of

Doctor of Philosophy

University of Washington

1994

Approved by_____
(Chairperson of Supervisory Committee)

Program Authorized
to Offer Degree_____

Date_____

University of Washington

Abstract

Optimization Models For Understanding

Migration Patterns of Juvenile Chinook Salmon

by Richard A. Hinrichsen

Chairperson of the Supervisory Committee: Professor James J. Anderson
Fisheries Research Institute

There are striking geographical and temporal patterns of juvenile chinook migrations that are not well understood. Chinook populations that migrate to the sea during their first year of life—ocean-type populations—predominate in latitudes north of 56° N, while those migrating later—stream-type populations—predominate south of the Columbia River. In rivers where these two life history types are sympatric, ocean-types are typically distributed more coastally than stream-types. Controversy exists over whether these patterns are the result of postglacial dispersal, or a result of geographical gradients in natural selection.

In this dissertation, I explore the selective pressures on migration timing of chinook salmon by using increasingly complex dynamic optimization models. The optimization models predict that migration distance can strongly influence migration timing, but other biological and physical quantities are also important. Models also suggest that geographical patterns of "growth opportunity" *per se* do not drive age at migration patterns observed.

A dynamic optimization model reveals two types of optimal behavior that, when appropriately pieced together, produce an optimal migration strategy. One behavior is characterized as "feeding and predator avoidance" and the other, "active migration." The optimal behavior is determined by the signs of two model-derived "switching functions," and the value of the maximum current velocity relative to the swimming speed that maximizes growth. Optimal strategies determined numerically show that behavior often switches from initial feeding and predator avoidance, to active downstream migration as the fish develops and/or during changes in environmental conditions.

TABLE OF CONTENTS

Page

LIST OF FIGURES vi

LIST OF TABLES xv

PREFACE xix

CHAPTER 1 INTRODUCTION 1

1.1 Background 1

1.2 Literature review of juvenile migratory behavior 2

1.2.1 Migration timing 2

1.2.1.1 Latitudinal gradient 3

1.2.1.2 Migration distance gradient 5

1.2.2 Seasonal migration pattern 6

1.2.3 Diel migration pattern 7

1.2.4 Current velocity selection 9

1.3 Optimization modelling approach 10

1.3.1 Migration timing 10

1.3.2 Current velocity selection models 14

1.4 Research questions and problems 16

CHAPTER 2 A HEURISTIC MODEL OF AGE AT MIGRATION 20

2.1 Model Development 21

2.1.1 Growth 23

2.1.2 Survival 24

2.1.3 Fitness measure 25

2.1.4 Objective function 25

2.2 Necessary conditions 26

2.2.1 Example 1 27

2.2.1.1 Effect of migration distance 28

2.2.1.2 Effect of migration velocity 31

TABLE OF CONTENTS

Page

2.2.1.3 Effect of freshwater growth 32
2.2.1.4 Effect of temperature 36
2.2.1.5 The effects of other parameters 38
2.2.2 Example 2 39
2.2.2.1 Effect of migration distance 41
2.2.2.2 Effect of freshwater growth 43
2.2.2.3 Effect of predator density 46
2.2.2.4 Effect of predator search velocity 47
2.2.2.5 Effect of migration velocity 47
2.2.2.6 Effect of spawning time 50
2.2.2.7 Effect of other parameters. 51
2.2.3 More general sensitivity results 51
2.2.3.1 Effect of migration distance 52
2.2.3.2 Effect of ocean mortality 52
2.2.3.3 Effect of ocean growth 53
2.2.3.4 Effect of predator density 53
2.2.3.5 Effect of predator search velocity 54
2.2.3.6 Effects of migration velocity and freshwater growth 54
2.2.3.7 Effect of freshwater growth on size at migration 54
2.3 Summary 55
2.4 Discussion 56

CHAPTER 3 MORE REALISTIC GROWTH AND FECUNDITY ASSUMPTIONS 58

3.1 Development of more realistic relationships 61
3.1.1 Ocean growth 61
3.1.2 Freshwater growth 62
3.1.3 Fecundity 63
3.2 Parameter effects. 64
3.2.1 Effect of food density 64

TABLE OF CONTENTS

Page

3.2.2 Effect of migration distance 66
3.2.3 Effect of predator density 67
3.2.4 Effect of other parameters 68
3.3 Summary 69
3.4 Discussion 69

CHAPTER 4 SEASONAL EFFECTS 71

4.1 Model development 74
4.1.1 Temperature dependent growth 74
4.1.1.1 Consumption 75
4.1.1.2 Respiration and specific dynamic action 76
4.1.1.3 Waste losses (egestion and excretion) 77
4.1.2 Temperature dependent depredation rate 77
4.1.3 Mean daily temperature data 79
4.2 Simulation results and sensitivity 80
4.2.1 Effect of migration distance 83
4.2.2 Effect of food availability 84
4.2.3 Effects of temperature function parameters 85
4.2.4 Effect of other parameters 86
4.3 Summary 87
4.4 Discussion 88

CHAPTER 5 A MORE GENERAL APPROACH: DYNAMIC OPTIMIZATION MODELLING 91

5.1 Model development 96
5.1.1 Control variables: current velocity and swimming velocity 97
5.1.1.1 Current velocity 97
5.1.1.2 Swimming velocity 98
5.1.2 State variables: downstream displacement and weight 99

TABLE OF CONTENTS

Page

5.1.2.1 Downstream displacement 99
5.1.2.2 Weight 100
5.1.3 Fitness measure 105
5.1.3.1 Freshwater survival 108
5.1.3.2 Estuarine survival 110
5.1.3.3 Ocean survival 111
5.1.3.4 Fecundity 112
5.1.4 Egg-to-fry survival 112
5.2 Optimization model summary 113
5.3 Discussion 113

CHAPTER 6 MODEL ANALYSIS 116

6.1 More simplifying assumptions 118
6.2 Applying the maximum principle 121
6.3 The value function 122
6.3.1 Co-state variables 123
6.3.2 The Hamiltonian 124
6.3.2.1 When the co-state variable λ_1 is positive 126
6.3.2.2 When the co-state variable λ_1 is nonpositive 133
6.3.3 The canonical equations and optimal control parameters 138
6.3.4 Transversality conditions 139
6.4 Summary 140
6.5 Discussion 143

CHAPTER 7 EFFECTS OF FLUCTUATING LIGHT, TURBIDITY, AND CURRENT VELOCITY ON MIGRATION BEHAVIOR 147

7.1 Introduction 147
7.2 An autonomous case 149
7.2.1 Optimal solution types 150

TABLE OF CONTENTS

Page

7.3 Light sensitive predation 154
7.3.1 Numerical example (estuary entry time fixed) 155
7.3.1.1 Singular path? 156
7.3.1.2 The optimal strategy 157
7.3.2 Numerical example (estuary entry time free) 160
7.3.2.1 Note on applying the maximum principle 163
7.4 Fluctuating current velocity 164
7.4.1 Numerical example 165
7.5 Summary 167
7.6 Discussion 169

CHAPTER 8 SUMMARY AND DISCUSSION 171

8.1 Overview 171
8.2 Summary by chapter 172
8.3 Discussion 179
8.3.1 Age at migration 179
8.3.2 Applications to the Columbia River System 188
8.3.2.1 Response to increased flow or drawdown 188
8.3.2.2 Long-term effects of dams 189

LIST OF REFERENCES 191

APPENDIX A CO-STATE VARIABLE RESULTS 211

APPENDIX B MAXIMIZING THE HAMILTONIAN 218

APPENDIX C AN AUTONOMOUS CASE 237

APPENDIX D NUMERICAL METHODS 264

LIST OF FIGURES

Number *Page*

FIGURE 1.1 4
Distribution of stream- and ocean-type juvenile chinook salmon life-histories in the North Pacific (Taylor, 1990). Shading represents the approximate fraction of each early life-history type. A completely blackened circle represents 100% stream-type, and an open circle represents 100% ocean-type. The number next to each circle is the number of populations surveyed. Regions surveyed are (clockwise from left): Kamchatka R., south-western Alaska, lower Yukon R., upper Yukon R., south-central Alaska, south-eastern Alaska and northern British Columbia, central British Columbia, Fraser River, Vancouver Island and coastal Washington, lower Columbia R., upper Columbia R., coastal Oregon, and California.

FIGURE 1.2 6
Distribution of stream (darkened fish) and ocean-type (white fish) chinook salmon life-history types in tributaries of the Columbia River (Taylor, 1990). 1, upper Willamette R.; 2, lower Willamette R.; 3, upper Deschutes R.; 4, lower Deschutes R.; 5, John Day R.; 6, Tucannon R.; 7, Grande Ronde R.; 8, Imnaha R.; 9, Little Salmon R.; 10, South Fork Salmon R.; 11, Bear Valley Cr.; 12, Marsh Cr.; 13, Middle Fork Salmon R.; 14, upper Salmon R.; 15, East Fork Salmon R.; 16, Lemhi R.; 17, Yakima R.; 18, Wenatchee R.; 19, Gray's R.; 20, Elochoman R.; 21, Klatskanie R.; 22, Methow R.; 23, lower Wenatchee R.; 24, Klickitat R.; 25, Washougal R.; 26, Gray's Harbor; 27, Cowlitz R.; 28, Columbia R. (Vernita Bar); 29, Snake R. (Hells Canyon Reach).

FIGURE 1.3 11
The optimal age at migration occurs when the marginal immediate costs equal the marginal future profits. Migration prior to the optimal time, though it brings higher pre-migratory survival, brings with it a low future profit due to high migration and ocean mortality. Migration after the optimal time, though it brings lower migration and ocean mortality, brings higher pre-migratory mortality and lower fecundity (presumably because of forgone ocean growth).

FIGURE 1.4 12
Fitness and the ratio of growth rate to mortality rate for the freshwater and ocean environments (here it is assumed that migration mortality is incorporated into the ocean mortality function). t^* is the time when a habitat shift from freshwater to the ocean maximizes fitness. Notice that it corresponds to the point where the freshwater and ocean ratios of growth rate to mortality rate intersect. This graph is based on the approach of Gilliam (1982).

FIGURE 1.5 16

LIST OF FIGURES

Number *Page*

Fitness and the ratio of growth rate to mortality rate for the slow current and swift current habitats. w_s is the size at which a habitat shift from slower to faster currents maximizes fitness.

FIGURE 2.1 30
Optimal migration timing is an increasing function of migration distance. For short migration distances ($a < a_{crit}$), outmigration is immediate. As migration distance increases, optimal migration timing approaches a maximum.

FIGURE 2.2 32
For predator search velocities less than $ar_f/2$, an increase in migration velocity results in later migration. When predator search velocities exceed $ar_f/2$, there is a critical migration velocity, below which increasing migration velocity results in later migration, and a above which, increasing migration velocity results in earlier migration. When predator search velocity and migration velocity fall above the dashed curve to the upper right, migration is immediate.

FIGURE 2.3 34
The curve above represents the values of predator density and freshwater growth rate that give zero marginal change of age at migration with respect to freshwater growth. Large values of predator density (above the curve) give a negative marginal change, small values (below the curve), a positive marginal change.

FIGURE 2.4 36
Optimal migration timing as a function of freshwater growth rate. For small freshwater growth rates (less than r_{crit}), immediate migration is favored. When freshwater growth rate approaches $r_o - \mu$, a lifetime freshwater residence strategy is favored. For intermediate freshwater growth rates, an increase in freshwater growth leads to earlier migration.

FIGURE 2.5 38
Isoclines of optimal age at migration. Below the dashed curve, age at migration declines with increasing freshwater growth rate; above the dashed curve, it increases. An increase in temperature produces a change in freshwater growth rate, Δr_f, in predator search velocity, $\Delta\zeta > 0$, and hence in migration timing Δt_m^*. $\Delta t_m^* < 0$ whenever Δz is large enough relative to Δr_f. $\Delta t_m^* < 0$ is guaranteed whenever $(\Delta t_m^* / dr_f)\, \Delta r_f < 0$ (see A and B above, the arrows represent the vector $(\Delta r_f, \Delta\zeta)$).

FIGURE 2.6 43

LIST OF FIGURES

Number *Page*

The indicator function increases with migration distance. Migration distance is constrained to lie between 0, where $\Delta J < 0$, and $t_s z$, where $\Delta J > 0$. For values of the migration distance less than a_{crit}, immediate migration is optimal; otherwise, lifetime freshwater residence is optimal. The migration distance at the vertex violates the constraint on a.

FIGURE 2.7 45
Null cline of the indicator function when the root of the denominator exceeds the root of the numerator in (2.26). For values of migration distance less than a_1, immediate migration is optimal, regardless of r_f. When migration distance is between a_1 and a_2, immediate migration is optimal for small values of r_f, and lifetime freshwater residence is optimal for larger values of r_f. When migration distance exceeds a_2, only lifetime freshwater residence is optimal.

FIGURE 2.8 46
Null cline of the indicator function when the root of the numerator exceeds the root of the denominator in (2.26). When migration distance is less than a_1, immediate migration is optimal; when it is greater than a_2, lifetime freshwater residence is optimal. In both of these cases, changing r_f does not influence the optimal strategy. However, when the migration distance is between a_1 and a_2, increasing r_f can change the optimal strategy from lifetime freshwater residence to immediate migration (negative effect).

FIGURE 2.9 49
The fitness difference as a function of migration velocity. In this case the horizontal asymptote is positive, and the optimal strategy is lifetime freshwater residence for all values of migration velocity, z, satisfying $z \geq a / t_s$.

FIGURE 2.10 50
The fitness difference as a function of migration velocity. In this case the horizontal asymptote is negative, and the optimal strategy is lifetime freshwater residence for migration velocities between a / t_s and z_{crit}. If z exceeds z_{crit}, then immediate migration is optimal.

FIGURE 3.1 66
Optimal migration time can be forced to decrease with food density if the von Bertalanffy anabolism exponent, ϕ, is large enough. However, theoretically, and in practice, this exponent lies near 2/3, where time of migration decreases with food density.

LIST OF FIGURES

Number *Page*

FIGURE 3.2 68
The log of age at migration as a function of predator density. As the terms leading to limited growth (metabolism, handling time) are reduced from their estimated values to zero, through the multiplier *d*, age at migration becomes and increasing function of predator density. This demonstrates how making the freshwater growth function limiting rather than exponential, changes the relationship between predator density and age at migration.

FIGURE 4.1 76
Temperature dependent food consumption functions for chinook/coho, and pink/sockeye (Hewitt & Johnson, 1992).

FIGURE 4.2 79
The proportion of the maximum consumption as a function of temperature for walleyr, smallmouth bass (Hewitt & Johnson 1992), and northern squawfish (Vigg & Burley, 1991).

FIGURE 4.3 80
Nonlinear least squares fit of Snake River daily average temperature data recorded at Anatone Gage, Washington, 1975-1982 (Conner *et al.*, 1993).

FIGURE 4.4 82
Comparison of log fitness vs. age-at-migration curves when temperature is constant and when it fluctuates. Notice that in the presence of fluctuating temperatures, the optimal migration occurs almost half a year earlier. The constant temperature model actually produces a poor strategy—migrate during the summer when predation is high.

FIGURE 4.5 84
Influence of migration distance on optimal age at migration. The step function described by the curve of asterisks describes the global optimum age at migration, while the lines represent local optimums. Notice that the optimal age at migration leaps discontinuously between years as migration distance increases, but the optimal time of year for migration changes little.

FIGURE 4.6 86
The effect of temperature fluctuations on the log(fitness) curve. The maxima correspond to the minima of the temperature curve. As the fish ages, the effect of temperature is less severe, owing to its larger size, and consequently, its greater ability to escape enemies.

LIST OF FIGURES

Number *Page*

FIGURE 5.1 93
Chinook life cycle summary. Lifetime reproductive success depends on survival in the ❶ freshwater, ❷ estuarine, and ❸ ocean habitats, as well as ❹ fecundity and egg-to-fry survival.

FIGURE 5.2 99
The control variables: swimming velocity and current velocity. Depicted is a chinook fry swimming against the current, which therefore has a negative swimming velocity. Since swimming velocity is measured relative to the current velocity, the migration velocity is $u + v$.

FIGURE 5.3 101
Typical growth curve as a function of swimming speed, where weight and temperature are fixed. Growth is concave in swimming speed, and there is one unique maximum value, $v = .48 \text{ m} \cdot s^{-1}$. Growth is negative for swimming speeds either too small, $|v| \leq .21 \text{ m} \cdot s^{-1}$, or too great, $|v| \geq .71 \text{ m} \cdot s^{-1}$. This curve was derived based on a Holling (1959) type II feeding curve, and a metabolic cost curve in Hewitt & Johnson (1991). It represents the growth rate of a fish weighing 5 g at a temperature of 15° C.

FIGURE 6.1 127
Optimal current and swimming velocities as determined by maximizing the Hamiltonian when λ_1 is positive.[a] In figure (a) the maximum current velocity exceeds the maximum growth speed. In figure (b) the reverse is true. When the switching function σ_1 is negative, ❶, behavior is driven by predator avoidance and feeding. When it is positive, ❷, behavior is driven by the need to migrate to the ocean and take advantage of its tremendous growth potential. When it is zero, behavior is intermediate to ❶ and ❷, and the current velocity is not uniquely determined (unless $u_{\max} = 0$).

FIGURE 7.1 152
Optimal strategy types. (a) The juvenile initially holds station until it grows above a critical weight, then continually migrates downstream until it reaches the estuary at t_f (strategy S1). (b) The juvenile begins downstream migration immediately, ceasing only when it reaches the estuary; it then holds station until t_f (strategy S2).

FIGURE 7.2 158
Effective predator density diminishes due to increased weight of the fish and during the onset of high turbidity. As turbidity subsides, the switching function falls negative and the fish returns to feeding and predator avoidance behavior. As the fish

continues to growth, the switching function rises again to a positive value, and the fish resumes active migration. This interrupted migration strategy occurs when the time of estuary entry, t_f , is fixed.

FIGURE 7.3 159
Downstream displacement plotted as a function of weight. The first increment in displacement is caused by an increase in turbidity, the second by the natural decrease in capture probability due to larger size. When the fish is not migrating downstream, it is holding station showing a feeding and predator avoidance behavior. There is no "critical weight" *per se* at which migration begins. Rather, active migration results from a combination of factors both external and internal—increased turbidity and increased weight.

FIGURE 7.4 161
Influence of turbidity on optimal time of estuary entry. There are two maxima of the fitness curve as a function of estuary entry time, the one on the left, corresponding to the period or turbidity, and the other corresponding to decreased capture probability due to natural growth. As the turbidity intensity parameter, κ, increases from 0, the global maximum switches from $t_f^* = 82.48$ d to the maxima corresponding to an increase in turbidity $t_f^* = 73.18$ d. This fitness curve is bimodal, and estuary entry times lying between the two modes are suboptimal. This leads to two possible optimal behavior (usually only one of which is truly optimal): either ignore the increased turbidity altogether, or initiate an uninterrupted seaward migration.

FIGURE 7.5 162
The co-state variable corresponding to downstream displacement increases in response to a sufficient increase in turbidity intensity parameter, κ. As κ increases from 0 to .0055 (representing a .55% decrease in the capture probability), the co-state variable varies from $\lambda_1 = .2670$ to $\lambda_1 = .2773$, making the switching function positive at an earlier date (8.3 days earlier), and therefore making an earlier migration optimal.

FIGURE 7.6 166
The influence of freshets on the optimal time of estuary entry. (b) Of the four freshets of equal intensity starting at 71, 74, 77, and 80 days respectively, those timed closest to the optimal time of estuary entry in the absence of freshets, t_f^*, have the most influence. t_f^* represents a good measure of the approximate time of migration readiness. (a) Freshets that occur too early (relative to t_f^*) do not influence time of estuary entry (see ❶), but those that do not occur to early, do have

influence (see ❷).

FIGURE 7.7 167
A well timed freshet can increase the co-state variable associated with displacement, λ_1, making the switching function zero earlier, and therefore leading to earlier seaward migration.

FIGURE 8.1 183
(a) Detection time if 46 PIT-tagged subyearling salmon at Lower Granite Dam, water temperature, flow, and temperature-dependent specific rate of respiration of a 5-gram subyearling. Migration timing may be attributed to a decrease in habitat suitability. As summer progresses, (b) temperatures rise, (c) respiration rate increases, and (d) flows decrease. The temperature-dependent specific respiration rate function is taken from Hewitt & Johnson (1992).

FIGURE 8.2 184
Comparison of 1981-82 flow, temperature, and specific rate of respiration of a 5-gram fish at the Snake River Anatone USGS gauge (RK 269) and the East Fork of the Salmon R. above Big Boulder Creek (USGS gauge 13297453).

FIGURE 8.3 186
Detection time of PIT-tagged subyearling salmon at Lower Granite Dam, water temperature, and a temperature-dependent consumption function for northern squawfish. The subyearlings were tagged between 30 May and 2 July of 1991 in the Snake River drainage between RK211 and RK250 above Lower Granite Dam. Mean daily water temperature data were recorded at Billy Creek (RK 265). (a) The peak of detection occurred in mid July, and most emigrated by September. Note that this peak in migration corresponds to periods of high temperature (b), which also corresponds to peak consumption rate of northern squawfish (c). The temperature dependent consumption function (d) is a generalized gamma, and is taken from Vigg & Burley (1991).

FIGURE 8.4 187
Comparison of fitness curves showing the influence of simple spatial structure. Curve ❶ uses the seasonal temperatures of 1981-82 from the Anatone Gauge (RK269 of the Snake R.), no spatial river structure, and a migration distance of 800 km. Curve ❷ also uses a migration distance of 800 km, but in the first 10 km, temperatures of East Fork Salmon R. 1981-82, and over the last 790 km, the warmer Anatone Gauge temperatures apply. Predation parameters were set to $\theta = .11$ $km^{-1}$and $\zeta = 1400$ $km \cdot yr^{-1}$, and the remain parameters are as given in TABLE 4.4.

Number *Page*

A juvenile optimally migrates during the first year when ❶ applies, and during the second year if ❷ applies. This occurs because the colder temperatures in ❷ give reduced predation (due to a temperature-dependent consumption rate), giving the juvenile an opportunity to remain in the upper river and grow for a year (under reduced predation conditions), before migrating through regions of more aggressive predators.

FIGURE B.1 220
The optimal choice of the current velocity depends on the sign of the switching function, σ_1. Note that since λ_1 is positive, so is σ_2 . When σ_1 is positive (case 1), the maximizing u is clearly u_{max}, when it is negative (case 2), the maximizing u is either u_{max}, $-v$, or 0, depending on whether $-v$ lies to the right, within, or to the left of the interval $[0, u_{max}]$ respectively. When σ_1 is zero (case 3), the maximizing u is either u_{max}, any value in the interval $[-v, u_{max}]$, or any value in the interval $[0,u_{max}]$, depending on wheter $-v$ lies to the right, within, or to the left of $[0, u_{max}]$ respectively.

FIGURE B.2 222
When σ_1 is positive, v^* maximizes the sum of L_1 and $\lambda_2 g$, subject to $-v_{max} \le v \le v_{max}$.

FIGURE B.3 224
When σ_1 is negative, v^* maximizes the sum of L_2 and $\lambda_2 g$ subject to $-v_{max} \le v \le v_{max}$. Note that the slope of the the left-most linear piece of L_2 is steeper than its right-most linear piece, since $\sigma_2 = \lambda_1 + \theta k > |\lambda_1 - \theta k| = |\sigma_1|$.

FIGURE B.4 227
In this case the switching function σ_1 is zero, and the goal is to maximize the sum of the functions L_3 and $\lambda_2 g$ with respect to v, while observing the constraint, $-v_{max} \le v \le v_{max}$.

FIGURE B.5 229
The maximizing choice of the current velocity depends on the sign of the switching function, σ_2 . Note that since λ_1 is nonpositive, σ_1 is negative (assuming $\theta k > 0$). When σ_2 is negative (case 1), then Y is strictly decreasing in u, and therefore the maximizing current velocity is 0. When σ_2 is positive (case 2), the maximizing current velocity is u_{max}, $-v$, or 0, depending on whether $-v$ lies to the right of, within, or to the left of the interval $[0, u_{max}]$ respectively. When σ_2 is zero (case 3), the maximizing current velocity is any value in $[0, u_{max}]$, any value in $[0, -v]$, or 0, depending on whether $-v$ lies to the right of, within, or to the left of the interval

Number *Page*

[0, u_{max}] respectively.

FIGURE B.6 231
If σ_2 is positive, v^* is identified by maximizing the sum L_4 and $\lambda_2 g$, while observing the constraint, $-v_{max} \le v \le v_{max}$.

FIGURE B.7 233
If σ_2 is positive, v^* is the value of v that maximizes the sum of L_2 and $\lambda_2 g$, while observing the constraint, $-v_{max} \le v \le v_{max}$. Note that the right-most linear piece of L_2 is steeper than the left-most linear piece, because $|\sigma_1| = -\lambda_1 + \theta k > \lambda_1 + \theta k = \sigma_2$.

FIGURE B.8 235
When the switching function σ_2 is zero. The goal is to maximize the sum of the functions L_5 and $\lambda_2 g$ with respect to v, where $-v_{max} \le v \le v_{max}$.

FIGURE D.1 266
Pseudo code for the shooting method.

FIGURE D.2 269
Arguments and method of the routine **shoot()** (Press *et al*., 1988).

LIST OF TABLES

Number *Page*

TABLE 1.1 8
Summary of diel observations of juvenile chinook salmon in various Pacific Northwest Rivers (Ledgerwood *et al.*, 1991).[a]

TABLE 1.2 13
Model descriptions.

TABLE 2.1 22
Assumptions of the heuristic model.

TABLE 2.2 22
Heuristic model summary.

TABLE 2.3 23
Heuristic model variables and functions.

TABLE 2.4 28
Parameter effects (example 1).

TABLE 2.5 39
Parameter effects (example 2).

TABLE 2.6 57
Latitude and migration timing.

TABLE 3.1 60
Model assumptions.

TABLE 3.2 61
Model summary.

TABLE 3.3 63
Parameters and their estimates.

TABLE 3.4 64
Parameter sensitivity.

TABLE 4.1 72
Model assumptions.

TABLE 4.2 73

LIST OF TABLES

Number *Page*

Model summary.

TABLE 4.3 74
Main model variables and functions.

TABLE 4.4 81
Functions, parameters, and their estimates.

TABLE 4.5 83
Sensitivity results.

TABLE 4.6 89
Lethal water temperatures in some California rivers. The estimates were derived from USGS data.[a]

TABLE 5.1 94
Model assumptions.

TABLE 5.2 95
General optimization model summary.

TABLE 5.3 96
Main parameters and functions.

TABLE 6.1 117
General optimal control problem.[a]

TABLE 6.2 119
Simplifying assumptions of this chapter.[a]

TABLE 6.3 120
The simplified optimal control problem.

TABLE 6.4 121
Special notation.

TABLE 6.5 128
Optimal choices of current velocity corresponding to different choices of the swimming velocity when λ_1 is positive.

TABLE 6.6 131

LIST OF TABLES

Number *Page*

Optimal swimming velocity summary when the switching function σ_1 is negative.[a]

TABLE 6.7 133
Optimal swimming velocities when the switching function σ_1 is zero.

TABLE 6.8 135
Optimal choices of current velocity corresponding to different choices of the swimming velocity when λ_1 is nonpositive.

TABLE 6.9 136
Optimal swimming velocity summary when the switching function σ_2 is positive.

TABLE 6.10 138
Optimal swimming velocities when the switching function σ_2 is zero.

TABLE 7.1 149
Further model simplifications.[a]

TABLE 7.2 150
Model assumptions (autonomous case with fixed estuary entry time).[a]

TABLE 7.3 150
Optimal control problem (autonomous case with fixed estuary entry time).

TABLE 7.4 151
Maximum principle applied to the autonomous case.[a]

TABLE 7.5 153
Optimal strategies based on the initial sign of the growth and switching functions.

TABLE 7.6 154
Functions, parameters, and their estimates.

TABLE 8.1 188
Factors and the gradient(s) they address.

TABLE B.1 221
Optimal choices of migration velocity corresponding to different choices of the swimming velocity when λ_1 is positive.

TABLE B.2 226

LIST OF TABLES

Number *Page*

Optimal swimming velocity summary when the switching function σ_1 is negative.

TABLE B.3 228
Optimal swimming velocities when the switching function σ_1 is zero.

TABLE B.4 230
Maximizing choices of current velocity corresponding to different choices of the swimming velocity when λ_1 is nonpositive.

TABLE B.5 234
Optimal swimming velocity summary when the switching function σ_2 is positive.

TABLE B.6 236
Optimal swimming velocities when the switching function σ_2 is zero.

TABLE C.1 238
Optimal control problem (autonomous case with fixed estuary entry time).

TABLE C.2 238
Special notation.

TABLE C.3 239
Optimal swimming velocity summary when $u_{\max} > v_{\max}$.

TABLE C.4 263
Optimal strategies based on the initial sign of the growth and switching functions.

PREFACE

This dissertation contains a succession of increasingly more complex models to describe the migration patterns of juvenile chinook salmon, focusing on the adaptive significance of the relationship between age at migration and geographical distribution, and migration behavior itself. I take the behavioral ecology approach of optimization modelling, designed to help understand why animals behave as they do. This approach stands in contrast to those that predict behavior solely on the basis of proximate mechanisms. These two methods present two different—although related through physiological constraints—ways to understand juvenile chinook behavior. When held together, they give broader perspective than either approach alone.

My approach is simple. I develop parsimonious models aimed at capturing the *basic* tradeoffs of different behaviors, respecting certain physiological constraints, where benefits and costs are measured in terms of survival and reproduction. These simple models, although frequently attacked for not including all relevant information, harbor the greatest potential for yielding useful biological insights. Furthermore, in simple models, components that drive solutions are more easily identified. For example, in CHAPTER 6, signs of the "switching functions," which measure the costs and benefits of movement downstream, determine which of two general behavior types— "feeding and predator avoidance" or "active downstream migration"— is optimal.

With the risk of invoking hostility from all quarters, I encroach upon the territory of researchers working to understanding migration behavior from a particular point of view shaped by their salmon habitat of interest. However, I believe an *integrated* approach, one that considers patterns of growth and mortality in streams, rivers, estuaries, and the ocean, for example, is essential for understanding the adaptive significance of migration timing and behavior. Would selection favor a seaward migration over a distance of 3,200 km from the headwaters of the Yukon River if the Pacific Ocean did not harbor tremendous growth potential?

Lastly, I want to stress that my work does not pretend to *explain* geographical and temporal patterns of migration, and I do not believe that any of the models are "correct," nor could they ever be. But I do believe that the models are *useful* since they suggest new hypotheses for migration behavior and suggest experiments for further understanding this behavior. This is usually the most that can be hoped for when modelling biological phenomena.

Seattle, October 1994 *R. A. Hinrichsen*

ACKNOWLEDGMENTS

I wish to express sincere appreciation to Professors Jim Anderson, Mark Kot, Juris Vagners, Ray Hilborn, and Robert Francis for serving on my supervisory committee, and providing valuable insight into the problem of applying optimization models to chinook migration behavior. Mark Kot served as my initial advisor, offering his knowledge of mathematical biology and showing great patience with my topic shift. Juris Vagners pointed out intricacies of my optimal control problem and recommended exploring modern stochastic optimization techniques. Ray Hilborn stressed the importance of exploring alternative hypotheses. My greatest debt of gratitude is owed to Jim Anderson, whose mind has not let mine rest, and who has willingly shared his ideas, insights, and time. He also procured steady long-term financial support for my work.

I also gratefully acknowledge Brian Spence, Oregon State University, for his e-mails concerning migration timing of coho salmon, Marc Mangel, University of California, Davis, for recommending his article of salmon life history related work; Eric Taylor, University of British Columbia, for supplying his chinook data, and allowing me to use his illustrations of the geographic distribution of chinook salmon; and finally, the inspirational Tom Quinn, whose graduate course on Pacific salmon supplied the necessary background for this research.

I also owe special thanks to the Bonneville Power Administration which gave me financial support through (Contract Number DE-BI79-89BP02347, Project Number 89-108).

To my brother,

Steven Todd Hinrichsen

March 20, 1964 – June 29, 1993

CHAPTER 1 INTRODUCTION

1.1 Background

Chinook salmon *(Oncorhynchus tshawytscha)* and other Pacific salmon species may have evolved as late as .5 to 1 million years ago (Neave, 1958) or as early as two or three million years ago (Thomas *et al.*, 1986). They are anadromous and semelparous, like all *Oncorhynchus* species, and are distinguished by their large adult size and by their broad variation in age at seaward migration, length of estuarine and ocean residence, ocean distribution, and age at maturity. Spawning populations have a geographical range extending south to California's Ventura River (34°N) and north to Point Hope, Alaska, and east to the Mackenzie and Coppermine rivers (Hallock & Fry, 1967; McPhail & Lindsey, 1970; Lee *et al.*, 1980; McLeod & O'Neil, 1983; Taylor, 1990). On the Asian coast, they range from northern Hokkaido to the Anadyr River (Berg, 1948; Shmidt, 1950; Hikita, 1956; Vronskiy, 1972; Major *et al.*, 1978).

The downstream migration of juveniles is both "facultative" and "obligatory" in the sense that it can be initiated by apparent overcrowding, absence of food, abundance of predators, high flow conditions, or other exogenous factors ("facultative" migration), and also by their stage of ontogeny or smolt condition ("obligatory" migration) (Baker, 1978). Smolting is a developmental process characterized by a set of physiological, morphological, and behavioral changes that prepare salmon for a salt water environment (Dickhoff & Sullivan, 1987). It is marked by dermal purine deposition (silvery skin),

osmoregulation, and an increase in thyroid hormones. The rate of smolting varies among populations for either genetic or environmental reasons, and contributes to variation in the age and season of migration.

Two early life history types (races) are identified based on age at migration from freshwater to saltwater (Gilbert, 1913; Clarke *et al*., 1992). One race, designated "stream-type," spend one or more years as fry or parr in fresh water before migrating to sea. The second race, "ocean-type", migrates to sea during their first year of life, normally within 3 months of emergence from spawning gravel (Healey, 1991).

1.2 Literature review of juvenile migratory behavior

The following literature review focuses on studies of juvenile chinook migratory behavior separated into four categories: migration timing, seasonal migration patterns, diurnal migration patterns, and stream velocity selection. The first three categories could all be placed under the heading of migration timing. The questions asked are "In what year after emergence does the fish migrate?", "During what time of the year?", and "During what time of the day?" Each of these questions is important, for there are many processes, acting over small to large time scales, exogenous or endogenous, that create hourly, seasonal, and yearly migration patterns.

1.2.1 Migration timing

There are two important geographic patterns observed in juvenile chinook migration timing: (1) chinook populations are predominantly "ocean-type" south of the Columbia River (coastal Oregon rivers and streams, California rivers such as the Sacramento and San Joaquin Rivers), and "stream-type" north of the Skeena River (56° N.); and (2) in

rivers where they are sympatric, (e.g. the Columbia and Fraser Rivers), “ocean-type” populations tend to be distributed in coastal regions, while “stream-type” populations are distributed inland.

Although these general patterns are quite striking, there are exceptions. For example, the Hells Canyon reach of the Snake River (located between RK 240.5 and RK 396.6), despite its distance its long distance from the ocean, is rearing habitat for ocean-type chinook. The Vernita Bar spawning populations (located between RK 345 and RM 397) on the Columbia River, are also ocean-type. There are also exceptions to the more northern distribution of stream-type populations: stream-type chinook populations exist in two upper tributaries of the Sacramento R. of California—Mill and Deer Creeks (F. Fisher, Stockton, CA, pers. comm.).

1.2.1.1 Latitudinal gradient

The latitudinal gradient (FIGURE 1.1) has been studied by Taylor (1990), who looked at the pattern from three points of view: zoogeography, growth, and selection.

Zoogeography. Chinook salmon likely survived the last (Wisconsinan) glaciation in two main refugia: (i) “Beringia,” a northern region consisting of the lower Yukon and exposed portions of the Bering Sea and Siberia; and “Cascadia,” defined as areas south of glaciers west of the Continental Divide (Lindsey & McPhail, 1986; McPhail & Lindsey, 1986). During deglaciation, chinook dispersed and settled along the Pacific Coast. According to the hypothesis, “stream-type” chinook persisted in the Beringia, and “ocean-type”, in the Cascadia, and after deglaciation, they maintained their north-south distribution.

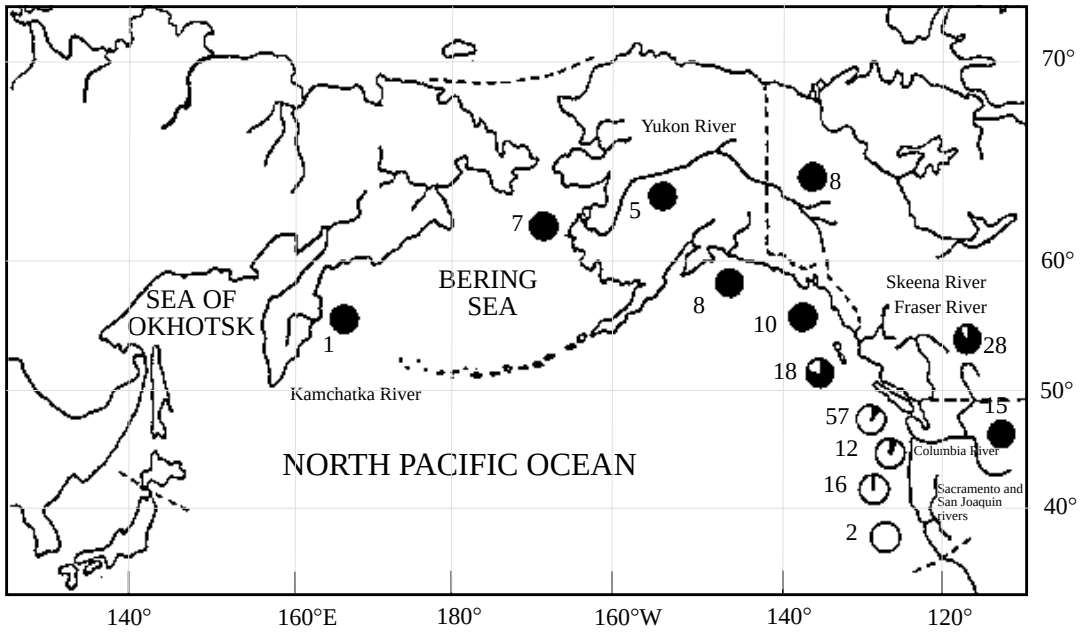

FIGURE 1.1 Distribution of stream- and ocean-type juvenile chinook salmon life-histories in the North Pacific (Taylor, 1990). Shading represents the approximate fraction of each early life-history type. A completely blackened circle represents 100% stream-type, and an open circle represents 100% ocean-type. The number next to each circle is the number of populations surveyed. Regions surveyed are (clockwise from left): Kamchatka R., south-western Alaska, lower Yukon R., upper Yukon R., south-central Alaska, south-eastern Alaska and northern British Columbia, central British Columbia, Fraser River, Vancouver Island and coastal Washington, lower Columbia R., upper Columbia R., coastal Oregon, and California.

Growth. Next is the “growth opportunity” point of view. Stream-type chinook are generally associated with regions of lower growth opportunity than ocean-type chinook. The north-south temperature gradient contributes to a like gradient in growth opportunity (i.e. regions to the south present higher growth-opportunity than northern regions). Since smolting contributes to the propensity for juveniles to move downstream, and smolting is

driven by temperature-related variables such as photo-period and growth, this pattern is not surprising.

Selection. Selection for size at migration, coupled with selection for migration during seasonal time "windows," might promote genetic differences in juvenile life-history. Locomotor and osmo-regulatory performance are inhibited at low temperatures (*i.e.*, cold climates north of 56°) (Brett, 1967; Knutsson & Garv, 1976; Beamish, 1978; Webb, 1978; Virtanen & Oikari, 1984). Therefore, larger smolt size may be selected in the cold northern environments, because larger smolts have an increased performance benefit (Brett & Glass, 1973; McCormick & Naiman, 1984; Hargreaves & LeBrasseur, 1986). This benefit of larger smolt size could lead to longer freshwater residence times in the north. Age at migration is in part, inherited in salmonids—a condition necessary if selection is to play a role in shaping it (Rich & Holmes, 1928; Ricker, 1972; Refstie *et al.*, 1977; Thorpe & Morgan, 1978; Carl & Healey, 1984; Taylor, 1988, 1989a,b).

1.2.1.2 Migration distance gradient

The migration distance pattern observed in migration timing data is quite simple: south of 56° N, longer migrations generally produce longer freshwater residence times (FIGURE 1.2). Two important selection-based factors are thought to explain why this pattern exists (Taylor, 1990). Larger migration distances, select for large smolt size at migration, due to (1) increased energetic demands (Gilhousen, 1980; Taylor & McPhail, 1985) and (2) greater exposure to freshwater predators (Larsson, 1985; Ruggertone, 1986) relative to short migrations.

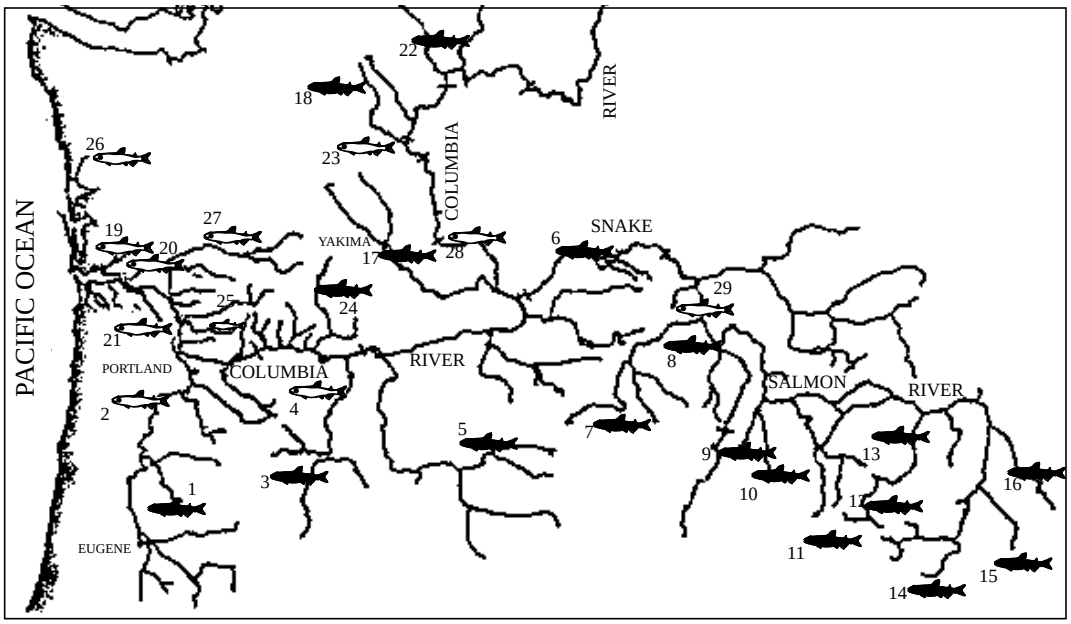

FIGURE 1.2 Distribution of stream (darkened fish) and ocean-type (white fish) chinook salmon life-history types in tributaries of the Columbia River (Taylor, 1990). 1, upper Willamette R.; 2, lower Willamette R.; 3, upper Deschutes R.; 4, lower Deschutes R.; 5, John Day R.; 6, Tucannon R.; 7, Grande Ronde R.; 8, Imnaha R.; 9, Little Salmon R.; 10, South Fork Salmon R.; 11, Bear Valley Cr.; 12, Marsh Cr.; 13, Middle Fork Salmon R.; 14, upper Salmon R.; 15, East Fork Salmon R.; 16, Lemhi R.; 17, Yakima R.; 18, Wenatchee R.; 19, Gray's R.; 20, Elochoman R.; 21, Klatskanie R.; 22, Methow R.; 23, lower Wenatchee R.; 24, Klickitat R.; 25, Washougal R.; 26, Gray's Harbor; 27, Cowlitz R.; 28, Columbia R. (Vernita Bar); 29, Snake R. (Hells Canyon Reach).

1.2.2 Seasonal migration pattern

Seasonal patterns of migration timing are hypothesized to be based on water velocity, turbidity, and temperature—correlated factors that likely work together. Observations show that juveniles tend to migrate with higher stream flows (Mains and Smith, 1964; Raymond, 1968; Reimers, 1968; Salo, 1969; Wetherall, 1970; Stober *et al.* 1973; Becker, 1973a; Anonymous, 1976; Kjelson *et al.*, 1982); during periods of increased water

turbidity (Junge and Oakley, 1966); and with fluctuations in water temperature (Mains & Smith, 1964; Becker, 1973b). Downstream movement of fry is typically greatest between February and May, and is earlier in more southern populations (Healey, 1991).

1.2.3 Diel migration pattern

Natural light intensity appears to be the major environmental factor controlling diel migration patterns of salmonid fry (Mains & Smith, 1964; Smith, 1974;Godin, 1982). Studies on diel movements abound, and do not show consistent results, but the majority of the studies demonstrate that chinook juveniles migrate mostly at night (TABLE 1).

One selection-based hypothesis that can explain this diurnal pattern is that juveniles migrate mainly at night to avoid predators (Neave, 1955). If migrating during the nighttime confers a fitness advantage, then we should look for mechanisms that produce the behavior. Nighttime movement has been described as “passive” by some, the idea is that movement is a result of loss of visual contact with surroundings (McDonald, 1960), or a reduction of rheotactic response (Hoar, 1953). However, Dauble *et al.* (1989) suggests that migration is not controlled solely by passive mechanisms.

TABLE 1.1 Summary of diel observations of juvenile chinook salmon in various Pacific Northwest Rivers (Ledgerwood *et al*., 1991).[a]

Race	Location	Time of Largest Catch	Source
stream	Central Ferry Bridge (Snake R.)	At night between 0300 and 0600h.	Mains & Smith 1964
stream	Byer's Landing	At night. 70%between 1800 and 0600h.	Mains & Smith 1964
stream	John Day (Columbia R.)	During daylight between 0700 and 2100h.	Sims *et al*. 1976
stream	Lower Monumental (Snake R.)	At night (92%).	Smith 1974
stream	Mayfield (Cowlitz R.)	At night. 92% between 2000 and 0800h.	Allen 1965
stream	Upper Mayfield (Cowlitz R.)	At night.	Smith *et al*. 1968
stream	North Fork (Clackamas R.)	At night.	Korn *et al*. 1967
stream	Rocky Reach (Columbia R.)	At night.	Leman 1978
stream	John Day (Columbia R.)	At night (92%).	Sims *et al*. 1976
stream	The Dalles (Columbia R.)	At night. 94% between 1900 and 0700h.	Long 1968
stream	The Dalles (Columbia R.)	During daylight. 89% between 0700h and 2100h.	Sims *et al*. 1976 Nichols 1979
stream	The Dalles (Columbia R.)	During daylight.	Nichols 1979
stream	Hanford Reach (Columbia R.)	At night. Peak between 2200 and 0400h	Dauble *et al*. 1989
ocean	Puget Island and Jones Beach (Columbia R. estuary)	During daylight. 90% between 0600 and 2100h.	Dawley *et al*. 1986
ocean	Sixes R. (Oregon)	At night.	Reimers 1973
ocean	John Day (Columbia R.)	During daylight.	Sims *et al*. 1976
ocean	John Day (Columbia R.)	At night (88%)	Sims and Ossiander 1981
ocean	The Dalles (Columbia R.)	At night. 67% between 1900 and 0700h.	Long 1968
ocean	The Dalles (Columbia R.)	During daylight.	Sims *et al.* 1976 Nichols & Ransom 1980
ocean	The Dalles (Columbia R.)	During daylight.	Nichols & Ransom 1980
ocean	Skagit River (Washington)	At night. Peak between 2000 and 0300h.	Davis 1981

[a] All sources except Dauble *et al*. (1989) and Davis (1981) are included in the Ledgerwood *et al*. (1991) analysis.

1.2.4 Current velocity selection

Despite the wide variation in migration timing observed among chinook populations, there appears to be one feature that is consistent throughout their range: larger fish are usually associated with swifter currents than smaller fish (Chapman & Bjornn, 1969; Lister & Genoe, 1970; Wickmire & Stevens, 1971; Everest & Chapman, 1972; Schaffter, 1980; Allen & Hassler, 1986; Dauble *et al.*, 1989). Swifter currents typically have a greater food delivery rate ($\mathrm{cal} \cdot \mathrm{s}^{-1}$), and can carry greater feeding opportunity for the juveniles (Elliot, 1967; Everest & Chapman, 1972; Fausch, 1984). As a trade-off, adjacent velocities selected by the fish may also be swift, requiring a greater energetic investment to feed (Jenkins, 1969; Fausch, 1984). Furthermore, the faster currents—typically located midstream—may bring a higher predation risk than slower, inshore currents. This underscores a trade-off inherent in many ecological processes: the trade-off between growth and the risk of predation.

From an adaptationist's viewpoint, the relationship between current velocity and size may be favored by natural selection. Smaller fish may be more vulnerable to predators, and increase survival changes by remaining in slower moving currents often associated with cover (Solomon, 1981). A social hypothesis is also possible. The larger fish are likely more socially dominant than the smaller ones (Newman, 1956; Kalleberg, 1958; Jenkins, 1969; Bassett, 1978), and may defend territories containing the swifter currents, presumably because such territories offer greater food delivery rates.

1.3 Optimization modelling approach

1.3.1 Migration timing

Some researchers, taking an adaptationist's viewpoint, have recently developed an optimization model to describe the relationships between initial length, survival and growth in fresh and salt water, and migration timing (Bohlin *et al*., 1993a; Mangel, 1994). Bohlin *et al.* (1993a) argue that

> "If fish migrate to increase growth rate and thereby fecundity (Gross, 1987), and if postmigratory mortality is negatively size dependent, then the benefit of early migration would be faster growth (as a result of longer time spent in the more productive environment), and the cost would be increased mortality (as a result of smaller body size at migration). The optimal migration time may therefore be the date at which the profit (benefit minus the cost) is maximized … The individual optimal might be predicted from life history theory by assuming that natural selection tends to favour reaction norms which maximize the lifetime fitness or reproductive value."

This problem can be described mathematically by representing the profit or "fitness" as the log of lifetime reproduction, where lifetime reproduction is the product of pre-migratory survival, the survival after the onset of migration, and fecundity, then determining the effect of a marginal increase of age at migration. At the optimal age at migration, the marginal change in profit is zero. The problem allows for both immediate and future ramifications for decisions. So, for example, migrating out of freshwater during a period of increased predation is not necessarily optimal, because the migration may lead to even worse predation along the migratory route, or in the estuary or ocean. The problem can be viewed along a time continuum, where at each moment, a fish makes the decision to remain in freshwater, or begin its seaward migration. The point at which migration

optimally begins is the time when the marginal benefit of delaying migration outweighs the marginal costs (FIGURE 1.3).

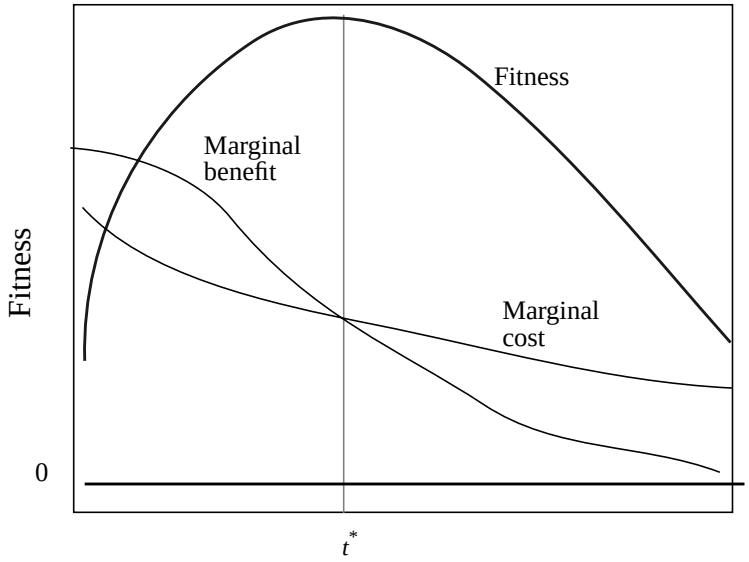

FIGURE 1.3 The optimal age at migration occurs when the marginal immediate costs equal the marginal future profits. Migration prior to the optimal time, though it brings higher pre-migratory survival, brings with it a low future profit due to high migration and ocean mortality. Migration after the optimal time, though it brings lower migration and ocean mortality, brings higher pre-migratory mortality and lower fecundity (presumably because of forgone ocean growth).

Similar approaches have been used to predict habitat shifts of bluegill (Gilliam, 1982; Werner & Gilliam, 1984). In fact, prediction of migration timing amounts to a habitat shift problem. Gilliam's (1982), chief result is that given the choice of two habitats (*e.g.*, freshwater and ocean habitats), with growth and mortality rates, g_1, μ_1; and g_2, μ_2 respectively, a juvenile optimally chooses the habitat of maximum g/μ (FIGURE 1.4). This "rule" or result, however, assumes that growth rates and mortality rates *do not*

depend explicitly on time, and so must be used with caution. Although the Bohlin model does not predict the same "rule," it gives consistent qualitative results: all else being equal, the larger g_1, the longer a juvenile should wait before making a transition from freshwater to saltwater, and the higher μ_2, the earlier a juvenile should migrate.

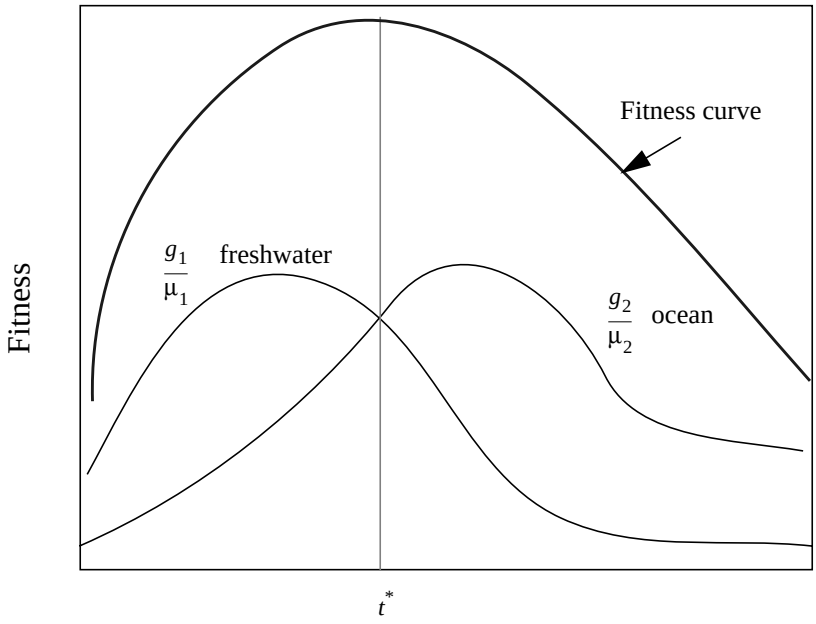

FIGURE 1.4 Fitness and the ratio of growth rate to mortality rate for the freshwater and ocean environments (here it is assumed that migration mortality is incorporated into the ocean mortality function). t^* is the time when a habitat shift from freshwater to the ocean maximizes fitness. Notice that it corresponds to the point where the freshwater and ocean ratios of growth rate to mortality rate intersect. This graph is based on the approach of Gilliam (1982).

Can the three models (Mangel, Bohlin and Gilliam) be used to explore the yearly, seasonal, and daily patterns of migration? Each has its advantages and disadvantages (TABLE 1.2). Since Gilliam is not time-explicit, it is questionable whether it can address

any of the questions adequately, since seasonal temperature is known to strongly influence patterns of growth and mortality. Let us assume that when considering yearly averages of growth and survival, it can be used to predict year of migration. Then all three can predict year of migration, only Bohlin can predict within-year migration timing, and none are appropriate for predicting daily migration pattern.

TABLE 1.2 Model descriptions.

Model	Time Horizon	Migration Timing	Fitness Criterion	State Variable(s)	Time explicit growth and survival?
Bohlin	fixed, 1 year	Continuous	Weight at end of year	Weight	yes
Mangel	free[a]	Discrete (specific time of year)	Expected Reproduction	Weight or Length	yes
Gilliam	infinite	Continuous	Expected Reproduction	Weight (size)	No

[a] "free" indicates that the final time is free to be varied in the optimization.

How well do these models predict the relationship between migration timing and latitude? The Bohlin and Gilliam models predict that delayed migration of northern chinook stocks is not a result of freshwater growth alone. They predict that poorer growth in the north should result in earlier migration of northern populations! They also predict that delayed migration in the north can only be a result of (i) poorer ocean or migration survival for northern juveniles, (ii) poorer pre-migration survival of southern stocks, or (iii) better marine growth for southern populations. Of the three possibilities, (iii) is unlikely, while (i) and (ii) are plausible. Note that these hypotheses are not mutually exclusive, and all can act together to shape behavior.

Mangel (1994) showed, in his analysis of young atlantic salmon migration timing, that increasing “food utilization efficiency,” a scaling factor of both ocean and freshwater growth rates, could lead to earlier migration. However, more model runs are required to determine how freshwater and ocean survival and growth, varied independently, influence migration timing, and if it can predict the observed relationship between migration timing and latitude.

Do the models predict that of the chinook stocks located on the Columbia or Fraser River, coastal populations migrate prior to inland populations? Assuming that size specific ocean growth and survival are the same for upstream and downstream populations, the Bohlin and Gilliam models could agree with the migration pattern if (i) size-specific migration survival is poorer for upriver populations, or (ii) size-specific pre-migration survival is better for upriver populations. Both of these scenarios are plausible, and (i) is especially likely considering that upstream salmon probably encounter a greater number of freshwater predators during their seaward migration. Considering the importance of (i) and (ii), there is a need to show how freshwater survival changes explicitly as a function of migration distance and its correlated variables such as current velocity, temperature, and predation. Unfortunately, none of the three models treat migration distance explicitly.

1.3.2 Current velocity selection models

The problem of current velocity selection can also be approached through optimization modeling, as one of optimal microhabitat selection. The most promising models consider not only growth (Fausch 1984), where the usual approach is to maximize rate of energy gain, but also survival (Gilliam 1982; Clark & Levy 1988; Leonardsson, 1991). A given

current velocity choice may be profitable for feeding, but may also be more dangerous. The degree of profit or danger depends on the size of the individual (Werner & Hall, 1988; Bugert & Bjornn, 1991; Bugert *et al.,* 1991). Gilliam's model once again is applicable to stream velocity selection, if we partition the river cross-section into regions of differing stream velocities, so that a finite number of mutually exclusive regions are defined, each having an average current velocity. Typically midstream habitats will have higher current velocity than habitats near shore.

How well can existing models predict the movement of salmon in to faster currents as they grow? Let us first assume that the most profitable stream positions, those maximizing potential growth, are associated with faster currents, and the "safest" regions are in nearshore areas, associated with slower currents. Then smaller juveniles, being more vulnerable to predators would likely forego the more profitable growth positions in favor of cover nearshore. As they grow, predation risk diminishes, and the juvenile can move into faster, more profitable currents. Gilliam's model could predict such a shift since it is based on maximizing g/μ (FIGURE 1.5).

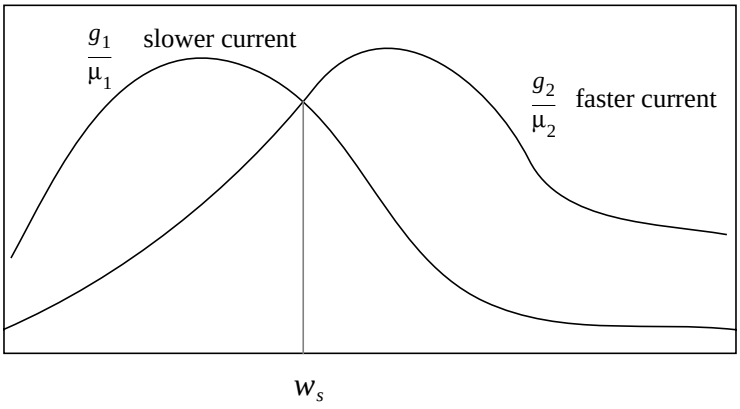

FIGURE 1.5 Fitness and the ratio of growth rate to mortality rate for the slow current and swift current habitats. w_S is the size at which a habitat shift from slower to faster currents maximizes fitness.

1.4 Research questions and problems

The literature abounds with observations and patterns concerning the early life history of chinook salmon. Observations show latitude and migration distance patterns of migration timing, and seasonal and diurnal patterns as well. Now that much data on the early life history of chinook has been tabulated and general patterns recognized, the time is ripe to ask the question, “What accounts for these patterns?” This question brings us to the realm of behavioral ecology. I will strive to view the question in two ways: “What survival or reproductive benefit does the behavior hold” (the adaptationist’s question); “What mechanism accounts for the behavior.” (the mechanist’s question). The bulk of this work focuses on the adaptationist’s question, and in the case of migrating salmon, is less studied than mechanisms.

The approach I take is to derive migration behaviors based on maximizing a measure of lifetime salmon fitness, and compare these simulated behaviors to actual observations. These behaviors are derived independently from the known behavioral mechanisms (smolting and ontogenetic switch from positive rheotaxis to negative rheotaxis), but are later compared to the known mechanism induced migration behavior. My hope is that the behaviors produced by the selective pressures acting in the fitness optimization, match the behaviors produced by known mechanisms, giving an independent understanding of behavior that is lacking. This more general approach—looking at behavior from more than one point of view—was advocated by Tinbergen (1963). In reality, however, it is only through the physiology of the salmon and the mechanisms of behavior, that salmon could achieve the optimal solutions predicted by the fitness model. Therefore, ultimately, the survival and reproductive value of behavior must be considered together with mechanisms to fully understand why salmon behave as they do.

Specifically, I will address the following behavioral questions:

1. What accounts for the relationship between early life history type and latitude? (i.e. why are ocean-type chinook associated with lower latitudes (the Oregon coast and California), and the stream-type chinook with higher latitudes (greater than 56°N)?).
2. In rivers where both ocean- and stream-type chinook are present (i.e the Fraser R. and the Columbia R.), why do ocean-type typically inhabit the lower reaches, while stream-type inhabit the upper reaches?
3. Why do chinook salmon typically begin their seaward migration between the months of February and May?
4. Why do chinook juveniles migrate mostly at night?

5. Why do juveniles typically move from regions of slower to swifter stream currents as they grow?

Chapters 2 and 3 address questions (1) and (2), and static optimization models are constructed to account for selective pressures that shape migration timing. Sensitivity analyses are preformed to observe how migration timing varies with both freshwater "growth opportunity" (related to latitude), and migration distance. Other model parameters are varied to examine whether the models yield sensible results.

Chapter 4 introduces seasonality into an model. Seasonality is shown to affect both the time of year and year of migration. Hence life history type (ocean- or stream-type) may be influenced by seasonal fluctuations of temperature and its related variables: growth opportunity, predation, and stream velocity.

In Chapter 5, I develop an optimal control model that is able to address both seasonal and diurnal migration timing, (3) and (4), as well stream velocity selection, (5). This model treats swimming velocity and current velocity as control variables (also known as decision variables). The sum of these variables gives migration velocity. The advantage of this model over the previous models, is that migration and feeding decisions are made on a continuous basis, and—in this respect—is more realistic.

Chapter 6 outlines the model analysis, and gives the basic mathematical results along with their biological interpretation. The importance of the "switching functions" is discussed, and is described in terms of the marginal increase in fitness with respect to displacement. Two important behaviors are identified that comprise an optimal migration strategy, and

fall into the categories of (a) predator avoidance and feeding, and (b) active migration. These results are quite general.

In Chapter 7, fluctuations in light intensity and current velocity are considered. Their influence on the optimal migration strategy is quantified by comparison to a simplified, autonomous (time does not enter the differential equations explicitly) version of the dynamic optimization model.

Appendix D contains outlines of the algorithms used to construct numerical solutions to the dynamic optimization model. The other appendices contain detailed information on model analysis I deemed too technical to be included in the main text.

CHAPTER 2 A HEURISTIC MODEL OF AGE AT MIGRATION

A heuristic model of optimal age at migration developed in this chapter includes numerous simplifying assumptions, but strives for general biological insight. The advantage of such assumptions is that parameter sensitivity can be obtained over an entire parameter range without resorting to numerical schemes. Also, the resulting optimization problem will be straightforward: static and one dimensional. However, the disadvantages can be many, depending on the specific question asked, and it is possible to "get the right answer for the wrong reason." The more complex models developed in later chapters are designed to expose some of these errors.

Why use a simple heuristic model, when a more complex one may better capture reality? One reason is that the results of complex models can be difficult to interpret. The heuristic model is developed to build intuition about the survival and reproductive tradeoffs associated with several habitat variables including stream velocity, migration distance, temperature, and growth. The more complex models of later chapters do not reveal their secrets easily—even though general relationships may exist, they are difficult to uncover. A simple model may offer insight into these more complex and mathematically cumbersome models. Where the complex models appear to give a "counter-intuitive" result, a heuristic model may show that the result follows from basic assumptions.

2.1 Model Development

The model contains parameters and state variables included to address questions about latitude and migration distance gradients in age at migration. It consists of two state equations, governing the change in weight and migration distance; a control or "decision" parameter—age at seaward migration; and a fitness measure—expected reproduction. For simplicity, I assume that a juvenile has a very straightforward migration strategy: (i) initially it holds station, swimming against the river current; (ii) at some unspecified time, known as the age at migration or the "switching time," t_m, the juvenile migrates seaward in an average river velocity u, and with average swimming velocity, v; (iii) the fish matures and returns to spawn at a fixed time, t_s. One important feature of this model is that migration distance enters explicitly, and it will therefore be possible to predict changes in optimal age as a function migration distances. Also, depredation is size-dependent and the benefits of delayed migration (increased migration survival) and the benefit of earlier migration (increased ocean growth) are both present.

TABLE 2.1 Assumptions of the heuristic model.

Assumption
Both ocean and freshwater growth are exponential
Temporal fluctuations of the environmental variables temperature, current velocity, predator density and search velocity, food abundance are ignored
Spawning time is fixed
Ocean survival is constant
Migration velocity is constant
Capture probability is a decreasing function of salmon weight. A predator's likelihood of capturing a juvenile decreases with increasing juvenile weight
Freshwater mortality is a result of depredation alone

TABLE 2.2 Heuristic model summary.

Maximize: $\max_{t_m} J(t_m) = -\int_{t_m}^{t_m + a/z} (\dot{x} + \zeta)\,\theta k(w)\,dt - \int_{t_m + a/z}^{t_s} \mu\,dt + \log(w(t_o))$

Subject to:

$$\dot{x} = \begin{cases} 0 & \text{if } 0 \le t < t_m \\ z & \text{if } t \ge t_m \end{cases}$$

$$\dot{w} = \begin{cases} r_f w & \text{if } 0 \le t < t_m + a/z \\ r_o w & \text{if } t_m + a/z \le t \le t_s \end{cases}$$

$$0 \le t_m \le t_s - a/z$$

TABLE 2.3 Heuristic model variables and functions.

variable or function	definition	variable or function	definition
t	time	t_m	age at migration
r_f	freshwater growth rate	t_s	spawning time
a	migration distance	$J(t_m)$	objective function
θ	predator density	$w(t)$	weight
μ	ocean mortality rate	$x(t)$	downstream displacement
ζ	predator search velocity	$k(w)$	capture probability
z	migration velocity	$S_f(t)$	freshwater survival probability
r_o	ocean growth rate	$S_o(t)$	ocean survival probability
$R(t_m)$	expected fecundity		

2.1.1 Growth

In freshwater and in the ocean, growth is exponential with parameters r_f and r_o respectively. Although exponential growth is unrealistic, the growth functions are mathematically convenient, each utilizing a single parameter only. Since growth is much greater in the ocean, I assume that $r_o > r_f$. The freshwater growth equation is

$$\dot{w} = r_f w \text{ with solution } w(t) = w_0 exp(r_f t), \text{ where } 0 \le t \le t_m, \tag{2.1}$$

and the ocean growth equation is

$$\dot{w} = r_o w \text{ with solution } w(t) = w_0 exp(r_f t_m)\, exp(r_o t), \text{ where } t_m < t \le t_s. \tag{2.2}$$

2.1.2 Survival

Freshwater survival is based on predator encounter rate and capture probability. The predator encounter rate is a product of predator density, θ, and the sum of migration velocity, $\dot{x}$, and predator search velocity, ζ:

$$\text{predator encounter rate} \;=\; (\dot{x} + \zeta)\,\theta. \tag{2.3}$$

I assume that during station holding, $\dot{x} = 0$, and during migration $\dot{x} = z$, where z is the sum of swimming and current velocity, hereafter called the migration velocity.

The capture probability, $k(w)$, is assumed to decrease with weight (*i.e.*, as the juvenile grows it becomes less susceptible to predators). Assuming that the probability of death due to predation in a time interval of length Δt is

$$Pr\{\text{death in } \Delta t\} \;=\; (z + \zeta)\,\theta k(w)\,\Delta t, \tag{2.4}$$

the probability that the fish is alive at time t, during freshwater residence, is

$$S_f(t) \;=\; exp\left(-\int_0^t (z + \zeta)\,\theta k(w)\,dt\right). \tag{2.5}$$

Assuming a constant ocean mortality rate, μ, ocean survival is given by

$$S_o(t) \;=\; exp\left(-\int_0^{t_m + a/z} (z + \zeta)\,\theta k(w)\,dt\right) exp\left(-\int_{t_m + a/z}^{t_s} \mu\,dt\right), \text{ where } t > t_m + \frac{a}{z}. \tag{2.6}$$

Although ocean mortality rate is known to vary with size, this relationship is ignored. Fortunately, the selective pressure for larger size at migration is still present in the capture

probability function, which can be modified to include early ocean mortality. Since freshwater depredation is most severe during migration, it may be optimal to delay migration until the juvenile is sufficiently large to escape high predation risk.

2.1.3 Fitness measure

The fitness measure is expected reproduction, $R = l \cdot m$, where l is the probability of survival from emergence to spawning, and m is the number of eggs produced by a female, assumed to be directly proportional to spawning weight, $w(t_s)$. Expected reproduction may therefore be written as

$$R(t_m) = S_f(t_m + \frac{a}{z})\, S_o(t_s)\, w(t_s)\,. \tag{2.7}$$

Although the scalar multiplier of spawning weight that yields the egg number has been ignored in (2.7), the optimal age at migration is unaltered by its absence.

2.1.4 Objective function

It is easier to work with the log of expected reproductive success than expected reproductive success itself,

$$J(t_m) = -\int_0^{t_m} \zeta\theta k(w)\, dt - \int_{t_m}^{t_m + a/z} (z+\zeta)\,\theta k(w)\, dt \qquad \text{(freshwater)} \tag{2.8}$$

$$-\int_{t_m + a/z}^{t_s} \mu\, dt \qquad \text{(ocean)}$$

$$+\log(w_s) + r_f t_m + r_o\left(t_s - t_m - \frac{a}{z}\right), \qquad \text{(fecundity)}$$

where J is the objective function. The goal is to maximize this objective function with respect to the age at migration, t_m.

2.2 Necessary conditions

In the usual way, I approach the optimization problem by finding first and second order necessary conditions satisfied by an optimum. There are three possibilities for an optimal age at migration, t_m^*: either it lies at one of the points 0 or t_s, or it lies somewhere between these points. In the latter case, the conditions $dJ(t_m^*)/dt_m = 0$, and $d^2J(t_m^*)/dt_m^2 \le 0$ must hold, where

$$dJ/dt_m = -(z+\zeta)\theta\cdot\left[k(w(t_m + a/z)) - k(w(t_m))\right] - \zeta\theta k(w(t_m)) + \mu + r_f - r_o \quad , \qquad (2.9)$$

and $$d^2J/dt_m^2 = z r_f w(t_m)\,\theta k_w(w(t_m)) - (z+\zeta) r_f w\left(t_m + \frac{a}{z}\right)\theta k_w\left(w\left(t_m + \frac{a}{z}\right)\right). \qquad (2.10)$$

Although much can be said about these equations without specifying an explicit form of the capture probability function (See “More general sensitivity results” on page 51), it is instructive to present two examples, incorporating different functions $k(w)$, and explore their salient, and potentially different features. The analysis will proceed by identifying the optimal age at migration as a function of model parameters, then varying the parameters to gauge the “sign” of their effect. The “sign” of an effect is deemed positive if increasing the parameter produces an increase in age at migration, and negative otherwise.

Of particular interest are the effects produced by varying the distance traveled to the ocean and the freshwater growth rate. Do the parameter sensitivities qualitatively match the observed patterns of geographical distribution (i.e. younger age at migration for shorter migration distances, and delayed migration for slower growing fish)? The results must be interpreted cautiously, since the sensitivities conducted do not generally consider covariation among the parameters. The sensitivities are conducted by varying one parameter, while holding the rest constant.

2.2.1 Example 1

In the first example I assume that the capture probability function is inverse to weight, $k(w) = \frac{1}{w}$, and that the initial weight is 1, $w_0 = 1$. The second order necessary condition is

$$d^2J/dt_m^2 = z\theta r_f w(t_m)\,(-w^{-2}(t_m)) - (z+\zeta)\,\theta r_f w(t_m+\frac{a}{z})\,(-w^{-2}(t_m+\frac{a}{z})), \quad (2.11)$$

$$= -z\theta r_f e^{-r_f t_m} + (z+\zeta)\,\theta r_f e^{-r_f t_m} e^{-r_f a/z} = \theta r_f e^{-r_f t_m}[-z + (z+\zeta)\,e^{-r_f a/z}] \le 0.$$

The second derivative of the objective function is therefore nonpositive only when

$$(z+\zeta)\,e^{-r_f a/z} - z \le 0.$$

The first order necessary condition is

$$dJ/dt_m = \frac{\theta}{w^*}\,((z+\zeta)\,(1-e^{-ar/z}) - \zeta) + (\mu + r_f - r_o) = 0,$$

yielding an optimal weight at migration of

$$w^* = exp(r_f t_m^*) = \theta \cdot \left(\frac{z - (z+\zeta) e^{-a r_f / z}}{r_o - \mu - r_f} \right). \quad (2.12)$$

In this case, the spawning time parameter, t_s has no influence on the optimal migration timing. This peculiarity will also be found in “More general sensitivity results” on page 51, and is an artifact of the exponential growth functions and assumed concavity of fitness function (with respect to t_m). Notice that, by (2.12), except for the freshwater growth parameter, if increasing a parameter produces a positive (negative) effect on optimal weight at migration, w^*, then it will also have a positive (negative) effect on optimal age at migration. I use the results frequently in the sensitivity analyses (TABLE 2.4).

TABLE 2.4 Parameter effects (example 1).

parameter	effect[a]
freshwater growth rate, r_f	+ or -
migration distance, a	+
predator density θ	+
ocean mortality rate, μ	+
predator search velocity, ζ	-
migration velocity, z	+ or -
ocean growth rate, r_o	-

[a] It is possible that the effect of the given parameter is 0 or has the indicated sign.

2.2.1.1 Effect of migration distance

By examining the first and second derivative of the objective function, I deduce that increasing a favors a delayed outmigration. When a is less than $\tilde{a} = -(z/r_f) \log(z/(z+\zeta))$, the fitness function decreases with outmigration timing,

and the optimal choice is immediate migration. When the migration distance exceeds $\tilde{a}$, the second derivative of the objective function is negative, and immediate migration is favored whenever

$$a \leq a_{crit} = -\frac{z}{r_f} \log \left(\frac{\theta z - (r_o - \mu - r_f)}{\theta \cdot (z + \zeta)} \right), \text{ (where } \theta z > r_o - \mu - r_f); \tag{2.13}$$

otherwise, delayed migration is favored. Note that when θz is only slightly larger than $r_o - \mu - r_f$ (relative to $(z + \zeta)\,\theta$), then a_{crit} is large, and the optimal strategy for all realistic values of a is immediate outmigration. When θz is much greater than $(r_o - \mu - r_f)$ (relative to $(z + \zeta)\,\theta$), then immediate migration is favored only for short migration distances.

The critical migration distance increases with ocean growth rate and predator search velocity; and it decreases with predator density, ocean mortality and freshwater growth rate. The influence of migration velocity on the critical migration distance is more difficult to determine.

As a gets larger, the optimal migration timing t_m^* reaches a limit, namely

$$\lim_{a \to \infty} t_m^* = \left(\frac{1}{r_f}\right) \log \left[\frac{\theta z}{r_o - \mu - r_f} \right]. \tag{2.14}$$

The effect of varying the migration distance is summarized below (FIGURE 2.1):

- For migration distances smaller that a critical distance, a_{crit}, selection favors immediate migration. This critical distance increases with ocean growth rate and predator search velocity, and decreases with predator density, ocean mortality and freshwater growth rate.

- As migration distance increases above the critical distance, delayed migration is favored, and migration timing increases with migration distance. As migration distance becomes large, the optimal migration timing approaches $r_f^{-1}\log\left[\theta z \cdot (r_o - \mu - r_f)^{-1}\right]$.

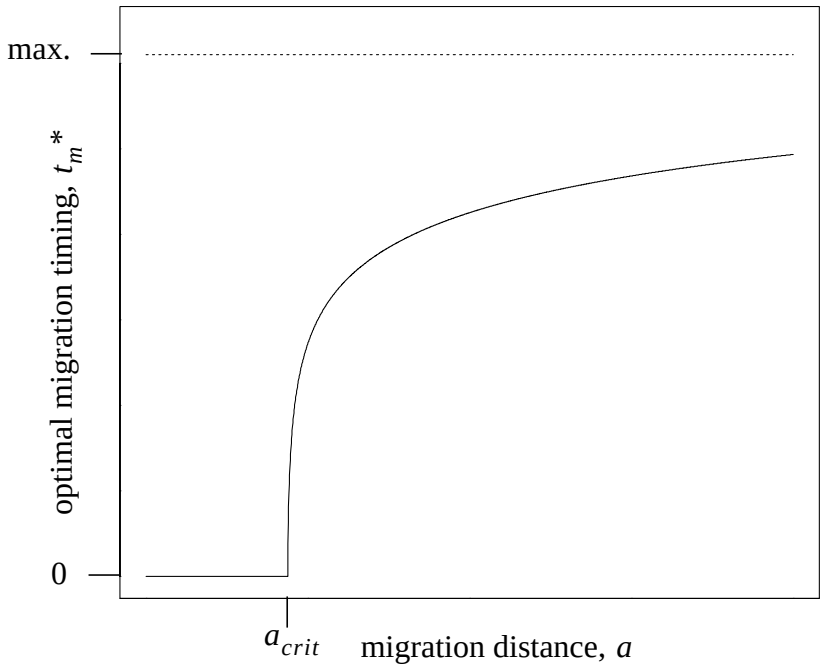

FIGURE 2.1 Optimal migration timing is an increasing function of migration distance. For short migration distances ($a < a_{crit}$), outmigration is immediate. As migration distance increases, optimal migration timing approaches a maximum.

2.2.1.2 Effect of migration velocity

Migration velocity has a more complicated effect. Increasing the velocity does not reduce the number of encounters due to the juvenile's movement, but *does* decrease the number of encounters due to active predator searching. To gauge how this effects migration timing, I examine the marginal change in migration timing with respect to migration velocity:

$$\frac{d}{dz}t_m^* = \frac{dw^*}{dz}\frac{e^{-r_f t_m^*}}{r_f} = \frac{\theta}{(r_o - \mu - r_f)}\left[1 - e^{-ar_f/z}\left(\frac{(z+\zeta)\,ar_f}{z^2} + 1\right)\right]\frac{e^{-r_f t_m^*}}{r_f}. \quad (2.15)$$

I am interested in values of z that make the numerator zero, (*i.e.*, where $\frac{d}{dz}t_m^* = 0$). This occurs where

$$\zeta = \frac{z^2 \cdot (e^{ar_f/z} - 1)}{ar_f} - z. \quad (2.16)$$

A plot of (2.16) shows that there are two possibilities: (a) when predator search velocity is less than or equal to $ar_f/2$, an increase in migration velocity produces later migration; (b) otherwise, there is a critical migration velocity below which an increase in migration velocity produces later migration, and above which an increase in migration velocity produces earlier migration (FIGURE 2.2).

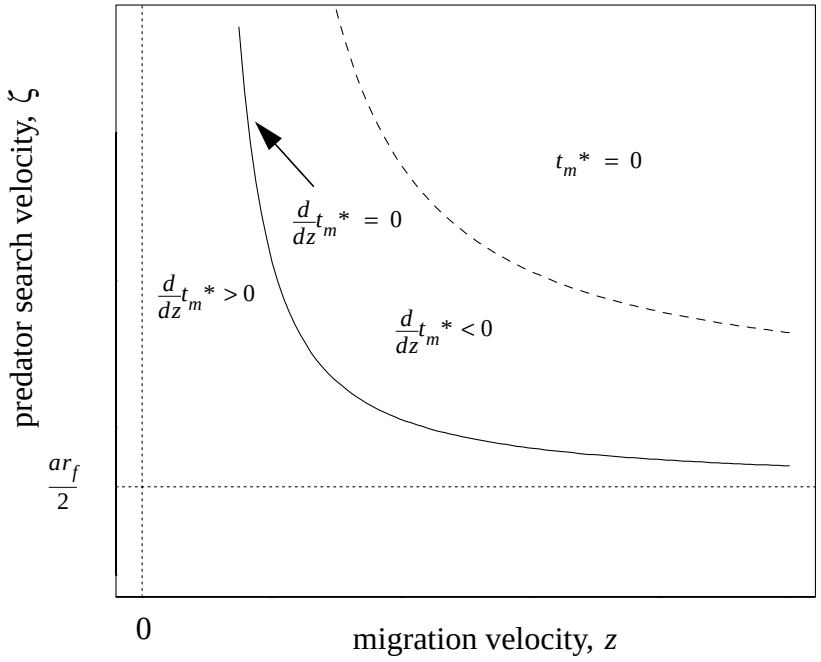

FIGURE 2.2 For predator search velocities less than $ar_f/2$, an increase in migration velocity results in later migration. When predator search velocities exceed $ar_f/2$, there is a critical migration velocity, below which increasing migration velocity results in later migration, and a above which, increasing migration velocity results in earlier migration. When predator search velocity and migration velocity fall above the dashed curve to the upper right, migration is immediate.

2.2.1.3 Effect of freshwater growth

The influence of freshwater growth is also more complex than that of migration distance. Migration timing may either increase or decrease with freshwater growth, depending on the values of the parameters. I strive to partition the parameter space into regions where migration time increases, decreases, and shows no effect.

For sufficiently small values of r_f, the objective function has negative slope over all points $t_m \geq 0$, and therefore, immediate outmigration is optimal.

As r_f increases beyond a critical value r_{crit}, migration is delayed. This critical growth rate satisfies the equation

$$\theta \cdot \left(\frac{z - (z+\zeta)\, e^{-a r_{crit}/z}}{r_o - \mu - r_{crit}} \right) = 1, \tag{2.17}$$

guaranteed to have a positive solution whenever $\theta\zeta > \mu - r_o$ (this is true since I assumed that $r_o - \mu - r_f > 0$, θ and ζ are both positive).

The critical freshwater growth rate increases with ocean growth rate and predator search velocity, and decreases with ocean mortality rate and migration distance. The influences of predator density and migration velocity are more difficult to determine.

The derivative of t_m^* with respect to r_f is given below.

$$exp\,(r_f t_m^*)\ (r_f \frac{d}{dr_f} t_m^* + t_m^*) = \theta \frac{(r_o - \mu - r_f)\ (z+\zeta)\, e^{-a r_f/z} a/z + z - (z+\zeta)\, e^{-a r_f/z}}{(r_o - \mu - r_f)^2}$$

$$\frac{d}{dr_f} t_m^* = \theta e^{-r_f t_m^*} \frac{[\,(r_o - \mu - r_f)\, a/z - 1]\ (z+\zeta)\, e^{-a r_f/z} + z}{(r_o - \mu - r_f)^2 r_f} - \frac{t_m^*}{r_f} \tag{2.18}$$

Setting this quantity equal to zero, and solving for θ produces

$$\theta = exp\left\{ r_f \frac{[\,(r_o - \mu - r_f)\, a/z - 1]\ (z+\zeta)\, e^{-a r_f/z} + z}{(r_o - \mu - r_f)\ (z - (z+\zeta)\, e^{-a r_f/z})} \right\} \cdot \frac{r_o - \mu - r_f}{z - (z+\zeta)\, e^{-a r_f/z}} \tag{2.19}$$

The function on the right of the above equation (viewed as a function of r_f) has two vertical asymptotes: one at $r_f = (-z/a) \log [\,z/(z+\zeta)\,]$ and the other at $r_f = r_o - \mu$.

As the freshwater growth, r_f, decreases toward $(-z/a)\log[z/(z+\zeta)]$, the R.H.S. of (2.19) approaches $+\infty$, and when r_f increases toward $r_o - \mu$, it also approaches $+\infty$ (FIGURE 2.3).

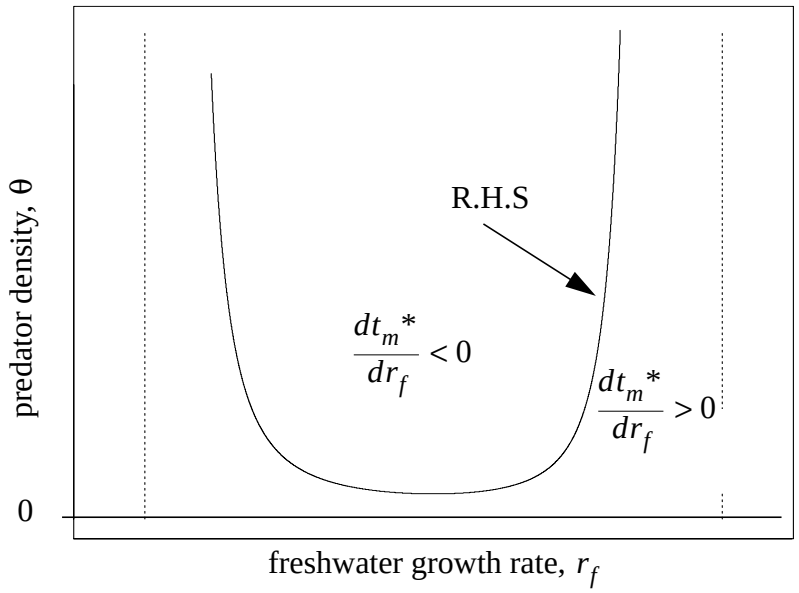

FIGURE 2.3 The curve above represents the values of predator density and freshwater growth rate that give zero marginal change of age at migration with respect to freshwater growth. Large values of predator density (above the curve) give a negative marginal change, small values (below the curve), a positive marginal change.

The results of this analysis are summarized in the three observations below (FIGURE 2.4):

- When freshwater growth rate is small, immediate migration is favored, because remaining in freshwater at a small size leads to higher mortality, and the fish must forego some ocean growth. Increasing the freshwater growth rate at this low level exerts greater pressure to take advantage of growing before enduring predation during migration; therefore, $dt_m^*/dr_f > 0$.

- When freshwater growth rate is sufficiently large (close to ocean growth rate – ocean mortality rate), there is little or no advantage of migrating to the ocean, and lifetime freshwater residence is best. Increasing the freshwater growth rate at this high level exters greater pressure to stay in freshwater, therefore, $dt_m^* / dr_f > 0$.

- For intermediate values of freshwater growth rate, neither immediate migration or lifetime freshwater residence is favored. The fish leave earlier to take advantage of a longer ocean growth period, and leave at a larger weight (meaning better freshwater survival). Increasing freshwater growth rate from this intermediate value favors earlier outmigration.

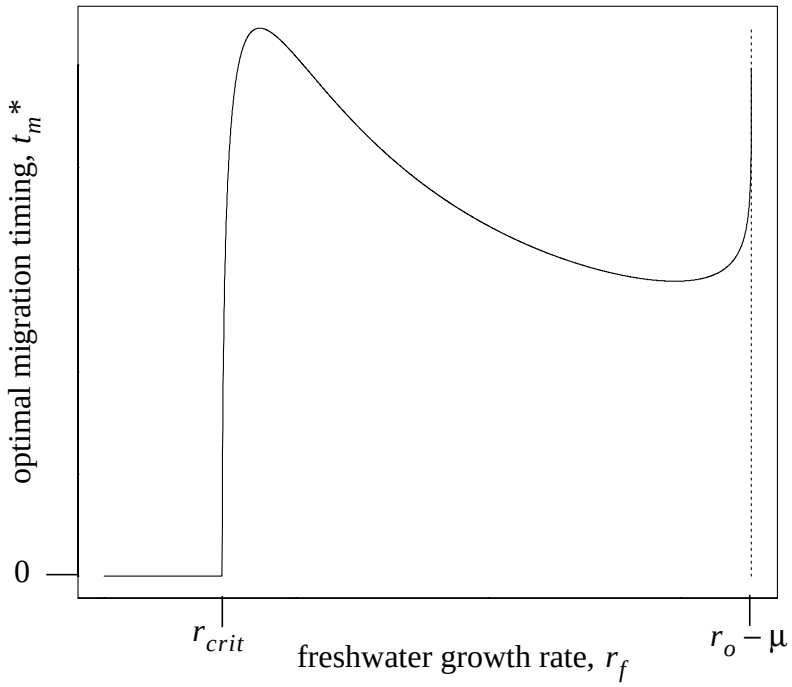

FIGURE 2.4 Optimal migration timing as a function of freshwater growth rate. For small freshwater growth rates (less than r_{crit}), immediate migration is favored. When freshwater growth rate approaches $r_o - \mu$, a lifetime freshwater residence strategy is favored. For intermediate freshwater growth rates, an increase in freshwater growth leads to earlier migration.

2.2.1.4 Effect of temperature

Knowing the effect of temperature hinges on knowing the relationship between the temperature and the model parameters, and the relationship between these temperature-influenced parameters and optimal age at migration. Freshwater temperature influences the freshwater growth rate and the predator search velocity, and can have a strong effect on the optimal migration timing. When food is scarce, increasing temperatures lead to a decrease in growth rate due to high metabolic costs, that the fish is unable to offset with a higher consumption rate. In a food rich environment, however, increasing temperatures

may lead to a higher consumption rate that surpasses the metabolic costs, leading to a higher growth rate. When the temperature is too high, it is lethal. Increasing the freshwater temperature increases the predator search velocity, which in turn favors an earlier migration (TABLE 2.4). Based on these two parameters, freshwater growth and predator search velocity, it is clear that the sign of the effect of temperature can be either positive or negative depending on the *level* of these parameters, and whether an increase in temperature leads to an increase or decrease in freshwater growth (FIGURE 2.5). Other factors influenced by temperature include migration velocity (a function of swimming performance and current velocity) and predator density, and these must be included for a comprehensive treatment of the influence of temperature.

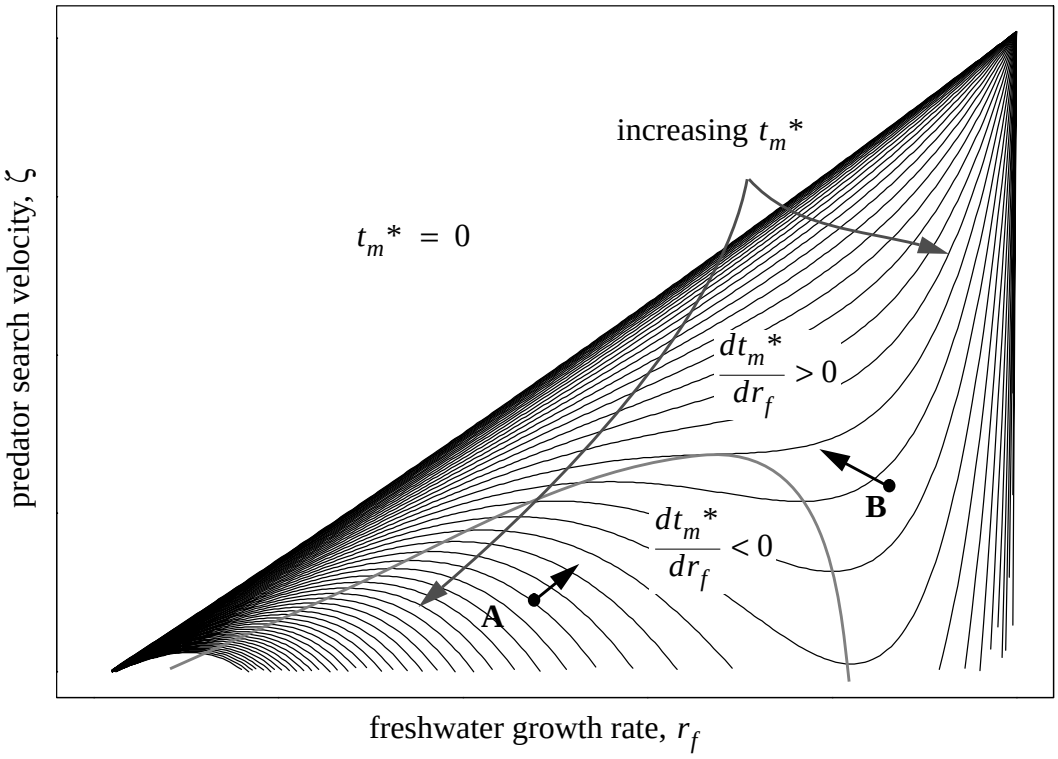

FIGURE 2.5 Isoclines of optimal age at migration. Below the dashed curve, age at migration declines with increasing freshwater growth rate; above the dashed curve, it increases. An increase in temperature produces a change in freshwater growth rate, Δr_f, in predator search velocity, $\Delta\zeta > 0$, and hence in migration timing Δt_m^*. $\Delta t_m^* < 0$ whenever $\Delta\zeta$ is large enough relative to Δr_f. $\Delta t_m^* < 0$ is guaranteed whenever $(\Delta t_m^* / dr_f)\, \Delta r_f < 0$ (see A and B above, the arrows represent the vector $(\Delta r_f, \Delta\zeta)$).

2.2.1.5 The effects of other parameters

The only parameters that do not show a monotonic effect on migration timing are freshwater growth rate and migration velocity. An increase in predator search velocity or an increase ocean growth rate make earlier migration more favorable. The former makes a longer freshwater residence time more costly due to decreased freshwater survival, and the

latter makes the ocean more attractive. Increasing migration distance, predator density, ocean mortality rate, makes a delayed (not immediate) outmigration optimal.

2.2.2 Example 2

It is not clear how robust the above sensitivity results are with respect to the choice of capture probability function. To examine robustness, I select a different capture probability function, and see how the sensitivity results compare with the first example (TABLE 2.5). This process, although it does not represent an exhaustive treatment, can offer some insight, especially in the case where the resulting sensitivities differ from the previous. For this second example, only the capture probability function will change—all other model characteristics will remain the same (see TABLE 2.1 & TABLE 2.2). Sensitivity analysis for a wider class of capture probability functions will be explored in the next paragraph (See “More general sensitivity results” on page 51).

TABLE 2.5 Parameter effects (example 2).

parameter	**effect**[a]
freshwater growth rate, r_f	+ or -
migration distance, a	+
predator density θ	+
ocean mortality rate, μ	+
predator search velocity, ζ	-
migration velocity, z	-
ocean growth rate, r_o	-
spawning time, t_s	-

[a] In all cases, it is possible for the effect to be 0, or to have the given sign.

Let $k(w) = -\log(w)$, and assume $e^{-1} < w < 1$, so that the function remains between 0 and 1 as a true probability. The second derivative evaluated at this capture probability function is

$$d^2J/dt_m{}^2 = -z\theta r_f + (z+\zeta)\theta r_f = \zeta\theta r_f, \tag{2.20}$$

demonstrating that J is a linear function of age at migration. This leaves three possibilities for an optimal strategy, depending on the slope of the line:

(i) Immediate migration, $t_m^* = 0$, if the slope is negative,

(ii) Lifetime freshwater residency, $t_m^* = t_s$, if the slope is positive,

(iii) Migration at ny age 0 and t_s, if the slope is zero.

I proceed by building an indicator function whose sign determines the optimal migration timing, namely $\Delta J = J(t_s) - J(0)$. When the indicator function, ΔJ, is positive, then $t_m^* = t_s$, when it is negative, then $t_m^* = 0$.

$$\Delta J = J(t_s) - J(0) = \int_0^{t_s} \zeta\theta \log(w(t))\, dt + \log(w_0) + r_f t_s \tag{2.21}$$

$$-\left[\int_0^{a/z} (z+\zeta)\theta \log(w(t))\, dt - (t_s - a/z)\mu + \log(w_0) + r_f a/z + r_o(t_s - a/z)\right]$$

$$= \theta\zeta \cdot \left(\log(w_0)\, t_s + \frac{r_f t_s^2}{2}\right) - (z+\zeta)\theta\left(\log(w_0)\frac{a}{z} + \frac{r_f}{2}\left(\frac{a}{z}\right)^2\right) + \left(t_s - \frac{a}{z}\right)(r_f + \mu - r_o)$$

Assuming that $w_0 = e^{-1}$, we obtain

$$\Delta J = \left(\frac{r_f t_s^2}{2} - t_s\right)\theta\zeta - \left(\frac{r_f}{2}\left(\frac{a}{z}\right)^2 - \frac{a}{z}\right)(z+\zeta)\,\theta + \left(t_s - \frac{a}{z}\right)(r_f + \mu - r_o)\,. \qquad (2.22)$$

To insure that $k(w) \geq 0$, I stipulate that

$$-\log\left(e^{-1}e^{r_f t_s}\right) = 1 - r_f t_s \geq 0. \qquad (2.23)$$

I also must assume that the duration of the ocean-ward migration is less than or equal to the life-span of the fish, *i.e.*,

$$\frac{a}{z} \leq t_s. \qquad (2.24)$$

2.2.2.1 Effect of migration distance

As in example 1, age at migration increases with migration distance. Migration distance is allowed to vary between 0 and $t_o z$ only, so that constraint (2.24) is satisfied.

Migration distance zero. When the migration distance is zero, the indicator function is

$$\Delta J|_{a=0} = \left(\frac{r_f t_s^2}{2} - t_s\right)\theta\zeta + t_s \cdot (r_f + \mu - r_o)\,,$$

a parabola in t_s which is negative between $t_s = 0$ and $t_s = t'$, and positive for $t_s > t'$, where

$$t' = \left[1 + \frac{(r_o - \mu - r_f)}{\theta\zeta}\right]\frac{2}{r_f}. \qquad (2.25)$$

Using (2.23), and the assumption that ocean growth rate exceeds the sum of the ocean mortality and freshwater growth rate, (*i.e.*, $(r_o - \mu - r_f) > 0$), the spawning time is guaranteed to lie between 0 and t', and therefore the indicator function is negative, making immediate migration optimal.

Migration distance at maximum. When $a = t_s z$, the indicator function is

$$\Delta J|_{a = t_s z} = -\theta z t_s \cdot \left(\frac{r_f t_s}{2} - 1\right) > 0,$$

making lifetime freshwater residence the optimal strategy.

General relationship. In general, the indicator functions defines a parabola in a that opens downward, with its vertex at a value too great for a to attain under constraints (2.23) and (2.24), namely

$$a_{vertex} = \frac{z}{r_f}\left[\frac{r_o - \mu - r_f}{(z + \zeta)\,\theta} + 1\right].$$

Thus, the indicator function is monotonically increasing from $a = 0$, where immediate migration is optimal to $a = t_s z$, where lifetime freshwater residence is optimal. For some migration distance between these two values, a_{crit}, the indicator function is zero and both strategies are optimal (FIGURE 2.6).

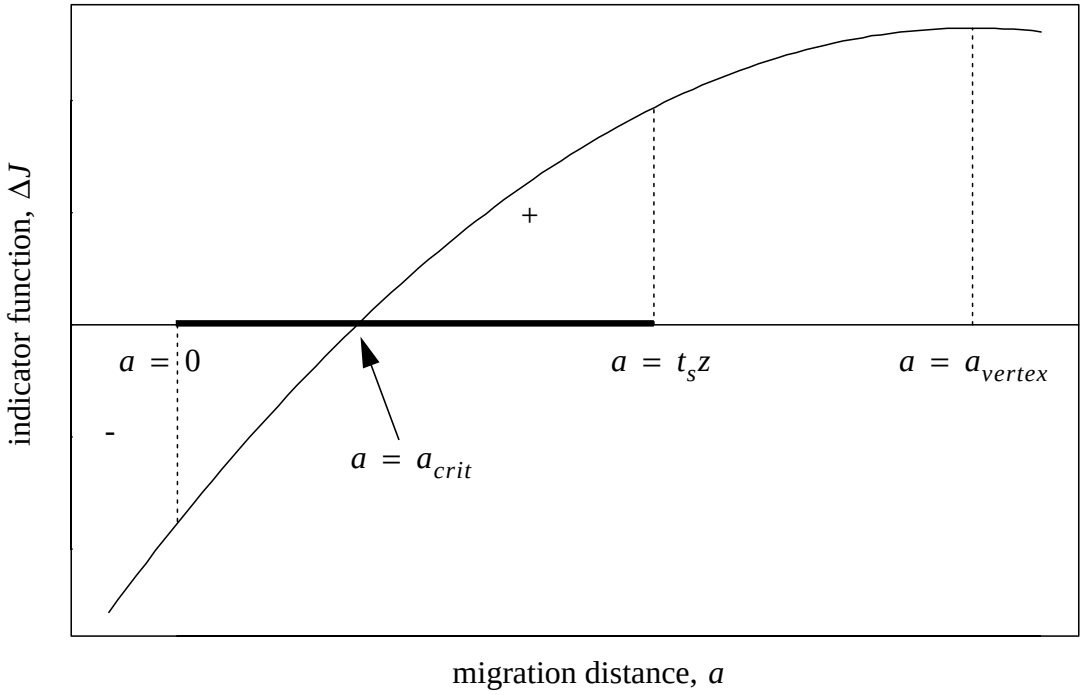

FIGURE 2.6 The indicator function increases with migration distance. Migration distance is constrained to lie between 0, where $\Delta J < 0$, and $t_s z$, where $\Delta J > 0$. For values of the migration distance less than a_{crit}, immediate migration is optimal; otherwise, lifetime freshwater residence is optimal. The migration distance at the vertex violates the constraint on a.

2.2.2.2 Effect of freshwater growth

Next, I investigate the effect of freshwater growth rate. The indicator function is a linear function of freshwater growth rate whose slope can be positive, zero, or negative depending on the value of the parameters. I show that the effect of freshwater growth rate on age at migration can be positive or negative, depending on the value of migration distance.

Null cline analysis. It is helpful to examine the null cline of the indicator function, (i.e. the values of the parameters making the indicator function zero). Notice that the indicator function is zero whenever

$$r_f = \left[\frac{-\frac{a}{z}\left(r_o - \mu + (z+\zeta)\,\theta\right) + t_s\left(\theta\zeta + (r_o - \mu)\right)}{-\frac{(z+\zeta)\,\theta}{2}\left(\frac{a}{z}\right)^2 + \left(t_s - \frac{a}{z}\right) + \frac{\zeta\theta t_s^2}{2}} \right]. \qquad (2.26)$$

The numerator of the R.H.S of (2.26) is positive when $a = 0$, is decreasing and linear in a, and has a root at the point

$$a = \frac{z t_s\left(\theta\zeta + (r_o - \mu)\right)}{\left(r_o - \mu + (z+\zeta)\,\theta\right)},$$

(which is less than $t_s z$, as required by (2.24)).

The denominator of the R.H.S. of (2.26) is a parabola that opens downwards when considered a function of a. When $a = 0$, the denominator is positive, and therefore it has two real roots: one positive, and the other negative. The positive root is the one of interest, since migration distance is assumed positive.

There are two possibilities: (a) the root of the denominator exceeds the root of the numerator, or (b) it does not. In the case of (a) increasing r_f can have a negligible effect on migration timing or increase it (FIGURE 2.7). In the case of (b), increasing r_f can have a negligible effect on migration timing, or decrease it (FIGURE 2.8).

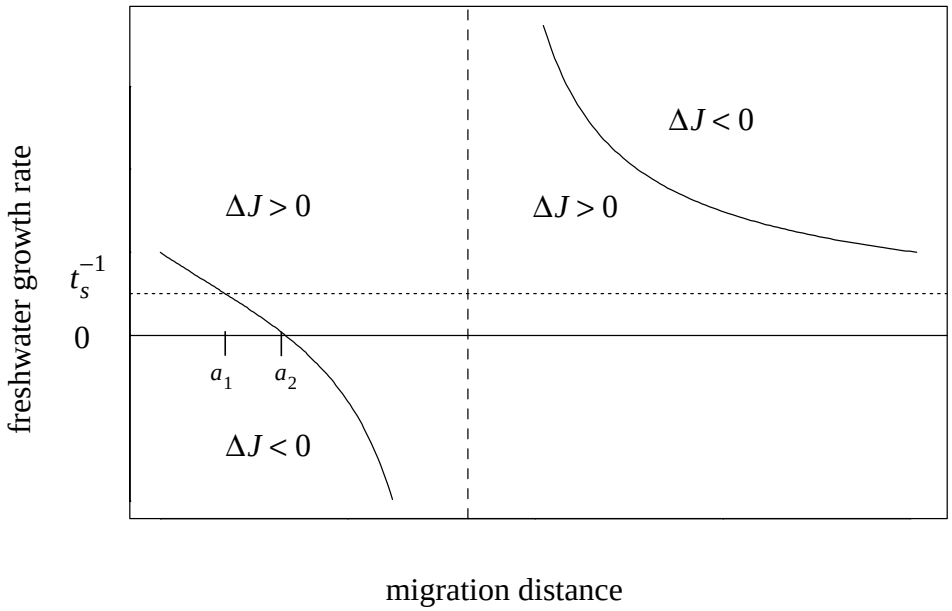

FIGURE 2.7 Null cline of the indicator function when the root of the denominator exceeds the root of the numerator in (2.26). For values of migration distance less than a_1, immediate migration is optimal, regardless of r_f. When migration distance is between a_1 and a_2, immediate migration is optimal for small values of r_f, and lifetime freshwater residence is optimal for larger values of r_f. When migration distance exceeds a_2, only lifetime freshwater residence is optimal.

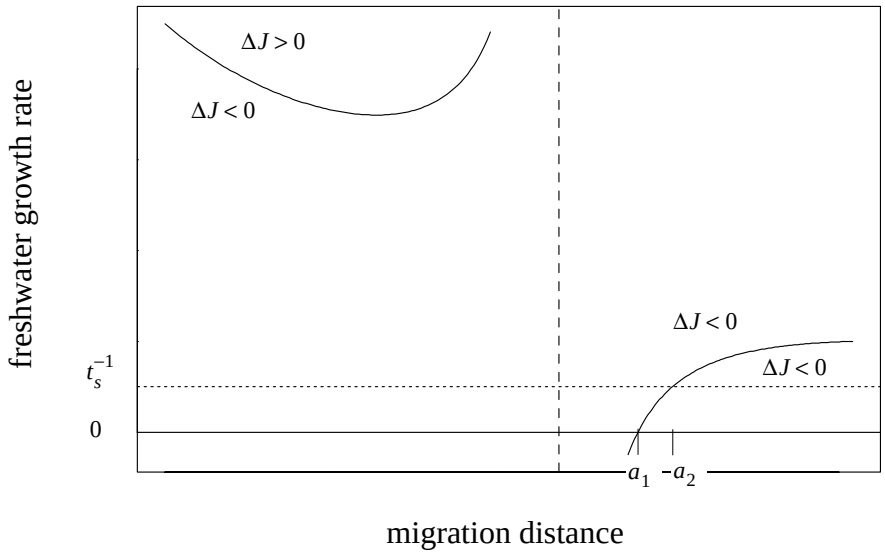

FIGURE 2.8 Null cline of the indicator function when the root of the numerator exceeds the root of the denominator in (2.26). When migration distance is less than a_1, immediate migration is optimal; when it is greater than a_2, lifetime freshwater residence is optimal. In both of these cases, changing r_f. does not influence the optimal strategy. However, when the migration distance is between a_1 and a_2, increasing r_f. can change the optimal strategy from lifetime freshwater residence to immediate migration (negative effect).

2.2.2.3 Effect of predator density

The indicator function is a linear function of predator density. When predator density is zero, the indicator function is

$$\Delta J|_{\theta = 0} = -(t_s - a/z)\ (r_o - r_f - \mu)\,,$$

and is therefore negative since and both $(t_s - a/z)$ and $(r_o - r_f - \mu)$ are assumed positive. Only when the slope of the line defined by ΔJ and θ is positive, is it possible for lifetime freshwater residence to be optimal (i.e. $\Delta J > 0$); otherwise, the indicator function is negative over its entire range, making immediate outmigration optimal over all values of θ. Therefore the effect of θ on age at migration is either negligible or positive.

2.2.2.4 Effect of predator search velocity

The indicator function is a linear function of predator search velocity, ζ, with slope

$$slope = \left[\frac{r_f t_s^2}{2} - t_s - \frac{r_f}{2}\left(\frac{a}{z}\right)^2 + \frac{a}{z}\right]\theta = (t_o - \frac{a}{z})\left[\frac{r_f}{2}(t_s + \frac{a}{z}) - 1\right]\theta$$

$$\leq (t_s - \frac{a}{z})\,[r_f t_s - 1]\,\theta \leq 0.$$

Therefore, increasing the predator search velocity can only lower the indicator function, and consequently, has a nonpositive effect on age at migration.

2.2.2.5 Effect of migration velocity

I next examine how increasing the migration velocity, z, changes the migration timing. Considering ΔJ a function of z,

$$\lim_{z \to \infty} \Delta J = \left(\frac{r_f t_s^2}{2} - t_s\right)\theta\zeta + \theta a + t_s \cdot (r_f + \mu - r_o). \qquad (2.27)$$

The R.H.S. of (2.27) is a horizontal asymptote of ΔJ as a function of z. When z achieves its lower bound of a/t_s,

$$\Delta J|_{z = a/t_s} = -\left[\frac{r_f t_s^2}{2} - t_s\right]\theta z \geq 0. \qquad (2.28)$$

To determine the slope of ΔJ as a function of z, I take the derivative:

$$\frac{d(\Delta J)}{dz} = \frac{\theta r_f a^2}{2z^2} + \frac{a}{z^2}(r_f + \mu - r_o) + \frac{\theta\zeta r_f a^2}{z^3} - \frac{\theta\zeta a}{z^2}.$$

This equation provides two important pieces of information about ΔJ as a function of z. (1) as z decreases to zero, the third term on the R.H.S. dominates, and the derivative is positive; (2) there is only one value of z satisfying $\frac{d(\Delta J)}{dz} = 0$.

Note also that the horizontal asymptote always lies below $\Delta J|_{z = a/t_s}$.

$$\lim_{z \to \infty} \Delta J - \Delta J|_{z = a/t_s} = (\frac{r_f t_s}{2} - 1)\,\theta\zeta + (r_f + \mu - r_o) - a\theta\frac{r_f}{2} < 0$$

Piecing together these results leaves two possibilities: (a) lifetime freshwater residence is optimal for all values of z satisfying the constraint $z \geq a/t_s$ (FIGURE 2.9); and (b) as z increases from a/t_s, the optimal strategy switches from lifetime freshwater residence to immediate migration (FIGURE 2.10).

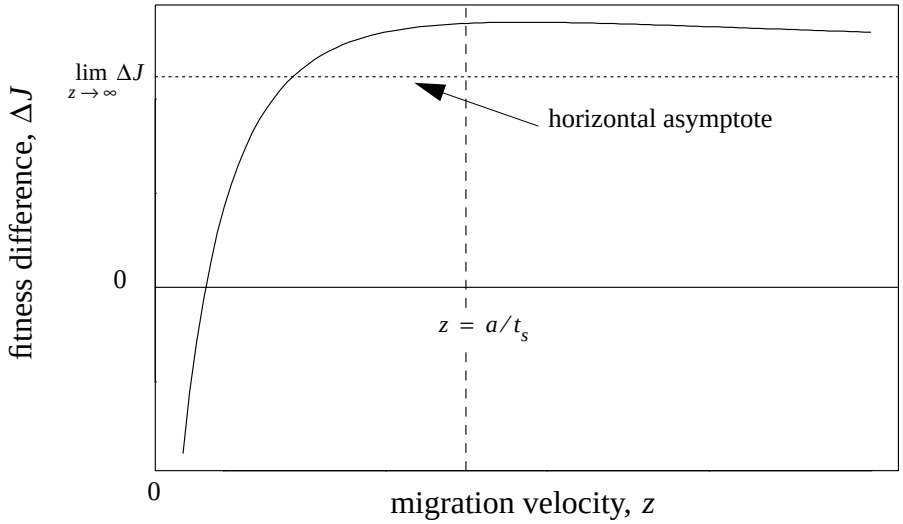

FIGURE 2.9 The fitness difference as a function of migration velocity. In this case the horizontal asymptote is positive, and the optimal strategy is lifetime freshwater residence for all values of migration velocity, z, satisfying $z \geq a / t_s$.

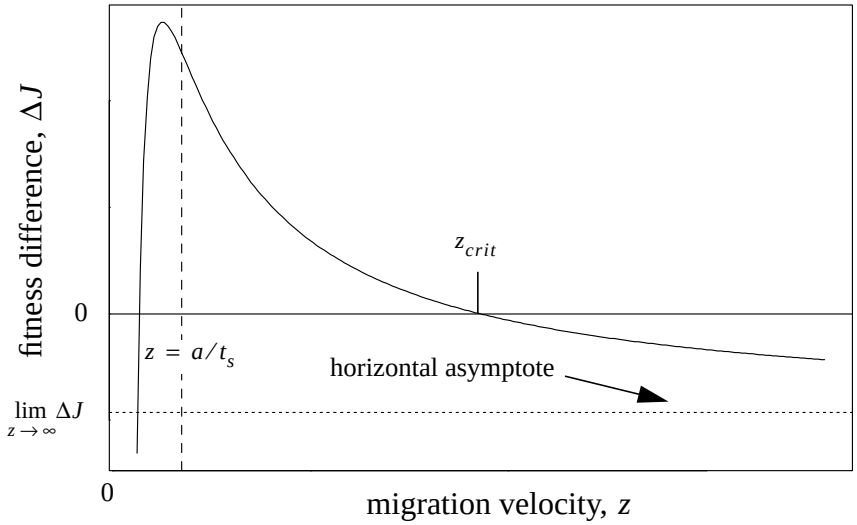

FIGURE 2.10 The fitness difference as a function of migration velocity. In this case the horizontal asymptote is negative, and the optimal strategy is lifetime freshwater residence for migration velocities between a / t_s and z_{crit}. If z exceeds z_{crit} , then immediate migration is optimal.

2.2.2.6 Effect of spawning time

The graph of ΔJ as a function of spawning time, t_s, defines a parabola that opens upwards, with its vertex at the point

$$t_{s,\,vertex} = \frac{(r_o - r_f - \mu)}{\zeta \theta r_f} + \frac{1}{r_f}. \qquad (2.29)$$

$t_{s,\,vertex}$ exceeds the upper bound on spawning time, r_f^{-1}, since the first term on the R.H.S. of (2.29) is positive, and therefore ΔJ decreases for $\frac{a}{z} \le t_s \le r_f^{-1}$. At the point $t_s = \frac{a}{z}$,

$$\Delta J\Big|_{t_s = \frac{a}{z}} = -\left(\frac{r_f}{2}\left(\frac{a}{z}\right)^2 - \frac{a}{z}\right)\theta z > 0,$$

which demonstrates that for small values of spawning time, the optimal strategy is lifetime freshwater residence. Increasing t_s to r_f^{-1} can lead to two possible outcomes: (a) ΔJ remains positive, or (b) it becomes negative. In either case, it is impossible to switch from the lifetime freshwater residence to the immediate migration strategy by increasing t_s. Therefore increasing the time of spawning can either produce no effect on age at migration or decrease it.

2.2.2.7 Effect of other parameters

The remaining parameters ocean mortality, μ, and ocean growth, r_o, are both linearly related to the indicator function. The indicator function increases with ocean mortality and decreases with ocean growth. When r_o is large enough, ΔJ is negative, and when small, can be either negative or positive. When increasing the ocean mortality rate, the only possible switch in strategy is from immediate migration to lifetime freshwater residence. Therefore age at migration increases with ocean mortality and deceases with ocean growth.

2.2.3 More general sensitivity results

In this more general sensitivity analysis, I focus on a class of capture probability functions, $k(w)$, that decrease with weight, and produce an optimal age at migration determined by the equation

$$-\theta \cdot (z+\zeta)\, k(w^* e^{a r_f / z}) + \theta z k(w^*) + \mu + r_f - r_o = 0, \tag{2.30}$$

and satisfies (2.10), i.e.

$$zk_w(w^*) - (z+\zeta)\, e^{ar_f/z} k_w(w^* e^{ar_f/z}) < 0, \tag{2.31}$$

where $w^* = w(t_m^*)$. This general class of capture probability functions includes the function form example 1, but not example2. Except for the case of the freshwater growth parameter, r_f, if an increase in the parameter produces an increase (decrease) in w^*, then it also produces produces an increase (decrease) in t_m^*. I take advantage of this fact below.

2.2.3.1 Effect of migration distance

The effect of migration distance on migration timing may be determined by examining the derivative of the optimal migration weight with respect to migration distance. Differentiating implicitly in (2.30),

$$-(z+\zeta)\, k_w(w^* e^{ar_f/z}) \left[w^* \frac{r_f}{z} e^{ar_f/z} + e^{ar_f/z} \frac{d}{da} w^* \right] + zk_w(w^*) \frac{d}{da} w^* = 0$$

$$\frac{d}{da} w^* = \frac{(z+\zeta)\, k_w(w^* e^{ar_f/z}) \left[w^* \frac{r_f}{z} e^{ar_f/z} \right]}{zk_w(w^*) - (z+\zeta)\, k_w(w^* e^{ar_f/z})\, e^{ar_f/z}} \tag{2.32}$$

The numerator of the R.H.S of (2.32) is negative since $k_w < 0$, and the denominator is negative by (2.10), therefore $\frac{d}{da} w^*$, and age at migration increases with migration distance.

2.2.3.2 Effect of ocean mortality

Next I examine how a marginal increase in the ocean mortality rate influences the migration timing. Differentiating (2.30) implicitly,

$$-(z+\zeta)\,\theta k_w(w^* e^{ar_f/z})\,e^{ar_f/z}\frac{d}{d\mu}w^* + \theta z k_w(w^*)\frac{d}{d\mu}w^* + 1 = 0$$

$$\frac{d}{d\mu}w^* = \frac{-1}{\theta z k_w(w^*) - (z+\zeta)\,\theta k_w((w^*)e^{ar_f/z})\,e^{ar_f/z}}. \tag{2.33}$$

By (2.10), the denominator is negative, and therefore increasing the ocean mortality increases the age at migration.

2.2.3.3 Effect of ocean growth

A richer ocean environment should lead to earlier and earlier migration, to take advantage of increased growth, the following equation shows that this is indeed the case:

$$\frac{d}{dr_o}w^* = \frac{1}{\theta z k_w(w^*) - (z+\zeta)\,\theta k_w(w^* e^{ar_f/z})\,e^{ar_f/z}}. \tag{2.34}$$

By (2.10), the denominator is negative, making the derivative of the age at migration with respect to ocean growth negative.

2.2.3.4 Effect of predator density

Increasing predator density increases the predator encounter rate in freshwater during both station holding and migration. The encounter rate is greatest during migration, and if predator density is large, delaying migration is the best strategy, as demonstrated below:

$$\frac{d}{d\theta}w^* = \frac{(z+\zeta)\,k(w^* e^{ar_f/z}) - zk(w^*)}{\theta z k_w(w^*) - (z+\zeta)\,\theta k_w(w^* e^{ar_f/z})\,e^{ar_f/z}}$$

Using (2.30) in the numerator,

$$\frac{d}{d\theta}w^* = \frac{(\mu + r_f - r_o)/\theta}{\theta z k_w(w^*) - (z+\zeta)\,\theta k_w(w^* e^{ar_f/z})\,e^{ar_f/z}} > 0. \quad (2.35)$$

Therefore migration timing increases with predator density.

2.2.3.5 Effect of predator search velocity

Increasing the predator search velocity increases the predator encounter rate due to predator movement uniformly over the juveniles freshwater residence. Delaying migration only serves to increase the amount of time the juvenile is at risk in freshwater, and therefore, an earlier migration is optimal, as demonstrated below:

$$\frac{d}{d\zeta}w^* = \frac{k(w^* e^{ar_f/z})}{z k_w(w^*) - (z+\zeta)\,k_w(w^* e^{ar_f/z})\,e^{ar_f/z}} < 0. \quad (2.36)$$

2.2.3.6 Effects of migration velocity and freshwater growth

Migration timing does not necessarily change monotonically with either migration velocity or freshwater growth rate as I discovered in Example 1 above. Their sensitivies depend on the choice of parameters, and the capture probability function.

2.2.3.7 Effect of freshwater growth on size at migration

Although the sign of the effect of freshwater growth on age at migration is dependent on the value of the model parameters (See “Effects of migration velocity and freshwater growth” on page 54), the sign of its effect on *size at migration* is easily determined, and

found to be positive. Taking the derivative of the optimal size at migration with respect to freshwater growth yields

$$\frac{d}{dr_f} w^* = \frac{(z+\zeta)\,\theta k_w (w^* e^{ar_f/z})\, w^* e^{ar_f/z} a/z - 1}{\theta z k_w (w^*) - (z+\zeta)\,\theta k_w (w^* e^{ar_f/z})\, e^{ar_f/z}} > 0. \tag{2.37}$$

This quantity is positive because the denominator is negative by (2.10), and the numerator is negative because the capture probability function decreases with weight. Therefore increasing freshwater growth rate increases the optimal *size at migration.*

2.3 Summary

The results of this chapter may be summarized as follows: increasing predator search velocity or ocean growth tends to decrease the optimal age at migration, while increasing migration distance, predator density, or ocean mortality rate tends to increase the optimal age at migration. Two of the model parameters, freshwater growth rate and migration velocity can have either a positive or negative effect on age at migration, depending on the value of the other parameters. Temperature influences both ocean and freshwater growth rate, and mortality rates, and since the effect of these variables on age at migration may counterbalance each other, it is not clear what its net effect is.

Except in the case of freshwater growth, the sign of a parameter's effect on optimal weight at migration is the same as the sign of its effect on age at migration (i.e early migration means smaller weight). Increasing freshwater growth increases optimal size at migration, but may at the same time, *decrease* optimal age at migration.

2.4 Discussion

What insight has been gleaned from this endeavor? One lesson is that some variable's influence, (i. e. migration distance, predator density, ocean mortality rate, ocean growth rate, predator search velocity), on age at migration is easily understood, while others are not (migration velocity and freshwater growth). Assuming the model correctly identifies the inherent tradeoffs associated with these variables, variables whose influence in not easily understood are connected to selective pressures that, in combination, both reward and punish early migration. For example, increasing freshwater growth diminishes the cost of early migration, providing an opportunity to begin ocean feeding sooner and with less cost during migration. On the other hand, delaying migration confers a survival advantage to the juvenile by decreasing migration mortality. These benefits are in competition with one another, tugging age at migration in opposite directions, and depending on the other parameters, either side can win the tug-o-war.

The model does predict an increase in age at migration with migration distance (assuming all else is equal), but its predictions on latitudinal gradient are less clear. Assuming the *hypothetical* relationships between latitude and the parameters in TABLE 2.6, there are influences of increasing latitude that favor earlier migration with respect to some parameters (predator density and ocean growth rate), and later migration with respect to others (ocean mortality rate and predator search velocity). As pointed out earlier a general pattern of decreasing freshwater growth rate with latitude, could lead to either earlier or later migration depending on the value of other parameters.

TABLE 2.6 Latitude and migration timing.

parameter	Hypothetical Influence of Latitude on parameter	Corresponding influence on age at migration[a]
freshwater growth rate, r_f	-	?
predator density θ	-	-
ocean mortality rate, μ	+	+
predator search velocity, ζ	-	+
migration velocity, z	?	?
ocean growth rate, r_o	+	-

[a] A question mark indicates that the sign of the influence is unknown (as predicted by the model), or no hypothetical relationship was assumed.

The “success” of demonstrating an increase in age at migration with migration distance must be interpreted cautiously, since it applies under the stipulation that “all else is equal.” In reality, of course, all else is seldom equal, and the relationship between migration and other model parameters must be understood—especially since local conditions of temperature, food abundance, current velocity, and predation risk, for example, can change radically with migration distance.

CHAPTER 3 MORE REALISTIC GROWTH AND FECUNDITY ASSUMPTIONS

In the previous chapter, I developed a heuristic model which assumed both ocean and freshwater growth were exponential, and that fecundity was directly proportional to size. However, in reality, growth is exponential—or at least nearly exponential—only for small young fish and tapers off as the fish grows. Moreover, fecundity is not usually found to be proportional to weight, but some fractional exponent of weight (Healey & Heard, 1984). What is gained by including more realistic assumptions? Analyzing and comparing a model that includes more realistic assumptions at this point could reveal what results from the heuristic model hinge on unlikely assumptions. I seek to understand how the sensitivity results derived in the last chapter hold up when confronted with more realistic growth and fecundity assumptions.

One of the drawbacks of including these more realistic assumptions is that the mathematics becomes more complicated. The heuristic model optimization could be carried out, in most cases, by examining first and second derivatives of the objective function. Unfortunately, for the objective function in this chapter, derivatives are not obtainable, and maximization must be accomplished through numerical schemes (Press *et al*., 1988). The simpler model revealed parameter sensitivities easily, requiring basic calculus only, and the influence of parameters could be readily determined over the entire

range of the parameter space. Here, for practicality, we must settle for knowing a parameter's influence over some restricted range of the parameter space.

Again, as in the previous chapter, the main focus will be on the relationship between age at migration, latitude and migration distance, although the effect of other variables will be considered as well. The parameter estimates will be based on various literature values or regressions on data found in the literature when possible; otherwise, reasonable values are assigned (TABLE 3.2). The maximization scheme used is based on functional values alone since derivative information is not available (Brent, 1973). It proceeds by fitting successive parabolas to the objective function, until the optimal age at migration is found to within a nominal error tolerance. Each objective function evaluation requires simultaneous numerical integration to determine weight and fitness, these are performed using either the fourth-order Runga-Kutta or Bulirsch-Stoer method (Press *et al*., 1988).

TABLE 3.1 Model assumptions.

Assumption[a]
Ocean and freshwater growth functions reflect diminishing returns
Fecundity is proportional to weight at spawning raised to a fractional exponent
Temporal fluctuations of the environmental variables temperature, current velocity, predator density and search velocity, food abundance are ignored
Spawning time is fixed
Ocean survival is constant
Migration velocity is constant
Capture probability is a decreasing function of salmon weight. A predator's likelihood of capturing a juvenile decreases with increasing juvenile weight
Freshwater mortality is a result of depredation alone

[a] The first two assumptions differ from the assumptions of the previous chapter.

TABLE 3.2 Model summary.

Maximize: $\underset{t_m}{}$ $J(t_m) = -\int_{t_m}^{t_m + a/z} \theta(\dot{x} + \zeta) k(w)\, dt - \int_{t_m + a/z}^{t_s} \mu dt + \log[m(w(t_s))]$

Subject to: $\dot{x} = \begin{cases} 0 & \text{if } 0 \le t < t_m \\ z & \text{if } t \ge t_m \end{cases}$

$\dot{w} = \begin{cases} g_f(w) & \text{if } 0 \le t < t_m + a/z \\ g_o(w) & \text{if } t_m + a/z \le t \le t_s \end{cases}$

$0 \le t_m \le t_s - a/z$

3.1 Development of more realistic relationships

3.1.1 Ocean growth

Both freshwater and ocean growth equations are assumed to follow a generalized von Bertalanffy growth model,

$$\dot{w} = \alpha w^{\phi} - \beta w, \tag{3.1}$$

where the R.H.S. represents the difference between anabolism (growth assimilation) and catabolism (respiration). Theoretically, the exponent ϕ assumes the value $2/3$, however, it is instructive to vary this quantity in the upcoming sensitivity analysis. As it varies from $2/3$ to 1, growth varies from the standard von Bertalanffy, which is limited, to exponential, which is unlimited. Thus, the parameter represents a bridge between ocean growth in the current chapter (limited growth), to that in the previous chapter (unlimited, exponential growth).

3.1.2 Freshwater growth

The freshwater growth function I consider here includes, handling time, food density, and metabolic costs:

$$g_f(w) = \frac{c\tau\rho\gamma(w)\,v}{1+\rho\gamma(w)\,h(w)\,v} - c\alpha_2 w^{\beta 2} v^{\eta} - c\alpha_1 w^{\beta 1}, \qquad (3.2)$$

where the first term on the R.H.S. represents rate of energy consumed, second and third terms represent rate of energy lost to active and standard metabolism respectively (Ware 1978). $\rho(t)$ represents the food density on the stream surface, and $\gamma(w)$, the width of the intersection between the reactive field cross section and stream surface. The fraction of the ration available for work and growth is τ. The handling time, $h(w)$, is the time required for a fish to apprehend and consume one calorie of food. The conversion factor, c, converts calories to grams.

One important characteristic of this growth function is that, like the von Bertalanffy growth function, growth is limited. As a fish in freshwater grows, it consume more and more food to offset its increased metabolic demand, otherwise its growth is very poor. The freshwater environment is relatively poor in food compared with the ocean environment and growth slows quickly after a boom (if food is available). Assuming the parameter estimates of TABLE 3.2, as weight becomes large the freshwater growth function is approximately

$$g_f(w) \cong c\tau\rho w^{0.345} v - c\alpha_2 w^{0.76} v^{\eta} - c\alpha_1 w^{0.624},$$

showing that the exponents of weight for the metabolic terms dominate the exponent of weight for the anabolic term. Therefore, as weight becomes large, growth tends to zero, (*i.e.*, growth is limited).

TABLE 3.3 Parameters and their estimates.

Parameter Description	Parameter or Relationship	Estimate	Data Source
standard metabolism $(\text{cal} \cdot \text{s}^{-1})$	α_1	3.646584×10^{-4}	Brett (1965)
	β_1	0.6239528	Brett (1965)
active metabolism $(\text{cal} \cdot \text{s}^{-1})$	α_2	3.651952×10^{-3}	Brett (1965)
	β_2	0.7609603	Brett (1965)
	η	2.360445	Brett (1965)
oxycalorific equivalent	q	$3.42\ \text{cal} \cdot \text{mg}^{-1}$	Webb (1974)
calories to grams conversion factor	c	$1.6949 \times 10^{-4}\ \text{g} \cdot \text{cal}^{-1}$	White & Li (1985)
swimming speed	v	$0.6\ \text{m} \cdot \text{s}^{-1}$	Brett (1965)
handling time	$h(w)$	$18w^{-0.69}\ \text{s} \cdot \text{cal}^{-1}$	Ware (1978)
reaction field	$\gamma(w)$	$0.02w^{0.345}/\sqrt{\pi}$ m	Ware (1978)
food density	ρ	$1\ \text{cal} \cdot \text{m}^{-2}$	
net food conversion efficiency	τ	0.7	Brett & Groves (1979)
distance from redd to estuary	a	613 km	
current speed	u	$1\ \text{m} \cdot \text{s}^{-1}$	
initial weight	w_0	3.38 g	
capture probability	$k(w)$	w^{-1}	
predator density	θ	$1\ \text{km}^{-1}$	
predator search velocity	ζ	$115\ \text{km} \cdot \text{yr}^{-1}$	
ocean growth rate $(\text{g} \cdot \text{yr}^{-1})$	$g_o(w)$	$25.870w^{2/3} - 0.7888w$	Parker & Larkin (1959)
ocean mortality rate	$\mu_o(w)$	$.316\ \text{yr}^{-1}$	Parker (1962)
fecundity	$m(w)$	$48.94w^{0.548}$	Healey & Heard (1984)

3.1.3 Fecundity

Studies confirm significant fecundity-size relationships within chinook populations (Galbreath & Ridenhour 1964; Healey & Heard 1984). Theoretically, the fecundity is

proportional to the cube of length, and using an allometric relationship, I relate fecundity to weight through the relationship

$$m(w) = a_m w^{b_m}. \tag{3.3}$$

TABLE 3.4 Parameter sensitivity.

parameter	parameter range	age at migration range (yr.)	effect	heuristic model effect
freshwater food density, ρ	1 to 10 $\mathrm{cal \cdot m^{-2}}$	1.0 to 4.5	+	+ or -[a]
freshwater swimming metabolism coefficient, α_2	1.826×10^{-3} to 5.478×10^{-3}	1.78 to .60	-	NA[b]
freshwater standard metabolism coefficient, α_1	1.823292×10^{-4} to 5.469876×10^{-4}	1.14 to .93	-	NA
migration distance, a	30 to 1500 km	.06 to 2.09	+	+
predator density, θ	.02 to 1.0 $\mathrm{km^{-1}}$	1.48 to 1.04	-	+
ocean mortality rate, μ	0.00 to 3.16 $\mathrm{yr^{-1}}$	1.02 to 1.35	+	+
predator search velocity, ζ	86.25 to 143.75 $\mathrm{km \cdot yr^{-1}}$	1.21 to .90	-	-
current velocity, u	0 to 3 $\mathrm{m \cdot s^{-1}}$	1.03 to 1.05	+	+ or -
initial weight, w_0	1.69 to 5.07 g	1.15 to .94	-	NA
spawning time, t_s	2.5 to 7.5 yr	1.00 to 1.05	+	+

[a] Assuming that the effect exponential freshwater growth parameter of the previous chapter may be compared to the freshwater food density of this chapter.

[b] NA indicates that no analogous parameter exists in the heuristic model, or it does exist but was not varied.

3.2 Parameter effects

3.2.1 Effect of food density

All else being equal, what effect does an increase of food density have on age at migration? There are two competing points of view:

1. When food density is larger, freshwater habitat is more attractive due to increased growth potential, and this should lead to delayed ocean migration.

2. When food density is larger, a juvenile will grow faster, outgrowing its predators more quickly. The juvenile optimally migrates earlier to take advantage of a longer ocean growth period.

Both of these hypotheses are short-sighted, and do not consider all of the factors at play. The first neglects the benefits of a longer ocean growth period, the second, the advantage of migrating at a large size to avoid being eaten. However, looking at these two hypotheses shows the countervailing selective pressures produced by a increase in food density, and the question is, “Which force is strongest?”

In this simplified case, where there are no seasonal effects on parameters considered, the first point of view prevails. Simply stated, the small increment in weight at spawning produced by an earlier migration does not compensate for the corresponding decrease in freshwater survival. It is possible to perturb parameters of the model so that hypothesis 2 wins out, but this required making the benefits of prolonged ocean growth unreasonably high (FIGURE 3.1).

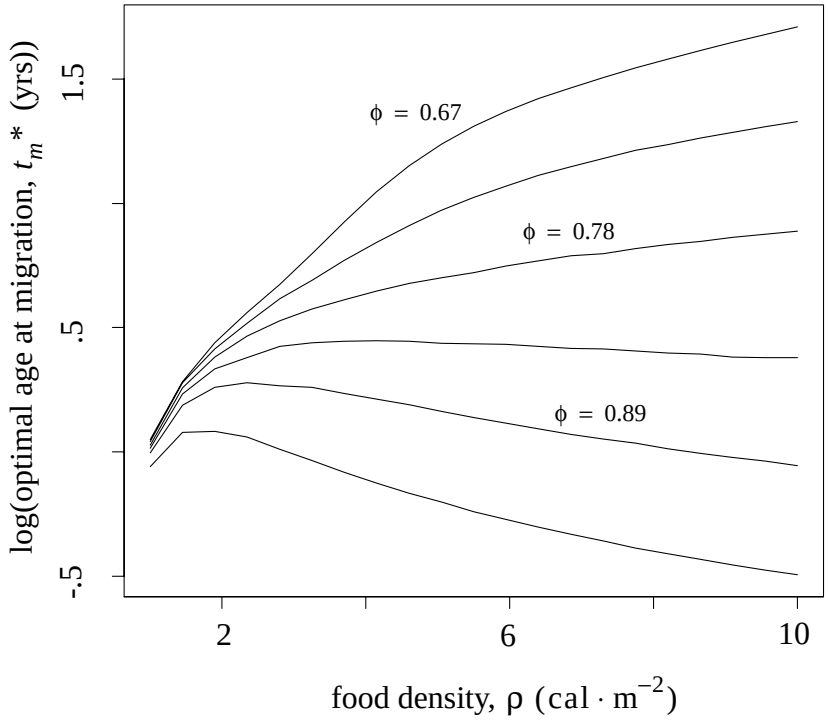

FIGURE 3.1 Optimal migration time can be forced to decrease with food density if the von Bertalanffy anabolism exponent, ϕ, is large enough. However, theoretically, and in practice, this exponent lies near 2/3, where time of migration decreases with food density.

3.2.2 Effect of migration distance

As in the case of the previous heuristic model, with exponential growth and fecundity linear with weight, age at migration increases with migration distance. This appears to be a robust result: when the migration corridor presents greater risk to the migrant (relative to the risk it experiences during station holding) it should invest a greater amount of time in growth before migrating.

3.2.3 Effect of predator density

Interestingly, the effect of predator density (+) is contrary to that predicted by the previous heuristic model (-). When predator density is larger, both the predation rate during station holding and during migration increases. There are two possible strategies for the juvenile:

1. Migration is delayed to decrease the risk during migration.
2. Migration is earlier to decrease the time at risk in freshwater, with some compensation through a longer ocean growth period.

Under the assumptions of exponential growth strategy 1 is favored, but when more realistic, limited growth assumptions are added, strategy 2 is favored. Under limited growth assumptions, the benefit to migration survival given by delayed migration does not counter balance the benefit of decreased time at risk during station holding and a prolonged period of ocean growth. This occurs, at least in part, because a limited freshwater growth curve does not offer the same benefit of prolonged freshwater residence offered by exponential growth (FIGURE 3.2).

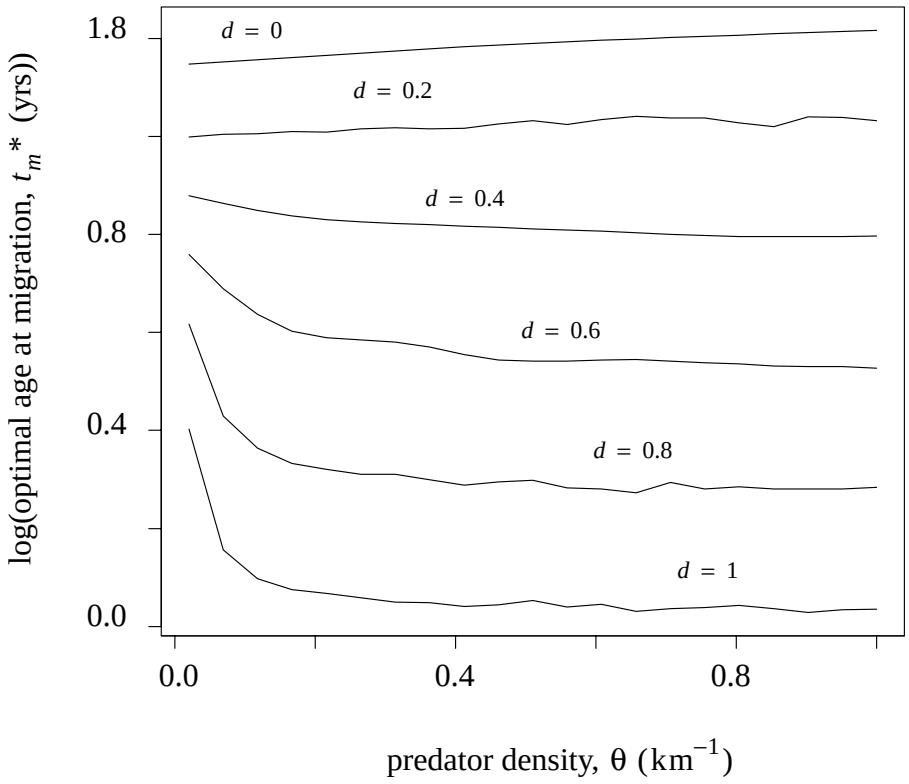

FIGURE 3.2 The log of age at migration as a function of predator density. As the terms leading to limited growth (metabolism, handling time) are reduced from their estimated values to zero, through the multiplier *d*, age at migration becomes and increasing function of predator density. This demonstrates how making the freshwater growth function limiting rather than exponential, changes the relationship between predator density and age at migration.

3.2.4 Effect of other parameters

The influence of freshwater growth rate (as determined by food intake, and metabolism), migration distance, ocean mortality rate, predator search velocity, and current velocity are all consistent with the heuristic case (TABLE 3.4).

3.3 Summary

Varying freshwater growth parameters reveals that as freshwater growth increases, so does optimal age at migration. The sign of this effect reverses, however, as the influence of limited ocean growth is decreased—becoming more exponential in nature. The effects of migration distance, predator ocean mortality rate, predator activity, current velocity, and spawning time are all consistent with the heuristic model. Predator density, however is inconsistent with the heuristic model: its increase results in a decrease in age at migration. This is partially, if not wholly, due to the introduction of the limiting effects of handling time and metabolism on growth. By reducing these limiting effects, it is possible to reverse the sign of the effect so that age at migration increases with predator density.

3.4 Discussion

Except in the case of predator density, adding more realistic growth and fecundity assumptions did not change the signs of the parameter effects. The effect of predator density changed from “+” in the heuristic case to “-” in the more general setting. I was able to show that by reducing the influence of metabolic cost terms and handling time, making freshwater growth less limited, it was possible to reverse the effect of predator density (from - to +) on age at migration, making it consistent with the heuristic model result (FIGURE 3.2). This was done while leaving the ocean growth and fecundity relationships unchanged, indicating that the reverse in the effect of predator density was, in part, if not wholly, attributable to the addition of limited freshwater growth. A simple biological argument makes sense of this result. When predator density is increased, risk of predation is greater in freshwater, and is most intense during the period of migration when the predator encounter rate is highest. If a resulting delay in migration is optimal, then the

benefit of growth during this delay had better offset the increased depredation risk during the delay. But the more limited freshwater growth becomes, the less likely this offset will occur, and therefore, as we discovered, the optimal age at migration actually decreases with predator density.

A similar argument shows why reducing the effect of limiting ocean growth results in a switch from a positive effect of freshwater growth on age at migration to a negative effect on age at migration (FIGURE 3.1). For if an increase in freshwater growth leads to earlier migration, then the increased ocean growth must offset the greater predation experienced during the earlier migration. As ocean growth becomes more limited, however, this offset becomes less likely, making age at migration increase with freshwater growth.

Although I present more realistic assumptions in this chapter, and, to some degree, illustrate the robustness of heuristic model results, there are still many simple assumptions present that certainly do not hold in reality, and these must be examined more closely. For example, how does introducing the effect of seasonally varying temperature influence the sensitivity results? By including seasonality, is the year of migration influenced as well as the season of migration? These questions are addressed in the following chapter.

CHAPTER 4 SEASONAL EFFECTS

Until now, I have held important environmental and biological variables such as current velocity, food availability, predator activity, and growth parameters, constant over time. In reality, this assumption does not hold. Mean daily temperature (averaged over many years), for example, follows a periodic function, and is known to influence growth and predator activity. Do these temperature fluctuations influence migration timing? Quantitative studies relating temperature and migration timing are scarce (Jonsson & Rudd-Hansen 1985; Bohlin *et al.*, 1993b), but show clear relationships. There is good reason that a relationship between temperature and migration timing exists, for smolt development is controlled by the temperature related variables such as growth rate and photoperiod, and the more developed a smolt, the more likely it will migrate (Dickhoff & Sullivan, 1987). Other seasonally related factors such as increasing stream velocity are also thought to promote downstream movement (Kjelson *et al*., 1982).

In this chapter, I include the influence of seasonality (TABLE 4.1), and as in previous chapters, focus on how migration timing affects individual fitness, and calculate the optimal age at migration based on hypothesized selective pressures. Including seasonality changes the nature of the objective function, producing local maxima that represent optimal within-year timing, and a global maximum that gives the optimal age at migration. The model suggests that temperature regime changes not only the optimal *within-year* migration timing but also, the optimal *year* of migration. As in the previous

chapters, I catalogue the effects of changing mean food availability, migration distance, and other parameters, and then compare the results to those of previous chapters.

TABLE 4.1 Model assumptions.

Assumption
Ocean and freshwater growth functions reflect diminishing returns
Fecundity is proportional to weight at spawning raised to a fractional exponent
Some temporal fluctuations of temperature related variables are considered: predator activity, food abundance, metabolic processes, food consumption[a]
Spawning time is fixed
Ocean survival is constant
Migration velocity is constant
Capture probability is a decreasing function of salmon weight
Freshwater mortality is a result of depredation alone

[a] This assumption differs from that of the previous chapter, where seasonality is ignored.

TABLE 4.2 Model summary.

Maximize: t_m

$$J(t_m) = -\int_{t_0}^{t_m + a/z} \theta(t)\ (\dot{x} + \zeta(t))\, k(w,t)\, dt - \int_{t_m + a/z}^{t_s} \mu dt + \log\left[m(w(t_s))\right]$$

Subject to:

$$\dot{x} = \begin{cases} 0 & \text{if} \quad t_0 \le t < t_m \\ z & \text{if} \quad t \ge t_m \end{cases}$$

$$\dot{w} = \begin{cases} g_f(w,t) & \text{if} \quad t_0 \le t < t_m + a/z \\ g_o(w,t) & \text{if} \quad t_m + a/z \le t \le t_s \end{cases}$$

$$t_0 \le t_m \le t_s - a/z$$

$$x(t_0) = 0$$

$$w(t_0) = w_0$$

TABLE 4.3 Main model variables and functions.

variable or function	definition	variable or function	definition
t	time	t_m	age at migration
$g_f(w, t)$	freshwater growth rate	t_s	spawning time
a	migration distance	$J(t_m)$	objective function
μ	ocean mortality rate	$w(t)$	weight
$\zeta(t)$	predator search velocity	$x(t)$	downstream displacement
z	migration velocity	$k(w, t)$	capture probability
$g_o(w, t)$	ocean growth rate	$\theta(t)$	predator density
t_0	time of emergence	w_0	initial weight
$m(w)$	fecundity		

4.1 Model development

Model changes include a new temperature dependent growth function and predation rate, and also a periodic mean daily temperature function. To sync the seasonal variation with the emergence date, time 0 will correspond to the beginning of a new year, and the emergence date is redefined as t_0 (TABLE 4.3).

4.1.1 Temperature dependent growth

The rates of food consumption, excretion, and metabolism are all influenced by temperature. And to capture this influence, I use the Fish Bioenergetics 2 model[1] (Hewitt & Johnson, 1992). This model is based on the balanced energy equation

$$\text{Consumption} = (\text{Metabolic Loss}) + (\text{Waste Loss}) + (\text{Growth}),$$

1. The Model 2 software package is available through the University of Wisconsin Sea Grant Institute. For more information, contact: Communications Office, University of Wisconsin Sea Grant, 1800 University Ave., Madison, WI 53705-4094. The software package runs only on IBM/compatibles.

or, using variables defined later in this chapter:

$$C = (R + S) + (F + U) + \Delta B.$$

Water temperature, fish size, energy density, and food availability are the primary factors affecting this energy budget. The computations are based on specific rates—grams of food per gram of predator per day.

4.1.1.1 Consumption

Consumption—the rate at which food is consumed by a fish—is determined by calculating a maximum consumption as an allometric function of weight, then scaling it by a parameter representing food availability and a function representing temperature dependent feeding activity. The basic equations for calculating consumption are:

$$C = C_{max} \cdot P \cdot f_c(T), \tag{4.1}$$

$$C_{max} = a_c w^{b_c}, \tag{4.2}$$

where C_{max} is the maximum specific feeding rate, w is fish weight, C is the specific feeding rate (consumption), P is a proportionality constant, a_c and b_c are allometric function parameters, T is water temperature, and $f_c(T)$ is the water temperature dependence function. Temperature dependent functions have been developed for several salmon species: chinook, coho, pink, and sockeye. The function is calculated using the Thornton & Lessem (1978) algorithm.

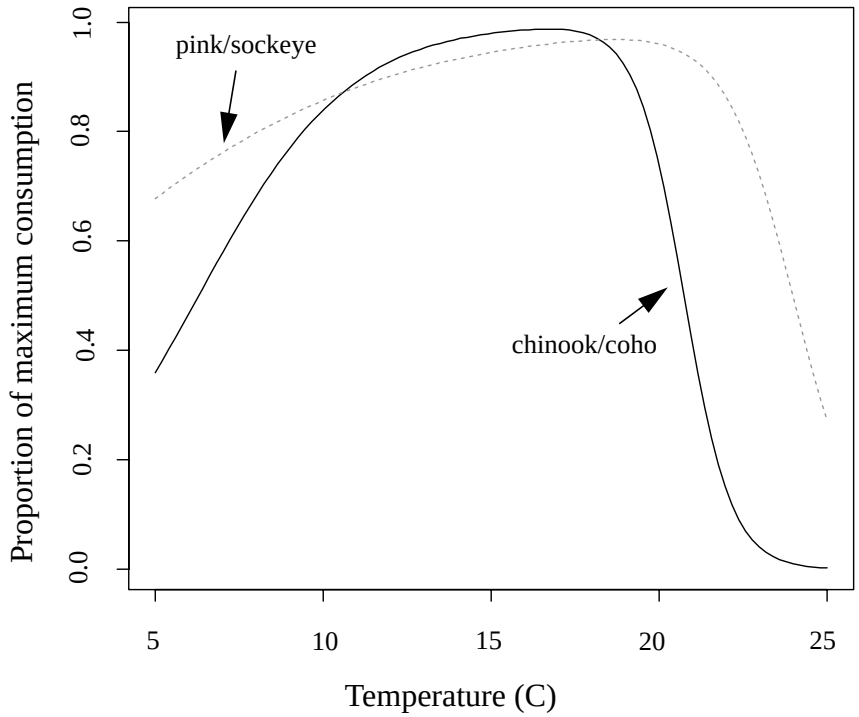

FIGURE 4.1 Temperature dependent food consumption functions for chinook/coho, and pink/sockeye (Hewitt & Johnson, 1992).

4.1.1.2 Respiration and specific dynamic action

Respiration is the amount of energy used by fish for metabolism—determined by calculating standard metabolism as an allometric function of weight, then increasing that value through a temperature dependent function and an activity factor. Specific dynamic action is then added to this quantity to determine the total metabolic rate. The equations are given by

$$R = a_r w^{b_r} f_r(T) \cdot activity \tag{4.3}$$

$$S = SDA \cdot (C - F), \tag{4.4}$$

where R is the specific rate of respiration, a_r and b_r are parameters of the allometric relationship for standard metabolism, $f_r(T)$ is the water temperature dependence function, $activity$ is the increment for active metabolism, S is the energy lost to specific dynamic action, SDA is the proportion of assimilated energy lost to specific dynamic action, and F is the specific rate of egestion.

4.1.1.3 Waste losses (egestion and excretion)

Energy not available for growth and not lost in metabolism is lost through egestion (fecal waste) and excretion (nitrogenous waste). The corresponding model equations are

$$F = PF \cdot C \tag{4.5}$$

$$U = a_u T^{b_u} \cdot exp(\gamma_u P) \cdot (C - F), \tag{4.6}$$

where F is the waste lost through egestion, PF represents the fraction of consumption that appears as fecal matter, and U is the waste lost through excretion. PF will change over time as the digestibility of diet changes.

4.1.2 Temperature dependent depredation rate

Recall that predation rate is governed by the movement of juveniles and the activity of the predators. In equation form, it is described as

$$\theta(t)\ (|\dot{x}(t)| + \zeta(t))\, k(w, t),$$

where $\theta(t)$ is the predator density, $\dot{x}(t)$ is the migration velocity, $\zeta(t)$ is the predator search velocity, and $k(w, t)$ is the capture probability. Predator search velocity, capture probability, and predator density are all functions of temperature. Until some temperature threshold is realized, increasing temperature leads to increased predator activity (and

hence predator search velocity and capture probability). Since capture probability scales predator search velocity, let us assume that the influence of temperature on predation rate is strictly through the capture probability function. To model this influence, I scale a maximum capture probability function by a temperature dependent function,

$$k(w,t) = k_{max}(w) \cdot f_{pred}(T(t)). \quad (4.7)$$

The temperature dependent scaling function is similar to the consumption function $f_c(T)$: it gauges the influence of temperature on predator consumption of salmon. Using this fact, I use the function $f_c(T)$, calibrated for the appropriate predator as the scaling function, $f_{pred}(T)$ (FIGURE 4.2).

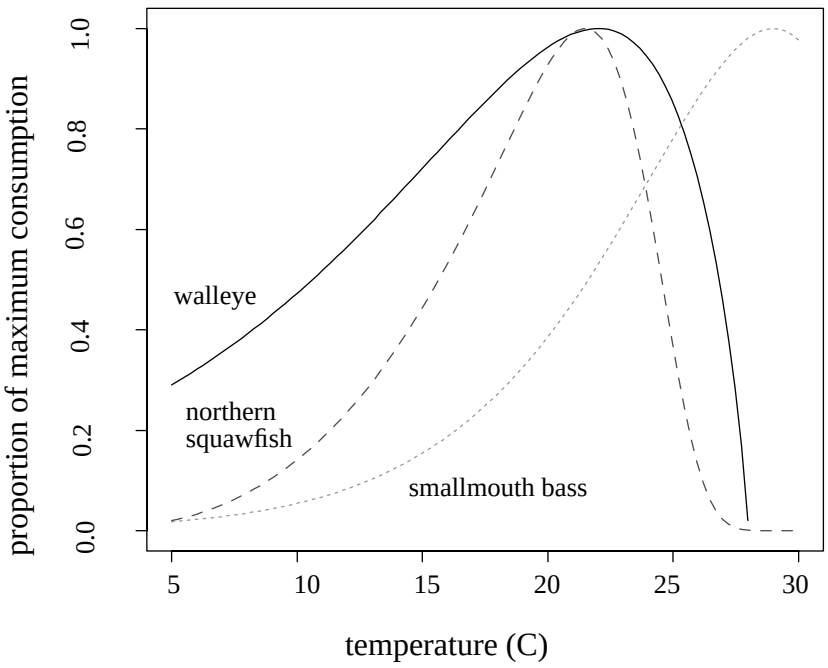

FIGURE 4.2 The proportion of the maximum consumption as a function of temperature for walleyr, smallmouth bass (Hewitt & Johnson 1992), and northern squawfish (Vigg & Burley, 1991).

4.1.3 Mean daily temperature data

Now that I have shown the importance of temperature on important biological variable, I proceed to show how the time series of daily water temperatures, measured at a fixed location, may be modeled. Since mean temperature patterns are periodic (with period of one year) and are linked to photoperiod, I choose to use the standard sine function:

$$T(t) \;=\; L + A \cdot \sin\left(\frac{2\pi\,(t-\phi)}{365}\right), \tag{4.8}$$

where L is a mean annual temperature level, A is the amplitude of the sin curve, and $2\pi\phi/365$ is the phase angle. The temperature function is fit to data using nonlinear least squares, and the fit is remarkably good for some data sets (FIGURE 4.3).

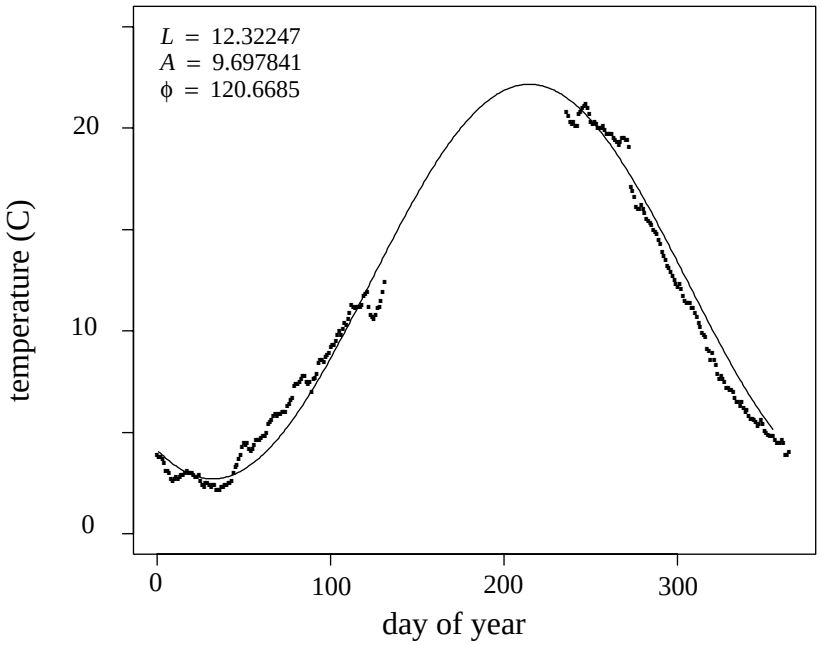

FIGURE 4.3 Nonlinear least squares fit of Snake River daily average temperature data recorded at Anatone Gage, Washington, 1975-1982 (Conner *et al.*, 1993).

4.2 Simulation results and sensitivity

Including seasonal effects changes the nature of the fitness vs. age-at-migration curve. In the absence of seasonal effects, the curve has one hump, and the optimal migration time changes continuously as a function of model parameters. When seasonal effects are present, each year contains a hump, and the top of each hump corresponds to a global or local maximum (FIGURE 4.4). The sensitivity analysis will focus on the influence of

parameters on both the year, and the time of year that fish migrate. Most parameters have a large influence on the year of migration, but little on the day of year.

TABLE 4.4 Functions, parameters, and their estimates.

Parameter Description	Parameter or Relationship	Units	Estimate	Data or Parameter Source
consumption	$C(t)$	d^{-1}	see reference (chinook)	Hewitt & Johnson (1992)
respiration	$R(t)$	d^{-1}	see reference (chinook)	Hewitt & Johnson (1992)
specific dynamic action	$S(t)$	d^{-1}	see reference (chinook)	Hewitt & Johnson (1992)
egestion	$E(t)$	d^{-1}	see reference (chinook)	Hewitt & Johnson (1992)
excretion	$U(t)$	d^{-1}	see reference (chinook)	Hewitt & Johnson (1992)
proportion of maximum capture probability	$f_{pred}(T)$		see reference (walleye)	Hewitt & Johnson (1992)
amplitude of temperature function	A	C	9.697841	Connor *et al.* (1993)[a]
mean level of temperature function	L	C	12.32247	Connor *et al.* (1993)
phase angle parameter of temperature function	ϕ	d	120.6685	Connor *et al.* (1993)
swimming speed	v	m/s	0.6	Brett (1965)
distance from redd to estuary	a	km	200	
current speed	u	m/s	1	
initial weight	w_0	g	3.38	
maximum capture probability	$k_{max}(w)$	none	w^{-1}	
predator density	θ	km^{-1}	1.5	
predator search velocity	ζ	$\text{km} \cdot \text{yr}^{-1}$	115	
ocean growth rate	$g_o(w)$	$\text{g} \cdot \text{yr}^{-1}$	$25.870w^{2/3} - 0.7888w$	Parker & Larkin (1959)
ocean mortality rate	$\mu_o(w)$	yr^{-1}	.316	Parker (1962)
fecundity	$m(w)$	eggs	$48.94w^{0.548}$	Healey & Heard (1984)
spawning time	t_s	yr	5.0	
emergence date	t_0	yr	1/6 (March 1)	

[a] The temperature function parameters where estimating using nonlinear regression on data contained in the indicated report.

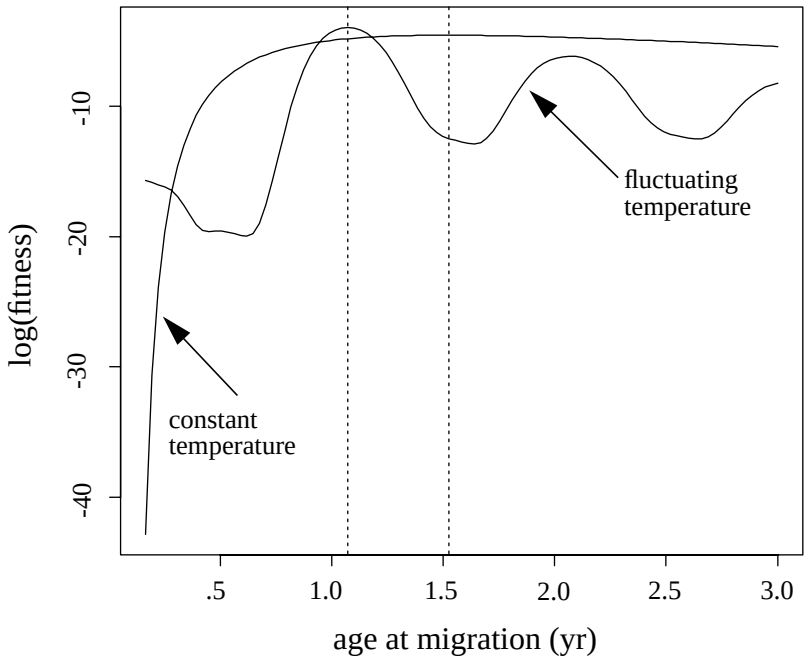

FIGURE 4.4 Comparison of log fitness vs. age-at-migration curves when temperature is constant and when it fluctuates. Notice that in the presence of fluctuating temperatures, the optimal migration occurs almost half a year earlier. The constant temperature model actually produces a poor strategy—migrate during the summer when predation is high.

TABLE 4.5 Sensitivity results.

parameter	parameter range	age at migration range (yr)	effect	effect (no seasonality)
food availability, *Pvalue*	0 to 1	.17 to 1.07	+	+[a]
migration distance, a	50 to 2000 km	.17 to 4.06	+	+
predator density, θ	.2 to 6.0 km^{-1}	1.07 to 1.07	0[b]	+
ocean mortality rate, μ	0.00 to .632 yr^{-1}	1.07 to 1.07	0	+
predator search velocity, ζ	86.25 to 143.75 $km \cdot yr^{-1}$	1.21 to .90	-	-
current velocity, u	0 to 3 $m \cdot s^{-1}$	1.03 to 1.05	+	+
initial weight, w_0	1.69 to 5.07 g	1.15 to .94	-	-
spawning time, t_s	2.5 to 7.5 yr	1.00 to 1.05	+	+
amplitude of temp. function A	7.27 to 12.12 C	1.07 to .17	-	NA[c]
mean level of temp. function, L	13 to 17 C	.25 to 1.09	+	NA
phase angle of temp. function, ϕ	60 to 180 d	.90 to 1.23	+	NA

[a] Although this food availability parameter is different from the one included in the case where seasonality is absent (previous chapter), in both cases, its increase results in greater food availability and hence greater growth.

[b] An effect of 0 indicates that no change in the age at migration was observed when varying the parameter over the given range.

[c] NA indicates that no analogous parameter exists in the model where seasonality is absent.

4.2.1 Effect of migration distance

In previous chapters I showed that increasing migration distance leads to a delay in migration. The same is true in the presence of fluctuating temperature. However, because the optimization problem admits several local minima, one of which may become a global minimum by changing migration distance, the optimal age at migration does not vary smoothly. In other words, the best time of year to migrate stays relatively fixed as migration distance varies, but when migration distance exceeds a certain threshold, optimal age at migration jumps discontinuously to the next year (FIGURE 4.5).

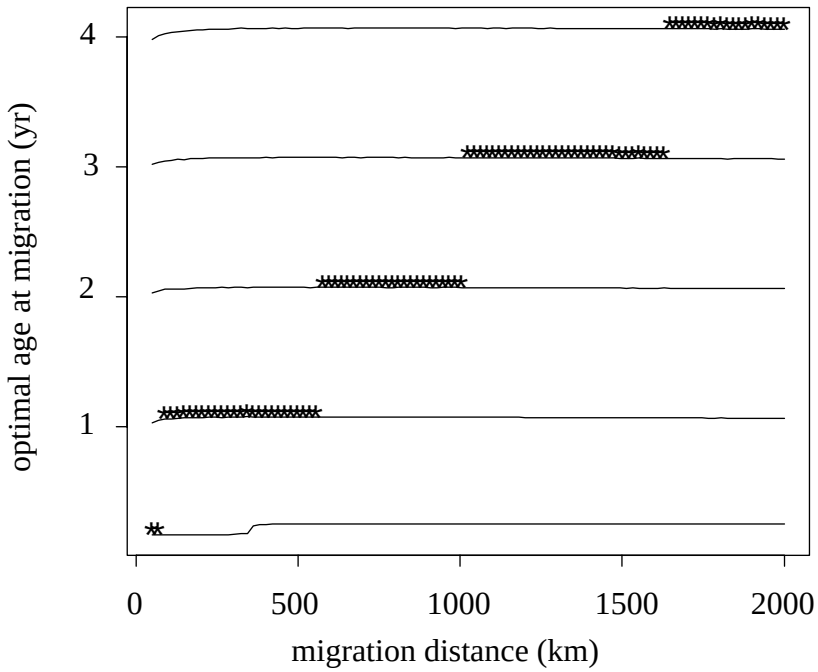

FIGURE 4.5 Influence of migration distance on optimal age at migration. The step function described by the curve of asterisks describes the global optimum age at migration, while the lines represent local optimums. Notice that the optimal age at migration leaps discontinuously between years as migration distance increases, but the optimal time of year for migration changes little.

4.2.2 Effect of food availability

The P-value is defined as the proportion of the maximum consumption that is influenced by food availability. As the P-value increases, so does food availability, and therefore I can gauge the qualitative influence of an increase in food availability by increasing the P-value. Using such a technique, I determined that an increase in food availability led to decrease in age at migration—the same result obtained in the absence of seasonality (TABLE 4.5).

4.2.3 Effects of temperature function parameters

Of the three temperature function parameters, the phase angle parameter, which defines the time of year at which temperature rises above the mean temperature, has the most influence, and its main influence is exerted on within-year migration timing. A rule of thumb, based on the many simulations, is that fish optimally migrate at a time when temperatures have reached a minimum, and predation risk is diminished (FIGURE 4.6). This time of minimum temperature is controlled by the phase angle parameter. As the amplitude of the temperature fluctuations diminishes, this relationship begins to break down (FIGURE 4.4). In contrast, depending on their levels, the amplitude and average temperature parameters mainly influence year of migration, affecting within-year migration timing to a lesser degree. Like migration distance, their influence yields a discontinuous movement of optimal age at migration from year to year.

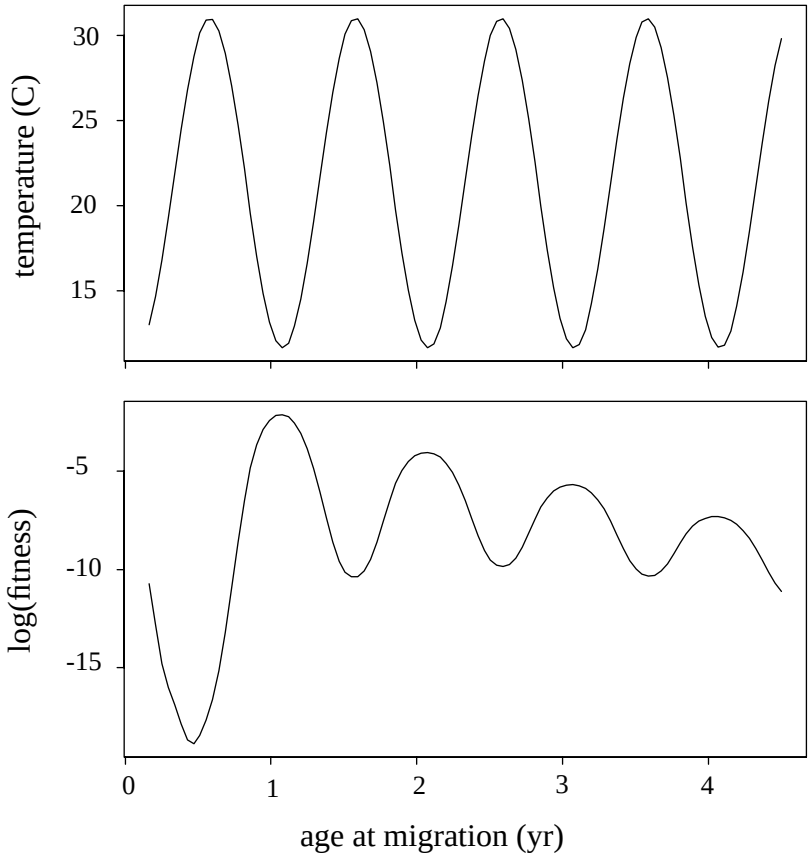

FIGURE 4.6 The effect of temperature fluctuations on the log(fitness) curve. The maxima correspond to the minima of the temperature curve. As the fish ages, the effect of temperature is less severe, owing to its larger size, and consequently, its greater ability to escape enemies.

4.2.4 Effect of other parameters

Largely, the remaining parameters show an influence on migration timing consistent with the case where seasonality was ignored. The exceptions are predator density and the ocean mortality rate which showed no effect on age at migration over their given range (TABLE 4.5). This appears to be a result of the anchoring of within-year optimal migration timing

by the temperature curve, making specific times of the year best for migration. Rather than producing a continuous effect on optimal migration timing, migration timing either varies little—not at all in the case of predator density and ocean mortality (for the parameter estimates used)—or jumps between years.

4.3 Summary

In this chapter I included temporal fluctuations in food consumption, metabolic processes, and predator activity. The temporal fluctuations in these variables were driven by a periodic temperature function of given average temperature, phase angle, and amplitude. The objective function has yearly humps corresponding to the best within-year migration timing, the tallest hump representing the global maximum. As a result, seasonal temperature fluctuations exerted a strong influence on the age at migration, not only determining the optimal *within-year* migration timing, but also the optimal *year* of migration. The best time of migration corresponds to times of low temperature, when predator activity is at a minimum. As fish grow, the influence of seasonality decreases because larger fish are less susceptible to predators.

The sign of the parameter effects were consistent with the case where seasonality was absent. The phase angle parameter defines the time of minimum temperature, and therefore is responsible for anchoring the optimal age at migration to a particular time of year. Other parameters have little to no effect on within-year migration timing (TABLE 4.5), but can strongly influence the optimal year of migration (*e.g.*, migration distance) (FIGURE 4.5).

4.4 Discussion

The simulations show that the best time to migrate is when predator activity is at its lowest, (*i.e.*, during winter months). Although this seems a reasonable result, it is not usually witnessed in nature. One may argue, from a physiological standpoint, that during the cold winter months smolt development is retarded and is hence an unlikely time to migration. On the other hand, one ought to ask, if winter is the best time to migrate, why do the fish not migrate to the ocean at a less developed state, and relying on smolt development with increased exposure to saltwater, as is witnessed in some ocean-type fry (Reimers 1973)? My point is that although one may appeal to smolt physiology for an explanation of migratory behavior, one wonders what survival or reproductive benefit is produced by the population-specific smolt development schedule—a schedule depending strongly on endogenous, as well and exogenous factors.

I believe the results of this chapter raise an important question: *If* predator activity is least during winter months, why do not all salmon populations migrate at that time? I believe the answer depends on knowing the temporal patterns of survival, not only in freshwater, but also in the ocean and estuary. For winter migration may eliminate some freshwater mortality, but what about size-dependent ocean and estuary mortality? Many agree that larger fish are better able to handle the insult of a more osmotically challenging saltwater environment (Brett & Glass, 1973; McCormick & Naiman, 1984; Hargreaves & LeBrasseur, 1986), and that they are better able to escape predators (Werner & Hall, 1988; Bugert & Bjornn, 1991; Bugert *et al.*, 1991). These factors ought to be incorporated in the ocean mortality function, and could yield more realistic migration timing patterns.

Another result of the simulations shows that, all else being equal, increasing the mean yearly temperature, increases freshwater residency. In reality, colder climes produce populations with greater freshwater residence times than warmer ones. Recall that ocean-type populations predominate in the south, and stream-type, in the south. However, the sensitivity performed on mean temperature assumed *all other factors were equal*, and certainly the other important factors vary with latitude, such as freshwater predator abundance, and the performance demands of the ocean environment: osmo-regulator and locomotor performance is inhibited in colder waters (Brett, 1967; Knutsson & Garv, 1976; Beamish, 1978; Webb, 1978; Virtanen & Oikari, 1984). Another factor ignored was the possibility of lethal temperatures. In some parts of California, a yearlong stay in certain freshwater regions is not feasible, since summer temperature are routinely lethal in their habitat (TABLE 4.5). I believe that including the patterns of freshwater predation, size-dependent saltwater readiness, and lethal temperatures, would yield more realistic latitudinal patterns.

TABLE 4.6 Lethal water temperatures in some California rivers. The estimates were derived from USGS data.[a]

Gauge Station	Station No.	Lat. S	No. days mean temp. > 25° (C)					
			1988	1989	1990	1991	1992	1993
Merced R. near Stevinson, CA	11272500	37° 22’	32	--[b]	--	34	59	--
San Joaquin R. near Newman, CA	11274000	37° 21’	55	--	--	--	--	24
Tuolumne R. at Modetso, CA	11290000	37° 38’	91	25	--	49	--	--
San Joaquin R. near Vernalis, CA	11303500	37° 40’	0	--	70	36	57	19
Sacramento R. below Wilkins Slough near Grimes, CA	11390500	39° 01’	0	0	0	0	0	0
Sacramento R. at Freeport, CA	11447650	38° 27’	--	0	2	2	9	0

[a] Lethal temperatures are estimated at > 25.1 C (Brett, 1952).

[b] The symbol “--” indicates that the year contained too many missing daily temperatures for an accurate estimate.

The parameter effects of this chapter were in qualitative agreement with those of the previous chapter, where seasonality was ignored. As before, age at migration increased with food availability, migration distance, current velocity, and spawning time; and decreased with predator activity and initial weight. Of special interest are the predator density and ocean mortality rate which showed no influence on age at migration over their chosen range. This is an artifact of added seasonality. The only parameter with a strong influence on with-year migration timing is the phase angle: all other parameters show their main influence on between-year age at migration (see for example FIGURE 4.5). This suggests the possibility of carrying out the optimization in two phases: (i) determine the optimal with-year migration timing, then (ii) given this best time of the year to migrate, what year should the migration take place. The first phase can be accomplished using a continuous variable (time of the year), and second with a discrete, “yes or no” variable: should the fish migrate this year or not? The continuous approach of the first phase was the approach of Bohlin *et al.* (1993), while the discrete approach of the second phase as used by Mangel (1994). The approach I use integrates these two phases.

CHAPTER 5 A MORE GENERAL APPROACH: DYNAMIC OPTIMIZATION MODELLING

The study of migratory behavior is not limited to understanding age at migration. There is a rich complex of behaviors leading up to migration and during migration itself—behaviors promoted by ontogeny and environmental changes. Studies show that although there is much variation in behavior among chinook populations, some common behavior patterns are evident[1]: fry initially inhabit the stream or river margin, but move into higher velocity locations as they grow; fry migrate mostly at night; fry move with freshets.

Models of the previous chapters are not able to capture the continuous decision process involved with these migration and feeding behaviors. The previous models assumed that once migration began, it continued at a constant rate until estuary entry. To capture the mosaic of behaviors considered in this chapter, the fish must be able to cease migration during different hours of the day and migrate in different cross-sections of the river or stream. Migration, considered at this level, involves a continuous decision process: at each instant the fish must be able to choose its migration velocity and its proximity to shore. The previous models presented static optimization problems involving only a single decision (*i.e.*, when to migrate), and do not apply here. Fortunately, there exists a modelling framework able to deal with the problem of a continuous decision process

1. See sections 1.2.3, 1.2.4, and 1.3.2 of CHAPTER 1.

rather than a static one: *dynamic optimization modelling* (Oster & Wilson 1984; Smith 1984; Mangel & Clark 1988).

As in the case of the static optimization problem of previous chapters, behavior is viewed as an organ shaped by natural selection into a form which optimizes the salmon's fitness. The assumptions underlying this class of models are that (a) each behavior allowed by the model is phyletically feasible, and (b) the organism either possesses or can develop a mechanism for achieving nearly optimally solutions to behavioral problems (Mangel & Clark 1988).

The model, as it is presented in this chapter, takes its most general form, making a minimal number of assumptions (TABLE 5.1). In later chapters, special cases will be considered and simplifying assumptions made. Attention is given to each phase the salmon life-cycle including freshwater, estuarine, and ocean residence (FIGURE 5.1), although the main focus is on behavior during freshwater residence and migration. The additional problems of identifying optimal estuarine residence time and age at maturity are subsumed by the general form of the model, but receive no treatment in upcoming chapters.

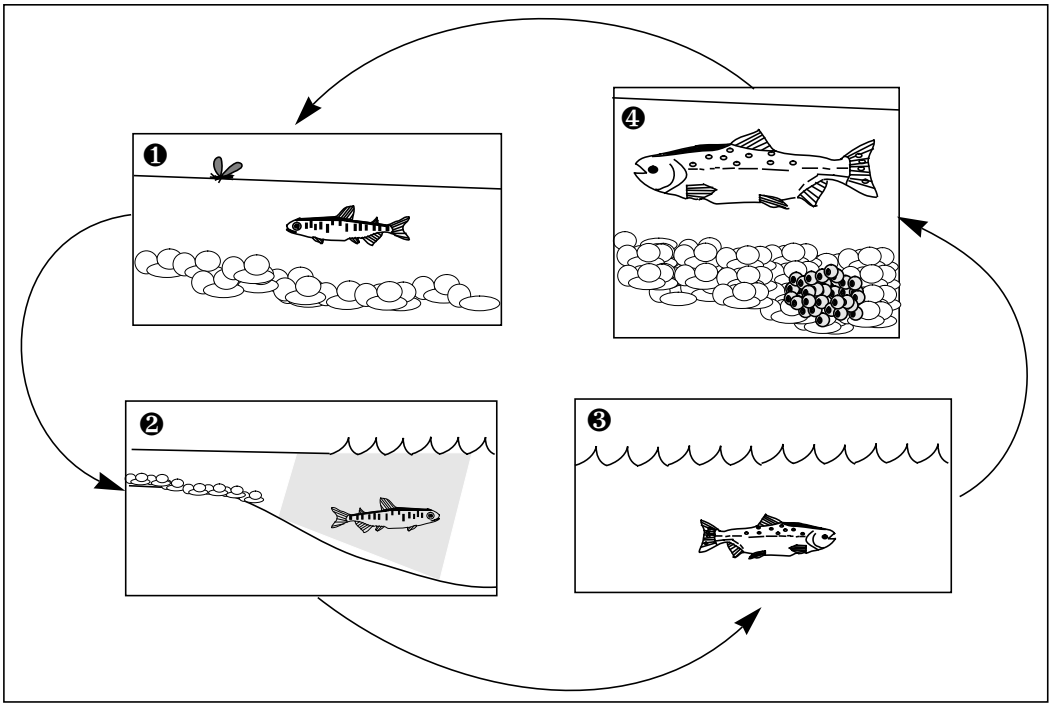

FIGURE 5.1 Chinook life cycle summary. Lifetime reproductive success depends on survival in the ❶ freshwater, ❷ estuarine, and ❸ ocean habitats, as well as ❹ fecundity and egg-to-fry survival.

TABLE 5.1 Model assumptions.

Assumption
Ocean growth is based on a von Bertalanffy growth equation, with parameters that are allowed to vary with time.
Estuarine growth is weight and time dependent and not locked down to a particular form.
Freshwater growth is time, space, and size dependent. It is based on a Holling type II disk equations for consumption, and metabolic costs determined by fish size and temperature.
Fecundity a function of weight at spawning.
Freshwater residence time, estuary residence time, and spawning time are free.
Emergence time is fixed.
Ocean mortality rate decreases with weight.
Migration velocity is allowed to vary continuously as the sum of swimming velocity and current velocity control variables.[a]
Movement is one dimensional, measured in the upstream/downstream direction.
Capture probability is a decreasing function of salmon weight, and allowed to vary with time.
Freshwater mortality is a result of depredation alone.

[a] This assumption differs from that of the previous chapters, where once migration began, it did not cease until the arrived in the estuary or ocean, and migration velocity was assumed constant.

TABLE 5.2 General optimization model summary.

Maximize: u, v, t_f, t_e, t_s	$-\int_{t_0} (\lvert u+v \rvert + \zeta(x,t))\,\theta(u,x,t)\,k(x,w,t)\,dt + \Phi(w(t_f), t_f, t_e, t_s)$	(objective functional)
Subject to:	$\dot{x} = u+v$	(displacement state eq.)
	$\dot{w} = g(v,x,w,t)$	(weight state eq.)
	$0 \le u \le u_{max}(x,t)$	(stream velocity constraint)
	$\lvert v \rvert \ge v_{max}(w)$	(swimming velocity constraint)
	$x(t_0) = 0,\ w(t_0) = w_0$	(initial conditions)
	$t_0 \le t \le t_f$	

TABLE 5.3 Main parameters and functions.

	Variable or function	Unit	Description
	t	s	Time
	$u(t)$	$\mathrm{m} \cdot \mathrm{s}^{-1}$	Current velocity (control variable)
	$v(t)$	$\mathrm{m} \cdot \mathrm{s}^{-1}$	Swimming velocity (control variable)
	$z(t)$	$\mathrm{m} \cdot \mathrm{s}^{-1}$	Migration velocity
	$x(t)$	m	Downstream displacement (state variable)
	$w(t)$	g	Salmon weight (state variable)
	$u_{max}(x,t)$	$\mathrm{m} \cdot \mathrm{s}^{-1}$	Maximum current velocity
	$v_{max}(w)$	$\mathrm{m} \cdot \mathrm{s}^{-1}$	Maximum swimming velocity
	a	m	Distance from redd to estuary
growth	$g(v,x,w,t)$	$\mathrm{g} \cdot \mathrm{s}^{-1}$	Growth rate of juvenile
parameters	C	$\mathrm{cal} \cdot \mathrm{s}^{-1}$	Consumption rate
and functions	d	$\mathrm{cal} \cdot \mathrm{s}^{-1}$	Food delivery rate
	$N(v,x,w,t)$	$\mathrm{cal} \cdot \mathrm{s}^{-1}$	Net energy gain
	c	$\mathrm{g} \cdot \mathrm{cal}^{-1}$	Calories to grams conversion constant
	$\rho(t)$	$\mathrm{cal} \cdot \mathrm{m}^{-2}$	Prey density
	τ	dimensionless	Net conversion efficiency
	$\gamma(w,t)$	m	Reactive field diameter
	$h(w)$	$\mathrm{s} \cdot \mathrm{cal}^{-1}$	Handling time
survival	$\theta(u,x,t)$	m^{-1}	Predator density
parameters	$\zeta(x,t)$	$\mathrm{m} \cdot \mathrm{s}^{-1}$	Predator search velocity
and functions	$k(x,w,t)$	dimensionless	Capture probability
	$\mu_o(w,t)$	s^{-1}	Ocean mortality rate
	$\mu_e(w,t)$	s^{-1}	Estuary mortality rate
other	t_s	s	Spawning time
	t_f	s	Time that the juvenile arrives in the estuary
	t_e	s	Time that the juvenile enters the ocean (from the estuary)
	t_0	s	Time of emergence
	$m(w)$	egg number	Fecundity

5.1 Model development

A model must be selected that is able to (a) describe the range of salmon behaviors observed, (b) treat decision making as a state dependent dynamic process, (c) consider

past and future costs and benefits, and (d) realistically link the state dynamics with decisions. It must also be mathematically and numerically manageable. Achieving all of these desirable qualities simultaneously is difficult—if not impossible—and eventually, some simplifying assumptions will be made.

In the dynamic optimization modelling framework I present, six elements are present: an *objective functional* which values various behaviors, a set of *control variables* representing the continuous choices available to the juvenile, *control parameters* representing discrete choices, a set of *state variables* representing the state of the juvenile—in this case the size and downstream location of the juvenile, *control variable constraints* specifying the range of available choices, and *boundary conditions* on the state variables (TABLE 5.2).

5.1.1 Control variables: current velocity and swimming velocity

At any given time, a juvenile makes two decisions: the current velocity in which it swims, and its swimming velocity. These represent the control variables.

5.1.1.1 Current velocity

After emergence, juveniles have a range of current velocities in which to swim. Current velocity is typically zero at the shoreline, and is typically maximal near midstream. Let $u(t)$ represent the chosen current velocity at time t. Then

$$0 \le u(t) \le u_{max}(x(t), t), \tag{5.9}$$

where $u_{max}(x, t)$ represents the maximum current velocity at downstream position x and time t.

5.1.1.2 Swimming velocity

Juveniles also choose their swimming velocity, $v(t)$, measured relative to the current velocity. Swimming velocity ranges from zero to the fatigue speed of the fish, $v_{max}(w)$, which is a function of weight. Therefore,

$$|v(t)| \leq v_{max}(w(t)), \tag{5.10}$$

where $w(t)$ is fish weight at time t. Fish swimming downstream have positive swimming velocity, and those swimming upstream, a negative swimming velocity.

Since the swimming velocity is measured relative to the current velocity, the actual migration velocity, $z(t)$, is the sum of the current velocity and swimming velocity at time t (FIGURE 5.2),

$$z(t) = u(t) + v(t). \tag{5.11}$$

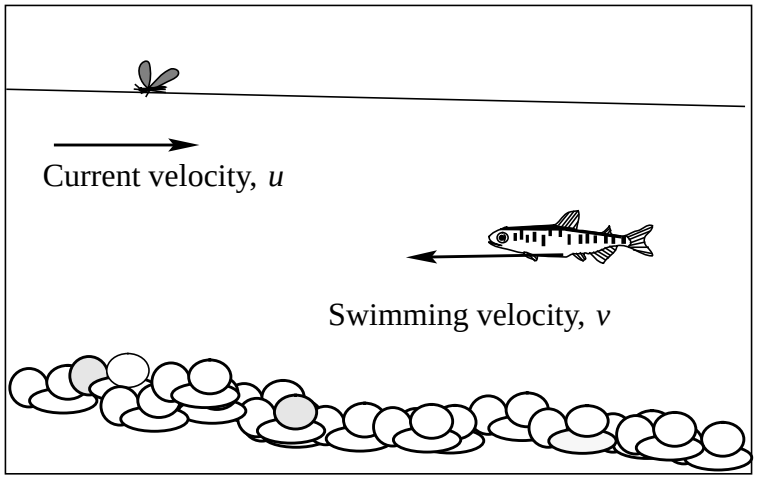

FIGURE 5.2 The control variables: swimming velocity and current velocity. Depicted is a chinook fry swimming against the current, which therefore has a negative swimming velocity. Since swimming velocity is measured relative to the current velocity, the migration velocity is $u + v$.

5.1.2 State variables: downstream displacement and weight

Two state variables are defined for a juvenile: its weight $w(t)$, and its downstream position, $x(t)$, measured relative to the point of emergence. Since fish make dynamic decisions based on weight and position, it is essential to know how these states evolve over time.

5.1.2.1 Downstream displacement

The first simplifying assumption I make, is that movement is tracked only in the upstream or downstream direction—no lateral movement is accounted for. This assumption makes the change in downstream position of the juvenile easy to compute:

$$\dot{x}(t) = u(t) + v(t). \tag{5.12}$$

This is the rate of displacement relative to the stream substrate. The positive direction is taken to be downstream, and the juvenile is assumed to be at position $x = 0$ at $t = t_0$, a total distance of a meters from the estuary.

Within this framework, the juvenile can control its freshwater residence time, and migration behavior through adjusting the values of u and v through time. When $v(t) = -u(t)$, the juvenile is holding station, when $v(t) + u(t) < 0$, it is migrating upstream, and when $v(t) + u(t) > 0$, it is migrating downstream.

5.1.2.2 Weight

5.1.2.2.1 Freshwater growth

Weight changes according to the amount of food the juvenile consumes, its standard metabolic costs, and its active metabolic costs. Feeding activity involves an inherent trade-off. If the fish is entirely inactive, then even though its metabolic cost is minimal, no food is obtained, and consequently, weight declines. When activity is too great, metabolic costs overtake the benefit of food intake, and weight again declines. The juvenile is faced with choosing an activity level that strikes a balance between the rate of food intake and metabolic costs (FIGURE 5.3). The growth function is assumed to be concave in swimming speed, capturing the essential features described above. The speed at which growth is maximized is denoted by $v_g(x, w, t)$.

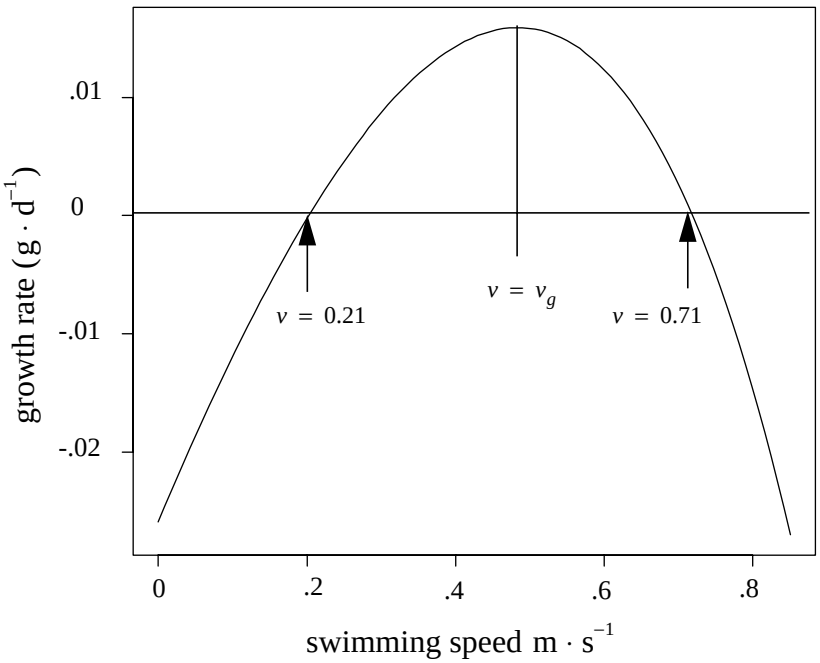

FIGURE 5.3 Typical growth curve as a function of swimming speed, where weight and temperature are fixed. Growth is concave in swimming speed, and there is one unique maximum value, $v = .48$ m · s^{-1}. Growth is negative for swimming speeds either too small, $|v| \leq .21$ m · s^{-1}, or too great, $|v| \geq .71$ m · s^{-1}. This curve was derived based on a Holling (1959) type II feeding curve, and a metabolic cost curve in Hewitt & Johnson (1991). It represents the growth rate of a fish weighing 5 g at a temperature of 15° C.

Weight changes according to the dynamical equation

$$\dot{w}(t) = g(v, x, w, t), \tag{5.13}$$

where g is a growth function which depends on the swimming velocity, location, weight, and time. I express growth in terms of consumption, metabolic loss (active and inactive), and waste loss,

$$\text{Growth} = \text{Net Energy Gain} - \text{Metabolic Loss},$$

$$g(v, x, w, t) = N(v, x, w, t) - M(v, x, w, T(t)) \tag{5.14}$$

The form of the growth function is taken from a combination of functions found in the literature. The net energy rate, $N(v, x, w, t)$, which consists of the portion of the ration available for work or somatic growth is calculated according to Ware (1978), and the metabolic rate, $M(v, x, w, T)$, according to Hewitt & Johnson (1991). The function $T(t)$ gives water temperature as a function of time, and from here forward, T will represent temperature (C).

Net energy gain. The energy available for work or somatic growth is known as the net energy gain. To calculate this function, measures of food consumption and loss due to specific dynamic action are needed. Food consumption depends on the food delivery rate, and to capture the advantages of searching for food at a faster rate, I assume that the rate of food delivery increases with swimming speed. Juvenile chinook are also assumed to be surface feeders (Becker, 1973a)—although a similar derivation is possible for a general drift feeder—to simplify the form of the intake function. The food delivery rate is directly proportional to the swimming speed of the juvenile:

$$d = \rho(x, t)\,\gamma(x, w, t)\,|v|, \tag{5.15}$$

where $\rho(t)$ is the prey density on the stream surface, and $\gamma(w, t)$ is the width of the intersection between the reactive field cross section and the stream surface. When the juvenile adopts a "sit-and-wait" strategy ($v = -u$, picking off food from the surface as it floats within visual range, the delivery rate is $d = \rho(x, t)\,\gamma(x, w, t)\,u$.

As the delivery rate increases, not all food delivered will be consumed, because consumption rate, C, is limited by handling time of food items. A Holling (1959) Type II feeding curve is used to model this phenomenon:

$$C = \frac{d}{1 + d \cdot h(w)}, \tag{5.16}$$

where an average of $h(w)$ seconds must be devoted to handling a single calorie of food, then the time spent handling food, and d is the food delivery rate. Not all of the food consumed is available for work. Some is lost in nitrogenous and fecal waste, and to specific dynamic action (Ware, 1980). The ratio of net energy to energy consumed is called the *net conversion efficiency,* $\tau(t)$.

Incorporating the expressions for the food delivery rate (5.15), and the food consumption rate (5.16), the rate of net energy gain is

$$N(v, x, w, t) = \frac{\tau(t)\,\rho(x, t)\,\gamma(x, w, t)\,|v|}{1 + \rho(x, t)\,\gamma(x, w, t)\,h(w)\,|v|}. \tag{5.17}$$

Metabolic Rate. The metabolic rate consists of energy lost through respiration, and is calculated by first calculating an allometric function of weight, then increasing that value through a water temperature dependence function and a factor representing activity. Activity will be an increasing function of swimming velocity. The respiration function is given explicitly by

$$R_g(v, w, T) = \alpha_R w^B \cdot f_R(T) \cdot ACT(v, T), \tag{5.18}$$

where the water temperature dependence function for respiration is given by

$$f_R(T) = exp(\theta_R T),$$

and the activity function is given by

$$ACT(v, T) = exp((TO_R - (TM_R \cdot T))|v|).$$

The variables, θ_R, TO_R, TM_R, represent parameters that need to be estimated.

5.1.2.2.2 Estuarine growth

Upon arriving in the estuary, a juvenile salmon faces a new set of challenges: new predators, new food habits, and higher salinities. These new challenges necessitate the use of estuarine specific survival and growth equations—both relevant to ultimate reproductive success of the individual.

Observations indicate that estuarine growth varies seasonally. Estimates of the instantaneous increase in mean weight are $2.1–2.7\% \cdot d^{-1}$ in the Campbell River estuary (Levings *et al*., 1986), $5.5\% \cdot d^{-1}$ in the Nanaimo estuary (Healey 1982), and $3.5\% \cdot d^{-1}$ in the Nitinat estuary (Healey, 1982). Reimers (1971) showed that in the Sixes River estuary, growth in the estuary was from late April to early June $0.9 \text{ mm} \cdot d^{-1}$, but was relatively poor during June to August ($0.07 \text{ mm} \cdot d^{-1}$). Neilson *et al.* (1985) suggested this decline in growth resulted from a combination of high temperatures that reduced growth efficiency and competition for food.

These observations suggest using an exponential growth equation with a time varying rate of increase for the duration of estuarine growth. However, unlimited growth is unrealistic,

and some amount of time growth should taper off, as it does when a von Bertalanffy is applied. If I were to assume exponential growth instead, it would be difficult to get fish to leave the estuary at all (unless the growth rate was assumed sufficiently small), because the estuarine residence time, $t_e - t_f$ is assumed to be free.

5.1.2.2.3 Ocean growth

Of the three chinook habitat types I cover: stream, estuarine, and ocean, the ocean contains the greatest growth potential for salmon. For example, upon entering the ocean, chinook can average 10 cm in fork length, and after 5 yrs of ocean growth, average about 90 cm in fork length (Loeffel & Wendler, 1969). Data of Loeffel & Wendler (1969) show two important characteristics: ocean growth rate is greatest in the chinook's first year of life and tapers off with time, and there is a definite seasonal pattern of growth, with rapid summer growth and slow winter growth. Like Henry (1972), I use a Bertalanffy growth curve to model ocean growth (Ricker, 1976):

$$\dot{w} = a_o(t)\, w(t)^{2/3} - b_o(t)\, w(t) . \tag{5.19}$$

The first term, $a_o(t)\, w(t)^{2/3}$, describes anabolism, and the last term, $b_o(t)\, w(t)$, catabolism.

5.1.3 Fitness measure

The fitness measure is lifetime reproductive success, $R = l \cdot m$, where l is the probability of survival from emergence to spawning, and m is the number of eggs produced by a female at spawning. The probability of survival from emergence to spawning consists of three factors: the freshwater survival, $S(t_f)$, estuarine survival, $S_e(t_e)$ and ocean entry to

spawning survival, $S_o(t_s)$. Since survival factors and reproduction are typically size dependent, growth in freshwater, the estuary, and the ocean is also considered.

Expected lifetime reproduction is defined by

$$R = S(t_f)\, S_e(t_e)\, S_o(t_s)\, m(w(t_s)) .$$

(I have ignored the egg-to-fry survival in the above expression since, assuming it is constant, it does not influence the optimal solution sought.) I could attempt to maximize lifetime reproductive success directly with respect to the control variables and control parameters, however, there it is more convenient to use the natural log of reproductive success,

$$J = \log(R) .$$

In the context of dynamic optimization, J is a functional that depends on the control variables u and v as well as control parameters t_f, t_e, and t_s: all of the variables that represent choices. This functional is

$$J(u, v, t_f, t_e, t_s) =$$

$$-\int_{t_0}^{t_f} (|u+v| + \zeta(x,t))\,\theta(x,t)\,k(w,t)\,dt \qquad \text{(freshwater)}$$

$$-\int_{t_f}^{t_e} \mu_e(w,t)\,dt \qquad \text{(estuary)}$$

$$-\int_{t_e}^{t_s} \mu_o(t)\,dt \qquad \text{(ocean)}$$

$$+ (\log(a_m) + b_m \log(w(t_s))) \qquad \text{(fecundity)}$$

The newly introduced variables appearing in this expression will be defined later.

For convenience, define a post-migration fitness component,

$$\Phi(w(t_f), t_f, t_e, t_s) = \qquad (5.20)$$
$$-\int_{t_f}^{t_e} \mu_e(w,t)\,dt - \int_{t_e}^{t_s} \mu_o(w,t)\,dt + \log(a_m) + b_m \log(w(t_s)).$$

Then the functional J can be simplified to

$$J(u, v, t_f, t_e, t_s) = \qquad (5.21)$$
$$-\int_{t_0}^{t_f} (|u+v| + \zeta(x,t))\,\theta(x,t)\,k(x,w,t)\,dt + \Phi(w(t_f), t_f, t_e, t_s).$$

Since the log is a monotone increasing function, control variables maximizing R also maximize J, and vise versa. In this formulation, $J(u, v, t_f, t_e, t_s)$ is the *objective functional*, or the *performance index*; it is the quantity we strive to maximize with respect to the control variables u and v, and the times, t_f, t_e, and t_s.

5.1.3.1 Freshwater survival

Predation is often implicated as the main cause of juvenile mortality after emergence, and heavy predation losses have been documented (Foerster & Ricker, 1941; Hunter, 1959). Unfortunately, little is known of the in-river losses due to other morality agents like disease, parasitism, and starvation. Throughout, I assume that predation is the sole source of mortality. When the other mortality factors are constant with respect to the control variables and parameters, then the optimal behavior is unaltered by their inclusion. Although this assumption is unrealistic, the influences of other mortality factors are likely qualitatively similar to the influence of predation: longer residence time means greater exposure risk, and risk decreases with juvenile weight.

Encounters with predators are due to a combination of predator and prey activities. The predator encounter rate (*i.e.*, an instantaneous rate giving the average number of predators encountered per second) increases with migration speed and also with predator search velocity. Predator search velocity is incorporated to allow for predator encounters whether or not the juvenile is stationary. Over a small increment of time, Δt, the probability of a predator encounter is

$$Pr\{\text{Encounter in } \Delta t\} = (|u + v| + \zeta(x, t))\,\theta(u, x, t)\,\Delta t, \tag{5.22}$$

where $\theta(u, x, t)$ is the predator density, and $\zeta(x, t)$ is the predator search velocity.

The predator density function represents predators per meter of river and is allowed to vary with current velocity. This allows for the possibility that predator densities may be smaller in nearshore areas, where more protective cover may exist (Solomon, 1981). Next, I assume that the probability that an encounter leads to a capture is a function of position, fish weight and time, $k(x, w, t)$. In most taxa, larger individuals are assumed to stand a better chance of escape than smaller ones (Werner & Gilliam, 1984).

Temperature also influences predation rate. Vigg & Burley (1991) observed that the daily ration of northern squawfish *(Ptycholcheilus oregonensis*), a major salmonid predator on the Columbia River, increased with temperature from about $0.5\ \text{salmonids} \cdot \text{predator}^{-1}$ at $8.0°\text{C}$ to $7.0\ \text{salmonids} \cdot \text{predator}^{-1}$ at $21.5°\text{C}$. The influence of temperature may be incorporated in the capture probability, $k(x, w, t)$, as a function of time, t, and downstream position, x.

Putting these elements together, I derive the probability that a juvenile survives from emergence to an arbitrary time t, during its freshwater residence. The probability of death between time t and $t + \Delta t$, is the probability of an encounter and a capture in this interval, namely,

$$Pr\{\text{death in } [t, t+\Delta t]\} = (|u(t) + v(t)| + \zeta(x, t))\,\theta(x, t)\,k(x, w, t)\,\Delta t. \quad (5.23)$$

The probability that the juvenile is alive at time $t + \Delta t$ is equal to the probability that it survives to time t times the probability that it remains alive between t and $t + \Delta t$:

$$S(t+\Delta t) = (1 - Pr\{\text{Death in } [t, t+\Delta t]\})\,S(t). \quad (5.24)$$

By substituting (5.23) into (5.24) and taking the limit as Δt tends to zero, we obtain the differential equation for survival during migration as

$$\frac{dS}{dt} = -(|u+v| + \zeta(x,t))\,\theta(u,x,t)\,k(x,w,t)\,S,$$

with the initial condition $S(t_0) = 1$.

The probability of surviving in-stream from emergence to an arbitrary time, t is then

$$S(t) = exp\left(-\int_{t_0}^{t} (|u+v| + \zeta(x,\xi))\,\theta(u,x,\xi)\,k(x,w,\xi)\,d\xi\right). \qquad (5.25)$$

The fish arrives at the estuary at time t_f—a control parameter—and begins its salt water residence.

5.1.3.2 Estuarine survival

Little is known about the mortality of juvenile salmon during estuarine residence, but in this general treatment, I allow estuarine mortality rate to vary with size and season. Specifically, I assume that the probability of death in an interval $[t, t+\Delta t]$ is proportional to Δt:

$$Pr\{\text{Death in } [t, t+\Delta t]\} = \mu_e(w,t)\,\Delta t, \quad t_f \le t \le t_e,$$

where $\mu_e(w,t)$ is the instantaneous estuary mortality rate. The probability of survival from time from the moment the juvenile enters the estuary to an arbitrary time $t+\Delta t$, prior to ocean entry, is the probability that it is alive at t times the probability that is does not die during $[t, t+\Delta t]$:

$$S_e(t+\Delta t) \;=\; S_e(t)\;(1-\mu_e(w,t)\,\Delta t)\,, \tag{5.26}$$

Subtracting $S_e(t)$ from both sides of (5.26), dividing by Δt, and then taking the limit as Δt tends to zero, yields the differential equation

$$\frac{dS_e}{dt} \;=\; -\mu_e(w,t)\,S_e(t)\,,$$

with boundary condition $S_e(t_f) \;=\; 1$; its solution is

$$S_e(t) \;=\; exp\left(-\int_{t_f}^{t}\mu_e(w,\xi)\,d\xi\right). \tag{5.27}$$

In the most general case, estuarine residence time, $t_e - t_f$, is left free, since it depends on control parameters t_e and t_f.

5.1.3.3 Ocean survival

As in the case of freshwater mortality, ocean mortality is thought to decline with size (Parker, 1962). Early during their ocean residence, salmon fall prey to fishes, birds, and mammals, and as they growth become potential prey for fewer and fewer species. At a weight of about 250 g salmon are no longer available to most birds. On the high seas, the number of predators that can take large salmon (*e.g.*, halibut and killer whales) is limited (Ricker, 1976). I assume that the probability of death in a small interval of time $[t,\, t+\Delta t]$ is proportional to Δt,

$$Pr\,\{\,\text{Death in }\;[t,\, t+\Delta t]\,\} \;=\; \mu_o(w,t)\,\Delta t,\;\; t_e \le t \le t_s,$$

where $\mu_o(w,t)$ is the weight and time dependent instantaneous ocean mortality rate, and t_s is the time that the chinook returns to spawn. Assuming the observations of and Parker

(1962) and Ricker (1976) are true, mortality rate falls rapidly for small weights, and approaches a constant as weight increases.

Following a development similar to that of the derivation of the estuarine survival function, the ocean survival is

$$S_o(t) = exp\left(-\int_{t_e}^{t} \mu_o(w, \xi)\, d\xi\right). \tag{5.28}$$

5.1.3.4 Fecundity

The next component of the fitness measure (reproductive success) considered here is fecundity. Many studies have confirmed significant fecundity-size relationships within chinook populations (Galbreath & Ridenhour, 1964; Healey & Heard, 1984). The majority of these studies relate the fork length of a mature female to the number of eggs. I relate fecundity to weight rather than length, using an allometric relationship between length and weight to convert length data to weight data. The form of the fecundity-weight relationship is

$$m(w) = a_m w^{b_m}, \tag{5.29}$$

where $m(w)$ is egg number and w is weight.

5.1.4 Egg-to-fry survival

To complete the description of survival during the chinook life cycle, we must consider egg-to-fry survival, which is the average number of eggs surviving to the fry stage divided by the average number of eggs deposited in a redd per female. Factors influencing egg

mortality include low dissolved oxygen concentrations, high percentage of small particles (fines) in the substrate, flooding and scouring, and dewatering. According to Healey (1991) the estimates of egg-to-fry survival are hard to interpret because of uncertainty in the estimates of both the potential eggs deposited and the numbers of fry produced. In the proposed model, I will assume that egg-to-fry survival is a constant, and since it merely scales the lifetime reproduction of a female, it has no influence on the solution to the optimal control problem at hand.

5.2 Optimization model summary

In this chapter, I presented a justification for approaching the problem of diel migration pattern and current velocity selection from a behavioral ecology perspective. By considering the possible selective pressures on shaping the behavior of young salmon, and couching them in equation form, I developed an optimization model that retained the ability to predict migration timing as in other chapters, but was much more general in that it treated diel migration and current velocity selection patterns. The resulting optimization problem was dynamic, and included current velocity and swimming velocity as control variables; time of entry into the estuary, time of ocean entry, and spawning time as control parameters; weight and downstream displacement as state variables, and the log of expected reproductive success as the objective functional.

5.3 Discussion

The dynamic optimization model presented here retains the ability to predict migration timing as previous chapters, but includes more detail on the migratory and pre-migratory behavior itself, such as diel migration and current selection. Although this behavior is

really the focus of the model, in its most general form, it is also able to predict time of entry in the estuary and ocean, as well as spawning time. These times are chosen so that the fitness criterion is as large as possible.

One must use such a general model cautiously. In the case where a general model does a good job of giving qualitative results consistent with observations of nature, one gains very little. Often, it is only when the model misses the mark that anything can truly be gleaned from the modelling experience. This fact together with the need to find numerical solutions to the optimization problem prompts the use of an incremental approach demonstrated in the treatment of age at migration in previous chapters. First, a very simple form of the model is assumed and its qualitative results are compared to nature. Observing the areas of inconsistencies with nature, hypothesis for the discrepancies are given, and new elements are added to the model to test the hypothesis. The results of this model are then weighed against reality, and the process continues.

Be aware that the models used here an in previous chapters are based on perfect knowledge, and that the behaviors predicted might be nearly optimal, but the salmon may have no known mechanism for achieving the optimal behavior. (Recall that I assumed from the outset that the organism either possesses or can develop a mechanism for achieving nearly optimal solutions.) A complex behavior such as migrating upstream to a ephemeral feeding area at exactly the right time, may be an optimal, but it is likely impossible based on known mechanisms. However, from a philosophical point of view, nature usually punishes inefficiency (sub-optimal behavior), and in response, animals can develop elaborate behaviors, which at first seem improbable, to “solve” ecological problems.

Although this model was developed specifically to analyze the problem of chinook migratory behavior, its use is not limited to this species. The rest of the genus *Oncorhynchus* is subject to the selective pressures operating on chinook, albeit to different degrees. Very simple migration strategies such as immediate migration after emergence displayed by pink salmon can be treated with the model as well as complex migration strategies, such as upstream to a lake prior to migration displayed by some sockeye populations.

CHAPTER 6 MODEL ANALYSIS

Now that the dynamic optimization model has been specified, it must be solved. A solution consists of swimming velocity and current velocity schedules, as well as estuary entry, ocean entry, and spawning times that make the fitness measure as large as possible. In mathematical terms, it consists of control variables and control parameters that maximize the objective functional. Since the problem involves optimizing with respect to functions of time (the control variables), the solution is not found by simply taking a derivative and setting it equal to zero—a technique applied to a typical static optimization problem. Rather, dynamic optimization problems are usually approached with the techniques of *dynamic programming* (Mangel & Clark, 1988) or *Pontryagin's Maximum Principle* (PMP) (Pontryagin *et al.*, 1962), and recently, with the modern computational techniques of genetic algorithms (Michalewicz *et al.*, 1992) and evolutionary programming (Fogel, 1994). In this chapter, I apply the PMP, or in more recent terminology, due to generalizations, *the maximum principle*.

Dynamic optimization problems are of two types: continuous and discrete time. In the continuous time case, the dynamic programming approach is equivalent to the maximum principle (Dixit, 1976), but in practice, optimal control is usually applied to continuous time problems, and dynamic programming, to discrete time problems. Dynamic programming is the technique applied by Mangel (1994) in his studies of salmon life history. It is a solution method that starts with the final stage of the life history

(reproducing individuals) and then links to previous stages working backwards through time (Mangel & Clark, 1988).

For some unusual problems, it is possible to find *analytical solutions* to optimal control problems using dynamic programming or the maximum principle, but in practice, numerical techniques must be applied. My strategy for solving the optimal control problem is to apply an analytical technique to simplify the computer algorithms used to obtain numerical solutions. Besides simplifying the algorithms, these analytic findings can reveal qualitative information about the solution useful for biological insight.

TABLE 6.1 General optimal control problem.[a]

Maximize: u, v, t_f, t_e, t_s	$-\int_{t_0}^{t_f} (\lvert u+v\rvert + \zeta(x,t))\,\theta(u,x,t)\,k(x,w,t)\,dt + \Phi(w(t_f), t_f, t_e, t_s)$	(objective functional)
Subject to:	$\dot{x} = u+v$	(displacement state eq.)
	$\dot{w} = g(v,x,w,t)$	(weight state eq.)
	$0 \le u \le u_{max}(x,t)$	(stream velocity constraint)
	$\lvert v\rvert \ge v_{max}(w)$	(swimming velocity constraint)
	$x(t_0) = 0,\ x(t_f) = a,\ w(t_0) = w_0$	(initial and final conditions)
	$t_0 \le t \le t_f,\ t_f \le t_e \le t_s.$	(control parameter constraints)

[a] This general model has control constraints that depend on the state variables and an objective functional integrand that is not continuously differentiable in the control parameters (*i.e.*, it involves the absolute value of the sum of the control variables). Therefore it is a nonsmooth dynamic optimization problem.

The analytic technique I wish to apply is the maximum principle; however, as the general problem stands (TABLE 6.2), there are two difficulties preventing its use. First of all, the problem involves control parameters (*i.e.*, t_f, t_e, t_s), but the formulation of Pontryagin *et al.* (1962) allows no such parameters. However, Hestenes (1966) handles the control parameters in a formulation of the *general control problem of Bolza*. Secondly, (i) the control constraints are functions of the state variables, and (ii) the integrand of the objective functional is not continuously differentiable in the control variables. If the control problem involved (i) alone or (ii) alone, it would remain in the realm of Hestenes's work, but as it stands, it is a problem of *dynamic and nonsmooth optimization*[1], which requires a more general technique than the maximum principle (Clarke, 1989).

To side-step this last difficulty, I will assume that the control constraints are independent of the state variables—although in reality this assumption is violated—simplifying the problem so that it becomes a general control problem of Bolza. Removing the state dependence to the control constraints may not change the qualitative nature of the optimal solution, only its quantitative nature. This can be tested by applying nonsmooth techniques, dynamic programming, or stochastic optimization.

6.1 More simplifying assumptions

With the goal of first developing some intuitive results appearing in analytic rather than numerical form, I choose to make another simplifying assumption: that is to remove the relationship between current velocity and predator density. Unfortunately, this removes a

1. It is imprecise to call these problems optimal control problems. They are more accurately called *differential inclusion problems* which subsume problems in optimal control. The techniques to solve such problems generalize Pontryagin's Maximum Principle (Clarke, 1975).

selection pressure that favors small fish remaining inshore to avoid predators in swifter currents, and the solution will likely not reflect the fact that fish move into swifter waters as they develop. As an advantage, the optimization problem becomes simpler to analyze, and at least the selection pressure for diurnal patterns of migration is retained.

Another assumption made to simplify the optimization is that fitness is enhanced by a small increase in weight. This assumption makes the co-state variable associated with weight positive (See “Co-state variables” on page 123). It is a reasonable assumption since larger fish are generally more likely to avoid predators, and have a greater survival probability.

TABLE 6.2 Simplifying assumptions of this chapter.[a]

Assumption
A.1 Maximum current velocity does not vary with river kilometer, but is allowed to vary with time.
A.2 Maximum swimming speed does not vary with weight, but is allowed to vary with time.
A.3 Predator density does not vary with current velocity.
A.4 A marginal increase in fish size increases fitness.

[a] These assumptions result in a less general model than that presented in CHAPTER 5.

TABLE 6.3 The simplified optimal control problem.

Maximize: u, v, t_f, t_e, t_s	$-\int_{t_0}^{t_f} (\lvert u+v\rvert + \zeta(x,t))\,\theta(x,t)\,k(x,w,t)\,dt + \Phi(w(t_f), t_f, t_e, t_s)$	(objective functional)
Subject to:	$\dot{x} = u+v$	(displacement state eq.)
	$\dot{w} = g(v,x,w,t)$	(weight state eq.)
	$0 \le u \le u_{max}(t)$	(stream velocity constraint)
	$\lvert v\rvert \ge v_{max}(t)$	(swimming velocity constraint)
	$x(t_0) = 0,\ x(t_f) = a,\ w(t_0) = w_0$	(initial and final conditions)
	$t_0 \le t \le t_f,\ t_f \le t_e \le t_s.$	(control parameter constraints)

TABLE 6.4 Special notation.

Variable or function	Description
$u^*(t)$	Optimal current velocity.[a]
$v^*(t)$	Optimal swimming velocity.
$x^*(t)$	Optimal downstream displacement trajectory.
$w^*(t)$	Optimal weight trajectory.
t_f^*	Optimal time of arrival in the estuary.
t_e^*	Optimal time of ocean entry.
t_s^*	Optimal spawning time.
$\lambda_1(t)$	The co-state variable associated with downstream displacement.
$\lambda_2(t)$	The co-state variable associated with weight.
$\sigma_1(x, w, \lambda_1, t)$	The switching function when $\lambda_1(t)$ is positive
$\sigma_2(x, w, \lambda_1, t)$	The switching function when $\lambda_1(t)$ is nonpositive
$v_g(x, w, t)$	Maximum growth speed. It is the unconstrained swimming speed that maximizes growth.
$\tilde{v}_g(x, w, t)$	Constrained maximum growth speed. The swimming speed that maximizes growth, when constrained it is constrained by the maximum swimming speed. $\tilde{v}_g = min(v_g, v_{max})$.
$u_{crit}(x, w, \lambda_1, \lambda_2, t)$	Critical current velocity.[b] It is a critical value of the maximum current velocity used to determine the values of the current velocity and swimming velocity that maximize the Hamiltonian.
$\tilde{u}_{crit}(x, w, \lambda_1, \lambda_2, t)$	Constrained critical current velocity. It is the critical current velocity constrained by the maximum swimming speed. $\tilde{u}_{crit} = min(u_{crit}, v_{max})$.

[a] The policy functions use similar notation but are functions of the state and co-state variables.

[b] The critical current velocity is defined more clearly in APPENDIX B. It is useful in the case where the switching function is negative and the maximum swimming velocity exceeds the maximum current velocity.

6.2 Applying the maximum principle

The goal of applying the necessary conditions that comprise the maximum principle is to maximize the objective function with respect to the control variable functions and control parameters, and to use these optimal choices to help determine optimal state trajectories. In the discussion that follows, optimal choices of the control parameters, control variables,

and state variables are indicated by an asterisk "*" (TABLE 6.4). Using this convention, $u^*(t)$ and $v^*(t)$ represent optimal choices for the current velocity and swimming velocity variables, $x^*(t)$ and $w^*(t)$, optimal choices for the downstream displacement and weight variables, and t_f^*, t_e^*, and t_s^* represent optimal choices for the control parameters.

The maximum principle is applied in two phases. First, a function called the Hamiltonian is maximized with respect to its control variable arguments. Secondly, these maximizing arguments are used to construct a two-point boundary value problem whose solution includes the optimal state variable trajectories (*i.e.*, the optimal weight and downstream displacement schedules).

6.3 The value function

The *value function* at time t, $V(x, w, t)$, also known as the *optimal return function*, is defined as the unique value of the objective functional acquired by starting from a point (x, w, t) and proceeding optimally to the terminal time, in this case t_f. For convenience, the terminal time is the time of entry into the estuary, because at that point, the integration in the objective functional terminates. The value function is defined mathematically as

$$V(x, w, t) = \max_{u, v, t_f, t_e, t_s} \{ -\int_t^{t_f} (|u+v| + \zeta(x, \xi))\, \theta(x, \xi)\, k(w, \xi)\, d\xi + \Phi(w(t_f), t_f, t_e, t_s) \}. \quad (6.30)$$

The constraints on the control variables, terminal condition, and conditions on the control parameters must be observed in calculating the value function (TABLE 6.1). The value function is sometimes called the *fitness-to-go* in the behavioral ecology context, because it

represents the remaining fitness of the individual from time t, to the final time, t_f, assuming an optimal choice for the control variables u and v, and the control parameters t_f, t_e and t_s.

6.3.1 Co-state variables

$\lambda_1(t)$ and $\lambda_2(t)$ represent, respectively, the marginal contributions of the state variables $x(t)$ and $w(t)$ to the objective functional at time t. Mathematically, they are defined by

$$\lambda_1(t) = V_x(x, w, t) \text{ and } \lambda_2(t) = V_w(x, w, t).^1$$

These variables are called *co-state variables*. In economics, they are known as *shadow prices.* Biologically, they show how the fitness, measured over the juvenile's remaining lifetime, is influenced by a marginal increase in downstream displacement or weight. For example, if the co-state variable associated with displacement, λ_1, is positive, then remaining fitness is enhanced by an increase in downstream position; otherwise, if $\lambda_1 < 0$, then a downstream increment decreases remaining fitness. If $\lambda_1 = 0$ there is no advantage to being further upstream or downstream. In the analysis that follows, only the co-state variable associated with weight is assumed positive (see simplifying assumption A.4 of TABLE 6.2). This assumption cannot be imposed without specifying certain conditions on the model parameters and functions, because the co-state variables are dependent upon model functions and parameters. The following two results describe situations in which the co-state variables are known to be positive or nonnegative from the time of emergence to estuary entry (i.e. the *time horizon*). The proofs of these results are in APPENDIX A.

---

1. The notation denotes partial differentiation with respect to the subscript, (*i.e.*, $V_x = \frac{\partial V}{\partial x}$ and $V_w = \frac{\partial V}{\partial w}$). This notation is used throughout.

Result 6.1 *If k is decreasing in w and Φ is increasing in w, then $\lambda_2(t)$ is nonnegative for all t in the time horizon. If, in addition, either k is strictly decreasing in w, or Φ is strictly increasing in w, then $\lambda_2(t)$ is positive for all t in the time horizon.*

Result 6.2 *If u_{max} and g are increasing in x; k, ζ, and θ are decreasing in x; and k is decreasing in w; then $\lambda_1(t)$ is nonnegative for all t in the time horizon.*

6.3.2 The Hamiltonian

The first step of the maximum principle is to maximize the *Hamiltonian* with respect to its control variable arguments. The Hamiltonian consists of elements of the objective functional integrand and the state equations,

$$H(x, w, u, v, \lambda_1, \lambda_2, t) = \\ -(|u+v| + \zeta(x,t))\,\theta k(x, w, t) + \lambda_1(u+v) + \lambda_2 g(v, x, w, t). \tag{6.31}$$

In maximizing the Hamiltonian, the control constraints must be observed.

The maximizing control variable arguments will be "functions" of x, w, λ_1, λ_2 and t. These maximizing arguments are not really functions, since it is possible for multiple values of u and v to maximize the Hamiltonian at the same point $(x, w, \lambda_1, \lambda_2, t)$. The maximizing arguments, called *policy functions*[1], are denoted by $u^*(x, w, \lambda_1, \lambda_2, t)$ and $v^*(x, w, \lambda_1, \lambda_2, t)$ (Dixit, 1976). Whenever the value returned by one of these policy functions is a single point (*i.e.*, the singleton set), the set is represented by the point itself; otherwise, the entire maximizing set is specified. Do not confuse the policy functions with

1. This is a term borrowed from economics. To be more precise, these "functions" are actually *multifunctions* whose output can be a set containing more than one element.

the optimal controls themselves; the optimal controls are functions of time alone (TABLE 6.1). Although they are given similar notation, the context will make it clear which is meant. The optimal control variables are connected to their corresponding policy functions through

$$u^*(t) \in u^*(x^*(t), w^*(t), \lambda_1(t), \lambda_2(t), t) \text{ and} \tag{6.32}$$

$$v^*(t) \in v^*(x^*(t), w^*(t), \lambda_1(t), \lambda_2(t), t).^1 \tag{6.33}$$

The simple act of maximizing the Hamiltonian yields a great deal of information about the optimal behavior types, although more is needed before the optimal state and control paths can be constructed (FIGURE 6.1).

The analysis will proceed by considering two different cases: the first where the co-state variable associated with displacement is positive, and the second, where it is nonpositive. In both cases, I first determine what values of the current velocity are optimal given an arbitrary choice of the swimming velocity. This amounts to maximizing the Hamiltonian over cross-sections defined by fixed swimming velocity. This allows me to write u^* as a function of v. When the result is substituted into the Hamiltonian, the optimization problem becomes one-dimensional, involving only the swimming velocity, and it is easier to analyze. For the sake of brevity, only an outline of the methodology and results are presented in this chapter. A more complete demonstration of the Hamiltonian optimization may be found in APPENDIX B.

---

1. The distinction between an optimal control a policy function (which returns a set of values maximizing the Hamiltonian) is very important in the case of a singular path, where the optimal control is not uniquely determined by the policy function (Conrad and Clark 1987; Huffaker *et al.* 1992).

A function known as the switching function plays an important role in determining the optimal migration behaviors. There are two different switching functions used:

$$\sigma_1 = \lambda_1 - \theta k \text{ and } \sigma_2 = \lambda_1 + \theta k. \quad (6.34)$$

When the co-state variable associated with displacement is positive, σ_1 is used as the switching function; otherwise, σ_2 is the best choice. It turns out that behavioral changes will be determined by a change in sign of one of these switching functions. [1]

6.3.2.1 When the co-state variable λ_1 is positive

In this section, I present the optimal behavior results when the co-state variable associated with displacement is positive. There are three types of behavior that the fish show at any time: 1) a predator avoidance and feeding behavior and 2) an active migration behavior 3) a behavior intermediate to (1) and (2) that represents a singular case (FIGURE 6.1). These three behaviors correspond to when the switching function, σ_1, is negative, positive, and zero, respectively.

1. In linear optimal control problems involving a single control variable, the switching function is the multiplier of the control variable, as it appears in the Hamiltonian. It indicates whether the maximum or minimum value of the control variable is optimal. When the switching function is zero, there are infinitely many values of the control variable that maximize the Hamiltonian, and it is possible that the solution admits a *singular control*. The control problem presented here is not linear. However, the Hamiltonian is piecewise linear in $u + v$, the migration velocity. When the migration velocity is positive, its multiplier is σ_1; when negative, its multiplier is σ_2. It turns out, in maximizing the Hamiltonian, that the sign of the function, σ_1, provides the best indicator of the optimal controls when the co-state variable λ_1 is positive, and σ_2 provides the best indicator when λ_1 is nonpositive.

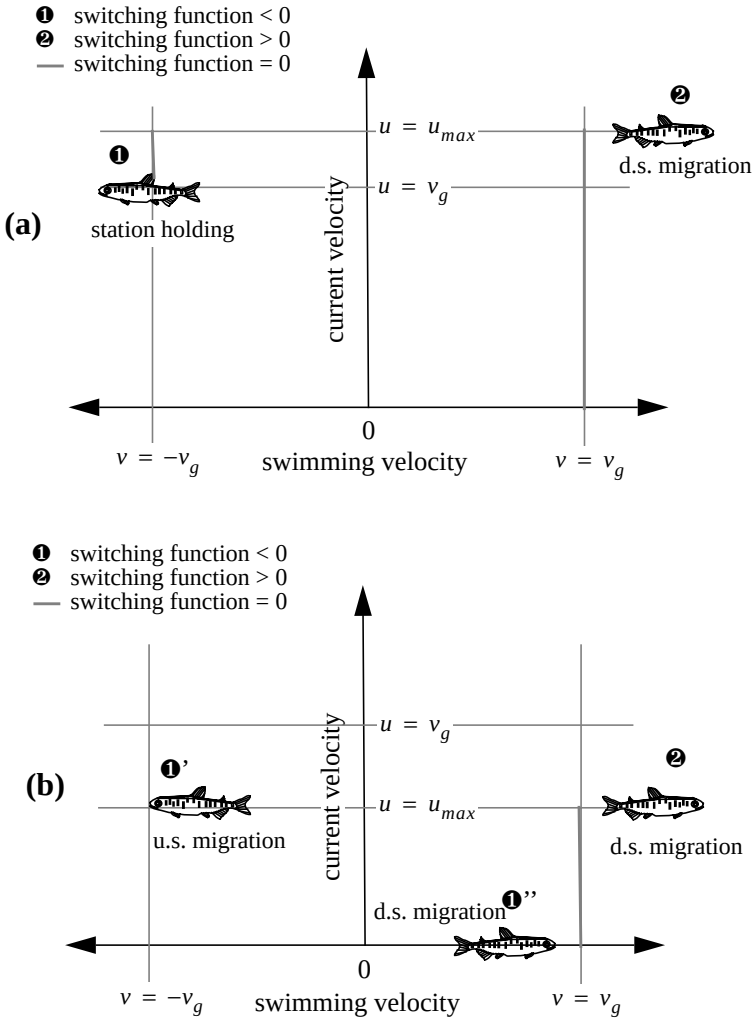

FIGURE 6.1 Optimal current and swimming velocities as determined by maximizing the Hamiltonian when λ_1 is positive.[a] In figure (a) the maximum current velocity exceeds the maximum growth speed. In figure (b) the reverse is true. When the switching function σ_1 is negative, ❶, behavior is driven by predator avoidance and feeding. When it is positive, ❷, behavior is driven by the need to migrate to the ocean and take advantage of its tremendous growth potential. When it is zero, behavior is intermediate to ❶ and ❷, and the current velocity is not uniquely determined (unless $u_{\max} = 0$).

[a] In all cases I assumed that the maximum swimming speed exceeded the maximum growth speed.

TABLE 6.5 Optimal choices of current velocity corresponding to different choices of the swimming velocity when λ_1 is positive.

Case Number	Sign of Switching Function σ_1	Swimming Velocity Condition	Optimal Current Velocities
1	+	none	$u^* = u_{max}$
2a	-	$v > 0$	$u^* = 0$
2b	-	$u_{max} + v < 0$	$u^* = u_{max}$
2c	-	$v \leq 0 \leq u_{max} + v$	$u^* = -v$
3a[a]	0	$v > 0$	$u^* = [0, u_{max}]$
3b	0	$u_{max} + v < 0$	$u^* = u_{max}$
3c	0	$v \leq 0 \leq u_{max} + v$	$u^* = [-v, u_{max}]$

Three different cases arise, depending on the sign of the switching function. Optimal current velocity depends on the sign of the switching function and the swimming velocity.

In cases 3a and 3c there is no single optimal choice for the current velocity. This is the case where the switching function is zero, and the problem may admit a singular path.

The results of the Hamiltonian maximization can be divided into three different cases depending on the sign of the switching function σ_1. In the following analysis, each of the three cases characterized by the sign of the switching function is considered separately, and I determine the optimal current and swimming velocities associated with each (TABLE 6.5). To guide intuition, recall that the switching function σ_1 is the difference of the marginal value of an increment in downstream displacement, λ_1, and the predation gradient, θk, which represents the marginal predation risk of migration over this increment of downstream displacement. When the predation gradient is small relative to λ_1, making σ_1 positive, downstream migration is optimal; otherwise, a behavior that keeps immediate predation risk low is best.

6.3.2.1.1 A positive switching function ($\sigma_1 > 0$)

When the predation gradient, θk, exceeds λ_1, then the switching function is positive and the optimal current velocity is known to be u_{max} (TABLE 6.5). A plot of the Hamiltonian along the curve $u = u_{max}$ shows that the optimal velocity is given by $\bar{v} = min(v', v_{max})$, where v' satisfies

$$\sigma_1 + \lambda_2 g_v(v', w, t) = 0. \tag{6.35}$$

When there is not solution to (6.35), then the maximizing velocity is $v^* = 0$. This occurs when $\sigma_1 + \lambda_2 g_v|_{v=0} < 0$, where g_v is a right-hand derivative. This represents an extreme case in which an increase in swimming velocity above zero serves only to decrease growth.

Overall, the behavior when the switching function is positive can be characterized as an *active downstream migration behavior*; a behavior driven more by the need to migrate than by immediate feeding and predator avoidance. A fish's best option is to actively migrate downstream, swimming in the swiftest current. Its swimming velocity is zero (in the case of severely depressed growth), or greater than its optimal growth velocity (provided that the optimal growth velocity does not exceed the maximum swimming speed, v_{max}).

6.3.2.1.2 A negative switching function ($\sigma_1 < 0$)

When predation gradient, θk, is less than λ_1, then the switching function is negative and the optimal current velocity lies along the curve

$$u = \begin{cases} 0 & if \quad v > 0 \\ u_{max} & if \quad v < -u_{max} \\ -v & if \; -u_{max} \le v \le 0 \end{cases} .$$

Optimizing the Hamiltonian over this curve yields the desired optimal swimming velocity (TABLE 6.6). The optimal strategy can be more complicated when the switching function is negative than when it is positive. When the switching function is positive, the optimal strategy is always downstream migration. When it is negative, the optimal strategy may involve no migration, downstream migration, or even upstream migration, *depending on the value of the maximum current speed* relative to the maximum growth velocity. When the maximum current speed exceeds the maximum growth speed, then the fish holds station, swimming against the current at a rate that maximizes growth. Here, the fish has the best of both worlds: it minimizes its expected risk of predation (its predator encounter rate is smallest when stationary), and it maximizes its growth.

What happens when the maximum current velocity drops below the maximum feeding speed? One thing is known for sure: it is *impossible* for a fish to have the best of both worlds. For if it minimizes predation risk by remaining stationary (with respect to the substrate), its growth is not maximal, and conversely, if its growth is maximal (*i.e.*, it is swimming at its maximum growth speed), then its predator encounter rate is not minimal since it is not stationary. The fish must choose a swimming velocity that balances the trade-off between feeding and predation, and this means that the optimal strategy will consist of swimming more slowly than the optimal growth speed while migrating either upstream or downstream. When the maximum current velocity is zero, downstream migration is optimal and the optimal current velocity choice is zero. When the maximum

current velocity approaches the optimal growth speed, *upstream migration* is optimal and the optimal current velocity choice is u_{max}.

The possibility of upstream migration is surprising since, in essence, migrating upstream serves to increase the length of the migration route, and consequently the number of predator encounters. What compensates for this detriment? The answer is—growth during the upstream migration. Recall that predator encounters are less likely to lead to capture if the juvenile is larger. Therefore, if the maximum current velocity is less than the maximum growth speed, the juvenile may opt to swim upstream near its maximum growth speed (and in the swiftest current to reduce predator encounters), with the benefit of increased growth, and hence the possibility of better survival, *even though the strategy is known to lead to a greater number of encounters.*

TABLE 6.6 Optimal swimming velocity summary when the switching function σ_1 is negative.[a]

Possibility	u_{max} Condition	Optimal current and swimming velocities
i	$\tilde{v}_g < u_{max}$	$u^* = -v^*,\ v^* = -\tilde{v}_g$
iia	$0 \le u_{max} \le \tilde{u}_{crit}$	$u^* = 0,\ 0 \le v^* \le \tilde{v}_g$
iib	$0 < u_{crit} < u_{max} \le \tilde{v}_g$	$u^* = u_{max},\ -\tilde{v}_g \le v^* \le -u_{max}$
iic	$v_{max} > u_{max} = u_{crit} > 0$	Velocities given in (iia) and (iib) are both optimal.

Here the switching function is negative. The optimal swimming velocity depends on the value of u_{max} relative to the constrained maximum growth velocity $\tilde{v}_g = min(v_g, v_{max})$. When the maximum current velocity exceeds $\tilde{v}_g$ (possibility i), the juvenile optimally holds station swimming against the current at its optimal growth speed. If the maximum current velocity does not exceed the constrained maximum growth speed (possibility iia–c), the optimal velocities depend on the maximum current velocity relative to a critical value, u_{crit} or the constrained critical current velocity $\tilde{u}_{crit} = min(u_{crit}, v_{max})$.

[a] In iia-b the optimal swimming velocity is unique and lies in the specified interval.

6.3.2.1.3 Switching function zero ($\sigma_1 = 0$)

When the switching function is zero, the optimal swimming velocity is found by maximizing the Hamiltonian over the region

$$u = \begin{cases} [0, u_{max}] & if \quad v > 0 \\ \{u_{max}\} & if \quad v < -u_{max} \\ [-v, u_{max}] & if \ -u_{max} \le v \le 0 \end{cases}.$$

This maximization problem does not yield a unique current and swimming velocity (TABLE 6.7). Rather, unless $u_{max} = 0$, there are infinitely many current velocities maximizing the Hamiltonian. One consistent result, however, is that the optimal swimming speed is always $min\,(v_g, v_{max})$.

This case may correspond to a singular path. Although maximizing the Hamiltonian does not produce unique values of the current and swimming velocity when the switching function is zero, it does not mean that the optimal controls are not unique. More analysis is needed, and dynamics must be considered (See “The canonical equations and optimal control parameters” on page 138). It is also possible that the switching function is zero for only an instant of time, ruling out the possibility of a singular path.

TABLE 6.7 Optimal swimming velocities when the switching function σ_1 is zero.

Possibility	u_{max} Condition	Optimal Velocities
i	$\tilde{v}_g \leq u_{max}$	$u^* = [\tilde{v}_g, u_{max}]$ and $v^* = -\tilde{v}_g$, or
		$u^* = [0, u_{max}]$ and $v^* = \tilde{v}_g$
ii	$u_{max} < \tilde{v}_g$	$u^* = [0, u_{max}]$ and $v^* = \tilde{v}_g$

Here the switching function is zero. As in case 2, the optimal velocities depend on the maximum current velocity relative to the constrained maximum growth velocity. Regardless of the value of u_{max}, the optimal current velocity is not uniquely determined, while the swimming speed, $|v^*|$, is always equal to the constrained maximum growth speed. When $u_{max} < \tilde{v}_g$, the juvenile swims with the current, but when $\tilde{v}_g \leq u_{max}$, the juvenile optimally swims either with the current or against the current.

6.3.2.2 When the co-state variable λ_1 is nonpositive

In this section, I derive optimal behavior when the co-state variable associated with displacement is nonpositive (meaning that the marginal value of displacement downstream is zero or negative). The results show that there are three types of behavior that a fish shows at any given time: 1) predator avoidance and feeding, 2) active *upstream* migration, or (3) a behavior intermediate to (1) and (2) (FIGURE 6.1). These three behaviors correspond to when the switching function, σ_2, is positive, negative, and zero, respectively.

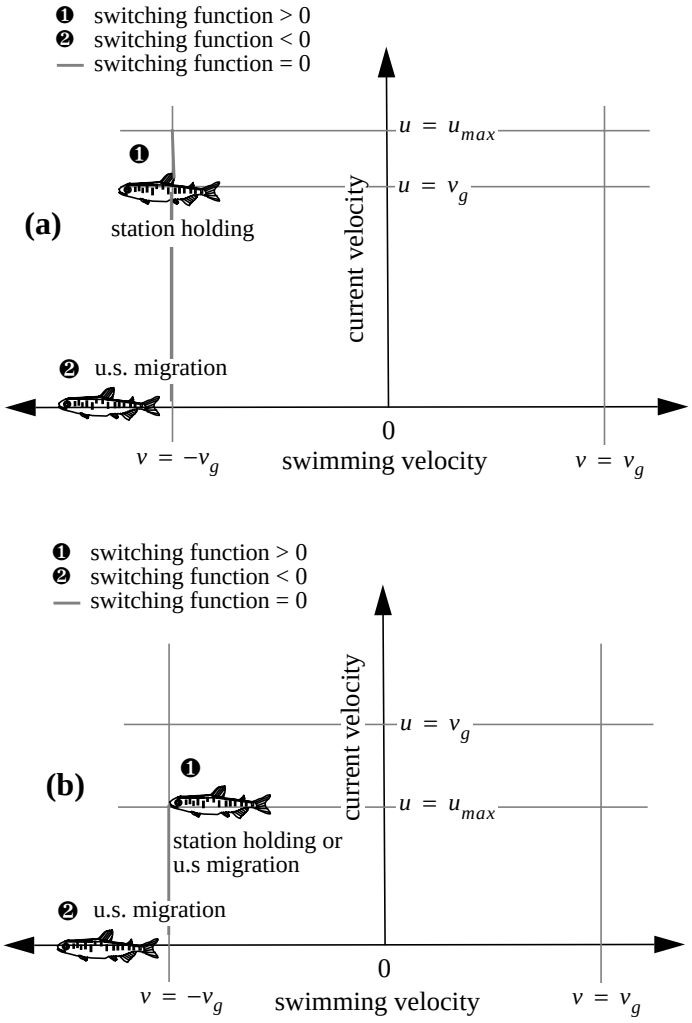

FIGURE 6.2 Optimal current and swimming velocities as determined by maximizing the Hamiltonian when λ_2 is nonpositive.[a] In figure (a) the maximum current velocity exceeds the maximum growth speed. In figure (b) the reverse is true. When the switching function σ_2 is positive, ❶, behavior is driven by predator avoidance and feeding—fish swim in the swiftest current holding station, or moving upstream. When it is negative, ❷, behavior is driven by the need to migrate upstream. When it is zero, a behavior intermediate to ❶ and ❷ is best.

[a] In all cases I assumed that the maximum swimming speed exceeded the maximum growth speed.

TABLE 6.8 Optimal choices of current velocity corresponding to different choices of the swimming velocity when λ_1 is nonpositive.

Case Number	Sign of the Switching Function σ_2	Swimming Velocity Condition	Optimal Current Velocities
1	-	none	$u^* = 0$
2a	+	$v > 0$	$u^* = 0$
2b	+	$u_{max} + v < 0$	$u^* = u_{max}$
2c	+	$v \le 0 \le u_{max} + v$	$u^* = -v$
3a	0	$v > 0$	$u^* = 0$
3b	0	$u_{max} + v < 0$	$u^* = [0, u_{max}]$
3c	0	$v \le 0 \le u_{max} + v$	$u^* = [0, -v]$

Three different cases arise, each depending on the sign of the switching function. Optimal current velocity depends on the sign of the switching function and the swimming velocity.

In cases 3a and 3c there is no single optimal choice for the current velocity. This is the case where the switching function is zero, and the problem may admit a singular path.

6.3.2.2.1 A negative switching function ($\sigma_2 < 0$)

When the predation gradient, θk, is less than $|\lambda_1|$, then the switching function σ_2 is negative and we need only optimize the Hamiltonian along the curve $u = 0$ (TABLE 6.5). A plot of the Hamiltonian restricted to this curve shows that the optimal velocity is given by $v^* = -min(|v''|, v_{max})$, where $v'' < 0$, and satisfies

$$\sigma_2 + \lambda_2 g_v(v'', x, w, t) = 0. \tag{6.36}$$

If $\sigma_2 + \lambda_2 g_v|_{v=0} > 0$ (g_v is a left-hand derivative), then (6.36) has no solution, and the maximizing swimming velocity is $v^* = 0$. This is an exceptional case where growth is so depressed that an increase in swimming speed above 0 decreases growth.

Overall, when the switching function σ_2 is zero, an *upstream migration behavior* is optimal. It is a behavior which is driven more by the need to migrate than by freshwater

predator avoidance and feeding. A fish's best option is to actively migrate upstream, swimming in the slowest current (typically nearshore). The optimal swimming velocity greater than its optimal growth velocity (provided that the optimal growth velocity does not exceed the maximum swimming speed, v_{max}), or zero if growth is too depressed.

6.3.2.2.2 A positive switching function ($\sigma_2 > 0$)

When the predation gradient, θk, is less than $|\lambda_1|$ the switching function is negative and the optimal current velocity lies along the curve

$$u = \begin{cases} 0 & if \quad v > 0 \\ u_{max} & if \quad v < -u_{max} \\ -v & if \quad -u_{max} \le v \le 0 \end{cases} \quad \text{(TABLE 6.6).}$$

TABLE 6.9 Optimal swimming velocity summary when the switching function σ_2 is positive.

Possibility	u_{max} Condition	Optimal current and swimming velocities
i	$\tilde{v}_g < u_{max}$	$u^* = \tilde{v}_g,\ v^* = -\tilde{v}_g$
iia	$u_{max} < \tilde{v}_g$ & $\lambda_2 g_v(-u_{max}, x, w, t) + \sigma_2 \le 0$	$u^* = u_{max}$, $v^* = -min(\lvert v'' \rvert, v_{max})$
iib	$u_{max} < \tilde{v}_g$ & $\lambda_2 g_v(-u_{max}, x, w, t) + \sigma_2 > 0$	$u^* = u_{max},\ v^* = -u_{max}$

The optimal swimming velocity depends on the value of u_{max} relative to the constrained maximum growth velocity $\tilde{v}_g = min(v_g, v_{max})$. When the maximum current velocity exceeds the constrained maximum growth speed (possibility i), the juvenile optimally holds station swimming against the current at its (constrained) optimal growth speed. If the maximum current velocity does not exceed the constrained maximum growth speed (possibility iia–b), the optimal velocities depend on the sign of $\lambda_2 g_v(-u_{max}, x, w, t) + \sigma_2$. The optimal behavior is characterized by station holding (in i and iib) or upstream migration in slack current at a swimming velocity that does not exceed the maximum growth speed.

The optimal strategy can be more complicated when the switching function σ_2 is positive than when it is negative. When the switching function is negative, the optimal behavior is

always upstream migration. When positive, the optimal strategy may involve upstream migration or station holding, *depending on the value of the maximum current speed relative to the maximum growth velocity.* When the maximum current speed exceeds the maximum growth speed, then the fish holds station, swimming against the current at a rate that maximizes growth. Here, the fish has the best of both worlds: it minimizes its expected risk of predation (its predator encounter rate is smallest when stationary), and maximizes growth.

When the maximum current velocity drops below the maximum feeding speed it is impossible for a fish to have the best of both worlds. For if it minimizes predation risk by remaining stationary (with respect to the substrate), its growth is not maximal, and conversely, if its growth is maximal (*i.e.*, it is swimming at its maximum growth speed), then its predator encounter rate is not minimal since it is not stationary. The fish must choose a swimming velocity that balances the feeding and depredation tradeoffs, and this means that the optimal strategy will consist of swimming more slowly than the optimal growth speed, holding station or moving upstream, always in the most rapid current.

6.3.2.2.3 Switching function zero ($\sigma_2 = 0$)

When the predation gradient, θk, equals λ_1, the switching function is zero, and the optimal swimming velocity is found by maximizing the Hamiltonian over the region

$$u = \begin{cases} 0 & if \quad v > 0 \\ [0, u_{max}] & if \quad v < -u_{max} \\ [0, -v] & if \; -u_{max} \le v \le 0 \end{cases} .$$

Unless $u_{max} = 0$, this maximization problem does not yield a unique current and swimming velocity (TABLE 6.7). Rather, there are infinitely many current velocities maximizing the Hamiltonian. One consistent result, however, is that the optimal swimming speed is always $-min(v_g, v_{max})$. This case may correspond to a singular path (compare to $\sigma_1 = 0$).

TABLE 6.10 Optimal swimming velocities when the switching function σ_2 is zero.

Possibility	u_{max} Condition	Optimal Velocities
i	$\tilde{v}_g \leq u_{max}$	$u^* = [0, \tilde{v}_g]$ and $v^* = -\tilde{v}_g$, or
ii	$u_{max} < \tilde{v}_g$	$u^* = [0, u_{max}]$ and $v^* = -\tilde{v}_g$

As in case 2, the optimal velocities depend on the maximum current velocity relative to the constrained maximum growth velocity. Unless $u_{max} = 0$, the optimal current velocity is not uniquely determined, while the swimming velocity is always equal to the negative of the constrained maximum growth speed. Notice that it is always optimal to swim against the current, and that since the migration velocity is always nonpositive, migration is allowed only in the upstream direction.

6.3.3 The canonical equations and optimal control parameters

The next step in the maximum principle is to develop a system of simultaneous differential equations called the canonical equations, whose solution gives the optimal state and co-state paths. The canonical equations consist of a set of four ordinary differential equations that govern the change in the optimal state variables and the co-state variables over time. To begin with, define

$$H^* = H|_{(u, v) = (u^*, v^*)}, \tag{6.37}$$

so that H^* is a function that does not include the control variable arguments—it is a function of x, w, λ_1, λ_2 and t alone.

According to the maximum principle, the co-state variables satisfy

$$\dot{\lambda}_1 = -H_x^* \text{ and} \tag{6.38}$$

$$\dot{\lambda}_2 = -H_w^*; \tag{6.39}$$

and the optimal state variables must satisfy the original state equations evaluated at u^* and v^*, namely

$$\dot{x} = u^* + v^* \text{ and} \tag{6.40}$$

$$\dot{w} = g|_{v^*}. \tag{6.41}$$

Recall that, in general, the policy functions, u^*, v^*; depend on $x, w, \lambda_1, \lambda_2, t$. Therefore, equations (6.38)–(6.41) represent a system of four simultaneous differential equations in 4 variables, without explicit dependence on u and v. These are the canonical equations. In the next section the boundary conditions will be specified, making it possible to solve these equations.

6.3.4 Transversality conditions

So far, only three boundary conditions are available for the canonical equations: $x(t_0) = 0$, $w(t_0) = w_0$, and $x(t_f^*) = a$; and furthermore, t_f^*, t_e^*, and t_s^* are unknown. It is therefore impossible to solve the system of equations without another boundary condition, and the values of t_f^*, t_e^*, and t_s^*. All of this information is supplied by the *transversality conditions*:

$$\lambda_2(t_f^*) = \Phi_w|_{w=w(t_f^*)},\ (\Phi_{t_f} + H)|_{t=t_f^*} = 0,\ \Phi_{t_e}|_{t_e=t_e^*} = 0, \text{ and } \Phi_{t_s}|_{t_s=t_s^*} = 0, \tag{6.42}$$

where I assume that $t_f^* < t_e^* < t_s^*$, (*i.e.*, ocean residence and estuarine residence time are not zero).

To summarize, the necessary conditions consist of a total of 4 canonical equations with three boundary conditions specified at the outset, and 4 transversality conditions. These 4 transversality conditions supply the 4th condition needed to solve the canonical equations as well as a set of 3 equations for determining the optimal values of the 3 control parameters, t_f^*, t_e^*, and t_s^*. The canonical equations, along with their boundary conditions, comprise a *two point boundary value problem* which can, in theory, be solved using some numerical routine. Two popular methods for solving this type of problem are the *shooting method* and the *relaxation method* (Press *et al*., 1988).

6.4 Summary

The optimal control problem was presented in a form that allowed application of the maximum principle. To avoid the need to resort to nonsmooth techniques, dependence of the control variable constraints on the state variables was omitted. In addition, for simplicity, the dependence of predator density on current velocity was also omitted. Once the problem was specified, the maximum principle was applied: the Hamiltonian was maximized with respect to the control variables to obtain the policy functions, the co-state and state equations were defined, and the transversality conditions were developed to supply enough boundary conditions to provide a boundary condition for the canonical equations and to determine the optimal control parameters.

A remarkable amount of information about the optimal controls was gleaned by simply maximizing the Hamiltonian (FIGURE 6.1). One important result is that optimal behavior

is largely controlled by the sign of the switching function (defined as σ_1 when $\lambda_1 > 0$, and σ_2 otherwise).

First focussing on the case where a marginal increase in downstream displacement is beneficial to fitness (*i.e.*, $\lambda_1 > 0$), the sign of the switching function σ_1 is informative. When it is positive, active downstream migration is optimal: the fish swims downstream in the swiftest current, at a speed that exceeds the maximum growth speed (if the maximum swimming speed permits).

When the switching function, σ_1, is negative, there are three possibilities: (i) if the maximum current velocity exceeds the maximum growth speed, then the fish holds station, migrating against the current, swimming at its maximum growth speed; (ii) otherwise, the juvenile either (a) migrates upstream, swimming in the most rapid current, and at a swimming velocity that exceeds the maximum current velocity, but is less than the optimal growth velocity or (b) swims downstream in a current of zero velocity, and at a swimming velocity that does not exceed the optimal growth velocity. Option (a) is optimal when the maximum current velocity is close to zero (relative to the maximum growth velocity), and option (b) is optimal when it is close to the maximum growth velocity.

When the switching function σ_1 is zero, maximizing the Hamiltonian gives more limited knowledge of the optimal controls. If the maximum current velocity exceeds the maximum growth speed, then one of two behaviors is optimal: (a) the fish swims against the current at its maximum growth speed and in a current velocity at least as great as its maximum growth speed; (b) the fish swims downstream in a current velocity not exceeding its maximum current velocity, with a swimming speed equal to its maximum

growth speed. Notice that, unless $u_{max} = 0$, the optimal current velocity is not uniquely determined, but is only known to lie in an interval; the swimming *speed*, however, always equals the maximum growth speed. If the maximum current velocity is less than the maximum growth speed, then option (a) is optimal.

Focussing next on the case where the co-state variable associated with displacement is nonpositive, the sign switching function σ_2 largely characterizes the optimal behaviors. When it is negative, a fish displays upstream migration behavior, swimming in slack current or near the shore ($u = 0$), while swimming upstream at a speed that exceeds the maximum growth speed (if the maximum swimming speed allows).

When the switching function σ_2 is positive, a fish shows feeding and predator avoidance behavior, but there are actually three possible behaviors based on the maximum current velocity. (a) If the optimal current velocity exceeds the maximum growth velocity, the fish holds station, swimming against the current at their maximum growth speed. Otherwise, the fish swims in the swiftest current either (b) holding station, or (c) migrating upstream with a swimming speed between the maximum growth speed and the maximum current velocity. Only one of these three behaviors is optimal at any given time.

When the switching function σ_2 is zero, a fish displays a behavior intermediate to when σ_2 is positive or negative. Unless $u_{max} = 0$, the optimal behavior is not actually uniquely determined by this case, and further analysis of the canonical equations is needed. However, it is known that the fish swims upstream at its constrained maximum growth velocity, swimming in any current from 0 to $min\,(\tilde{v}_g, u_{max})$.

This analysis shows that when the co-state variable associated with displacement is nonpositive, no downstream migration strategy is ever optimal.

6.5 Discussion

Probably the most useful result of this section is that behaviors are largely determined by the switching functions and the difference between the maximum current velocity and the maximum growth velocity. When the co-state variable associated with displacement is positive, the switching function is σ_1, and represents difference between (i) the marginal change in future fitness for a marginal increase in downstream displacement and (ii) the probability of death over a marginal increase in downstream displacement. The analysis shows that when the marginal value of and increment in downstream position exceeds the marginal cost of predation over that distance increment, then the juvenile optimally migrates downstream. This corresponds to the case where the switching function σ_1 is positive. The optimal behavior, at this point, is driven more by selection pressure to migrate to the ocean than pressure to avoid predators or feed. Because, during active migration, predation risk is not minimal and growth is not maximal (unless $v_{max} \leq v_g$).

What happens when the switching function σ_1 is negative? In this case, the fish is averse to active migration. Although the fish *will* move under low maximum current velocity conditions, behavior is driven more by feeding and predator avoidance. Movements when σ_1 is negative are more properly referred to as *appetitive movements* (Southwood, 1962) rather than migration. When maximum current velocity exceeds maximum growth speed, then the fish enjoys the best of both worlds—minimal predation and maximum growth—by holding station and swimming against the current at its optimal growth speed. If, on the

other hand, maximum current velocity is less than the maximum growth speed, the fish must make the best of a bad situation and some unexpected behavior ensues. For example, it is possible for the fish to move upstream! This occurs when the benefit to growth during the upstream movement (in the form of reduced predation risk in the future and other size-related benefits), exceeds the cost of greater predator encounters during this upstream movement. The other possibility (when maximum current velocity is less than the maximum growth speed) is that the fish moves downstream in a river current of zero (*i.e.*, near shore) with a swimming velocity less than is maximum growth speed. Here the fish accepts a higher predator encounter rate (*i.e.*, migration velocity is not zero), for the sake of increased growth rate. Another benefit is that less migration distance will need to be covered in the future.

When the switching function σ_1 is zero, maximizing the Hamiltonian produces less information on the optimal migration strategy. However it does appear to be an *intermediate strategy*, lying between the case where migration is the driving force of behavior, and the case where growth and predator avoidance are the driving forces. This case must be explored further by considering the dynamics of the canonical equations. A singular solution may show a smooth transition between growth and predator avoidance-driven behavior, and active migration behavior. If, on the other hand, the switching function σ_1 is zero only for an instant, there will be a abrupt change from one behavior to the other. This issue and others will be explored in later chapters, in which emphasis is placed on obtaining a numerical solution to the control problem.

The above discussion assumed that the co-state variable associated with displacement was positive. When it is nonpositive, the switching function is σ_2 rather than σ_1, and can be

interpreted as the difference between (i) the probability of death over a marginal increase in upstream displacement and (ii) the marginal change in future fitness for a marginal increase in upstream displacement. When this quantity is positive, cost of migration is too great and station holding is optimal; when it is negative, the benefit of upstream movement is high enough that the fish migrates upstream. The case where it is zero represents an intermediate strategy, where neither upstream movement or station holding behavior is better. In this case, the possibility of a singular solution must be explored.

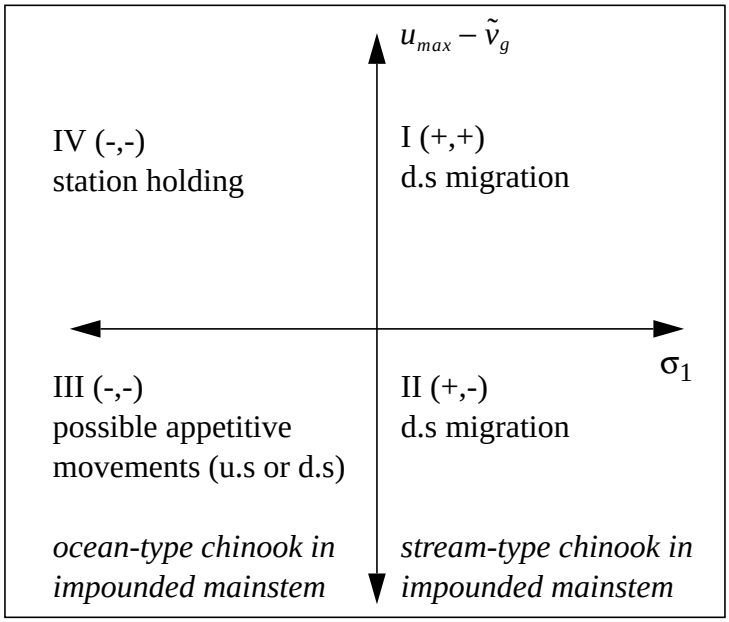

FIGURE 6.3 The juvenile chinook behavior space is partitioned into four quadrants defined by the sign of the switching function σ_1 (assuming $\lambda_1 > 0$) and the difference between the maximum current velocity and maximum growth speed. Behavior in quadrants I and II is characterized as downstream migration; III and IV, as predator avoidance and feeding behavior which involves station holding (III or possibly IV) or appetitive movements (IV only).

How do these model-derived behaviors compare with observed juvenile chinook movements? Observations of movements on the Snake River show that during the "migration" season, stream-type chinook move more swiftly through the Lower Granite reservoir than do ocean-type chinook. Zabel (1994) estimated an average migration rate of 5.22 (km/d) for 17 release groups of stream-type chinook, and 1.41 (km/d) for ocean-type chinook (only 1 release group) during the 1991 season. My optimization results suggest that ocean-type chinook migrate more slowly because their movements are appetitive, characterized by a negative switching function σ_1 and low current velocity. These ocean-type chinook rear in the mainstem of the Snake River, subject to low current velocities of impounded waters where station-holding feeding behavior is suboptimal because delivery rate of food is low, making appetitive movement best. In contrast, stream-type chinook rear in tributaries of the Snake River (*e.g.*, the Salmon and Clearwater Rivers), and when they reach the mainstem of the Snake River are moving more quickly downstream. This suggests that these fish have a positive switching function σ_1 in the mainstem (FIGURE 6.3).

CHAPTER 7 EFFECTS OF FLUCTUATING LIGHT, TURBIDITY, AND CURRENT VELOCITY ON MIGRATION BEHAVIOR

7.1 Introduction

Patterns of migration exhibited in salmon populations appear to be driven in part by fluctuations of light intensity. Migration has observed to occur mostly at night, or in some cases during freshets when turbidity is high. High turbidity can produce nighttime conditions and stimulate a “nighttime” migration response (Junge & Oakley, 1966). Once the juvenile is in a physiological state which predisposes it to downstream migration (*i.e.*, its smolt development is sufficient), a change in light can provide the environmental cue for migration to begin.

None of the previous chapters have dealt with fluctuating light intensity explicitly. However, if I can establish a link between the switching function, discussed in the previous chapter, and light intensity, then its influence can be quantified, because behavior is largely characterized by the switching function. Recall that when the switching function is negative, an active migration behavior is optimal, and when positive, a predator avoidance and feeding behavior is optimal. The switching function is comprised of three elements, the co-state variable associated with downstream displacement, the predator

density, and the capture probability. Fluctuating light levels can influence the capture probability, providing the link to the switching function I seek.

My approach to understanding the influence of fluctuating light levels is to compare solutions in the absence of fluctuating light levels—an *autonomous*[1] case, to solutions in its presence. This represents a controlled experiment—not on nature, but on the dynamic optimization model. What results do I expect? Just as seasonality modulated the fitness function in CHAPTER 4, making certain times of the year better for migration, I expect fluctuating light and current velocity will modulate the fitness functional of this chapter, making certain times of the day and year better for migration than others. So that the effects are not confounded, I eliminate time varying factors not related to current velocity or light, and I make some other simplifying assumptions for ease of model analysis (TABLE 7.2).

1. The term *autonomous* is used to indicate that the underlying canonical equations are not explicit functions of time.

TABLE 7.1 Further model simplifications.[a]

Assumption
The control parameters, t_e and t_s are treated as known
Maximum swimming velocity, v_{max}, is constant
Predator density, θ, and predator search velocity, ζ, are constant
Food density is constant
$t_f(u_{max} + v_{max}) \geq a$, allowing sufficient time to journey to the estuary.
The maximum current velocity exceeds the maximum swimming velocity[b]
Estuarine mortality rate is equal to ocean mortality rate and are constant

[a] The simplifications are in addition to those of the previous chapter.

[b] This simplifies the problem of maximizing the Hamiltonian (see FIGURE 6.1a).

7.2 An autonomous case

The simplest case I consider is an autonomous one that removes explicit time dependence of the model parameters. In this case the influence of light and current velocity fluctuations are deliberately omitted, so that their influence can be quantified later by way of comparison. This represents the “control” simulation. The assumptions for the autonomous case are summarized in TABLE 7.2.

TABLE 7.2 Model assumptions (autonomous case with fixed estuary entry time).[a]

Assumption
The maximum current velocity is constant
The growth function depends only on weight (not on time)
Predation rate depends only on weight (not on time)
Time of estuary entry, t_f, is treated as known

[a] The third and fourth assumptions will be relaxed when fluctuating light levels are considered (See "Light sensitive predation" on page 154)

TABLE 7.3 Optimal control problem (autonomous case with fixed estuary entry time).

Maximize: u, v	$-\int_0^{t_f} (\lvert u+v \rvert + \zeta)\, \theta k(w)\, dt \; + \Phi(w(t_f))$	(objective functional)
Subject to:	$\dot{x} = u + v$	(displacement equation)
	$\dot{w} = g(v, w)$	(weight equation)
	$0 \le u \le U_{max}$	(current velocity constraint)
	$\lvert v \rvert \le v_{max}$	(swimming velocity constraint)

7.2.1 Optimal solution types

By using the maximum principle—maximizing the Hamiltonian and building the canonical equations— it is possible to characterize all solutions to the autonomous case on the based simply on the initial sign of the growth function and the initial sign of the switching function (See APPENDIX C). The maximized Hamiltonian and the canonical

equations are easily determined by the techniques of the last chapter, and are summarized in TABLE 7.3.

TABLE 7.4 Maximum principle applied to the autonomous case.[a]

—Maximized Hamiltonian—

$$H^* = \begin{cases} -\theta\zeta k(w) + \lambda_2 g(v_g, w) & \text{if } \sigma < 0 \\ -(u_{max} + \tilde{v} + \zeta)\,\theta k(w) + \lambda_1 (u_{max} + \tilde{v}) + \lambda_2 g(\tilde{v}, w)^{\text{b}} & \text{if } \sigma > 0 \end{cases}$$

—Canonical Equations—

$$\dot{x} = \begin{cases} 0 & \text{if } \sigma < 0 \\ u_{max} + \tilde{v} & \text{if } \sigma > 0 \end{cases}$$

$$\dot{w} = \begin{cases} g(v_g, w) & \text{if } \sigma < 0 \\ g(\tilde{v}, w) & \text{if } \sigma > 0 \end{cases}$$

$$\dot{\lambda}_1 = 0$$

$$\dot{\lambda}_2 = \begin{cases} -\lambda_2 g_w(v_g, w) + \theta\zeta k_w(w) & \text{if } \sigma < 0 \\ -\lambda_2 g_w(\tilde{v}, w) + (u_{max} + \tilde{v} + \zeta)\,\theta k_w(w) & \text{if } \sigma > 0 \end{cases}$$

—Boundary Conditions—

$$x(t_0) = 0,\ x(t_f) = a,\ w(t_0) = w_0,\ \lambda_2(t_f) = d\Phi/dw$$

[a] The switching function can be zero for only an instant (APPENDIX C), and therefore the case where $\sigma = 0$ is omitted.

[b] $\tilde{v}$ is defined in CHAPTER 6.

For the autonomous optimal control problem presented above, one of the following three behaviors is optimal:

S1. Initially, the juvenile holds its station at $x = 0$, swimming against the current at its optimal growth speed. At some critical weight, it begins migrating downstream, swimming in the swiftest current, and actively swimming downstream at a speed greater than its optimal growth speed. The juvenile does not reach $x = a$ until t_f (assumed fixed).

S2. The juvenile begins migrating immediately after emergence, swimming at a speed greater than or equal to its optimal growth speed, and in the swiftest current. It ceases migration only when $x = a$. If the juvenile reaches a before t_f, then it holds its station at a, swimming against the current at its optimal growth speed.

S3. An infinite number of behaviors is optimal. At each instant the juvenile swims downstream at its optimal growth speed, or against the current at its optimal growth speed. Migration upstream is not permitted.

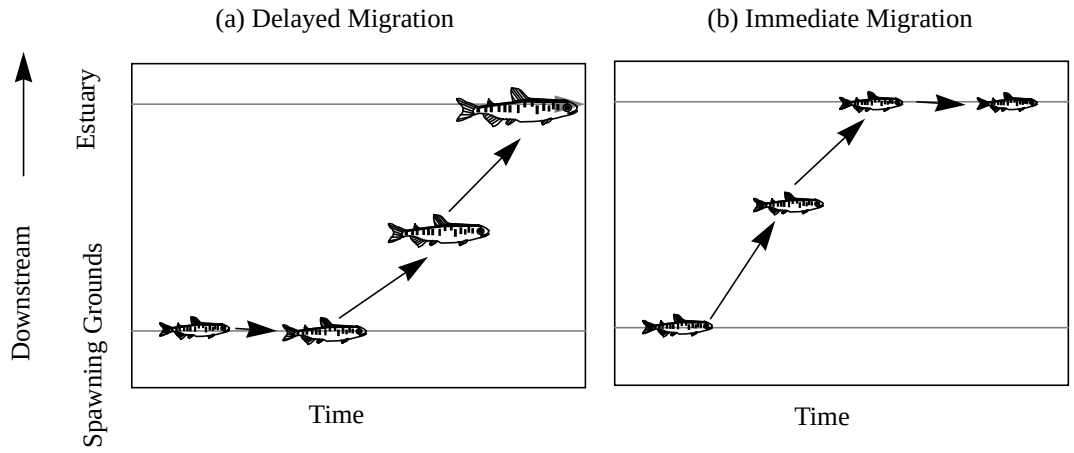

FIGURE 7.1 Optimal strategy types. (a) The juvenile initially holds station until it grows above a critical weight, then continually migrates downstream until it reaches the estuary at t_f (strategy S1). (b) The juvenile begins downstream migration immediately, ceasing only when it reaches the estuary; it then holds station until t_f (strategy S2).

The three strategies S1, S2, and S3 were discovered by considering the initial sign of the growth function evaluated at the maximum growth speed, $\tilde{v}_g(w_0)$, and the initial sign of

the switching function (TABLE 7.5). Be aware that certain sign combinations are impossible.

TABLE 7.5 Optimal strategies based on the initial sign of the growth and switching functions.

	$\sigma(w_0) < 0$	$\sigma(w_0) = 0$	$\sigma(w_0) > 0$
$g(v_g(w_0), w_0) < 0$	Impossible	Impossible	S2
$g(v_g(w_0), w_0) = 0$	Impossible	S3 or S2[a]	S2
$g(v_g(w_0), w_0) > 0$	S1	S2	S2

[a] S3 applies when $T(U_{max} + v_g(w_0)) > a$, S2 otherwise.

Strategy S1, when examined in a more general light, represents a strategy commonly found in juvenile chinook populations. The fish initially demonstrate a feeding and predator avoidance behavior, followed by a rapid downstream migration. The optimization model predicts that this strategy will occur when growth potential is good and the estuary entry time is not chosen too small. Strategy S2 is best when growth is poor, (*i.e.*, $g(v_g(w_0), w_0) < 0$) or when estuary entry time is small.

It is important to recognize the implications of fixing time of estuary entry in the autonomous formulation above. I assumed that the fish must choose a swimming velocity and current velocity schedule that would place them in the estuary at a pre-specified time, t_f. It is not immediately clear that if t_f is allowed to vary, that the three strategies, S1, S2, S3 represent a comprehensive list of optimal strategy types. The results of this section do generalize to the case where t_f is free, however, because the above results apply to *any given* t_f—including the optimal one.

TABLE 7.6 Functions, parameters, and their estimates.

Parameter Description	Parameter or Relationship	Units	Estimate	Data or Parameter Source
Metabolic cost	$M(t)$	$g \cdot s^{-1}$	see reference (chinook)	Hewitt & Johnson (1992)
oxycalorific equivalent	q	$cal \cdot mg^{-1}$	3.42	Webb (1974)
calories to grams conversion factor	c	$g \cdot cal^{-1}$	1.6949×10^{-4}	White & Li (1985)
handling time	$h(w)$	$s \cdot cal^{-1}$	$18w^{-0.69}$	Ware (1978)
reaction field	$\gamma(w)$	m	$0.02w^{0.345}/\sqrt{\pi}$	Ware (1978)
food density	ρ	$cal \cdot m^{-2}$	1.15	
net food conversion efficiency	τ	none	0.7	Brett & Groves (1979)
swimming speed	v	$m \cdot s^{-1}$	.6	Brett (1965)
migration distance	a	km	150	
current speed	u	$m \cdot s^{-1}$	1.0	
initial weight	w_0	g	3.38	
capture probability	$k(w, t)$	none	$\Omega(t)\, w^{-1}$	
predator density	θ	km^{-1}	.15	
predator search velocity	ζ	$km \cdot yr^{-1}$	252.288	
ocean growth rate	$g_o(w)$	$g \cdot yr^{-1}$	$25.870w^{2/3} - 0.7888w$	Parker & Larkin (1959)
ocean mortality rate	$\mu_o(w)$	yr^{-1}	$3.6915w^{-0.7675}$	Ricker (1976)
fecundity	$m(w)$	eggs	$48.94w^{0.548}$	Healey & Heard (1984)
spawning time	t_o	yr	4.0	

7.3 Light sensitive predation

The strategies derived under the assumption of autonomous canonical equations do not show the influence of fluctuating light levels as seen in the cycle of day and night and in situations of high turbidity. Given that predation is influenced by light levels, for example where predators are largely visual predators, light level may influence the capture probability, and consequently the switching function, making migration during low light

levels best. This would mean a flip-flop between an active migration strategy and a feeding and predator avoidance behavior: when light levels fall the active migration behavior is optimal, and when they rise again feeding and predator avoidance behavior is best. This intuitive insight is not complete, as the simulations will show, because migration timing also depends on the fish size. Premature downstream movement, before the fish is of sufficient size to adequately defend against predators in the estuary, or along the migration route is undesirable.

7.3.1 Numerical example (estuary entry time fixed)

This switching behavior can be easily illustrated by specifying a light sensitive capture probability function. For example,

$$k(w,t) = \left(\frac{1}{w}\right) \cdot \Omega(t), \tag{7.1}$$

where the function $\Omega(t)$ represents the influence of light intensity on the capture probability function. As light intensity decreases, it is assumed that $\Omega(t)$ decreases as well, so that the capture probability diminishes with nighttime or during a period of increased turbidity. For the sake of illustration, let

$$\Omega(t) = \begin{cases} 1 - \kappa(16)\,(t-72)^2\,(73-t)^2 & \text{if} \quad 72 < t < 73 \\ 1 & \text{otherwise} \end{cases}, \tag{7.2}$$

so that between 100 and 101 days after emergence, light levels drop due to high turbidity, decreasing the capture probability by a maximum of $100 \times \kappa\%$. On all other days, no decrease in predation rate is assumed to be the result of light fluctuation, but rather as a

result of increasing size. Although the daily fluctuations in light due to the earth's rotation are not explicitly treated here, the example will generalize.

Using the results obtained by maximizing the Hamiltonian (See "The Hamiltonian" on page 137.), and applying the shooting method to solve the resulting two-point boundary problem represented by the canonical equations and their boundary conditions, I obtain numerical solutions. The time of estuary entry, t_f is allowed to vary as a control parameter, and its optimal value is determined by using a numerical function maximizing algorithm known as Brent's Method (Brent, 1973; Press *et al.*, 1988).

7.3.1.1 Singular path?

Another important detail is that, in this example, the switching function cannot be zero for more than an instant of time, and therefore the problem does not admit a singular path. I demonstrate this by showing that if the switching function is zero over an interval, then the capture probability must also be constant over the same interval, leading to a contradiction.

To this end, suppose that the switching function is zero over an interval of time, I. Then since λ_1 is constant over the time horizon,

$$\dot{\sigma} = -\theta\dot{k} = -\theta\,(k_w\dot{w}^* + k_t) = 0 \text{ over } I, \tag{7.3}$$

which further implies that

$$\dot{w}^* = \frac{-k_t}{k_w} = \begin{cases} w^*\dot{\Omega}/\Omega & if \quad 72 < t < 73 \\ 0 & \text{otherwise} \end{cases} \text{ over } I. \tag{7.4}$$

In the example, however, whenever the switching function is zero, $\dot{w}^* > 0$, since $v^* = v_g$, and $g(v_g, w) > 0$ for all feasible values of w. Therefore I can only lie in the interval $(72.5, 73)$.

If a singular path exists, then the functions $\frac{g(v_g, w^*(t))}{w^*(t)}$ and $\dot{\Omega}/\Omega$ would have to be identical over I. However, there is nothing that links these two functions together (when the switching function is zero)—they were chosen independently, and a simple plot shows that for any value of w where they agree, they diverge after a step forward in time. The two functions can only agree for an instant of time, ruling out the possibility of a singular path.

7.3.1.2 The optimal strategy

As the fish grows, the capture probability diminishes, since it is inversely related to fish weight, making the quantity, $\theta k(w, t)$ (I call it the *effective predator density*), gradually smaller. When the turbidity increases, the effective predator density decreases rapidly. When it falls below the value of the co-state variable associated with displacement, the switching function rises to a positive value, and active migration begins (See “A positive switching function” on page 141.). After the turbidity subsides, the switching function falls negative once again and migration ceases in favor of a feeding and predator avoidance behavior (*i.e.*, holding station, and feeding at the maximum growth velocity). Once the fish’s growth drives the switching function positive once again, the fish migrates to the estuary (FIGURE 7.2 & FIGURE 7.2).

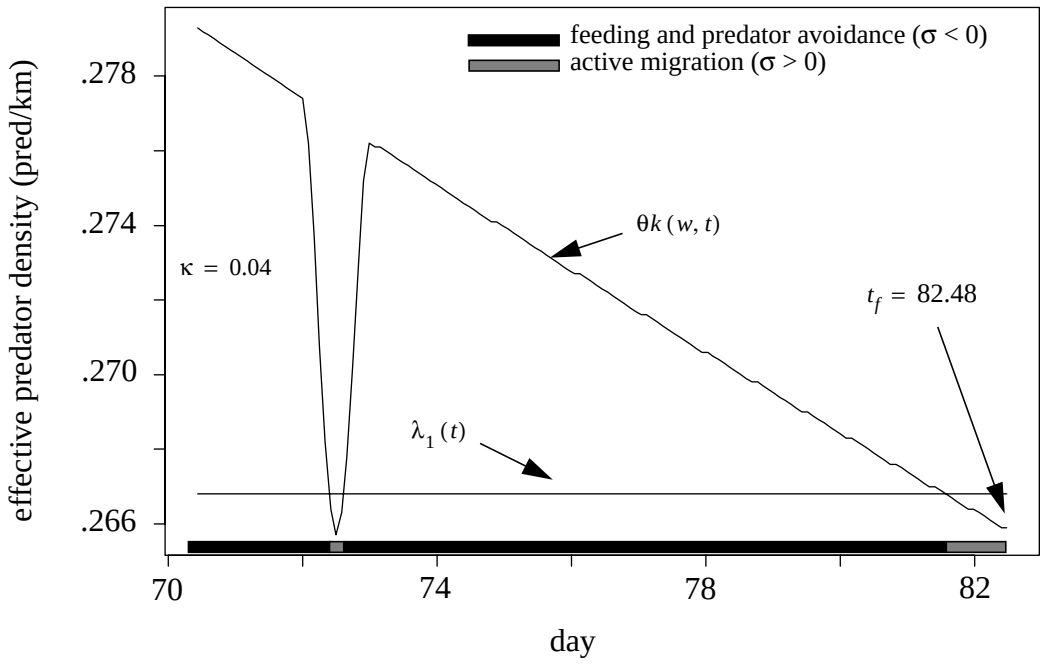

FIGURE 7.2 Effective predator density diminishes due to increased weight of the fish and during the onset of high turbidity. As turbidity subsides, the switching function falls negative and the fish returns to feeding and predator avoidance behavior. As the fish continues to growth, the switching function rises again to a positive value, and the fish resumes active migration. This interrupted migration strategy occurs when the time of estuary entry, t_f, is fixed.

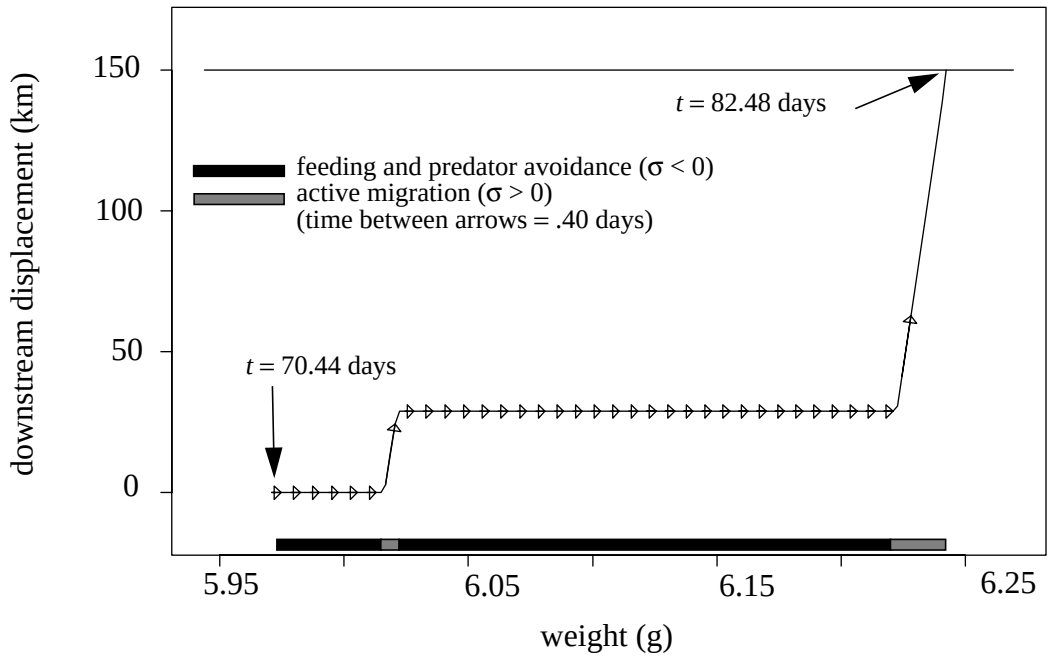

FIGURE 7.3 Downstream displacement plotted as a function of weight. The first increment in displacement is caused by an increase in turbidity, the second by the natural decrease in capture probability due to larger size. When the fish is not migrating downstream, it is holding station showing a feeding and predator avoidance behavior. There is no "critical weight" *per se* at which migration begins. Rather, active migration results from a combination of factors both external and internal—increased turbidity and increased weight.

Without this time fluctuation in the capture probability (or other model parameters and functions), the autonomous case prevails, interrupted migration behavior does not occur —there is simply one switch from feeding and predator avoidance to an uninterrupted, active migration. When fluctuations in capture probability occur, the dips represent windows of active migration opportunity during which predation is lower. By taking advantage of these opportunities, a migrant increases its expected freshwater survival.

There is a catch, however, because in this example, I assumed that the time of arrival in the estuary was fixed, and was not free to vary in the optimization. As this next example shows, when time is allowed to vary, optimal strategies can tend to either ignore the period of lower capture probability (my not migrating) or migrate during the period and continue to migrate to the estuary once it subsides—in other words an interrupted migration does not occur.

7.3.2 Numerical example (estuary entry time free)

In the previous example, I assumed that the time of estuary entry was “fixed”, and discovered an instance when an interrupted migration strategy was optimal. However, as we will discover in this section, this does not mean that this type of strategy is optimal when time of estuary entry is free to vary. In fact, for the functions and parameters used in the previous example (TABLE 7.6), the interrupted migration behavior does not appear to be optimal, regardless of the timing, duration, and magnitude in the decrease in capture probability.

When time of estuary entry is free to vary, there are just two optimal reactions to a decrease in capture probability: it should be ignored (the fish should continue to hold station), or it should stimulate a migration that does not cease until the fish has arrived in the ocean. This is clear from a plot of fitness as a function of estuary entry time. Generally, there are two humps in this curve, each corresponding to a candidate for the optimal time of estuary entry. One hump is due to the period of increased turbidity, and the other to the decreased capture probability due to fish growth (FIGURE 7.4).

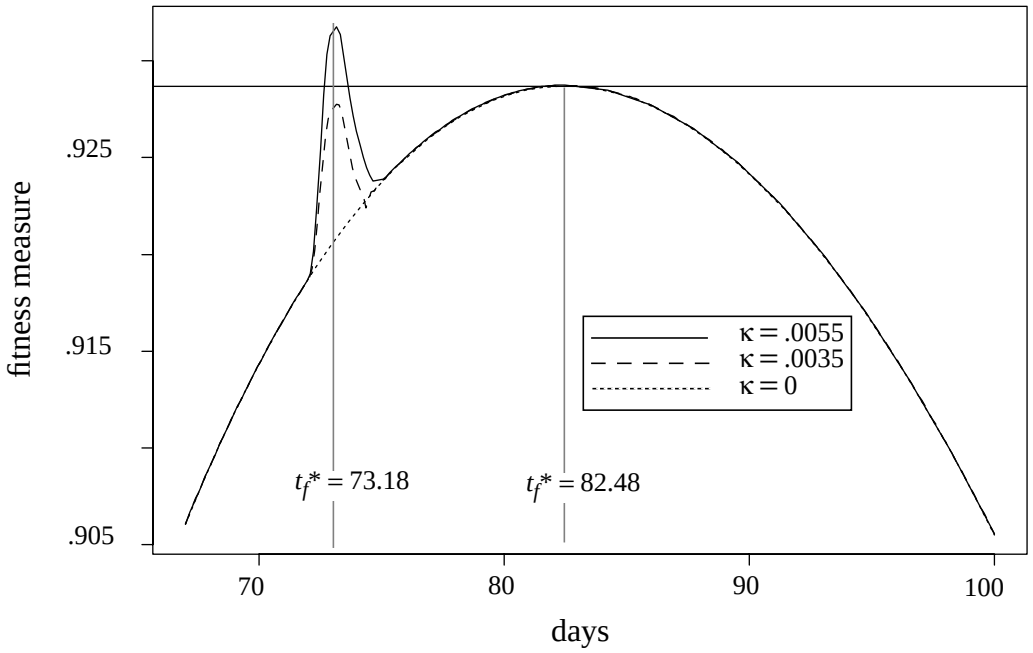

FIGURE 7.4 Influence of turbidity on optimal time of estuary entry. There are two maxima of the fitness curve as a function of estuary entry time, the one on the left, corresponding to the period or turbidity, and the other corresponding to decreased capture probability due to natural growth. As the turbidity intensity parameter, κ, increases from 0, the global maximum switches from $t_f^* = 82.48$ d to the maxima corresponding to an increase in turbidity $t_f^* = 73.18$ d. This fitness curve is bimodal, and estuary entry times lying between the two modes are suboptimal. This leads to two possible optimal behavior (usually only one of which is truly optimal): either ignore the increased turbidity altogether, or initiate an uninterrupted seaward migration.

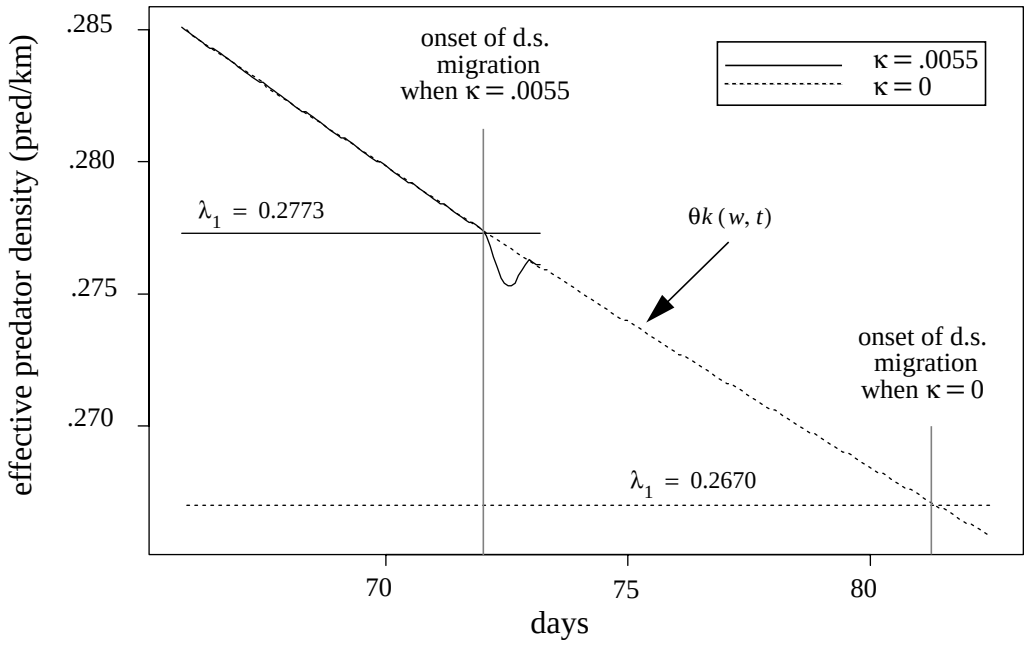

FIGURE 7.5 The co-state variable corresponding to downstream displacement increases in response to a sufficient increase in turbidity intensity parameter, κ. As κ increases from 0 to .0055 (representing a .55% decrease in the capture probability), the co-state variable varies from $\lambda_1 = .2670$ to $\lambda_1 = .2773$, making the switching function positive at an earlier date (8.3 days earlier), and therefore making an earlier migration optimal.

One surprising feature of the sensitivity of migration timing to a period of increased turbidity, is that it may take only a small change in capture probability to induce a much earlier migration. For example, FIGURE 7.5 shows that a .55% decrease in the capture probability over a one day period can induce migration. In the absence of increased turbidity, the capture probability must drop to .2670 before migration begins, but in its presence, the fish optimally migrate when the capture probability does not fall below .2773. Why should migration be so attractive during this minuscule change in capture

probability? (This is especially puzzling since the capture probability does not even come close to the low level necessary for migration in the absence of increased turbidity.) The answer is that earlier migration is attractive not only because of reduced capture probability, but also because of reduced exposure time to predators in freshwater, and longer growth opportunity in the ocean. Juveniles migrating early during elevated turbidity, might suffer greater mortality enroute to the ocean than a juvenile migrating later at a larger size, but suffer lower overall freshwater mortality because of a shorter freshwater residence time, and experience greater growth over its lifetime. This argument hinges on the assumption that an earlier migration is not prohibited by a large decrease in ocean survival for the smaller migrant. Otherwise, a larger decrease in the capture probability might be necessary to make earlier migration optimal.

7.3.2.1 Note on applying the maximum principle

When seasonal or daily fluctuations of model parameters are allowed, the fitness curve is not necessarily a simple concave function with respect to the estuary entry time, t_f, and the transversality condition $H + \Phi_{t_f} = 0$ can yield spurious solutions. In fact, for the example presented above, there are 3 solutions to $H + \Phi_{t_f} = 0$—two maxima and a minimum, only one of which is a global maximum—namely, $t_f^* = 73.18$, which all correspond to critical points of the fitness curve (FIGURE 7.4). Therefore, I take the cautious approach of first plotting the fitness curve as a function of t_f, (as in FIGURE 7.4) to avoid local maxima and minima, and to obtain a bracket on the optimal estuary entry time, t_f^*. Once the global solution is bracketed, I apply an algorithm that uses both inverse parabolic interpolation and golden section search—Brent's method (Press *et al*., 1989).

7.4 Fluctuating current velocity

During a freshet, when capture probability might diminish due to higher turbidity, the maximum current velocity increases. This occurs when there is a greater flow of water through a restricted cross-sectional area. In Davis (1981) all major salmonid outmigration occurred during a phase of a spring freshet, many other studies confirm that increases in flow correspond to higher catches of migrants (Mains & Smith, 1964; Raymond, 1968; Reimers, 1968; Salo, 1969; Wetherall, 1970; Stober *et al.*, 1973; Becker, 1973b; Anonymous, 1976; Kjelson *et al*., 1982; Hopkins & Unwin, 1987). As demonstrated earlier, (See “Light sensitive predation” on page 154) when the freshet grows in strength, turbidity can increase, making outmigration favorable. At the same time, there may be a benefit due to increased current velocity.

If the juvenile is in a sufficiently ready state to migrate to the ocean (*i.e.*, it is approaching the point at which the benefits of migration (better ocean growth) outweigh the costs (mortality), then migration during a freshet can serve to decrease migration time, decreasing the overall exposure time to predators on its seaward journey. To test this hypothesis in simulation, I allow fluctuations in the maximum current velocity over time, keeping all else equal (even turbidity levels), and like the previous section, gauge the simulated influence of increased current velocity on migration behavior.

7.4.1 Numerical example

I simulate the change in maximum current velocity through the equation

$$u_{max}(t) = \Omega_{current}\left(\frac{t - t_1}{t_2 - t_1}\right) \text{ (during a freshet } t_1 \le t \le t_2\text{),} \qquad (7.1)$$

$$\text{and } u_{max}(t) = 1.0 \text{ otherwise.}$$

where $\Omega_{current}(\xi) = 1 + \kappa(16)(\xi)^2(1-\xi)^2$. In this example, there will be a total of four consecutive freshets each lasting one day, starting at day 71,74,77, and 80 respectively. During each freshet, the current velocity increases by $100 \times \kappa\%$. For this example, I assume that the maximum current velocity doubles over the freshet, so that $\kappa = 1$. For the 'control' simulation, the current velocity is held constant at 1.0.

The simulations show that if the freshet is of sufficient duration and intensity, and is timed when the juvenile is in a sufficient state of readiness (*i.e.*, relatively large so that its capture probability is relatively small), then the juveniles optimally migrate with freshets (FIGURE 7.6). This occurs without the additional benefit of high turbidity, because the increased maximum current velocity associated with a freshet, reduces the travel time to the estuary, in turn reducing the time at risk to predators during migration. Mathematically, it occurs because a freshet timed prior to the optimal time of estuary entry in the absence of a freshet, serves to increase the co-state variable associated with downstream displacement, λ_1—a quantity interpreted as the marginal increase brought by an increase in downstream displacement. This means that the switching function turns positive sooner, making migration begin sooner (FIGURE 7.7).

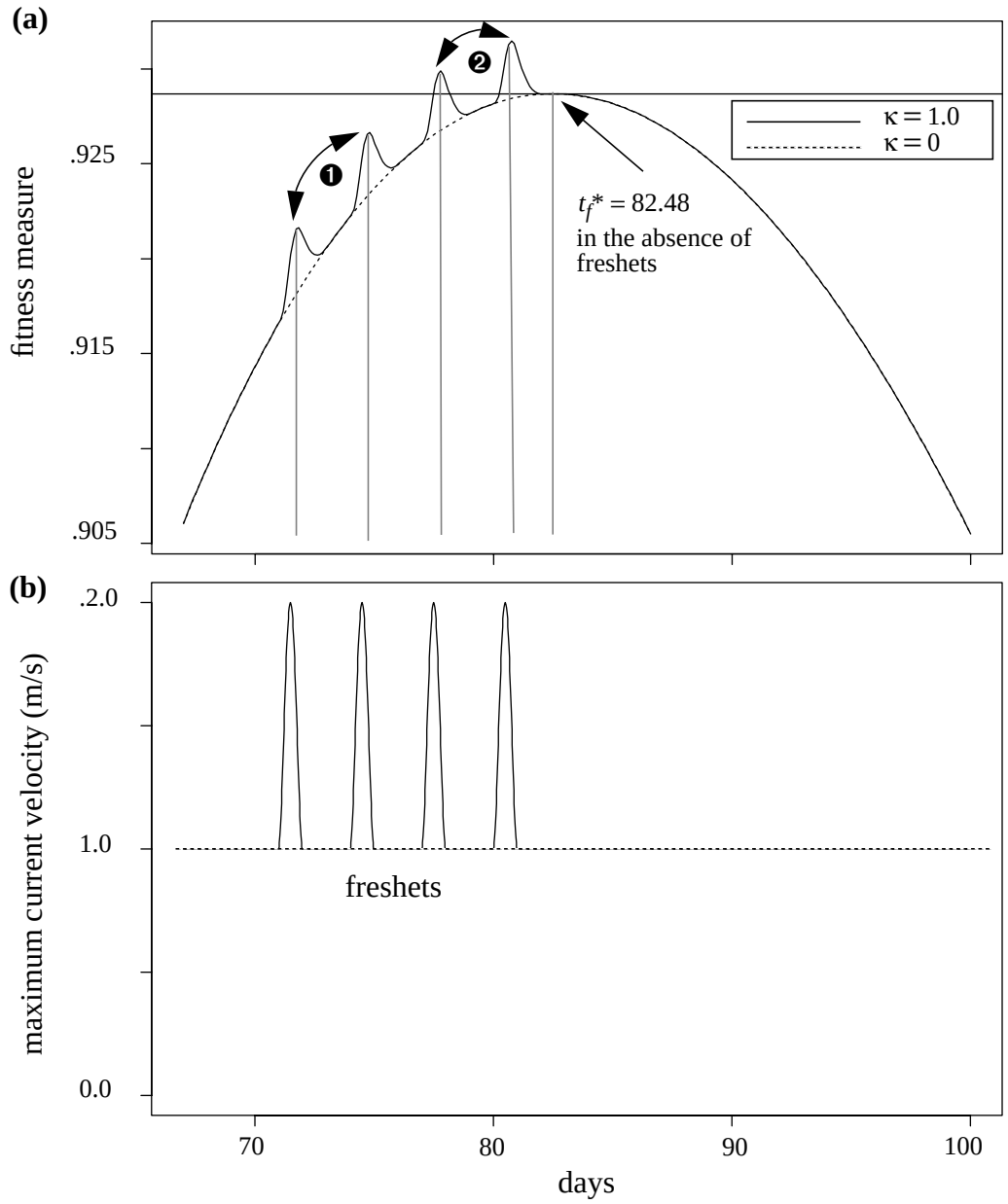

FIGURE 7.6 The influence of freshets on the optimal time of estuary entry. (b) Of the four freshets of equal intensity starting at 71, 74, 77, and 80 days respectively, those timed closest to the optimal time of estuary entry in the absence of freshets, t_f*, have the most influence. t_f* represents a good measure of the approximate time of migration readiness. (a) Freshets that occur too early (relative to t_f*) do not influence time of estuary entry (see ❶), but those that do not occur to early, do have influence (see ❷).

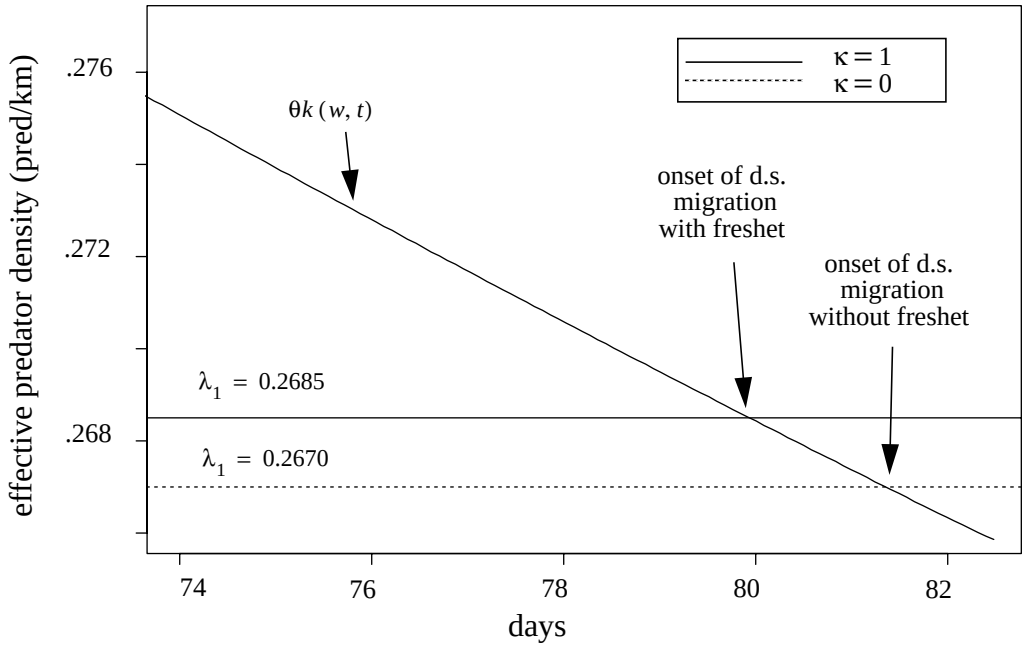

FIGURE 7.7 A well timed freshet can increase the co-state variable associated with displacement, λ_1, making the switching function zero earlier, and therefore leading to earlier seaward migration.

The two examples of fluctuating light levels and maximum current velocity, taken together, demonstrate that there can be two advantages of migrating with freshets: reduced time at risk (due to high current velocity), and lower average capture probability (due to high turbidity).

7.5 Summary

In the first section of this chapter, I developed an exhaustive list of optimal strategy types when time fluctuations in model parameters were ignored (the autonomous case). These strategies were then compared to the optimal strategies in the case where light levels and

maximum current velocities were allowed to fluctuate. This allowed me to gauge the influence of freshets and nighttime on migration behavior. In the autonomous case, one of three behaviors was found to be optimal:

S1. Initially, the juvenile holds station, swimming against the current at its optimal growth speed. At some critical weight, it begins migrating downstream, swimming in the swiftest current, and actively swimming downstream at a speed greater than its optimal growth speed. The juvenile does not reach the estuary until t_f (assumed fixed).

S2. The juvenile begins migrating immediately after emergence, swimming at a speed greater than or equal to its optimal growth speed, and in the swiftest current. It ceases migration only it is about to reach the estuary. If the juvenile reaches the estuary before t_f, then it holds station prior to entering the estuary, swimming against the current at its optimal growth speed.

S3. An infinite number of behaviors is optimal. At each instant the juvenile swims downstream at its optimal growth speed, or against the current at its optimal growth speed, and migration upstream is not permitted.

When time of estuary entry was fixed, it was possible for interrupted migrations, characterized by downstream movement during periods of relatively low capture probability, and station holding when it is higher. When time of estuary entry was allowed to vary in the optimization problem, interrupted migration ceased to be optimal, and the optimal strategy was S1—initial station holding followed by an unceasing seaward migration. In the case of fluctuating capture probability or maximum current velocity, the

reactions of the fish are similar, and exemplified by the optimal reaction to a freshet: either the freshet should be completely ignored (station holding), or the fish should migrate with the freshet, moving nonstop toward the estuary, migrating even after the freshet subsides. Fish ignore a freshet if it is not of sufficient strength or duration, or if it is not timed during a large enough size (*i.e.*, near the time marking the onset of migration in the absence of a freshet.)

7.6 Discussion

The methodology of this chapter follows a that of a controlled experiment, conducted not on nature, but on the dynamic optimality model. The questions posed— "What are the effects of fluctuation daylight? Fluctuating maximum current velocity?", are addressed by first analyzing the model in the absence of these fluctuations (the control), and then in their presence (the treatment). In the autonomous case, there were three strategy types found, with the first— station holding followed by an unceasing migration initiated at a critical weight—optimal whenever growth is initially positive (when maximized by v), and the time of optimal estuary entry is sufficiently greater that $a/(u_{max}+v_{max})$.

Comparing the optimal strategies in the case of fluctuation light levels or current velocity, shows that there are certain windows of opportunity created by lower capture probability (in the case of low light levels) and shorter travel time to the estuary (in the case of current velocity). One thing made clear by the simulations, however, is that migration during these "windows of opportunity" is optimal only if they offer either sufficiently shorter travel time, or capture probability, and if they are properly timed. Those windows of opportunity, timed prematurely are optimally ignored by the fish. In contrast, when it is

timed at a state of migration readiness (in this case, sufficiently near the optimal migration timing in the absence of these windows of opportunity), then the fish optimally migrate during the window of opportunity. I believe this result is crucial, and bears on the proper management of salmon stocks: if we are to increase current velocity in the rivers to aide fish during migration, this increase must be well-timed, synced with the physiological development, or the state of readiness to migrate.

Another result of the model (at least for the calibration used in the numerical examples), is that interrupted migrations do not occur. In fact, the only way I was able to induce a interrupted migration was by fixing the time of estuary entry. This is only a reasonable assumption if the fitness curve peeks at the fixed estuary entry time, t_f, and is very steep in a neighborhood of t_f. This was not what I expected, but after some thought, does make sense, in terms of the model used. Since spatial homogeneity was assumed, there are not special feeding spots that juveniles should migrate to, stop and feed, and continue on their way. Furthermore, fish are assumed to have perfect knowledge of the duration, intensity, and timing of all fluctuations in current velocity, and future growth, disallowing risk-taking behavior such as migrating with and early freshet rather than holding out for later freshet that might not materialize. To capture these types of strategies, a stochastic element and/or spatial heterogeneity must be added.

CHAPTER 8 SUMMARY AND DISCUSSION

8.1 Overview

In this work I focused on the migration behavior of salmon using a behavioral ecology approach. Specifically, I used optimization modelling to show how selective patterns shape geographical patterns of age at migration, seasonal and diurnal migration timing, and current velocity selection. The goal was to suggest explanations or hypothesis of migration behavior that could in turn possibly suggest new experiments and lead to further insight into why salmon behave as they do. In developing the models, I strove for parsimony and respect for the underlying salmon biology.

Like other models of habitat shifts (in this case salmon are shifting from a freshwater to an ocean habitat), I considered the growth and predation risk of both environments, but I also included the special cost of migration itself— in terms of energetic expenditure and predation risk enroute to the ocean. By approaching the problems using optimal control theory, it was possible to characterize optimal current velocity and swimming velocity choices based on the signs of the "switching functions" and the maximum current velocity relative to the swimming speed at which growth is maximal. Numerical and analytic solutions to the static optimization models (used in earlier chapters) led to insights into the selective pressures associated with of migration distance and growth opportunity and to insights about the selective pressures associated with daily and seasonal fluctuations in light and temperature. The selective pressures associated with each of these factors

influence age at migration as well as timing of migration, and the models are able to quantify the “sign” of the influence.

Analyzing salmon migration from this evolutionary perspective, provides new insight into behavior and aids in understanding the proximate mechanisms that determine behavior and the variation in life history types they produce. Ultimately, it is my hope that the results or indirect results (results due to further modelling or experiments) can be used to help manage salmon stocks properly.

8.2 Summary by chapter

Chapter 1 contains introductory material: a literature review, problems and questions that the research addresses, justification for a behavioral ecology approach to the problems and questions addressed, and the evidence for spatial and temporal patterns of chinook migration behavior.

In Chapter 2 I develop and analyze a simple heuristic model of age at migration, that is designed to build intuition, and to yield simple analytic results. The results may be summarized as follows: increasing predator search velocity, ocean growth tends to decrease the optimal age at migration, while increasing migration distance, predator density, or ocean mortality rate tends to increase the optimal age at migration. Two of the model parameters, freshwater growth rate and migration velocity can have either a positive or negative effect on age at migration, depending on the value of the other parameters. Temperature influences both ocean and freshwater growth rate, and mortality rates, and since the effect of these variables on age at migration may counterbalance each other, it is not clear what its net effect is. Except in the case of freshwater growth, the sign

of a parameter's effect on optimal weight at migration is the same as the sign of its effect on age at migration (*i.e.*, early migration means smaller weight). Increasing freshwater growth increases optimal size at migration, but at the same time can *decrease* optimal age at migration.

In Chapter 3 I add more realistic growth and fecundity assumptions to the model. The ocean growth is determined by a von Bertalanffy curve rather than exponential curve; fecundity is proportional to a fractional exponent of spawning weight, rather than directly proportional to spawning weight; and the exponential freshwater growth of Chapter 2 is replaced by a growth curve that is the difference between a Holling Type II feeding function and a metabolic cost function that depends on weight and swimming velocity. Varying freshwater growth parameters reveals that as freshwater growth increases, so does optimal age at migration. However, the sign of this effect reverses as the influence of limited ocean growth is decreased—becoming more exponential in nature. This shows that limited ocean growth is at least in part—if not wholly—responsible for the positive effect of freshwater growth rate. The effects of migration distance, predator ocean mortality rate, predator activity, current velocity, and spawning time are all consistent with the heuristic model. Predator density, however is inconsistent: its increase results in a decrease in age at migration. By reducing the limiting effects of handling time and metabolism, it is possible to reverse the sign of the effect so that age at migration increases rather than decreases with predator density.

In Chapter 4 I included seasonality by through temporal fluctuations in food consumption, metabolic processes, and predator activity. The temporal fluctuations in these variables were driven by a periodic temperature function of given mean annual temperature, phase

angle, and amplitude. The resulting objective function had yearly humps corresponding to the best within-year migration timing, the tallest hump representing the global maximum. As a result, seasonal temperature fluctuations exerted a strong influence on the age at migration, not only determining the optimal *within-year* migration timing, but also the optimal *year* of migration. The best time of migration corresponded to periods of low temperature, when predator activity was at a minimum. As fish grew, the influence of seasonality decreased because larger fish were assumed less susceptible to predators.

The sign of the parameter effects were consistent with the case were seasonality was absent. The phase angle parameter defines the time of minimum temperature, and therefore is responsible for anchoring the optimal age at migration to a particular time of year. Other parameters have little to no effect on within-year migration timing, but can strongly influence the optimal year of migration.

In Chapter 5, I justified approaching the problem of diel migration pattern and current velocity selection from a behavioral ecology perspective. By considering the possible selective pressures shaping the behavior of young salmon, and couching them in equation form, I developed an optimization model that retained the ability to predict migration timing as in other chapters, but was much more general in that it treated diel migration and current velocity choice. The resulting optimization problem was dynamic, and included current velocity and swimming velocity as control variables; time of entry into the estuary, time of ocean entry, and spawning time as control parameters; weight and downstream displacement as state variables, and the log of expected reproductive success as the objective functional.

In Chapter 6, the optimal control problem was presented in a form that allowed application of the maximum principle. To avoid resorting to nonsmooth techniques, dependence of the control variable constraints on the state variables was omitted. For simplicity, the dependence of predator density on current velocity was also omitted. Once the problem was specified, the maximum principle was applied: the Hamiltonian was maximized with respect to the control variables to obtain the policy functions, the co-state and state equations were defined, and the transversality conditions were developed to supply enough boundary conditions to solve the canonical equations and determine the optimal control parameters.

A remarkable amount information was gleaned by simply maximizing the Hamiltonian. One important result, is that optimal behavior is largely controlled by the sign of the appropriate switching function (defined as σ_1 when $\lambda_1 > 0$, and σ_2 otherwise).

First focusing on the case where a marginal increase in downstream displacement is beneficial to fitness (*i.e.*, $\lambda_1 > 0$), the sign of the switching function σ_1 is informative. When it is positive, active downstream migration is optimal: the fish swims downstream in the swiftest current, at a speed that exceeds the maximum growth speed (if the maximum swimming speed permits).

When the switching function σ_1 is negative, there are three possibilities: (i) if the maximum current velocity exceeds the maximum growth speed, then the fish holds station, migrating against the current, swimming at its maximum growth speed; (ii) otherwise, the juvenile either (a) migrates upstream, swimming in the most rapid current, and at a swimming velocity that exceeds the maximum current velocity, but is less than the

optimal growth velocity or (b) swims downstream in a current of zero velocity, and at a swimming velocity that does not exceed the optimal growth velocity. Option (a) is optimal when the maximum current velocity is close to zero (relative to the maximum growth velocity), and option (b) is optimal when it is close to the maximum growth velocity.

When the switching function σ_1 is zero, maximizing the Hamiltonian gives more limited knowledge of the optimal controls. If the maximum current velocity exceeds the maximum growth speed, then two strategy classes are optimal (a) the fish swims against the current at its maximum growth speed and in a current velocity at least as great as its maximum growth speed (b) the fish swims downstream in a current velocity not exceeding its maximum current velocity, with a swimming speed equal to its maximum growth speed. Notice that the optimal current velocity is not unique determined: it is only known to lie in an interval. The swimming *speed*, however, always equals the maximum growth speed. If the maximum current velocity is less than the maximum growth speed, then option (a) is optimal.

When the co-state variable associated with displacement is nonpositive, the sign switching function σ_2 largely characterizes the optimal behaviors. When it is negative, the fish display an “upstream migration” behavior, swimming in slack current or near the shore ($u = 0$), while swimming upstream at a speed that exceeds the maximum growth speed (if the maximum swimming speed allows).

When the switching function σ_2 is positive, fish show a “feeding and predator avoidance” behavior, but there are actually three possible behaviors based on the maximum current velocity. (a) If the optimal current velocity exceeds the maximum growth velocity, the fish

holds station, swimming against the current at its maximum growth speed. Otherwise, the fish swims in the swiftest current either (b) holding station, or (c) migrating upstream with a swimming speed between the maximum growth speed and the maximum current velocity. Only one of these three behaviors is optimal at any given time.

When the switching function σ_2 is zero, fish follow a strategy characterized as intermediate to when it is positive or negative. The optimal behavior is not actually uniquely determine by this case, and further analysis of the canonical equations is needed. However, it is known that the fish swims upstream at its constrained maximum growth velocity, swimming in any current from 0 (resulting in upstream migration) to the constrained maximum growth velocity (resulting in station holding).

When the co-state variable associated with displacement is nonpositive, no downstream migration strategy is optimal.

In Chapter 7 I explore how migration behavior is influenced by fluctuations in light intensity and maximum current velocity. In the first section I developed an exhaustive list of optimal strategy types when time fluctuations in model parameters were ignored (the autonomous case). These strategies were then compared to the optimal strategies in the case where light levels and maximum current velocities were allowed to fluctuate. This allowed me to gauge the influence of freshets and nighttime on migration behavior. In the autonomous case, one of three behaviors was found to be optimal:

S1. Initially, the juvenile holds its station, swimming against the current at its optimal growth speed. At some critical weight, it begins migrating downstream, swimming in the swiftest current, and actively swimming downstream at a speed greater than its optimal growth speed.

S2. The juvenile begins migrating immediately after emergence, swimming at a speed greater than or equal to its optimal growth speed, and in the swiftest current. It migrates nonstop to the estuary.

S3. An infinite number of behaviors is optimal. At each instant the juvenile swims downstream at its optimal growth speed, or against the current at its optimal growth speed. Migration upstream is not permitted.

When time of estuary entry was fixed, it was possible for interrupted migrations, characterized by downstream movement during periods of relatively low capture probability, and station holding when it is higher. When time of estuary entry was allowed to vary in the optimization problem, interrupted migration ceased to be optimal, and the optimal strategy was S1—initial station holding followed by a nonstop migration to the ocean. In the case of fluctuating capture probability or maximum current velocity, the reactions of the fish were similar, and exemplified by the optimal reaction to a freshet: either the freshet should be completely ignored (station holding), or the fish should migrate with the freshet, moving nonstop until arriving at the estuary. Fish ignored a freshet if it is not of sufficient strength or duration, or if it did not occur when the fish was of sufficient size (*i.e.*, near the time marking the onset of migration in the absence of a freshet.)

8.3 Discussion

8.3.1 Age at migration

Several factors can act separately or together, to produce relationship between “growth opportunity” and age at migration. Some of these factors are:

(i) *Ocean-challenge factor.* Focusing on the latitudinal gradient, since northern oceans represent a more osmotically challenging environment, the slower growing fish of these northern latitudes benefit by migrating out at a larger size (Taylor, 1990).

(ii) *Predation vs. migration distance factor.* Focusing on the migration distance gradient observed in the Columbia and Fraser Rivers, since areas of low growth opportunity are generally associated with upper tributaries (positively correlated with migration distance), and larger fish are more likely to survive longer migrations, it is beneficial for fish inhabiting these upper reaches to migrate later.

(iii) *Freshwater-predation factor.* Freshwater predation is reduced in regions of low growth opportunity, giving a greater survival value to longer freshwater residence.

(iv) *Lethal-temperature factor.* Focusing on the latitudinal gradient, fish inhabiting California rivers would be exposed to lethal summer temperatures if they resided in freshwater for a year.

(v) *Starvation factor.* Areas of high growth opportunity (*e.g.*, coastal streams of Oregon, California rivers, and lower altitude regions of the Fraser and Columbia Rivers) in the spring and early summer, become uninhabitable as food resources dwindle, and metabolic costs do not diminish enough to make up for it. Fish rearing in these regions migrate earlier than fish in regions of low growth opportunity.

(vi) *Temperature-related freshwater predation factor.* Regions having high summer temperatures can bring high predation rates due to temperature-elevated consumption rates of predators. In these regions, juveniles failing to migrate before temperature increases are confronted, not only with higher metabolic costs (vii), but also reduced survival. This factor is similar to (iv), but involves *fluctuations* in predation rather than mean predation rate.

(vii) *Zoogeographical factor.* The distribution of the ocean- and stream-type fish is a result of their post-glacial dispersal, with ocean-type dispersing to the south, and stream-type, to the north (Taylor, 1990).

Some of these factors have been addressed directly through modelling, others have not. I appeal to literature and model predictions to examine each. Most are based explicitly on adaptation, linking behavior directly to growth, reproduction, and survival.

The idea of an ocean challenge factor (i) is supported by studies of smolt performance, and may explain why Alaskan chinook salmon (even populations rearing near the ocean) are of stream-type. Locomotor and osmo-regulatory performance are inhibited at low temperatures (*i.e.*, cold climates north of 56°) (Brett, 1967; Knutsson & Garv, 1976; Beamish, 1978; Webb, 1978; Virtanen & Oikari, 1984). Therefore, larger smolt size may be selected in the cold northern environments, because larger smolts have an increased performance benefit (Brett & Glass, 1973; McCormick & Naiman, 1984; Hargreaves & LeBrasseur, 1986), leading to longer freshwater residence times in the north. It is uncertain if this factor has bearing on the age at migration pattern observed in river drainages where ocean- and stream-types are sympatric, because these fish enter the ocean in the same location.

A predation-migration distance factor (ii) could, at least in part, account for greater age at migration of upstream populations on rivers where ocean- and stream-type populations are sympatric. The models of chapters 2-4 show that *when all else is equal,* increased migration distance, creating greater predation risk enroute to the ocean, is optimally offset by delaying migration. However, all else is seldom equal, and the result must be used cautiously. For example, upper tributaries generally have lower growth opportunity, which in itself can produce pressure for earlier migration (according to the models of chapters 2-4). Furthermore, throwing at least some doubt on the importance of this factor, is the fact that there exist a few ocean-type populations that rear in inland locations on the mainstem of the Snake and Columbia Rivers. If at play, this predation-migration distance factor does not differentiate stream- and ocean-type populations in Alaska, since according to Taylor (1990), these populations are *all* stream-type, regardless of migration distance. In California, this factor can have little bearing since the majority of populations are ocean-type, but the two stream-type populations known to exist originate in Mill and Deer Creeks (F. Fisher, Stockton, CA, pers. comm.), upper tributaries of the Sacramento River.

The freshwater-predation factor (iii) may act if predation is less severe in regions of low growth opportunity making later migration more favorable than in high-growth-opportunity locations. If indeed predation is lower in areas of low growth opportunity, then models of chapters 2-4 suggest that the loss of growth experienced by greater freshwater residence time can be compensated by greater survival probability and larger size at migration and ocean entry. It is unclear if this growth-opportunity vs. predation pattern exists in nature. However, it is known that some important salmon predators are less abundant in upper tributaries. For example, the northern squawfish (*Ptychocheilus*

oregonensis), which is common in the pools formed by dams on the mainstem of the Columbia River, is scarce in lower order streams (Beecher *et al.*, 1988), and is known to prefer areas of slow to moderate flow, and temperatures of 20° C to 23° C. The smallmouth bass (*Micropterus dolomieui*), a lesser salmon predator on the Columbia River, prefers slight gradients (.078% to .473%), associated with higher order streams, and high water temperatures (21° C to 27° C). Predation is an important determinate of age at migration, and more research is needed to define its relationship to growth opportunity. In fact, it appears to be the only factor that *potentially* explains the pattern observed between growth opportunity age at migration throughout the chinook's range.

The lethal-temperature factor (iv) has limited application over the range of chinook salmon, but can be important in California rivers and streams where summer temperatures reach lethal levels(TABLE 4.5). The preponderance of ocean-type chinook in California may be due, to some extent, to a decrease in habitat suitability (Southwood, 1962) as temperatures rise.

The starvation factor (v) is similar to (iii) in that, in both, migration is prompted by a decrease in habitat suitability. A decrease in river flows accompanied by rising summer temperatures are correlated with fish migration in the Hanford Reach (Becker, 1973a). A decrease in flows can lead to a decrease in the rate of food drift (Waters, 1969), and can accompanied by an increase in temperature. These factors together could lead to starvation (or at least poor growth), making the river habitat unsuitable (FIGURE 8.1). In contrast, streams and rivers of lower growth opportunity (upper reaches of rivers or populations north of 56°N) may not warm enough in the summer to make metabolic costs prohibitive (FIGURE 8.2).

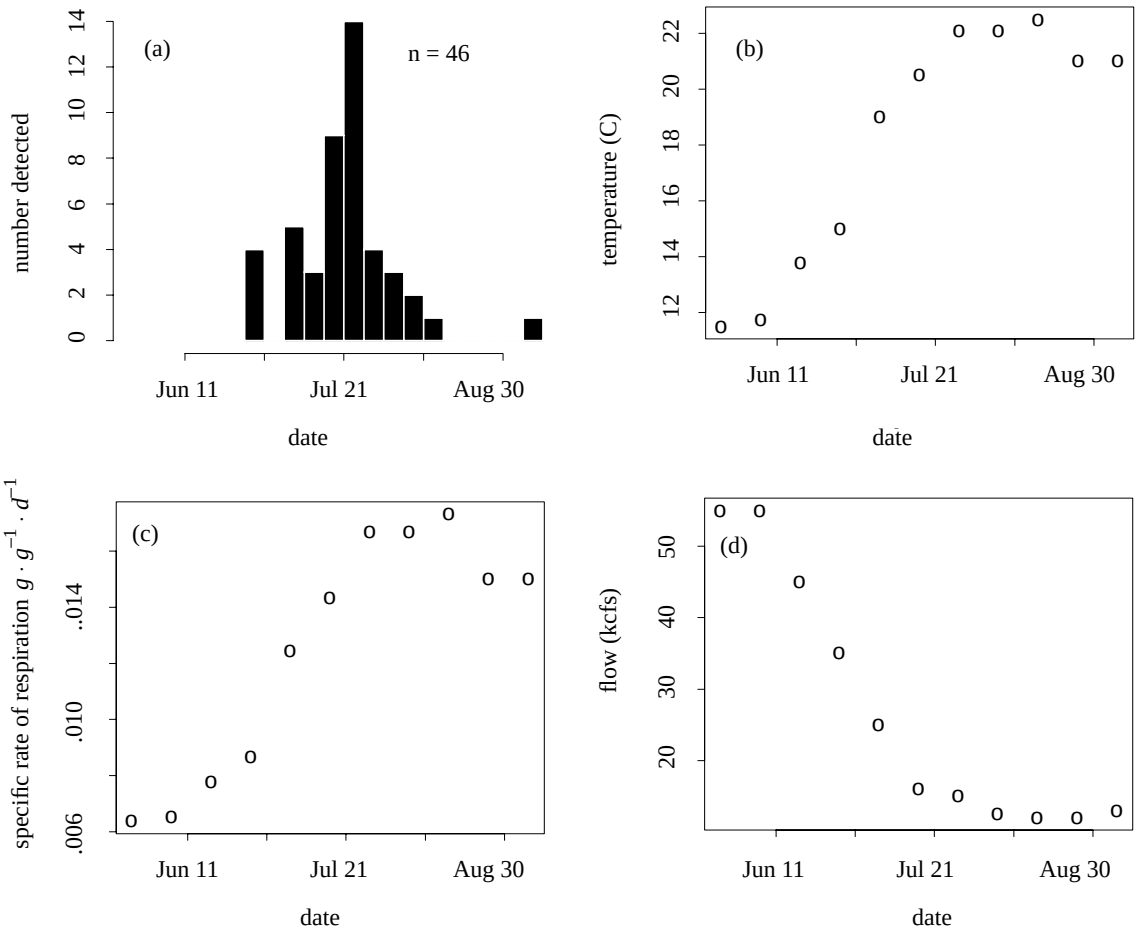

FIGURE 8.1 (a) Detection time if 46 PIT-tagged subyearling salmon at Lower Granite Dam, water temperature, flow, and temperature-dependent specific rate of respiration of a 5-gram subyearling. Migration timing may be attributed to a decrease in habitat suitability. As summer progresses, (b) temperatures rise, (c) respiration rate increases, and (d) flows decrease. The temperature-dependent specific respiration rate function is taken from Hewitt & Johnson (1992).

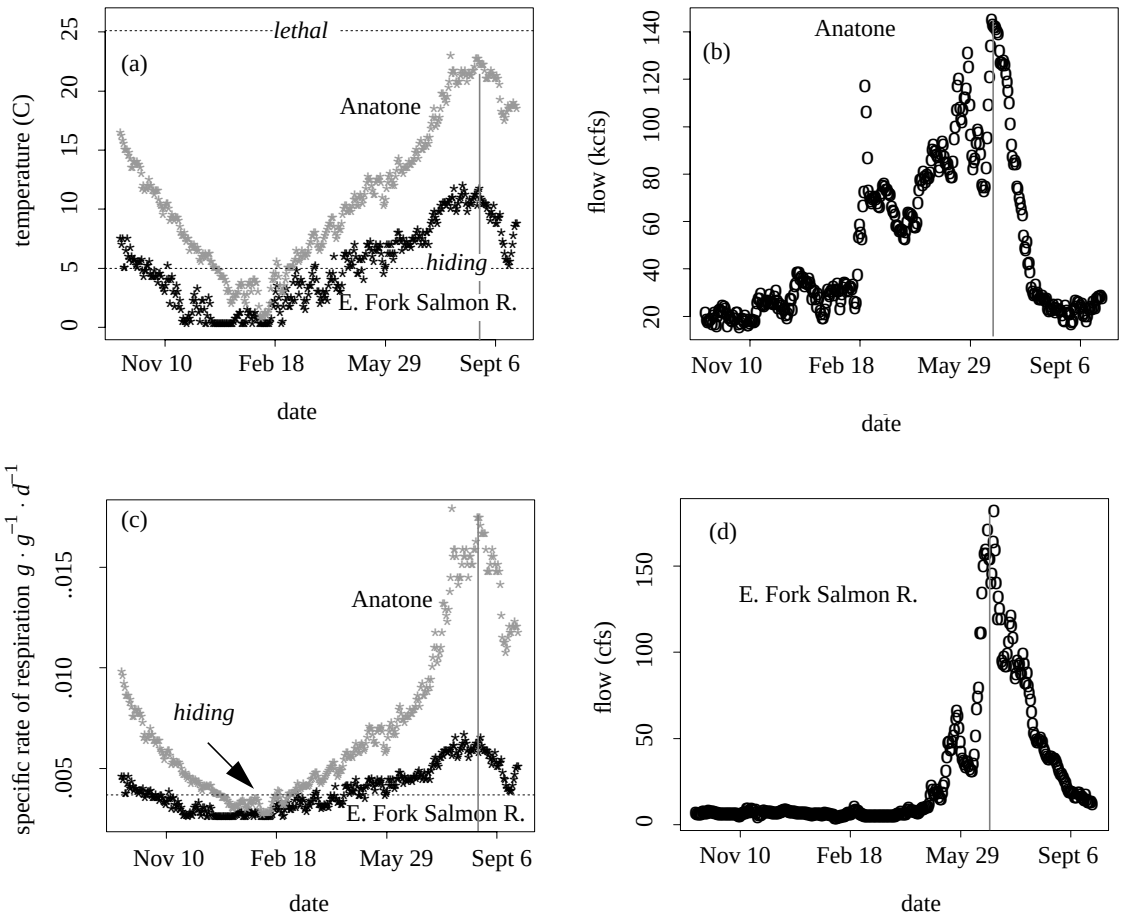

FIGURE 8.2 Comparison of 1981-82 flow, temperature, and specific rate of respiration of a 5-gram fish at the Snake River Anatone USGS gauge (RK 269) and the East Fork of the Salmon R. above Big Boulder Creek (USGS gauge 13297453).

Another factor that is linked with habitat suitability is the temperature-related freshwater predation factor (vi). As in (iv) and (v), migration is prompted by a decrease in habitat suitability due to increasing temperatures. The maximum consumption rate of salmon predators such as the northern squawfish, smallmouth bass, and walleye is known to increase as temperature rises, failing to diminish over the sublethal temperature range of

salmon (FIGURE 4.2). If the feeding activity of the predators is severe in the regions of high growth opportunity, one expects to see seaward migration, or at least migration out of these environs (FIGURE 8.3). The results of CHAPTER 4 suggest that age at migration can indeed decrease when temperature dependent predation is considered. To test importance of this selection pressure, one must understand the geographical distribution of salmon predators and temperature regime (FIGURE 8.2). A simple model run (FIGURE 8.4) demonstrates that spatial structure in temperature regime can be important in determining optimal age at migration.

The zoogeographical factor (vii) does not directly address the adaptive significance of the geographical distribution of stream- and ocean-type chinook, and it ignores the selection gradients that might have produced the observed distribution. Over the 13,500 years since the Wisconsinan glaciation, chinook salmon have produced approximately 2,700 generations. A combination of this large number of generations, consistent and strong geographically-varying selection pressures, heritability of migration behavior, and genetic variability, supplies conditions necessary and sufficient for local adaptation.

Various factors [*i.e.*, (iii), (v), (vi), and (vii)] could contribute to both the latitudinal gradient and the migration distance gradient in age at migration. Given that I have thrown some doubt on (vii), the remaining factors capable of explaining both gradients are: (iii) freshwater-predation, (v) starvation, and (vi) temperature-related freshwater. All other factors must be combined with others to explain both gradients (TABLE 8.1).

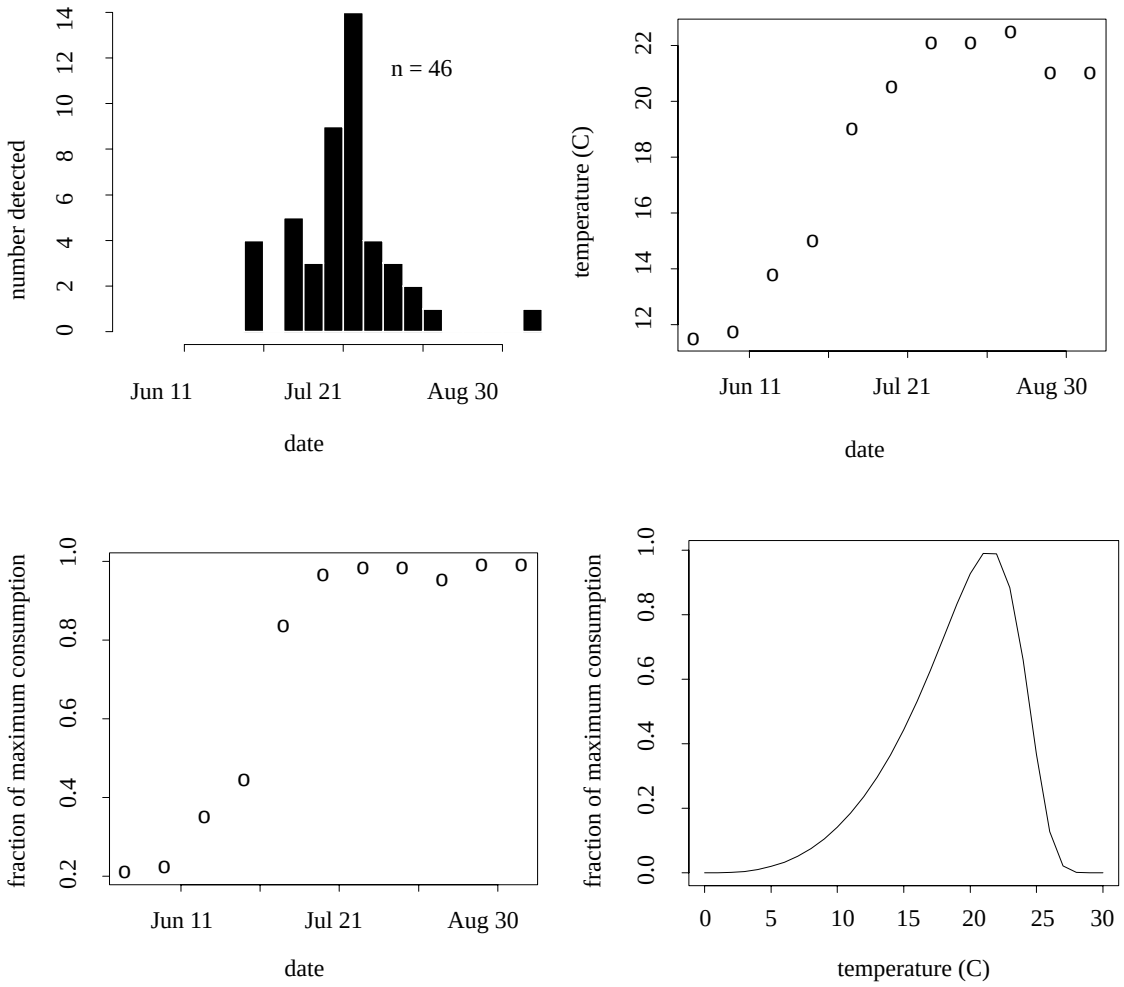

FIGURE 8.3 Detection time of PIT-tagged subyearling salmon at Lower Granite Dam, water temperature, and a temperature-dependent consumption function for northern squawfish. The subyearlings were tagged between 30 May and 2 July of 1991 in the Snake River drainage between RK211 and RK250 above Lower Granite Dam. Mean daily water temperature data were recorded at Billy Creek (RK 265). (a) The peak of detection occurred in mid July, and most emigrated by September. Note that this peak in migration corresponds to periods of high temperature (b), which also corresponds to peak consumption rate of northern squawfish (c). The temperature dependent consumption function (d) is a generalized gamma, and is taken from Vigg & Burley (1991).

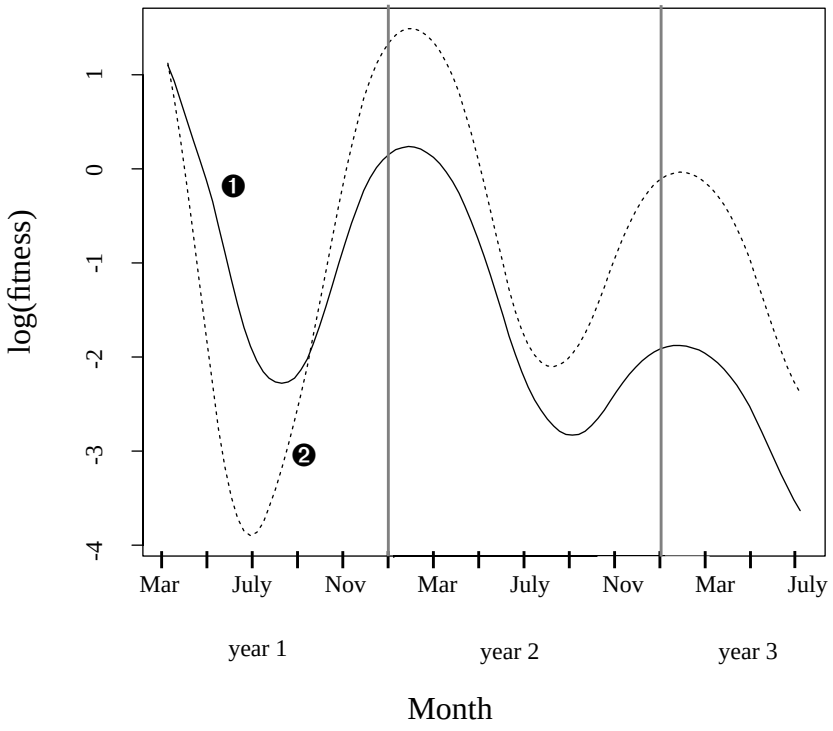

FIGURE 8.4 Comparison of fitness curves showing the influence of simple spatial structure. Curve ❶ uses the seasonal temperatures of 1981-82 from the Anatone Gauge (RK269 of the Snake R.), no spatial river structure, and a migration distance of 800 km. Curve ❷ also uses a migration distance of 800 km, but in the first 10 km, temperatures of East Fork Salmon R. 1981-82, and over the last 790 km, the warmer Anatone Gauge temperatures apply. Predation parameters were set to $\theta = .11$ km^{-1}and $\zeta = 1400$ km·yr^{-1}, and the remain parameters are as given in TABLE 4.4. A juvenile optimally migrates during the first year when ❶ applies, and during the second year if ❷ applies. This occurs because the colder temperatures in ❷ give reduced predation (due to a temperature-dependent consumption rate), giving the juvenile an opportunity to remain in the upper river and grow for a year (under reduced predation conditions), before migrating through regions of more aggressive predators.

TABLE 8.1 Factors and the gradient(s) they address.

Relationship addressed	Applicable factors
Latitudinal gradient	(i), (iii), (iv), (v), (vi), (vii)
Migration distance gradient	(ii), (iii), (iv), (v), (vi), (vii)

8.3.2 Applications to the Columbia River System

The Columbia River has both stream- and ocean-type populations present, with the stream-type fish typically distributed inland and the ocean-type distributed coastally. When ocean-type chinook are distributed inland, they typically rear in the mainstem of the Columbia or Snake Rivers, while, in contrast, stream-type chinook rear in tributaries which are associated with higher elevations and usually, colder annual temperatures. The fundamental differences in the behavior of these two life-history types that must be respected when managing the river for their mutual benefit.

8.3.2.1 Response to increased flow or drawdown

Of the two life-history types, the model suggests that ocean-type chinook will show less migration response to measures of increased flow. If, as suggested in CHAPTER 6 (See FIGURE 6.3), ocean-type chinook are operating in a “predator avoidance and feeding” mode, one expects that increasing flow can actually *reduce movement* of ocean-type chinook by making a station holding superior to active foraging (appetitive movement). In contrast, stream-type chinook, which are likely to be in a more aggressive downstream migratory state than ocean-type chinook, may truly benefit from a measure that increases

maximum current velocity and decreases travel-time (and consequently time at risk to predators) to the ocean.

These model-related predictions are borne out, to some extent, by data. Raymond *et al.* (1975) and Sims *et al.* (1976) found that even during high-flow years, large numbers of ocean-type chinook remained in John Day Reservoir for a protracted period compared with stream-type chinook. These early observations are supported by more recent studies of ocean-type migration as well. Giorgi *et al.* (1994) discovered that ocean-type chinook not only show protracted reservoir residence, but also upstream movements after marking, indicating that the these fish are not consistently displaced downstream. Note that these upstream movements support the notion that ocean-types are showing predator avoidance and feeding behavior along with low-flow induced appetitive movements.

8.3.2.2 Long-term effects of dams

Hydroelectric developments has had a strong impact on migration and survival of both stream- and ocean-type chinook salmon, as well as other salmon species. There is direct mortality due to passage through the turbines, spillways, and bypass systems at the dams. The cumulative effect of passage through a series of dams can produce high mortalities for upstream salmon stocks. For example, juveniles originating above the Lower Granite Dam must pass 9 dams (if they are not transported) enroute to the ocean.

From a lifetime-fitness perspective, fish have two possible strategies that fish can follow: lifetime freshwater residence (residualism), or migration to the ocean to feed (anadramy). It is possible that since the migration corridor is expensive (due to dams and predation in their impoundments), if there exists suitable year-round upstream habitat, residualism may

become more commonplace. This is possible if the conditions for natural selection are met (heritability, variability, and persistent, directional selection pressure). Of course, the stipulation of suitable year-round upstream habitat is essential. Earlier in this discussion, I argued that if habitat suitability decreases rapidly during the summer, due to temperature-related factors, there can be intense selective pressure for migration. Of the two life-history types, it seems most reasonable that stream-type chinook will have more suitable year-round habitat than ocean-type chinook, as well as a tendency to remain in freshwater longer, and therefore will be more likely to exhibit residualism.

Aside from considerations of age at migration, the reduced current velocities associated with impoundments, can also influence migration rates and feeding behavior. Although appetitive movements of ocean-type chinook appear to be important in waters with reduced current velocity, they may have been much less so when dams were absent and river currents were swift. At the same time these impounded waters made it possible for predators, such as the northern squawfish, typically absent from swift-moving sections of rivers and cooler waters, to thrive throughout the mainstem of the Columbia and Snake Rivers. The increased appetitive movements made more important by reduced current velocity, together with an increase in predators, probably led to a substantial increase in predation. Because increased movements could also, in theory, make the juveniles more visible to predators, exacerbating the problem of increased predator density.

LIST OF REFERENCES

Allen, M.A. & Hassler, T. J. (1986). Species profiles: life histories and environmental requirements of coastal fishes and invertebrates (Pacific Southwest)—chinook salmon. *U.S. Fish Wildl. Serv. Biol. Rep.* **82(11.49)**. US. Army Corps of Engineers, TR EL-82-4.

Allen, R. (1965). Juvenile fish collector operation at Lake Mayfield July1, 1964 to June 30, 1965. Report to Bureau of Commercial Fisheries, Contract 14-17-0001-1357. Wash. Dep. Fish., Olympia, 23 p.

Anonymous. (1976). Young king salmon survival and migrations in the delta. Fifth Annual Report (1975), Interagency Ecological Study Program for the Sacramento-San Joaquin Estuary. pp. 28-34.

Baker, R. R. (1978). The evolutionary ecology of animal migration. New York: Holmes & Meier Publishers.

Bassett, C. E. (1978). Effect of cover and social structure on position choice by brown trout (*Salmo trutta*) in a stream. M. S. Thesis, Michigan State Univ., E. Lansing: 181 p.

Beamish, F. W. (1978). Swimming capacity. In: *Fish Physiology, vol. 7, Locomotion*. (Hoar, W. S. & Randall, D. J., eds), pp. 101-187. New York: Academic Press.

Becker, C. D. (1973a). Food and growth parameters of juvenile chinook salmon, *Oncorhynchus tshawytscha*, in central Columbia River. *Fish. Bull.* **71**, 387–400.

Becker, C. D. (1973b). Columbia River thermal effect study: reactor effluent problems. *J. of the Water Pollution Control Federation.* **45**, 850-869.

Beecher, H.A., Dott, E.R. & Fernau, R.F. (1988). Fish species richness and stream order in Washington State streams. *Env. Biol. Fish*. **22**, 193-209.

Berg, L. S. (1948). Freshwater Fishes in the U.S.S.R. and Adjacent countries. Vol. 1. Academy of Sciences, U.S.S.R. Translated from Russian by Israeli Program for Scientific Translation, Jerusalem.

Bohlin, T., Dellefors, C. & Faremo, U. (1993a). Optimal time and size for smolt migration in wilds sea trout (*Salmo trutta*). *Can. J. Fish. Aquat. Sci.* **50**, 224-232.

Bohlin, T., Dellefors, C. & Faremo, U. (1993b). Timing of sea-run brown trout (*Salmo trutta*) smolt migration: effects of climatic variation. *Can. J. Fish. Aquat. Sci*. **50**, 1132-1136.

Brent, R. P. (1973). Algorithms for minimization without derivatives. Englewood Cliffs, N.J.: Prentice-Hall.

Brett, J. R. (1952). Temperature tolerance in young Pacific salmon, genus *Oncorhynchus*. *J. Fish. Res. Bd. Can.* **9**, 265-323.

Brett, J. R. (1965). The relation of size to rate of oxygen consumption and sustained swimming speed of sockeye salmon (*Oncorhynchus nerka*). *J. Fish. Res. Board Can.* **22,** 1491-1501.

Brett, J. R. (1967). Swimming performance of sockeye salmon (*Oncorhynchus nerka*) in relation to fatigue time and temperature. *J. Fish. Res. Bd Can.* **24**, 1731-1741.

Brett, J. R. & Glass, N. R. (1973). Metabolic rates and critical swimming speeds of sockeye salmon (*Oncorhynchus nerka*) in relation to size and temperature. *J. Fish. Res. Bd Can.* **30**, 379-387.

Brett, J.R & Groves, T.D.D. (1979). Physiological energetics. In: *Fish Physiology, Vol VIII: Bioenergetics and Growth* (Hoar, W. S., Randall, D. J. & Brett, J. R., eds) pp. 279-352. New York: Academic Press.

Bugert, R. M. and T. C. Bjornn. (1991). Habitat use by steelhead and coho salmon and their responses to predators and cover in laboratory streams. *Trans. Am. Fish. Soc.* **120**, 486-493.

Bugert, R. M., Bjornn, T. C. & Meehan, W. R. (1991). Summer habitat use by young salmonids and their responses to cover and predators in a small stream. *Trans Am. Fish. Soc.* **120**, 474-485.

Carl, L. M. & Healey, M. C. (1984). Differences in enzyme frequency and body morphology among three juvenile life history types of chinook salmon (*Oncorhynchus tshawytscha*) in the Nanaimo River, British Columbia. *Can. J. Fish Aquat. Sci.* **41**, 1070-1077.

Chapman, D. W. & Bjornn, T. C. (1969). Distribution of salmonids in streams, with special reference to food and feeding. In: *Symposium on Salmon and Trout in Streams.* (Northcote, T. G, ed) pp. 153-176. Vancouver: University of British Columbia.

Clark, W. C. & Levy, D. A. (1988). Diel vertical migrations by juvenile sockeye salmon and the antipredation window. *Am. Nat.* **131**, 271-290.

Clarke, F. H. (1975). The Euler-Lagrange differential inclusion. *Journal of Differential Equations* **19**, 80-90.

Clarke, F. H. (1989). Methods of dynamic and nonsmooth optimization. Montpelier, Vermont: Capital City Press.

Clarke, W. C., Withler, R. E. & Shelbourn, J. E. (1992). Genetic control of juvenile life history pattern in chinook salmon (*Oncorhynchus tshawytscha*). *Can. J. Fish. Aquat. Sci.* **49**, 2300-2306.

Connor, W. P., Burge, H. L., & Miller, W. H. (1991). Rearing and emigration of naturally produced Snake River fall chinook salmon juveniles. In: *Identification of the Spawning & Migratory Requirements of Fall Chinook Salmon in the Columbia River Basin* (Randorf, D. W. & Miller, W. H., eds). pp. 86-137. Portland: Bonneville Power Administration.

Conrad, J. M. & Clark, C. W. (1987). Natural resource economics. New York: Cambridge University Press.

Dauble, D.D., T.L. Page, T. L. & Hanf, R. W. (1989). Spatial distribution of juvenile salmonids in the Hanford Reach, Columbia River. *Fishery Bulletin.* **87**, 775-790.

Davis, S. K. (1981). Determination of body composition, condition, and migration timing of juvenile chum and chinook salmon in lower Skagit River, Washington. M. S. Thesis. University of Washington, Seattle. 97 pp.

Dawley, E. M., Ledgerwood, R. D., Blahn, T. H., Sims, C. W., Durkin, J. T., Kirn, R. A., Rankis, A. E., Monan, G. E. & Ossiander, F. J. (1986). Migration characteristics, biological observations, and relative survival of juvenile salmonids entering the Columbia River estuary, 1966-1983. Report to Bonneville Power Administration, Portland, Oregon. Contract DE-A179-848BP39652. Alaska Fish. Sci. Cent., Natl. Mar. Fish. Serv., NOAA, Seattle, WA 98112, 256 p.

Dickhoff, W. W. & Sullivan, C. V. (1987). Involvement of the thyroid gland in smoltification, with special reference to metabolic and developmental processes. *American Fisheries Society Symposium* **1**, 197-210.

Dixit, A. K. (1976). Optimization in economics. Oxford, England: Oxford University Press.

Elliott, J. M. (1967). Invertebrate drift in a Dartmoor stream. *Arch. Hydrobiol.* **63**, 202-237.

Everest, F. J. & Chapman, D.W. (1972). Habitat selection and spatial interaction by juvenile chinook salmon and steelhead trout in two Idaho streams. *J. Fish. Res. Board Can.* **29**: 91-100.

Fausch, K. D. (1984). Profitable stream positions for salmonids: relating specific growth rate to net energy gain. *Can. J. Zool.* **62**, 441-451.

Foerster, R. E. & Ricker, W. E. (1941). The effect of reduction of predaceous fish on survival of young sockeye salmon at Cultus Lake. *J. Fish Res. Board Can.* **5**, 315-336.

Fogel, D. B. (1994). Applying evolutionary programming to selected control problems. *Computers Math. Applic.* **27**, 89-104.

Galbreath, J. L. & Ridenhour, R. L. (1964). Fecundity of Columbia River chinook salmon. *Res. Briefs Fish Comm. Oreg.* **10**, 16–27.

Gilbert, C. H. (1913). Age at maturity of Pacific coast salmon of the genus *Oncorhynchus*. *Bull. U.S. Bureau Fish.* **32**, 57-70.

Gilhousen, P. (1980). Energy sources and expenditures in Fraser River sockeye salmon during their spawning migration. *Int. Pacfic Salmon Commn Bull.* No **22**.

Gilliam, J. F. (1982). Habitat use and competitive bottle-necks in size-structure fish populations. Ph.D. thesis. Michigan State Univ., east Lansing, MI.

Giorgi, A.E., Miller, D.R & Sandford, B.P. (1994). Migratory characteristics of juvenile ocean-type chinook salmon, Oncorhynchus tshawytscha, in John Day Reservoir on the Columbia River. *Fish. Bull.* **92**, 872-879.

Godin, J-G. J. (1982). Migrations of salmonid fishes during life history phases: daily and annual timing. In: *Salmon and Trout Migratory Behavior Symposium* (Brannon, E. L. & Salo, E. O., eds) pp. 22-50. Seattle: Univ. Wash.

Gross, M. R. (1987). Evolution of diadromy in fishes. *Am. Fish. Soc. Symp.* **1**, 14-25.

Hallock, R. J. & Fry, D. H., Jr. (1967). Five species of salmon, *Oncorhynchus*, in the Sacramento River, *California. Calif. Fish Game* **53**, 5-23.

Hargreaves, N. B. & LeBrasseur, R. J. (1986). Size selectivity of coho (*Oncorhynchus kisutch*) preying on chum salmon (*O. keta*). *Can. J. Fish. Aquat. Sci.* **43**, 581-586.

Healey, M. C. (1982). Juvenile Pacific salmon in estuaries: the life support system, p. 315–341. In*: Estuarine Comparisons* (Kennedy, V. S., ed) pp. 315-341. New York: Academic Press.

Healey, M. C. (1991). Life history of chinook salmon (*Oncorhynchus tshawytscha*). In: *Pacific Salmon Life Histories* (Groot C. & Margolis, L., eds) pp. 312-393. Vancouver: UBC Press.

Healey, M. C. & Heard, W. R. (1984). Inter- and intra-populations variation in the fecundity of chinook salmon (*Oncorhynchus tshawytscha*) and its relevance to life history theory. *Can J. Fish. Aquat. Sci.* **41**, 476-483.

Henry, K. A. (1972). Ocean distribution, growth and effects of the troll fishery on yield of fall chinook salmon from Columbia River hatcheries. *U.S. Natl. Mar. Fish. Serv., Fish. Bull.* **70**, 431–445.

Hestenes, M. R. (1966). Calculus of variations and optimal control theory. New York: John Wiley & Sons, Inc.

Hewitt, S.W. & Johnson, B. L. (1992). Fish bioenergetics model 2: an upgrade of a generalized bioenergetics model for fish growth for microcomputers. Madison, WI: University of Wisconsin Sea Grant Institute.

Hikitia, H. (1956). Pacific salmon (Genus: *Oncorhynchus)* known to occur in the coasts and rivers with Hokkaido. *Sci. Rep. Hokkaido Fish Hatch.* **11**, 25-44.

Hoar, W. S. (1953). The control and timing of migration. *Biol. Rev. Can. Phil. Soc.* **28**, 437-452.

Holling, C. S. (1959). Some characteristics of simple types of predations and parasitism. *Can. Entomol.* **91**, 385–398.

Hopkins, C. L. & Unwin, M. J. (1987). River residence of chinook salmon (*Oncorhynchus tshawytscha*) in the Rakaia River, South Island, New Zealand. *N.Z. J. Mar. Freshwat. Res.* **21**, 163-174.

Huffaker, R. G., Bhat, M. G., & Lenhart, S. M. (1992). Optimal trapping strategies for diffusing nuisance-beaver populations. *Natural Resource Modeling* **6**, 71-97.

Hunter, J. G. (1959). Survival and production of pink and chum salmon in a coastal stream. *J. Fish Res. Board Can.* 16, 835-886.

Jenkins, T. M., Jr. (1969). Social structure, position choice and micro-distribution of two trout species (*Salmo trutta* and *Salmo gairdneri*) resident in mountain streams. *Anim. Behav. Monogr.* 2, 56-123.

Jonsson, B. & Ruud-Hansen, J. (1985). Water temperature as the primary influence on timing of seaward migrations of Atlantic salmon (*Salmo salar*) smolts. *J. Fish. Aquat. Sci.* **42**, 593-595.

Junge, C. O. & Oakley, A. L. (1966). Trends in production rates for upper Columbia River runs of salmon and steelhead and possible effects of changes in turbidity. *Fish. Comm. Oregon, Res. Briefs.* **12**, 22-43.

Kalleberg, J. (1958). Observations in a stream tank of territoriality and competition in juvenile salmon and trout (*Salmo salar L. and S. trutta. L). Inst. Freshwat. Res. Drottningholm* Rep. No. **39,** 55-98.

Kjelson, M. A., Raquel, P. F. & Fisher, F. W. (1982). Life History of fall-run chinook salmon, *Oncorhynchus tshawytscha*, in the Sacramento-San Joaquin Estuary, California. In: *Estuarine Comparisons* (Kennedy, V., ed) pp. 393-411. New York: Academic Press.

Knutsson, S. & Garv, T. (1976). Seawater adaptation in Atlantic salmon (*Salmo salar L.*) at different experimental temperatures and photoperiods. *Aquaculture* **8**, 169-187.

Korn, L. M., Hreha, L. H., Montagne, R. G., Mullarkey, W. G. & Wagner, E. J. (1967). The effects of small impoundments on the behavior of juvenile anadromous salmonids. Final Report to U. S. Bureau of Commercial Fisheries. Contract 14-17-0001-597,767,917,1093, and 1238. *Fish Comm. Oreg. Res. Div.*, Clackamas, 127 p.

Larsson, P.-O. (1985). Predation on migratory smolts as a regulating factor in Baltic salmon. *Salmo salar L.*, populations. *J. Fish Biol.* **26**, 391-397.

Ledgerwood, R. D., Thrower, F. P. & Dawley, E. M. (1991). Diel sampling of migratory juvenile salmonids in the Columbia River estuary. *Fish. Bull., U.S.* **89**, 69-78.

Lee, D. S., Gilbert, C. R., Hocutt, C. H., Jenkins, R. E., McAllister, D. E. & Stauffer, J. R., Jr. (1980). Atlas of North American freshwater fishes. *N. Carolina Biol. Survey Publ.* No **1980-12**.

Leman, B. D. (1978). Coordinated spilling at Columbia River dams during low river flows; response by Public Utility Districts. Unpubl. manuscr. Chelan County, Public Utility District #1, Wenatchee, WA 15 p.

Leonardsson, K. (1991). Predicting risk-taking behavior from life-history theory using static optimization technique. *Oikos* **60**, 149-154.

Levings, C. D., McAllister, C. D. & Chang, B. D. (1986). Differential use of the Campbell River estuary, British Columbia, by wild and hatcher-reared juvenile chinook salmon (*Oncorhynchus tshawytscha*). *Can J. Fish. Aquat. Sci.* **43**, 1386-1397.

Lindsey, C. C. & McPhail, J. D. (1986). Zoogeography of fishes of the Yukon and Mackenzie Basins. In: *Zoogeography of North American Freshwater Fishes.* (Hocutt, C. H. & Wiley, E. O., eds) pp. 639-674. New York: Wiley and Sons.

Lister, D.B. & Genoe. H. S. (1970). Stream habitat utilization by cohabiting underyearlings of chinook (*Oncorhynchus tshawytscha*) and coho (*O. kisutch*) salmon in the Big Qualicum River, British Columbia. *J. Fish. Res. Bd. Canada* **27**:1215-1224.

Loeffel, R. E. & Wendler, J. O. (1969). Review of Pacific coast chinook and coho salmon resources with special emphasis on the troll fisher, p. 1–107. In: *Informal Committee on Chinook and Coho. Reports by the United States exploitation of northeast Pacific stocks of chinook and coho salmon, to 1964, vol. 1, report by the United States Section.*

Long, C. (1968). Diel movement and vertical distribution of juvenile anadromous fish in turbine intakes. *Fish. Bull., U. S.* **66**, 599-609.

Mains, E. M. and Smith, J. M. (1964). The distribution, size, time, and current preferences of seaward migrant chinook salmon in the Columbia Snake Rivers. *Fish. Res. Papers, Wash State Dept. Fish.* **2**, 5-43.

Major, R. L., Ito, J., Ito, S. & Godfrey, H. (1978). Distribution and origin of chinook salmon (*Oncorhynchus tshawytscha*) in offshore water of the north Pacific Ocean. *Int. N. Pacif. Fish. Commn Bull.* No **38**.

Mangel, M. & Clark, C. W. (1988). Dynamic modelling in behavioral ecology. Princeton, New Jersey: Princeton University Press.

Mangel, M. (1994). Climate change and salmonid life history variation. *Deep-Sea Research II.* **41**, 75-106.

McCormick, S. D. & Naiman, R. J. (1984). Osmoregulation in the brook trout, *Salvelinus foninalis-II*. Effect on size, age and photoperiod on seawater survival and ionic regulation. *Comp. Biochem. Physiol*. **79A**, 17-28.

McDonald, J. (1960). The behavior of Pacific salmon fry during their downstream migration to freshwater and saltwater nursery areas. *J. Fish Res. Bd. Can.* **17**, 655-676.

McLeod, C. L. & O'Neill, J. P. (1983). Major range extensions of anadromous salmonids and first record of chinook salmon in the Mackenzie River drainage. *Can. J. Zool.* **61**, 2183-2184.

McPhail, J. D. & Lindsey, C. C. (1970). Freshwater fishes of northwestern Canada and Alaska. *Fish. Res. Bd Can. Bull.* No **173**.

McPhail, J. D. & Lindsey, C. C. (1986). Zoogeography of the freshwater fishes of Cascadia (the Columbia system and rivers north to the Stikine). In: *Zoogeography of North American Freshwater Fishes.* (Hocutt, C. H. & Wiley, E. O., eds) pp. 615-637. New York: Wiley and Sons.

Michalewicz, Z., Jaikow, C. Z. & Krawczyk, J. B. (1992). A modified genetic algorithm for optimal control problems. *Computers Math. Applic.* **23,** 83-94.

Neave, F. (1955). Notes on the seaward migration of pink and chum salmon fry. *J. Fish. Res. Bd. Can.* **12**, 369-374.

Neave, F. (1958). The origin and speciation of *Oncorhynchus*. *Proc. Trans. R. Soc. Can. Ser. 3* **52**, 25-39.

Neilson, J. D., Green, G. H. & Bottom, D. (1985). Estuarine growth of juvenile chinook salmon (*Oncorhynchus tshawytscha*) as inferred from otolith microstructure. *Can. J. Fish. Aquat. Sci.* **42**, 899–908.

Newman, M. A. (1956). Social behavior and interspecific competition in two trout species. *Physiol. Zool.* **29**, 64-80.

Nichols, D.W. (1979). Passage efficiency and mortality studies of downstream migrant salmonids using The Dalles ice-trash sluiceway during 1978. Report to U.S. Army Corps of Engineers, Contract DACW 57-78-C-0058. Oreg. Dep. Fish Wildl., Portland, 28 p.

Nichols, D.W & Ransom, B. H. (1980). Development of The Dalles Dam ice and trash sluiceway as a downstream migrant bypass system, 1980. Final report to U. S. Army Corps of Engineers, Contract DACW57-78-C-0058. Oreg. Dep. Fish Wild., Portland, 37 p.

Oster, G. F. & Wilson, E. O. (1984). A critique of optimization theory in evolutionary biology. In: *Conceptual Issues of Evolutionary Ecology* (Sober, E., ed.) pp. 271-288. Cambridge, Massachusetts: MIT Press.

Parker, R. R. (1962). Estimations of ocean mortality rates for Pacific salmon (*Oncorhynchus*). *J. Fish. Res. Board Can.* **19**, 561–589.

Parker, R. R. & Larkin, P. A. (1959). A concept of growth in fishes. *J. Fish. Res. Bd. Can.* **16**, 721-745.

Poe, T. P., Hansel, H. C., Vigg, S., Palmer, D. E. & Pendergast, L. A. (1991). Feeding of predaceous fishes on out-migrating juvenile salmonids in John Day Reservoir, Columbia River. *Trans. Am. Fish. Soc.* **120**, 405–420.

Pontryagin, L. S., Boltyanskii, V. S., Gamkrelidze, R. V. & Mishchenko, E. F. (1962). The mathematical theory of optimal processes. New York: Wiley.

Press, H. P., Flannery, B. P. , Teukolsky, S. A. & Vetterling, W. T. 1988. Numerical recipes in C. Cambridge: Cambridge University Press.

Raymond, H. L. (1968). Migration rates of yearling chinook salmon in relation to flows and impoundments in the Columbia and Snake Rivers. *Trans. Amer. Fish. Soc.* **97**, 356-359.

Raymond, H.L., SIms, C.W., Johnsen, R.C. & Bentley, W.W. (1975). Effects of power peaking operations on juvenile salmon and steelhead trout migrations, 1974. Northwest Fish. Sci. Cent., Noatl. Mar. Fish. Serv., Seattle, WA. Report to U.S. Army Corps of Engineers: 46 p.

Refstie, T., Steine, T. A. & Gjerdre. T. (1977). Selection experiments with salmon. II. Proportion of Atlantic salmon smoltifying at 1 year of age. *Aquaculture* **10**, 239-242.

Reimers, P. E. (1968). Social Behavior among juvenile fall chinook salmon. *J. Fish. Res. Board Can.* **25**, 2005-2008.

Reimers, P. E. (1971). The length of residence of juvenile fall chinook salmon in the Sixes River, Oregon. Ph.D. thesis. Oregon State University, Corvallis, OR. 99p.

Reimers, P. E. (1973). The length of residence of juvenile fall chinook salmon in Sixes River, Oregon. *Res. Rep. Fish Comm. Oreg.* **4**, 3-43.

Rich, W. H. & Holmes, H. B. (1928). Experiments with marking young chinook salmon on the Columbia River, 1916 to 1927. *Bull. U.S. Bur. Fish.* **44**, 215-264.

Ricker, W. E. (1972). Hereditary and environmental factors affecting certain salmonid populations. In: *The Stock Concept in Pacific Salmon.* (Simon R. C. & Larkin, P.A., eds) pp. 19-160. Vancouver: University of British Columbia.

Ricker, W. E. (1976). Review of the rate of growth and mortality of Pacific salmon in salt water, and noncatch mortality caused by fishing. *J. Fish. Res. Board Can.* **33**, 1483–1524.

Ruggertone, G. T. (1986). Consumption of migrating juvenile salmonids by gulls foraging below a Columbia River dam. *Trans. Am. Fish Soc.* **115**, 736-743.

Salo, E. O. (1969). Final report for the period June 1, 1965 - September 30, 1968, Estuarine ecology research project. Fish. Res. Inst., Univ. of Washington, Seattle. 80pp.

Schaffter, R. G. (1980). Fish occurrence, size, and distribution in the Sacramento River near Hood, California during 1973 and 1974. *Calif. Fish Game Anad. Fish. Admin.* Rep. No. **80-3**. 76 pp.

Shmidt, P. Yu. (1950). Fishes of the Sea of Okhostsk, Smithonian Inst. Natn. Sci. Found. Translated from Russian by Istrali Program for Scientific Translation, Jeruselum.

Sims, C. W., Johnsen, R. C. & Bentley, W. W. (1976). Effects of power peaking operations on juvenile salmon and steelhead trout migrations, 1975. Final report to U.S Army Corps of Engineers, Contract DACW68-77-C-0025. Alaska Fish. Sci. Cent., Natl. Mar. Fish. Serv., NOAA. Seattle: 61 p.

Sims, C. W. & Ossiander, F. J. (1981). Migrations of juvenile chinook salmon and steelhead trout in the Snake River from 1973 to 1979, a research summary. Final report to U.S. Army Corps of Engineers, Contract DACW68-78-C-0038. Alaska Fish. Sci Cent., Natl. Mar. FIsh. Serv., NOAA, Seattle, WA 98112, 53 p.

Smith, J. M. (1984). Optimization theory in evolution, p. 289–315. In: *Conceptual Issues of Evolutionary Ecology* (Sober, E., ed.) pp. 289-315. Cambridge, Massachusetts: MIT Press.

Smith, J. R. (1974). Distribution of seaward migrating chinook salmon and steelhead trout in the Snake River above Lower Monumental Dam. Mar. Fish. Rev. **36**, 42-45.

Smith, J. R., Pugh, J. J. & Monan, G. E. (1968). Horizontal and vertical distribution of juvenile salmonids in upper Mayfied Reservoir, Washington. *U. S. Fish Wildl. Serv. Spec. Sci. Rep. Fish.* **566**, 11 p.

Solomon, D. J. (1981). Migration and dispersion of juvenile brown and sea trout. In: *Salmon and Trout Migratory Behavior Symposium* (Brannon E. L. & Salo E. O., eds) pp. 136-145. Seattle: School of Fisheries, University of Washington.

Southwood, T.R.E. (1962). Migration of terrestrial arthropods in relation to habitat. *Biol. Rev.* **37**, 171-214.

Stober, Q. J., Walden, S. J. & Griggs, D. T. (1973). Juvenile salmonid migration through north Skagit Bay. In: Ecological studies of the proposed Kiket Island nuclear power site (Stober, Q. J. & Salo, E., eds) pp. 35-67. Final Report. Fish. Res. Inst. Univ. Washington, **FRI/UW-7304.**

Taylor, E. B. (1988). Adaptive variation in rheotactic and agonistic behaviour in newly-emerged fry of chinook salmon (*Oncorhynchus tshawytscha*) from ocean- and stream-type populations. *Can J. Fish. Aquat. Sci.* **45**, 237-243.

Taylor, E. B. (1989a). Precocial male maturation in laboratory reared populations of juvenile chinook salmon, *Oncorhynchus tshawytscha*. *Can. J. Zool.* **67**, 1665-1669.

Taylor, E. B. (1989b). Adaptive diversification of juvenile life histories in the chinook salmon, *Oncorhynchus tshawytscha*, (Walbaum). Unpubl. Ph.D. Thesis, University of British Columbia, Vancouver.

Taylor, E. B. (1990). Environmental correlates of life-history variation in juvenil chinook salmon, *Oncorhynchus tshawytscha* (Walbaum). *J. Fish. Biol.* **37**, 1-17.

Taylor, E. B. & McPhail, J. D. (1985). Variation in burst and prolonged swimming performance among British Columbia populations of coho salmon, *Oncorhynchus kisutch. Can. J. Fish. Aquat. Sci.* **42**, 2029-2033.

Thomas, W. K., Withler, R. E. & Beckenbach, A. T. (1986). Mitochondrial DNA analysis of Pacific salmonid evolution. *Can. J. Zool.* **64**, 1058-1064.

Thornton, K. W. & Lessem, A. S. (1978). A temperature algorithm for modifying biological rates. *Trans. Amer. Fish. Soc.* **107**, 284-287.

Thorpe, J. E. & Morgan. R. I. G. (1978). Parental influence of growth rate, smolting rate and survival in hatchery reared Atlantic salmon, *Salmo salar. J. Fish Biol.* **13**, 549-556.

Tinbergen, N. (1963). On aims and methods of ethology. *Z. Tierpsychol.* **20**, 410-433.

Vigg, S. & Burley, C. C. (1991). Temperature-dependent maximum consumption of juvenile salmonids by norther squawfish (*Ptycholcheilus oregonensis*) from the Columbia River. *Can. J. Fish. Aquat. Sci.* **48**, 2491-2498.

Virtanen, E. & Oikari, A. (1984). Effects of low acclimation temperature on salinity adaptation in the presmolt salmon, *Salmo Salar L. Comp. Biochem. Physiol.* **78A**, 387-392.

Vronskiy, B. B. (1972). Reproductive biology of the Kamchatka River chinook salmon. *J. Ichthyol.* **12**, 259-273.

Ware, D. M. (1978). Bioenergetics of pelagic fish: theoretical change in swimming speed and ration with body size. *J. Fish. Res. Board Can.* **35**, 220-228.

Ware, D. M. (1980). Bioenergetics of stock and recruitment. *Can. J. Fish. Aquat. Sci*. 37, 1012–1024.

Waters, T. F. (1969). Invertebrate drift - ecology and significance to stream fishes. In: Symposium on Salmon and Trout in Streams (Northcote, T. G., ed) pp. 121-134. H.R. MacMillan Lectures in Fisheries. Vancouver: Inst. Fish. UBC.

Webb, P. W. (1974). Hydrodynamics and energetics of fish propulsion. *Bull. Fish. Res. Bd. Can.* **190**.

Webb, P. W. (1978). Temperature effects on acceleration performance in rainbow trout, *Salmo gairdneri. J. Fish. Res. Bd Can.* **35**, 1417-1422.

Werner, E. E. & Gilliam, J. F. (1984). The ontogenetic niche and species interactions in size-structured populations. *Ann. Rev. Ecol. Syst.* **15**, 393-425.

Werner, E. E. & Hall, D. J. (1988). Ontogenetic habitat shifts in bluegill: the foraging rate-predation risk trade-off. *Ecology.* **69**, 1352-1366.

Wetherall, J. A. (1970). Estimation of survival rates for chinook salmon during their downstream migration in the Green River, Washington. Ph.D. Thesis, College of Fisheries, University of Washington, Seattle. 170pp.

White, J. R. & Li, H. W. (1985). Determination of the energetic cost of swimming from the analysis of growth rate and body composition in juvenile chinook salmon, *Oncorhynchus tshawytscha. Comp. Biochem. Physiol.* **81A**: 25–33.

Wickmire, R. H. & Stevens, D. E. (1971). Migration and distribution of young king salmon, *Oncorhynchus tshawytscha*, in the Sacramento River near Collinsville. *Calif. Dept. Fish Game, Anad. Fish. Br. Admin.* Rep. No. **71-4**.

Zabel, R. W. (1994). Spatial and temporal models of migrating juvenile salmon with applications. Ph.D. Thesis, University of Washington, Seattle, WA.

APPENDIX A CO-STATE VARIABLE RESULTS

The two results that follow give sufficient conditions for the co-state variables to be nonnegative. Although both results are of interest, Result A.2 is of most concern here, since the optimal migration strategies were derived under the assumption that the co-state variable associated with weight, $\lambda_2(t)$, was positive. In contrast Result A.1 is less important since the optimal strategy was constructed both for the case where the co-state variable associated with displacement it is negative and when it is nonnegative. Furthermore, there is no good biological reason to assume that it is positive. As luck would have it, the proof of Result A.2 is both the simplest to prove and the most important.

Result A.1 *If* u_{max} *and* g *are increasing in* x; k, ζ, *and* θ *are decreasing in* x; k *is decreasing in* w; *and* Φ *is increasing in* w; *then* $\lambda_1(t)$ *is nonnegative for all* $\mathbf{t}$ *in the time horizon.*[1]

Proof

I prove that $\lambda_1(t) \geq 0$ by comparing the values, given by the value function, of two juveniles of identical weight beginning at different locations at time t. I show that the

1. The time horizon is assumed to be the time from emergence to the time of arrival in the estuary. Also, for convenience, T will represent the optimal time of estuary entry.

juvenile located further downstream enjoys a value (defined as the remaining fitness) at least as great as the value of the upstream fish at time t, so that $\lambda_1(t) = \frac{\partial V}{\partial x} \geq 0$.

In overview, I first assume that the upstream fish arrives in the estuary at its optimal terminal time follows its optimal velocity trajectories. I then use the optimal decisions followed by the upstream fish to construct a terminal time, a current velocity trajectory, and a swimming velocity trajectory, which if applied to the downstream fish, give an objective functional value at least as great as the value of the upstream fish. Since the value of the downstream fish must be at least as great as the objective functional evaluated at the terminal time and velocity trajectories I constructed, it must also be at least as great as the value of the upstream fish. Consequently, $\lambda_1(t) = \frac{\partial V}{\partial x} \geq 0$.

Suppose that at time t_1, fish 1 is located at position x and fish 2 is located at position $x + \Delta x$, downstream from fish 1, but upstream from the estuary. Suppose also that both fish weigh w a time t_1. For fish 1, let $\bar{T}_1$, optimal terminal time, and let $\bar{x}_1(t)$, $\bar{w}_1(t)$, $\bar{u}_1(t)$, and $\bar{v}_1(t)$ be the position, weight, current velocity, and swimming velocity respectively for each time t such that $t_1 \leq t \leq \bar{T}_1$. I next use the optimal terminal time and optimal trajectories for fish 1 to construct a decision scenario for fish 2. It is constructed so that: (i) the swimming speed of fish 2 always matches the swimming speed of fish 1, (ii) fish 2 is always at least as far downstream as fish 1, (iii) fish 2 weighs as least as much as fish 1 from time t_1 to $\bar{T}_1$, (iv) fish 2 arrives at the estuary at the same time as fish 1, and (v) fish1 has a migration speed which either matches or exceeds the migration speed of fish 2 from time t_1 to $\bar{T}_1$. Let $x_2(t)$, $w_2(t)$, $u_2(t)$ and $v_2(t)$ be the position, weight, current velocity, and swimming velocity of fish 2 at any time t from t_1 to $\bar{T}_1$, not necessarily optimal. Define $u_2(t)$ and $v_2(t)$ in the following manner:

Case 1. If $\bar{x}_1(t) < x_2(t)$ and

a. $0 < \bar{v}_1(t)$, then $u_2(t) = 0$ and $v_2(t) = -\overline{v_1}(t)$.

b. $-\bar{u}_1(t) \le \bar{v}_1(t) \le 0$, then $u_2(t) = -\bar{v}_1(t)$ and $v_2(t) = v_1(t)$.

c. $\bar{v}_1(t) < -\bar{u}_1(t)$, then $u_2(t) = u_1(t)$ and $v_2(t) = v_1(t)$.

Case 2. If $\bar{x}_1(t) \ge x_2(t)$, then $u_2(t) = u_1(t)$ and $v_2(t) = v_1(t)$.

I next show that (i)-(iv) hold.

Proof of (i). In both cases above, the swimming speed of fish 2 equals the swimming speed of fish 1 (*i.e.*, $|v_2(t)| = |\bar{v}_1(t)|$). Thus (i) holds.

Proof of (ii). If (ii) does not hold, then at some time t'' $x_2(t'') < \bar{x}_1(t'')$. By continuity of the displacement trajectories, at some time t', $x_2(t') = \bar{x}_1(t')$, and $x_2(\xi) \le \bar{x}_1(\xi)$ for any ξ such that $t' \le \xi \le t''$. Note that case 2 holds on from time t' to t'', and therefore $u_2(t) = \bar{u}_1(t)$ and $v_2(t) = \bar{v}_1(t)$. Hence the ordinary differential equations governing the displacement of fish 1 and fish 2 are identical from time t' to t'', with the same condition at t', namely, $x_2(t') = \bar{x}_1(t')$ Since the solution to an ordinary differential equation is unique, $x_2(t'') = \bar{x}_1(t'')$, contradicting the earlier statement that $x_2(t'') < \bar{x}_1(t'')$. Therefore (ii) must hold.

Proof of (iii). To prove (iii), I must show that from time t to $\bar{T}_1$, $\bar{w}_1 \le w_2$. $w_2(t') < w_3(t')$. Assume otherwise. Then by continuity of the weight trajectories, there exists a time t' such that $t \le t' \le \bar{T}_1$, $w_2(t') = \bar{w}_1(t')$, and $\lim_{\delta \to 0} (\dot{w}_2(t' + \delta) - \dot{\bar{w}}_1(t' + \delta)) < 0$, for $\delta > 0$. Using (i) and the fact that g does not

depend on the sign of the swimming velocity (*i.e.*, $g(v, x, w, t) = g(|v|, x, w, t)$), I may write

$$g(\bar{v}_1(t), \bar{x}_1(t), \bar{w}_1(t), t) = g(v_2(t), \bar{x}_1(t), \bar{w}_1(t), t). \qquad \text{(A.1)}$$

Consequently,

$$\lim_{\delta \to 0} \dot{w}_2(t' + \delta) =$$

$$\lim_{\delta \to 0} g(v_2(t' + \delta), x_2(t' + \delta), w_2(t' + \delta), t' + \delta)$$

$$= \lim_{\delta \to 0} g(\bar{v}_1(t' + \delta), x_2(t' + \delta), w_2(t' + \delta), t' + \delta) \quad \text{(by (A.1))}$$

$$= \lim_{\delta \to 0} g(\bar{v}_1(t' + \delta), x_2(t'), w_2(t'), t') \quad \text{(since } x_2, w_2, \text{ and } g \text{ are continuous in } t\text{)}$$

$$= \lim_{\delta \to 0} g(\bar{v}_1(t' + \delta), x_2(t'), \bar{w}_1(t'), t') \quad \text{(since } w_2(t') = \bar{w}_1(t')\text{).}$$

Furthermore, since x_1, w_1, and g are continuous in t,

$\lim_{\delta \to 0} \dot{\bar{w}}_1(t' + \delta) = \lim_{\delta \to 0} g(\bar{v}_1(t' + \delta), \bar{x}_1(t'), \bar{w}_1(t'), t')$. Therefore,

$\lim_{\delta \to 0} (\dot{w}_2(t' + \delta) - \dot{\bar{w}}_1(t' + \delta)) < 0$ implies that

$$\lim_{\delta \to 0} (g(\bar{v}_1(t' + \delta), x_2(t'), \bar{w}_1(t'), t') - g(\bar{v}_1(t' + \delta), \bar{x}_1(t'), \bar{w}_1(t'), t')) < 0.$$

But this is impossible since $\bar{x}_1(t') \le x_2(t')$, and g was assumed to be increasing in x. Therefore, (iii) holds.

Proof of (iv). If at some point in time, t', case 2 holds (*i.e.*, fish 1 and fish 2 are at the same position), then the two fish will swim together from t' to T, because they have identical

migration velocities. Therefore they will both arrive at a at time $\bar{T}_1$. If however, case 2 never holds, then $x_2(t)$ is decreasing from time t_1 to $\bar{T}_1$, so that $x_2(t) < a$, for t such that $t_1 \le t \le \bar{T}_1$. Define the function $y(t) = x_2(t) - \bar{x}_1(t)$. Then $y(t_1) = x_2(t_1) - \bar{x}_1(t_1) > 0$ since fish 2 is downstream from fish 1 at time t_1, and $y(\bar{T}_1) = x_2(\bar{T}_1) - \bar{x}_1(\bar{T}_1) = x_2(\bar{T}_1) - a < 0$ since $x_2(t)$ decreases from $x_2(t_1)$, where $x_2(t_1) < a$. But $y(t)$ is continuous. Therefore $y(t') = 0$ (*i.e.*, case 2 holds for some t' between t_1 and T). This contradicts the earlier statement that case 2 never holds. Hence the position trajectory of fish 2 satisfies the terminal condition (*i.e.*, $x_2(\bar{T}_1) = a$).

Proof of (v). To prove (v) I consider each case in the definition of the velocity trajectories for fish 2. In case 1a, $|u_2 + v_2| = |0 + \bar{v}_2| \le |\overline{u_1} + \overline{v_1}|$. In case 1b, $|u_2 + v_2| = |-\bar{v}_2 + \bar{v}_2| = 0 \le |\overline{u_1} + \overline{v_1}|$. In cases 1c and 2, $|u_2 + v_2| = |\overline{u_1} + \overline{v_1}|$. Therefore (v) holds.

Fish 1 has value $V(x, w, t)$, and fish 2 has value $V(x + \Delta x, w, t)$. By our hypothesis, k, θ, and ζ are decreasing in x, k is decreasing in w, and Φ is increasing in w. Therefore by (ii) $\bar{x}_1(t) \le x_2(t)$ and (iii) $\bar{w}_1(t) \le w_2(t)$, $k(x_2(t), w_2(t), t) \le k(\bar{x}_1(t), \bar{w}_1(t), t)$, $\theta(x_2(t), t) \le \theta(\bar{x}_1(t), t)$, $\zeta(x_2(t), t) \le \zeta(\bar{x}_1(t), t)$, and $\Phi(\bar{w}_1(\bar{T}_1), \bar{T}_1) \le \Phi(w_2(\bar{T}_1), \bar{T}_1)$ for all t in the time horizon. By these inequalities in addition to (v) $|\bar{u}_1(t) + \bar{v}_1(t)| \le |u_2(t) + v_2(t)|$ for all t in the time horizon, and (iv) $T_2 = \bar{T}_1$,

$$V(x, w, t_1) = -\int_{t_1}^{\bar{T}_1} (|\bar{u}_1 + \bar{v}_1| + \zeta(\bar{x}_1, t))\, \theta(\bar{x}_1, t)\, k(\bar{x}_1, \bar{w}_1, t)\, dt + \Phi(w_1(\bar{T}_1), \bar{T}_1)$$

$$\leq -\int_{t_1}^{T_2} (|u_2 + v_2| + \zeta(x_2, t))\,\theta(x_2, t)\,k(x_2, w_2, t)\,dt + \Phi(w_2(T_2), T_2)$$

$$\leq V(x + \Delta x, w, t_1).$$

Thus $\lambda_1(t_1) = \frac{\partial}{\partial x} V(x, w, t_1) \geq 0$. Since t_1 was arbitrary, $\lambda_1(t) = \frac{\partial}{\partial x} V(x, w, t) \geq 0$ for all t in the time horizon. ■

Result A.2 *If k is decreasing in w and Φ is increasing in w, then $\lambda_2(t)$ is nonnegative for all t in the time horizon. If, in addition, either k is strictly decreasing in w, or Φ is strictly increasing in w, then $\lambda_2(t)$ is positive for all t in the time horizon.*

Proof

I demonstrate that $\lambda_2(t)$ is nonnegative by comparing the value of two fish of different sizes released at position x at time t. I show that the larger fish enjoys a value at least as great as the value of the smaller fish, and hence the marginal contribution of w at an arbitrary time t is positive (*i.e.*, $\lambda_2(t) = \frac{\partial}{\partial w} V(x, w, t) \geq 0$).

Consider two different sized fish at time t_1. Fish 1 is the smaller fish weighing w, and fish 2 weighs $w + \Delta w$. Assume both fish are at position x at t_1. For fish 1, let $\bar{T}_1$ be the optimal terminal time, and let $\bar{u}_1(t)$, $\bar{v}_1(t)$, and $\bar{w}_1(t)$ be the optimal current velocity, swimming velocity, and weight respectively for t such that $t_1 \leq t \leq \bar{T}_1$. Suppose fish 2 chooses terminal time $\overline{T_1}$, and follows current velocity and swimming velocity controls $\bar{u}_1(t)$ and $\bar{v}_1(t)$ respectively, with resulting weight function $w_2(t)$. I may then show that fish 2 remains larger than fish 1 from time t to $\bar{T}$, (*i.e.*, $\bar{w}_1(t) \leq w_2(t)$ for

$t_1 \le t \le \bar{T}_1$). Suppose otherwise. By continuity of the weight trajectory, there exists a time t' such that both fish 1 and fish 2 weigh $\bar{w}_1(t')$. Consider weight trajectories moving backwards in time from t' to t: Fish 1 and fish 2 are of identical weight at t', they follow identical velocity decisions from time $t = t'$ to $t = 0$, and yet obtain different weights at time t. This is impossible since the ordinary differential equation governing weight must yield a unique solution. Therefore fish 2 always weighs more than fish 1.

At t_1, fish 1 has value $V(x, w, t_1)$, and Fish 2 has value $V(x, w + \Delta w, t_1)$. Assuming that k is decreasing in w and Φ is increasing in w, then $k(w_2(t), t) \le k(\bar{w}_1(t), t)$ and $\Phi(\bar{w}_1(\bar{T}_1), \bar{T}_1) \le \Phi(w_2(\bar{T}_1), \bar{T}_1)$. Therefore

$$V(x, w, t_1) \le -\int_{t_1}^{\bar{T}_1} (|\bar{u}_1 + \bar{v}_1| + \zeta(\bar{x}_1, t))\, \theta(\bar{x}_1, t)\, k(\bar{x}_1, w_2, t)\, dt + \Phi(w_2(\bar{T}_1), \bar{T}_1)$$

$$\le V(x, w + \Delta w, t_1),$$

and since t_1 was arbitrary, $\lambda_2(t) = \frac{\partial}{\partial w} V(x, w, t) \ge 0$. If, in addition, k is strictly decreasing in w or Φ is strictly increasing in w, then either $k(w_2(t), t) < k(\bar{w}_1(t), t)$ or $\Phi(\bar{w}_1(\bar{T}_1), \bar{T}_1) > \Phi(w_2(\bar{T}_1), \bar{T}_1)$. Therefore

$$V(x, w, t_1) < -\int_{t_1}^{\bar{T}_1} (|\bar{u}_1 + \bar{v}_1| + \zeta(\bar{x}_1, t))\, \theta(\bar{x}_1, t)\, k(\bar{x}_1, w_2, t)\, dt + \Phi(w_2(\bar{T}_1), \bar{T}_1)$$

$$\le V(x, w + \Delta w, t),$$

and since t_1 was arbitrary $\lambda_2(t) = \frac{\partial}{\partial w} V(x, w, t) > 0$. ■

APPENDIX B MAXIMIZING THE HAMILTONIAN

The Hamiltonian is maximized below as function of swimming velocity, v and current velocity, u. It is convenient to maximize the Hamiltonian in two separate cases: when the co-state variable associated with displacement is positive, and when it is nonpositive. A function known as the switching function, is used to help characterize the optimal migration behaviors. When the co-state variable λ_1 is positive, the switching function is defined as $\sigma_1 = \lambda_1 - \theta k$, when it is nonpositive, the switching function is $\sigma_2 = \lambda_1 + \theta k$.

This static maximization problem and can be solved by simply plotting cross-sections of the Hamiltonian, and appealing to first order derivatives when necessary. We first maximize with respect to u along cross-sections defined by fixed swimming velocities. The maximizing u's, each indexed by a value of fixed v , are then substituted into the Hamiltonian to make the problem single dimensional (in v).

For notational convenience, the arguments x, w and t are dropped from all functions, since they do not enter explicitly into the maximization problem. The arguments v, u, λ_1 and λ_2 are retained. So, for example, the growth function is denoted by $g(v)$ instead of $g(v, x, w, t)$. The maximizing choices of u and v will be denoted u^* and v^* respectively. These are not unique for any given point $(x, w, t, \lambda_1, \lambda_2)$. Do not confuse

the velocities u^* and v^*, which maximize the Hamiltonian, with the optimal controls, which are paths that maximize the objective functional J.

B.1 Positive displacement co-state variable

Any cross-section of the Hamiltonian defined by fixing v may be written as $H|_{v \text{ fixed}} = Y(u) + \text{constant}$, where

$$Y(u) = \lambda_1 (u+v) - |u+v|\theta k. \tag{B.1}$$

When $u \le -v$, $Y(u) = \sigma_2 (u+v)$, and when $u > -v$, $Y(u) = \sigma_1 (u+v)$. Any u that maximizes $Y(u)$ also maximizes $H|_{v \text{ fixed}}$. Therefore the problem of maximizing along a cross-section reduces to: maximize $Y(u)$ with respect to u, subject to $0 \le u \le u_{max}$. This problem is solved by inspection of a plot of $Y(u)$ (FIGURE B.1). The maximizing u depends on the sign of the switching function, σ_1, and the value of the fixed swimming velocity, v (TABLE B.1).

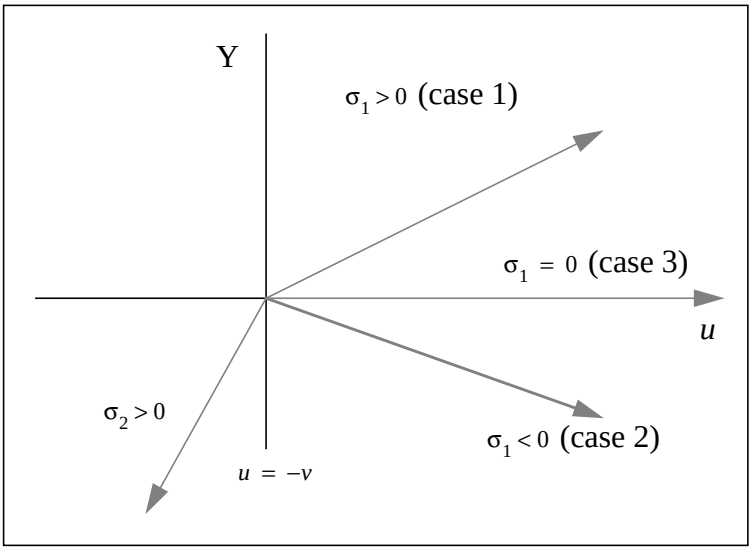

FIGURE B.1 The optimal choice of the current velocity depends on the sign of the switching function, σ_1. Note that since λ_1 is positive, so is σ_2 . When σ_1 is positive (case 1), the maximizing u is clearly u_{max}, when it is negative (case 2), the maximizing u is either u_{max}, $-v$, or 0, depending on whether $-v$ lies to the right, within, or to the left of the interval $[0, u_{max}]$ respectively. When σ_1 is zero (case 3), the maximizing u is either u_{max}, any value in the interval $[-v, u_{max}]$, or any value in the interval $[0,u_{max}]$, depending on wheter $-v$ lies to the right, within, or to the left of $[0, u_{max}]$ respectively.

TABLE B.1 Optimal choices of migration velocity corresponding to different choices of the swimming velocity when λ_1 is positive.

Case number	Sign of switching function σ_1	Swimming velocity condition	Maximizing current velocity
1	+	none	u_{max}
2a	-	$v > 0$	0
2b	-	$v < -u_{max}$	u_{max}
2c	-	$-u_{max} \le v \le 0$	$-v$
3a	0	$v > 0$	$[0, u_{max}]$
3b	0	$v < -u_{max}$	u_{max}
3c	0	$-u_{max} \le v \le 0$	$[-v, u_{max}]$

The maximizing current velocity depends on the sign of the switching function, and the value of v relative to 0 and $-u_{max}$. In cases 3a and 3c, the maximizing current velocity is any value in the specified interval.

We next consider the cases 1, 2 and 3 separately— each defined by the sign of the switching function σ_1. In all cases the Hamiltonian is written as a function of v alone, by restricting u to its known maximizing value for each given v (TABLE B.1). Each resulting restricted Hamiltonian is then the sum of $\lambda_2 g(v)$, a piece-wise linear function $L(v)$, and a constant (in v), making the one dimensional maximization quite simple. In each case, it is solved by inspecting a plot of $\lambda_2 g(v)$ and the piece-wise linear function L on the same coordinate system. Rather than explaining this methodology repeatedly for each individual case, we will simply derive the piecewise linear function, L, plot L and $\lambda_2 g$ on the same coordinate system, and derive maximizing velocity choices.

B.2.1 If the switching function σ_1 is positive

For case 1, $u^* = u_{max}$, and the Hamiltonian becomes $H = L_1 + \lambda_2 g + \theta\zeta k$, where the piece-wise linear function L_1 is given by

$L_1(v) = -(|u_{max} + v|)\,\theta k + \lambda_1 (u_{max} + v)$. When $u_{max} + v \le 0$,

$L_1(v) = (u_{max} + v)\,\sigma_2 + \lambda_2 g(v)$; when $u_{max} + v > 0$,

$L_1(v) = (u_{max} + v)\,\sigma_1 + \lambda_2 g(v)$.

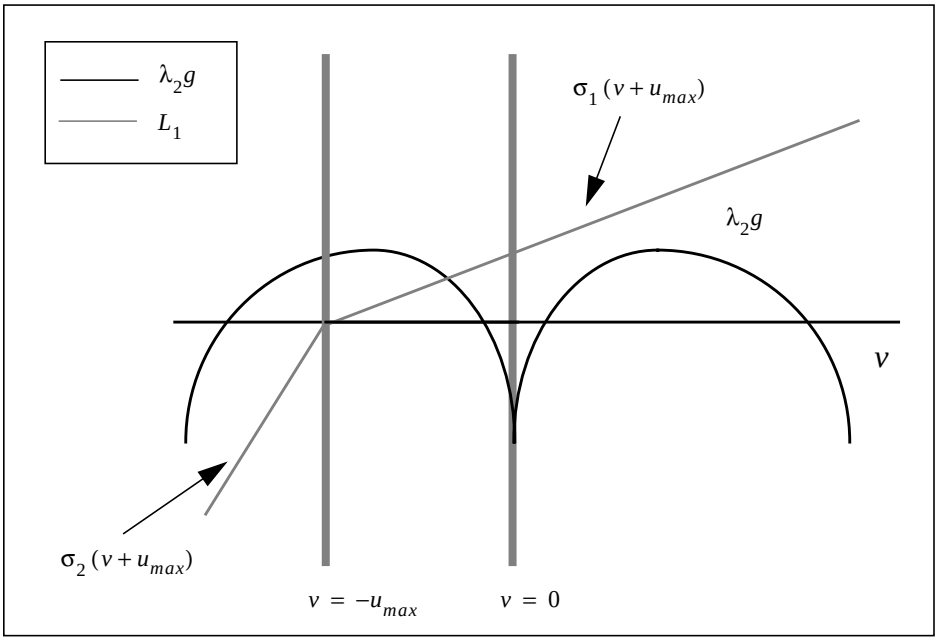

FIGURE B.2 When σ_1 is positive, v^* maximizes the sum of L_1 and $\lambda_2 g$, subject to $-v_{\max} \le v \le v_{\max}$.

Since L_1 is increasing in v and $\lambda_2 g$ is symmetric about $v = 0$, then v^* is nonnegative (FIGURE B.3). If $\sigma_1 + \lambda_2 g_v(0) < 0$ (g_v is a right-hand derivative), then $v^* = 0$; otherwise, as depicted in FIGURE B.3, the sum of the functions is largest at a point v'', where $\sigma_1 + \lambda_2 g_v(v'') = 0$ is zero. Therefore—applying the constraint $-v_{max} < v < v_{max}$—when $\sigma_1 + \lambda_2 g_v(0) \geq 0$, $v^* = min(v', v_{max})$.

B.3.2 If the switching function σ_1 is negative

For Cases 2a, 2b, and 2c, the Hamiltonian may be written as $H = \theta\zeta k + \lambda_2 g + L_2$, where the piece-wise linear function L_2 is

$$L_2(v) = \begin{cases} \sigma_2(v + u_{max}) & if \quad v < -u_{max} \\ 0 & if \ -u_{max} \leq v \leq 0. \\ \sigma_1 v & if \quad v > 0 \end{cases}$$

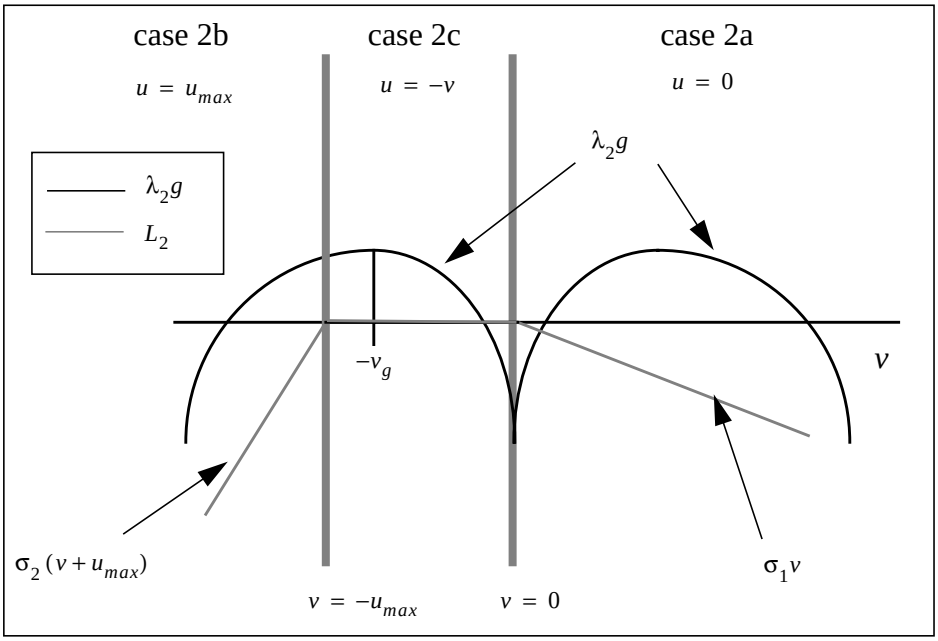

FIGURE B.3 When σ_1 is negative, v^* maximizes the sum of L_2 and $\lambda_2 g$ subject to $-v_{\max} \le v \le v_{\max}$. Note that the slope of the the left-most linear piece of L_2 is steeper than its right-most linear piece, since $\sigma_2 = \lambda_1 + \theta k > |\lambda_1 - \theta k| = |\sigma_1|$.

There identify 4 possibilities, each depending on u_{max} and u_{crit} defined below (FIGURE B.3):

i. If $min\,(v_g, v_{max}) < u_{max}$, then $v^* = -min\,(v_g, v_{max})$, and $u^* = -v^*$.

ii. If $0 \le u_{max} \le min\,(u_{crit}, v_{max})$, then $u^* = 0$ and

   a. $v^* = 0$ if $\lambda_2 g_v(0) + \sigma_1 \le 0$ (g_v is a right-hand derivative); otherwise

   b. $v^* = min\,(v', v_{max})$, where $\lambda_2 g_v(v') + \sigma_1 = 0$.

iii. If $0 < u_{crit} < u_{max} \leq min\,(v_g, v_{max})$, then $u^* = u_{max}$

a. $v^* = -u_{max}$ if $\lambda_2 g_v(-u_{max}) + \sigma_2 \geq 0$ $v^* = max\,(v', -v_{max})$; otherwise

b. $v^* = v''$ where $\lambda_2 g_v(v'') + \sigma_2 = 0$.

iv. If $v_{max} > u_{max} = u_{crit} > 0$ then there are two points which maximize the Hamiltonian—the velocities given by (iib), and those given by (iiib).

u_{crit} is defined either the critical value of u_{max} that ensures that the velocities in (iib) and (iiib) both maximize the Hamiltonian—such a value exists whenever $\lambda_2 g_v(0) + \sigma_2 < 0$ (g_v is a left-hand derivative), or 0 if no such critical value exists. These results are summarized in TABLE B.2.

TABLE B.2 Optimal swimming velocity summary when the switching function σ_1 is negative.

Possi-bility	u_{max} Condition	Derivative condition	Maximizing current velocity	Maximizing swimming velocity
i	$\tilde{v}_g < u_{max}$	none	$\tilde{v}_g$	$-\tilde{v}_g$
iia†	$0 \le u_{max} \le \tilde{u}_{crit}$	$\lambda_2 g_v\|_{v=0} + \sigma_1 \le 0$	0	0
iib		$\lambda_2 g_v\|_{v=0} + \sigma_1 > 0$	0	$min\,(v', v_{max})$
iiia	$0 < u_{crit} < u_{max} \le \tilde{v}_g$	$\lambda_2 g_v\|_{v=-u_{max}} + \sigma_2 \ge 0$	u_{max}	$-u_{max}$
iiib		$\lambda_2 g_v\|_{v=-u_{max}} + \sigma_2 < 0$	u_{max}	$max\,(v'', -v_{max})$
iv	$v_{max} > u_{max} = u_{crit} > 0$	none	The velocities of both (iib) and (iiib)	

The optimal swimming velocity depends on the value of u_{max} relative to the constrained maximum growth velocity $\tilde{v}_g = min\,(v_g, v_{max})$. If the maximum current velocity does not exceed the constrained maximum growth speed (ii-iv), the optimal velocities depend on the maximum current velocity relative to a critical value, u_{crit}, or the constrained critical current velocity $\tilde{u}_{crit} = min\,(u_{crit}, v_{max})$.

† g_v in (iia-b) is a right-hand derivative.

B.4.3 If the switching function σ_1 is zero

If $\sigma_1 = 0$, there are infinitely many points that maximize the Hamiltonian. In the case, the Hamiltonian (restricted to the maximizing choice of u) may be written as

$H = \theta\zeta k + \lambda_2 g + L_3$, where

$$L_3(v) = \begin{cases} \sigma_2 (v + u_{max}) & if\ v < -u_{max} \\ 0 & if\ -u_{max} \le v \end{cases}.$$

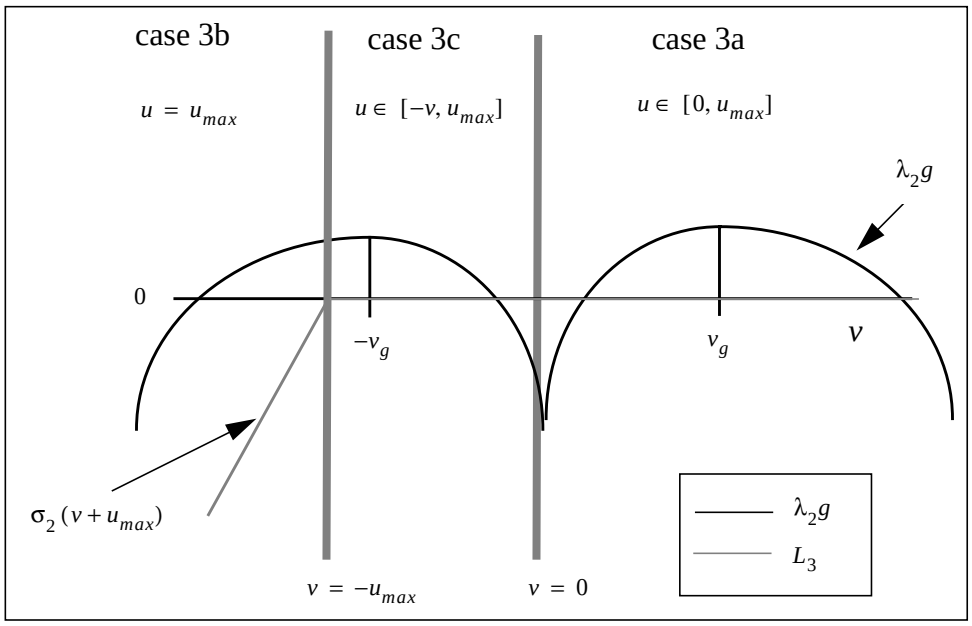

FIGURE B.4 In this case the switching function σ_1 is zero, and the goal is to maximize the sum of the functions L_3 and $\lambda_2 g$ with respect to v, while observing the constraint, $-v_{\max} \le v \le v_{\max}$.

Since L_3 is constant for $v \ge -u_{max}$, there is possibly more than one choice for v^* (FIGURE B.4). If $-u_{max} \le max(-v_g, -v_{max})$, both $v = max(-v_g, -v_{max})$, $u \in [-v, u_{max}]$ and $v = min(v_g, v_{max})$, $u \in [0, u_{max}]$ maximize the Hamiltonian; otherwise, the maximizing velocities are $v^* = min(v_g, v_{max})$ and $u \in [0, u_{max}]$. These results are summarized in TABLE B.3.

TABLE B.3 Optimal swimming velocities when the switching function σ_1 is zero.

Possibility	u_{max} Condition	Maximizing current velocity	Maximizing swimming velocity
i†	$\tilde{v}_g \le u_{max}$	$[\tilde{v}_g, u_{max}]$	$-\tilde{v}_g$
		$[0, u_{max}]$	$\tilde{v}_g$
ii	$u_{max} < \tilde{v}_g$	$[0, u_{max}]$	$\tilde{v}_g$

†The velocities of both rows of possibility (i) maximize the Hamiltonian.

In all cases, the swimming speed equal to the constrained maximum growth speed and the current velociy is not uniquely determined—it is only known to lie in the specified interval.

B.5 Nonpositive displacement co-state variable

The methodology of this section mirrors that of the previous. I will maximize the Hamiltonian (with respect to u) along all cross-sections defined by fixing v, then use this result to couch the problem in one dimension. Throughout the rest of the optimization, the switching function will be defined as $\sigma_2 = \lambda_1 + \theta k$ instead of σ_1.

As demonstrated before, cross-sections of the Hamiltonian may be written as $H|_{v \text{ fixed}} = Y(u) + \text{constant}$, where $Y(u)$ is defined in (B.1). Any u that maximizes $Y(u)$ also maximizes $H|_{v \text{ fixed}}$. By examining a plot of $Y(u)$, and respecting the constraint $0 \le u \le u_{max}$, it is possible to solve this maximization problem by inspection (FIGURE B.1). The maximizing u depends on the sign of σ_2, and the value of the fixed swimming velocity, v (TABLE B.4).

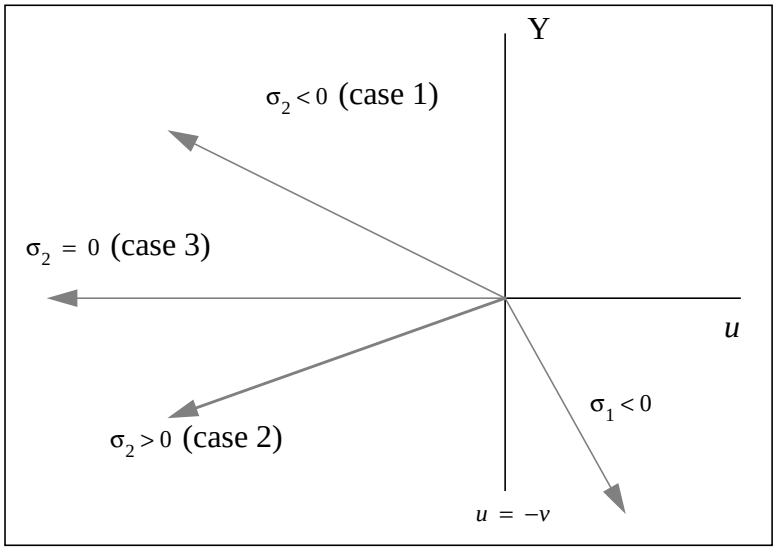

FIGURE B.5 The maximizing choice of the current velocity depends on the sign of the switching function, σ_2 . Note that since λ_1 is nonpositive, σ_1 is negative (assuming $\theta k > 0$). When σ_2 is negative (case 1), then Y is strictly decreasing in u, and therefore the maximizing current velocity is 0. When σ_2 is positive (case 2), the maximizing current velocity is u_{max}, $-v$, or 0, depending on whether $-v$ lies to the right of, within, or to the left of the interval $[0, u_{max}]$ respectively. When σ_2 is zero (case 3), the maximizing current velocity is any value in $[0, u_{max}]$, any value in $[0, -v]$, or 0, depending on whether $-v$ lies to the right of, within, or to the left of the interval $[0, u_{max}]$ respectively.

TABLE B.4 Maximizing choices of current velocity corresponding to different choices of the swimming velocity when λ_1 is nonpositive.

Case number	Sign of switching function σ_2	Swimming velocity condition	Maximizing current velocity
1	-	none	0
2a	+	$v > 0$	0
2b	+	$v < -u_{max}$	u_{max}
2c	+	$-u_{max} \le v \le 0$	$-v$
3a	0	$v > 0$	0
3b	0	$v < -u_{max}$	$[0, u_{max}]$
3c	0	$-u_{max} \le v \le 0$	$[0, -v]$

The maximizing current velocity depends on the sign of the switching function, and the value of the swimming velocity relative to 0 and $-u_{max}$. In 3b and 3c, it is any value in the specifed interval.

As before, we proceed by considering cases 1, 2 and 3 separately, and reducing the Hamiltonian to one dimension by restricting it to the known maximizing u (TABLE B.4). In all cases the Hamiltonian can be written as the sum of $\lambda_2 g(v)$, a piece-wise linear function $L(v)$, and a constant (in v). The maximizing velocities are found by placing the functions $\lambda_2 g(v)$ and $L(v)$ on the same plot.

B.6.1 If the switching function σ_2 is negative

When σ_2 is negative, the Hamiltonian is to be maximized over the curve $u = 0$ (TABLE B.4). This restricted Hamiltonian is $H = L_1(v) + \lambda_2 g(v) + \text{constant}$, where $L_1(v) = -|v|\theta k + \lambda_1 v$. When $v \le 0$, then $L_1(v) = v\sigma_2$; when $v > 0$, $L_1(v) = v\sigma_1$.

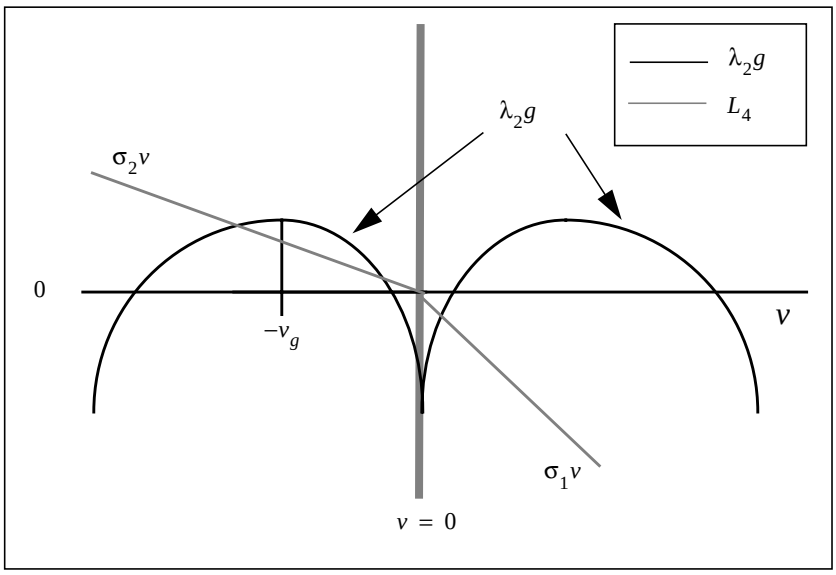

FIGURE B.6 If σ_2 is positive, v^* is identified by maximizing the sum L_4 and $\lambda_2 g$, while observing the constraint, $-\boldsymbol{v}_{\max} \le v \le v_{\max}$.

Since L_4 is decreasing in v, and $\lambda_2 g$ is symmetric about $v = 0$, the maximizing v is nonpositive (FIGURE B.3). If $\sigma_2 + \lambda_2 g_v(0) > 0$ (where g_v is a left-hand derivative), then $v^* = 0$; otherwise, $v^* = max(v'', -v_{max})$, where $\sigma_2 + \lambda_2 g_v(v'') = 0$ $(v'' < 0)$. v'' is less than the maximum growth velocity (in absolute value).

B.7.2 If the switching function σ_2 is positive

When the switching function σ_2 is positive, the Hamiltonian (restricted to maximizing choices of u) may be written as $H = \theta\zeta k + \lambda_2 g + L_2(v)$,

where

$$L_2(v) = \begin{cases} \sigma_2(v + u_{max}) & if \quad v < -u_{max} \\ 0 & if \; -u_{max} \le v \le 0 \\ \sigma_1 v & if \quad v > 0 \end{cases}$$

is the desired piece-wise linear function.

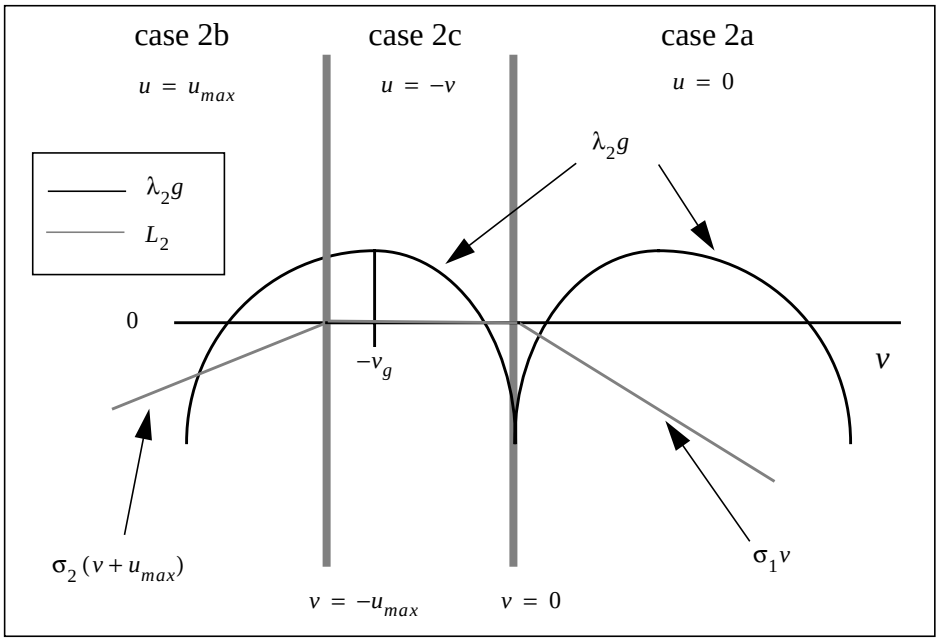

FIGURE B.7 If σ_2 is positive, v^* is the value of v that maximizes the sum of L_2 and $\lambda_2 g$, while observing the constraint, $-\boldsymbol{v}_{\max} \le v \le v_{\max}$. Note that the right-most linear piece of L_2 is steeper than the left-most linear piece, because $|\sigma_1| = -\lambda_1 + \theta k > \lambda_1 + \theta k = \sigma_2$.

Thre are two possibilities, depending on the maximum current velocity, u_{max} (FIGURE B.3):

i. If $min\,(v_g, v_{max}) < u_{max}$, then $v^* = -min\,(v_g, v_{max})$, and $u^* = -v^*$.

ii. If $0 \le u_{max} \le min\,(v_g, v_{max})$, then $u^* = u_{max}$ and

   a. $v^* = -u_{max}$ if $\lambda_2 g_v\,(-u_{max}) + \sigma_2 \ge 0$; otherwise,

b. $v^* = max(v'', -v_{max})$, where $\lambda_2 g_v(v'') + \sigma_2 = 0$ $(v'' < 0)$.

These results are summarized in TABLE B.2.

TABLE B.5 Optimal swimming velocity summary when the switching function σ_2 is positive.

Possi-bility	u_{max} condition	Derivatve condition	Maximizing current velocity	Maximizing swimming velocity
i	$\tilde{v}_g < u_{max}$	none	$\tilde{v}_g$	$-\tilde{v}_g$
iia	$u_{max} < \tilde{v}_g$	$\lambda_2 g_v(-u_{max}, x, w, t) + \sigma_2 > 0$	u_{max},	$-u_{max}$
iib	$u_{max} < \tilde{v}_g$	$\lambda_2 g_v(-u_{max}, x, w, t) + \sigma_2 \le 0$	u_{max},	$max(v'', -v_{max})$

The optimal swimming velocity depends on the value of u_{max} relative to the constrained maximum growth velocity $\tilde{v}_g = min(v_g, v_{max})$. When the maximum current velocity exceeds the constrained maximum growth speed (possibility i): the juvenile optimally holds station swimming against the current at its (constrained) optimal growth speed. If the maximum current velocity does not exceed the constrained maximum growth speed (possibility iia–b), the optimal velocities depend on the sign of $\lambda_2 g_v(-u_{max}, w, t) + \sigma_2$. The optimal behavior is characterized by station holding (in i and iib) or upstream migration in slack current at a swimming velocity that does not exceed the maximum growth speed.

B.8.3 If the switching function σ_2 zero

When the switching function σ_2 is zero (case 3), the Hamiltonian may be written as

$$H = \theta\zeta k + \lambda_2 g(v) + L_5(v),$$

where

$$L_5(v) = \begin{cases} 0 & if\ v < 0 \\ \sigma_1 v & if\ v \ge 0 \end{cases},$$

is a piece-wise linear function.

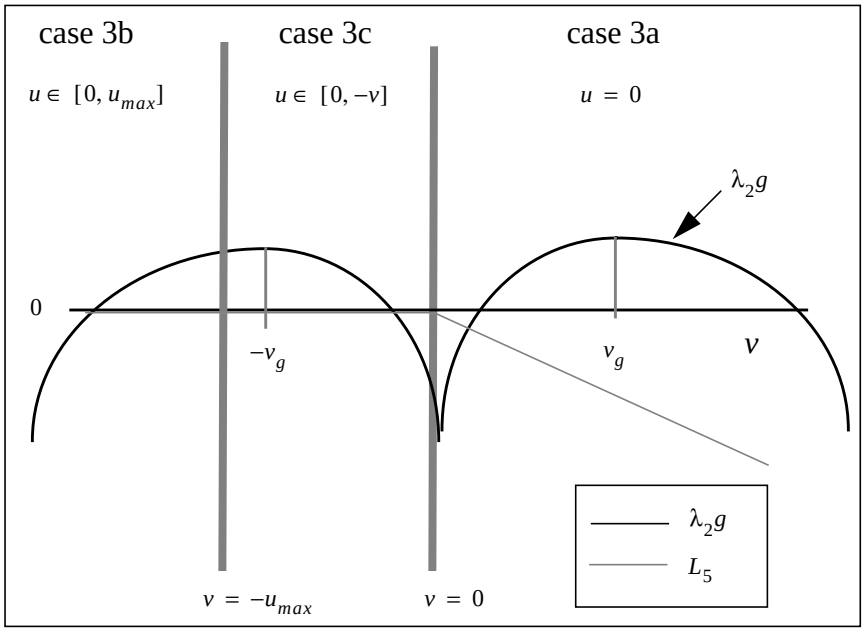

FIGURE B.8 When the switching function σ_2 is zero. The goal is to maximize the sum of the functions L_5 and $\lambda_2 g$ with respect to v, where $-v_{\max} \le v \le v_{\max}$.

Since $L_5(v)$ is strictly decreasing over $v \ge 0$ and $\lambda_2 g(v)$ is symmetric about $v = 0$, v^* is nonpositive (FIGURE B.4). Since $L_5(v) = 0$ over $v \le 0$, v^* is found by maximizing $\lambda_2 g(v)$. This, by definition, occurs at the point $v^* = max(-v_g, -v_{max})$. When $-u_{max} < v^*$, then u^* is any value in $[0, u_{max}]$; otherwise, it is any value in $[0, min(v_g, v_{max})]$. These results are summarized in TABLE B.6.

TABLE B.6 Optimal swimming velocities when the switching function σ_2 is zero.

Possibility	u_{max} condition	Maximizing current velocity	Maximizing swimming velocity
i	$\tilde{v}_g \leq u_{max}$	$[0, \tilde{v}_g]$	$-\tilde{v}_g$
ii	$u_{max} < \tilde{v}_g$	$[0, u_{max}]$	$-\tilde{v}_g$

As in case 2, the optimal velocities depend on the maximum current velocity relative to the constrained maximum growth velocity. Regardless of the value of u_{max}, the optimal current velocity is not uniquely determined, while the swimming velocity is always equal to the negative of the constrained maximum growth speed. Notice that it is always optimal to swim against the current, and that since the migration velocity is always nonpositive, migration is allowed only in the upstream direction.

APPENDIX C AN AUTONOMOUS CASE

In this appendix, I present a simplified version of the optimal control problem, where among other simplifications, state and time dependency is removed from the control constraints, and the system of canonical equations is autonomous. Specifically, the maximum current velocity, v_{max}, and the maximum swimming speed u_{max} are constants, the capture probability $k(w)$ is allowed to vary only with weight, the predation parameters θ and ζ are constants, the growth function does not depend explicitly on time, and the final time, also known as the time of estuary entry, T, is fixed. Furthermore, to avoid the complications of low maximum current velocity (see CHAPTER 6), the maximum current velocity is assumed to exceed the maximum swimming velocity. Also, $T(u_{max} + v_{max}) \geq a$, ensuring that the fish will be able to swim to $x = a$ within T time units.

For notational convenience T will denote the time of estuary rather than t_f. The optimal control problem is summarized in TABLE C.1. The switching function will be taken as $\sigma = \sigma_1$ throughout the appendix, since the assumption of autonomy make the co-state variable associated with displacement positive (See Result 6.2). Other special notation of this appendix is found in TABLE C.2.

Several special cases of this problem will be treated, demonstrating the limited number of optimal strategy types that arise from the model. In each case analyzed, the canonical

equations are developed based on the maximized Hamiltonian, and a qualitative analysis of their possible solutions is explored based on the initial sign of the switching function and growth function.

TABLE C.1 Optimal control problem (autonomous case with fixed estuary entry time).

Maximize: u, v	$-\int_0^T (\lvert u+v\rvert + \zeta)\,\theta k(w)\,dt + \Phi(w(t_f))$	(objective functional)
Subject to:	$\dot{x} = u + v$	(displacement equation)
	$\dot{w} = g(v, w)$	(weight equation)
	$0 \le u \le u_{max}$	(current velocity constraint)
	$\lvert v\rvert \le v_{max}$	(swimming velocity constraint)

TABLE C.2 Special notation.

Variable or function	Description
$u^*(t)$	Optimal current velocity.
$v^*(t)$	Optimal swimming velocity.
$x^*(t)$	Optimal downstream displacement path.
$w^*(t)$	Optimal weight path.
T	Optimal time of arrival in the estuary (fixed).
$\lambda_1(t)$	The co-state variable associated with downstream displacement.
$\lambda_2(t)$	The co-state variable associated with weight.
$\sigma(x, w, \lambda_1, t)$	The switching function.
$v_g(x, w, t)$	Maximum growth speed. It is the unconstrained swimming speed that maximizes growth.
$\tilde{v}_g(x, w, t)$	$\tilde{v}_g = min(v_g, v_{max})$.

TABLE C.3 Optimal swimming velocity summary when $u_{\max} > v_{\max}$.

Sign of switching function	Optimal current and swimming velocities
-	$u^* = \tilde{v}_g,\ v^* = -\tilde{v}_g$
+	$u^* = u_{max},\ v^* = \tilde{v}'$
0	$u^* \in [\tilde{v}_g, u_{max}]$ and $v^* = -\tilde{v}_g$, or $u^* \in [0, u_{max}]$ and $v^* = \tilde{v}_g$

C.1 The simplest case

In this section, a very simple case is explored and analyzed to the fullest, serving as an introduction of the methods used in a more complicated case. Specifically, I make the added simplifying assumptions:

A1. $u_{max} \geq v_{max}$

A2. ρ and v_{max} are such that $g(v_{max}, w) > 0$ for w in $[w_0, w_{max}]$, where w_{max} is the weight achieved by a fish swimming at its maximum swimming speed from time 0 to time t.

A3. The maximum growth velocity exceeds the maximum swimming velocity, (*i.e.*, $v_{max} < v_g(w)$ for w in $[w_0, w_{max}]$).

The canonical equations for this problem are developed using the results of TABLE C.3 which gives the values of current velocity and swimming velocity that maximize the Hamiltonian. It is best to consider cases #1, #2, and #3, separately, all determined by the switching function $\sigma(w) = \lambda_1 - \theta_1 k(w)$. The three cases correspond to $\sigma(w) > 0$, $\sigma(w) < 0$, and $\sigma(w) = 0$ respectively.

Case #1—when the switching function is negative. Assuming that $v_{max} < v_g(w)$, the optimal velocities are $u^* = u_{max}$ and $v^* = v_{max}$, and the resulting maximized $H^*(t) = H(t)\big|_{(u^*, v^*)}$. The maximized Hamiltonian is

$$H^*(t) = \sigma(w)(u_{max} + v_{max}) + \lambda_2(t)\, g(v_{max}, w) - \zeta\theta k(w), \quad \text{when } \sigma(w) > 0$$

Case #2—when the switching function is positive. The optimal velocities are $\bar{u} = v_{max}$ and $\bar{v} = -v_{max}$, giving the maximized Hamiltonian

$$H^*(t) = \lambda_2(t)\, g(v_{max}, w) - \zeta\theta k(w), \quad \text{when } \sigma(w) < 0.$$

Case #3—when the switching function is zero. The optimal velocities are given by

$(u^*, v^*) \in \{(u, v): \ v_{max} \le u \le u_{max}, v = -v_{max}\}$ or

$(u^*, v^*) \in \{(u, v): \ 0 \le u \le u_{max}, v = v_{max}\}$, and the maximized Hamiltonian is

$$H^*(t) = \lambda_2(t)\, g(v_{max}, w) - \zeta\theta k(w) \quad \text{when } \sigma(w) = 0$$

Combining these three results, the maximized Hamiltonian is

$$H^*(t) = \begin{cases} \lambda_2(t)\, g(v_{max}, w) - \zeta\theta k(w) & \text{if } \sigma(w) \le 0 \\ \sigma(w)(u_{max} + v_{max}) + \lambda_2(t)\, g(v_{max}, w) - \zeta\theta k(w) & \text{if } \sigma(w) > 0 \end{cases} \quad \text{(C.1)}$$

The canonical equations are then given by

$$\dot{\lambda}_2(t) = \begin{cases} \lambda_2(t)\, g_w(v_{max}, w^*) - \zeta\theta k_w(w^*) & \text{if } \sigma(w^*(t)) \le 0 \\ \lambda_2(t)\, g_w(v_{max}, w^*) - (\zeta + (u_{max} + v_{max}))\,\theta k_w(w^*) & \text{if } \sigma(w^*(t)) > 0 \end{cases} \quad \text{(C.2)}$$

$$\dot{w}^*(t) = g(v_{max}, w^*(t)), \quad \text{(C.3)}$$

$$\dot{\lambda}_1(t) = 0, \tag{C.4}$$

$$\dot{x}^*(t) = \begin{cases} 0 & \text{if } \sigma(w^*(t)) < 0 \\ u_{max} + v_{max} & \text{if } \sigma(w^*(t)) > 0 \end{cases} \tag{C.5}$$

$\dot{x}^*(t) \in [0, u_{max} - v_{max}] \cup [v_{max}, u_{max} + v_{max}]$ if $\sigma(w^*(t)) = 0$

There are two possibilities arising from these equations:

a. $\sigma(w^*(t)) > 0$ on $[0, T]$, or

b. $\sigma(w^*(t)) \leq 0$ for some t in $[0, T]$.

If the first possibility holds, then by (C.5), $x^*(t) = (u_{max} + v_{max})\,t$, and so at time T $x^*(T) = (u_{max} + v_{max})\,T$. By assumption, $x(T) = a$, and so $T = \dfrac{a}{(u_{max} + v_{max})}$. Therefore if $T > \dfrac{a}{(u_{max} + v_{max})}$, then the second possibility must be correct. Assume that $T > \dfrac{a}{(u_{max} + v_{max})}$. If $\sigma(w^*(t)) < 0$ holds throughout $[0, T]$, then $x(T) = 0$ which is only possible if $a = 0$: in which case the juvenile does not need to migrate at all. Next assume that $\sigma(w^*(t'')) > 0$ for some t'' in $[0, T]$; since λ_1 and θ are constants, and $k(w)$ is strictly decreasing in w, there exists a unique weight w' such that $\sigma(w') = \lambda_1 - \theta_1 k(w') = 0$. Since $g(v_{max}, \bar{w}(t)) > 0$ (by hypothesis), there must be a unique time t' such that $\bar{w}(t') = w'$. This means that the switching function is zero for only an instant of time, and therefore *no singular path is possible*.

In conclusion, when $a > 0$, the juvenile optimally waits until it grows to a critical size w' and then migrates downstream to the ocean at velocity $u_{max} + v_{max}$. The critical weight w', is that weight attained by a juvenile at time $T - a/(u_{max} + v_{max})$. Its growth is governed by (C.3). Interestingly, the exact forms of the functions $k(w)$ and $\Phi(w_T)$ are not required to solve for the trajectories x^* and w^*. The switching function is known to be

zero precisely at time $T - a/(u_{max} + v_{max})$ regardless of the precise form of $k(w)$. I merely used the fact that $k(w)$ is decreasing in w and $\Phi(w_T)$ is increasing in w_T. These facts were essential in showing that both λ_1 and λ_2 are nonnegative, and subsequently in maximizing the Hamiltonian.

An important question which arises from this example is "Under what conditions on the food density ρ is it guaranteed that assumptions (A2) and (A3) are satisfied?" The food density is expected to play an important role in shaping the optimal weight and displacement trajectories, and it would be nice to know under what conditions the simple solution described in the special case is optimal. Of course w_{max} will depend on ρ, and this dependence must be known to answer the question.

Fortunately, assumption (A2) is equivalent to $g(v_{max}, w_0) > 0$. To prove this, assume otherwise, so that $g(v_{max}, w_0) > 0$ and when $w(T) > w(0)$, there exists w' in $(w(0), w(T)]$ such that $g(v_{max}, w') \leq 0$. Since $g(v_{max}, w)$ is continuous in w, there exists a weight w'' in (w_0, w') such that $g(v_{max}, w'') = 0$. Solving the differential equation backwards in time starting with the time t'' such that $w(t'') = w''$ yields $w(t) = w''$ for t in $[0, t'']$. This contradicts that fact that $g(v_{max}, w_0) > 0$. When $w(T) < w(0)$, the same contradiction arises. Thus (A2) is indeed equivalent to $g(v_{max}, w_0) > 0$.

C.2 The general case where $v_{max} < u_{max}$.

Next I explore a more complicated situation under the assumption that the maximum swimming speed is less than the maximum current velocity, but the maximum swimming velocity is not restricted to be less than the maximum growth velocity—the velocity that

maximizes the unconstrained growth function. For convenience, in the remaining analysis, I will restrict the optimal growth velocity to be less than or equal to the maximum swimming speed, and the new optimal growth velocity will be defined as $\tilde{v}_g(w) = min(v_g(w), v_{max})$. This is the maximum of the growth function attained when the swimming speed is constrained to not exceed v_{max}.

In the forthcoming development, I will consider three possibilities that will help to characterize the optimal strategy types

1. $g(\tilde{v}_g(w_0), w_0) = 0.$
2. $g(\tilde{v}_g(w_0), w_0) > 0.$
3. $g(\tilde{v}_g(w_0), w_0) < 0.$

The maximizing paths can take on a very different character depending on the case which applies.

As in the last section, I proceed by first obtaining the maximized Hamiltonian, and then building the canonical equations. As before, I consider the three possible cases stemming from the sign of the switching function $\sigma(w) = \lambda_1 - \theta k(w)$. The optimal velocities for each case are found in TABLE C.3.

case #1—when the switching function is negative. The optimal velocities are $u^* = u_{max}$ and $v^* = min(v', v_{max})$, where $v' > 0$ satisfies

$$\sigma(w) + \lambda_2 g_v(v', w) = 0. \tag{C.6}$$

Since the swimming velocity can never exceed the maximum swimming velocity, v_{max}, it will be convenient to work with the quantity $\tilde{v}' = min(v', v_{max})$ instead of v'. Since

$g(v, w)$ is concave for $v > 0$, and the quantities $\sigma(w)$, and λ_2 are positive, v' exceeds the maximum growth velocity, $v_g(w)$. Working in terms of $\tilde{v}'$ and $\tilde{v}_g(w)$, it is known only that $\tilde{v}' \geq \tilde{v}_g(w)$. This gives

$$H_w^* = -\theta k_w(w)\ (u_{max} + \tilde{v}') + \lambda_2(t)\, g_w(\tilde{v}', w) - \zeta\theta k_w(w), \quad \text{when } \sigma(w) > 0.$$

case #2—when the switching function is positive. The optimal velocities are given by $u^* = \tilde{v}_g(w)$, and $v^* = -\tilde{v}_g(w)$ yielding

$$H_w^* = \lambda_2(t)\, g_w(\tilde{v}_g(w), w) - \zeta\theta k_w(w), \quad \text{when } \sigma(w) < 0.$$

case #3—when the switching function is zero. There are two possibilities for the optimal velocities: 1) $u^* \in [\tilde{v}_g(w^*), u_{max}]$ and $v^* = -\tilde{v}_g(w^*)$, or 2) $u^* \in [0, u_{max}]$ and $v^* = v_g$. In either case,

$$H^*{}_w = \lambda_2(t)\, g_w(\tilde{v}_g, w) - \zeta\theta k_w(w), \quad \text{when } \sigma(w) = 0.$$

The canonical equations are then given by

$$\dot{\lambda}_2 = \begin{cases} -\lambda_2 g_w(\tilde{v}_g(w^*), w^*) + \zeta\theta k_w(w^*) & \text{if } \sigma(w^*(t)) \leq 0 \\ -\lambda_2 g_w(\tilde{v}'(\lambda_1, \lambda_2, w^*), w^*) & \text{if } \sigma(w^*(t)) > 0 \\ \quad + [\zeta + u_{max} + \tilde{v}'(\lambda_1, \lambda_2, w^*)]\, \theta k_w(w^*) & \end{cases} \tag{C.7}$$

$$\dot{w}^* = \begin{cases} g(\tilde{v}_g(w^*), w^*) & \text{if } \sigma(w^*(t)) \leq 0 \\ g(\tilde{v}'(\lambda_1, \lambda_2, w^*), w^*) & \text{if } \sigma(w^*(t)) > 0 \end{cases} \tag{C.8}$$

$$\dot{\lambda}_1 = 0 \tag{C.9}$$

$$\dot{x}^* = \begin{cases} 0 & \text{if } \sigma(w^*(t)) < 0 \\ u_{max} + \tilde{v}'(\lambda_1, \lambda_2, w^*) & \text{if } \sigma(w^*(t)) > 0 \end{cases} \tag{C.10}$$

$\dot{x}^*(t) \in [0, u_{max} - \tilde{v}_g(w^*)] \cup [\tilde{v}_g(w^*), u_{max} + \tilde{v}_g(w^*)]$ if $\sigma(w^*) = 0$.

Before proceeding, it is useful to derive a result describing the behavior of the growth and switching functions in the event that, at the same instant, the growth function is zero and the switching function nonpositive.

C.2.0.1 Result. If $\sigma(w^*(t_1)) \leq 0$ and $\dot{w}^*(t_1) = 0$ at some time t_1 in $[0, T]$, then the switching function and the weight path are constant throughout $[0, T]$.

Proof: Assume that $\sigma(w^*(t_1)) = \lambda_1 - \theta_1 k(w^*(t_1)) \leq 0$ and $\dot{w}^*(t_1) = 0$ at time $t_1 \in [0, T]$. At the point t_1, the differential equation governing weight is

$$\dot{w}^* = g(\tilde{v}_g(w^*), w^*) \tag{C.11}$$

and the variables λ_1, λ_2, and x exert no influence on this differential equation. Since $w^*(t_1)$ is a stationary point of (C.11), the weight path is unable to deviate from $w^*(t_1)$, and hence remains there throughout $[t_1, T]$. Working backwards through time shows that the weight path must also be constant throughout $[0, t_1]$. ■

C.2.0.2 Corollary. If $\sigma(w^*(t_1)) \leq 0$ and $\dot{w}^*(t_1) = 0$ at some time t_1 in $[0, T]$, then $\sigma(w^*(t_1)) = 0$ and $w^*(t_1) = w_0$ on $[0, T]$.

Proof: By result C.2.0.1, if the switching function is nonpositive and the growth is zero then the switching function must be constant throughout $[0, T]$. Therefore

$\sigma(w^*(t)) = \sigma(w_0) \leq 0$. If $\sigma(w_0) < 0$, then the juvenile fails to migrate to the target $x = a$. Hence $\sigma(w^*(t)) = \sigma(w_0) = 0$ on $[0, T]$. ■

C.2.0.3 Result. If $\sigma(w^*(t_1)) = 0$ and $\dot{w}^*(t_1) \neq 0$ at some time t_1 in $[0, T]$, then the switching function remains zero for only an instant of time.

Proof: Assume that $\sigma(w^*(t_1)) = \lambda_1 - \theta_1 k(w^*(t_1)) = 0$ and $\dot{w}^*(t_1) \neq 0$ for some $t_1 \in [0, T]$. Then $\frac{d}{dt}\sigma(w^*(t_1)) = -k_w(w^*(t_1))\dot{w}^*(t_1) > 0$ since $\dot{w}^*(t_1) \neq 0$ and $k(w)$ is assumed to be strictly decreasing in w. Therefore the switching function departs from zero instantly, and hence remains zero for only an instant of time. ■

C.2.0.4 Result. If $\sigma(w_0) \neq 0$, and $\sigma(w^*(t_1)) = 0$ for t_1 in $[0, T]$, then the switching function remains zero for only an instant of time.

Proof: I proceed by showing that if $\sigma(w_0) \neq 0$, and $\sigma(w^*(t_1)) = 0$ for t_1 in $[0, T]$, then $\dot{w}^*(t_1) \neq 0$, and hence by result C.2.0.3, the switching function will remain zero for only an instant of time. If $\dot{w}^*(t_1) = 0$, then by corollary C.2.0.2 $\sigma(w^*(t_1)) = \sigma(w_0) \neq 0$, contradicting the hypothesis that $\sigma(w^*(t_1)) = 0$. Therefore $\dot{w}^*(t_1) \neq 0$, and by result C.2.0.3, the switching function remains zero for only an instant of time. ■

Armed with these results, I will explore all possible optimal strategies.

C.2.1 The case where $g(\tilde{v}_g(w_0), w_0) = 0$.

In this case, the juvenile can initially only maintain its weight by swimming at its maximum growth velocity—all other velocities lead to weight decrease. By corollary

C.2.0.2, it is impossible for the switching function to be initially negative, leaving only the possibilities that the initial value of the switching function positive or zero. These possibilities are examined below.

C.2.1.1 Switching function initially zero.

If $\sigma(w_0) = 0$, then by result Result 6.2, switching function and the growth rate remain zero throughout $[0, T]$, and the canonical equations are

$$\dot{\lambda}_2 = -\lambda_2(t)\, g_w(\tilde{v}_g(w^*), w^*) + \zeta\theta k_w(w^*) \tag{C.12}$$

$$\dot{w}^* = g(\tilde{v}_g(w^*), w^*(t)) = 0 \tag{C.13}$$

$$\dot{\lambda}_1 = 0 \tag{C.14}$$

$$\dot{x}^* = [0, u_{max} - \tilde{v}_g(w^*)] \cup [\tilde{v}_g(w^*), u_{max} + \tilde{v}_g(w^*)] \tag{C.15}$$

where v^* may be chosen as $\tilde{v}_g(w_0)$ or $-\tilde{v}_g(w_0)$ at each time in $[0, T]$. When $T(\tilde{v}_g(w_0) + u_{max}) < a$, I can rule out this possibility, for by (C.15), $\dot{x}^* \le u_{max} + \tilde{v}_g(w_0)$, and the juvenile has no hope of migrating a distance of a within time T, therefore I will assume that $T(\tilde{v}_g(w_0) + u_{max}) \ge a$. If $T(\tilde{v}_g(w_0) + u_{max}) = a$, then (C.15) becomes $\dot{x}^* = \tilde{v}_g(w_0) + u_{max}$, since this is the only choice of v and u satisfying the boundary condition $x(T) = a$. If $T(\tilde{v}_g(w_0) + u_{max}) > a$, equation (C.15) leaves infinitely many choices for $\dot{x}^*$, and it is only necessary for $x^*(T) = a$. Do each of these choices yield the same value of the objective functional? If so, then a maximizing displacement path is not unique.

Let x^* represent any displacement path satisfying $x(T) = a$. Then the objective functional becomes

$$-\int_0^T (|\dot{x}^*(t)| + \zeta)\,\theta k(w^*(t))\,dt + \Phi(w^*(T))$$

$$= -\int_0^T (|\dot{x}^*(t)| + \zeta)\,\theta k(w_0)\,dt + \Phi(w_0) \quad (\text{Since } \bar{w}(t) = w_0)$$

$$= -\theta k(w_0)\int_0^T (\dot{x}^*(t) + \zeta)\,dt + \Phi(w_0) \quad (\text{Since } \dot{x}^*(t) \geq 0)$$

$$= -k(w_0)\,\theta(a + T\zeta) + \Phi(w_0). \qquad (\text{Since } \int_0^T \dot{x}^*(t)\,dt = a)$$

Thus all solutions to (C.15) yield the same value of the objective functional, and hence all are maximizing displacement paths.

C.2.1.2 Switching function initially positive.

If the switching function is initially positive, (*i.e.*, $\sigma(w_0) > 0$), then the optimal swimming velocity is at least as great as the optimal growth velocity (*i.e.*, $\tilde{v}'(\lambda_1, \lambda_2(0), w_0) \geq \tilde{v}_g(w_0)$), and since $g(v, w)$ is concave in v, $\dot{w}^*(0) = g(v'(\lambda_1, \lambda_2(0), w_0), w_0) \leq g(\tilde{v}_g(w_0), w_0) = 0$, demonstrating that growth is initially nonpositive.

I next examine the case where growth is initially negative. Since the growth function is concave in v, his can occur only when $\tilde{v}_g(w_0) < v_{max}$. Is it possible for the juvenile to later grow back to size w_0 within time T? The answer is no. Otherwise, there exists a time $t_1 > 0$ such that $w^*(t_1) = w_0$ and $w^*(t_1 - \varepsilon) < w_0$ for all $\varepsilon > 0$, where $t_1 - \varepsilon > 0$.

Because I assumed that the switching function was initially positive, then the switching function must also be positive at t_1, since $\sigma(w^*(t_1)) = \sigma(w_0) > 0$, and therefore by the concavity of the growth function, $g(v'(\lambda_1, \lambda_2(t_2), w_0), w_0) < g(\tilde{v}_g(w_0), w_0)$. Next note that $w^*(t_1) - w^*(t_1 - \varepsilon) > 0$ and therefore $\dot{w}^*(t_1) \geq 0$. But $\dot{w}^*(t_1) \geq 0$ contradicts our earlier result that $\dot{w}^*(t_1) = g(\tilde{v}'(\lambda_1, \lambda_2(t_2), w_0), w_0) < g(\tilde{v}_g(w_0), w_0) = 0$. Thus when the switching function is initially positive and growth initially negative, the juvenile's weight immediately falls below w_0, and remains below w_0.

If the growth function is initially zero, then
$g(\tilde{v}'(\lambda_1, \lambda_2(0), w_0), w_0) = g(\tilde{v}_g(w_0), w_0) = 0$, and therefore
$\tilde{v}'(\lambda_1, \lambda_2(0), w_0) = \tilde{v}_g(w_0) = v_{max}$. I show that it is impossible for weight t deviate from w_0 on $[0, T]$. Suppose otherwise. Then there must exist a time t_1 such that $w^*(t_1) = w_0$, and $\dot{w}^*(t_1) \neq 0$. Since the switching function was positive at w_0, it must also be positive at $w^*(t_1)$. Furthermore,

$$\begin{aligned} \dot{w}^* &= g(\tilde{v}'(\lambda_1, \lambda_2(t_1), w^*(t_1)), w^*(t_1)) \\ &= g(\tilde{v}'(\lambda_1, \lambda_2(t_1), w_0), w_0) \\ &= g(v_{max}, w_0) = 0 \end{aligned} \tag{C.16}$$

But this contradicts our hypothesis that $\dot{w}^*(t_1) \neq 0$. Therefore weight never deviates from w_0. The switching function remains positive throughout $[0, T]$ and the juvenile optimally migrates downstream at speed $v_{max} + u_{max}$ throughout. This can only occur when $T(v_{max} + u_{max}) = a$.

C.2.1.3 Optimal initial value of the switching function.

I have now discussed some qualities of the solutions of the canonical equations in the event that $g(v_g(w_0), w_0) = 0$, and have discussed the outcomes resulting from the initial sign of switching function. I found switching function cannot be initially negative, and so can only be initially positive or zero. Under what conditions is it initially zero? I showed that if the $\sigma(w_0) = 0$, then $T(\tilde{v}_g(w_0) + u_{max}) \geq a$, otherwise the juvenile could not reach its downstream destination, a within the allotted time, T. Therefore, when $T(\tilde{v}_g(w_0) + u_{max}) < a$ the switching function is initially positive, and the juvenile begins its downstream migration immediately at time zero.

On the other hand, what if $T(\tilde{v}_g(w_0) + u_{max}) \geq a$? Is the initial value of the switching function initially zero, or is it positive? To answer this question, I appeal to the objective function directly, and evaluate it using the results of sections C.2.1.1 and C.2.1.2. In section C.2.1.1, I showed that when the switching function is initially zero, the weight of the juvenile remains at w_0 throughout $[0, T]$. In section C.2.1.2 I showed that when the switching function is initially positive, and $T(v_{max} + u_{max}) > a$, the juvenile's weight remains below w_0 throughout $(0, T]$. Let v_1^*, x_1^*, w_1^* represent the velocity, displacement, and weight trajectories in the case that the switching function is initially positive. When $\sigma(w_0) > 0$ and $T(v_{max} + u_{max}) > a$ the objective functional is

$$-\int_0^T (|\dot{x}_1^*(t)| + \zeta)\, \theta k(w_1^*(t))\, dt + \Phi(w_1^*(T))$$

$$< -\int_0^T (|\dot{x}_1^*(t)| + \zeta)\,\theta k(w_0)\,dt + \Phi(w_0) \quad \text{(Since } w_1^*(t) < w_0,\ t > 0\text{)}$$

$$= -\theta k(w_0)\int_0^T (\dot{x}_1^*(t) + \zeta)\,dt + \Phi(w_0) \quad \text{(Since } \dot{x}_1^*(t) \geq 0\text{)}$$

$$= -\theta k(w_0)\,(a + T\zeta) + \Phi(w_0)\,. \quad \text{(Objective func.when } \sigma(w_0) = 0\text{)}$$

This string of inequalities demonstrates that when the switching function is positive initially and $T(v_{max} + u_{max}) > a$, the value of the objective functional is inferior to that of the objective functional when the switching function is initially zero. Therefore the switching function is indeed initially zero.

In conclusion, whenever $g(v_g, w_0) = 0$ and $T(v_g(w_0) + u_{max}) < 0$, the switching function is initially positive, and as a result, the juvenile begins its migration at time zero. If on the other hand $g(v_g, w_0) = 0$, $T(v_g(w_0) + u_{max}) \geq 0$, and $T(v_{max} + u_{max}) > a$, then the switching function is initially zero, and an infinity of displacement paths are optimal whenever $T(\tilde{v}_g(w_0) + u_{max}) > 0$ (see section C.2.1.1).

The very last case I need to cover, is the case where $T(\tilde{v}_g(w_0) + u_{max}) = T(v_{max} + u_{max}) = a$. I showed earlier that when the switching function is initially positive and $\tilde{v}_g(w_0) = v_{max}$, then weight remains at w_0 throughout $[0, T]$ and the optimal strategy clearly consists of migrating downstream in the fastest current u_{max}, swimming downstream at the maximum swimming speed, v_{max}. Any other strategy does not allow the fish to arrive at a within time T. Interestingly, this strategy is also covered by case where the switching function is initially zero. This suggests that there

is no unique optimal initial value of the switching function, and that is only required to be negative.

C.2.2 The case where $g(\tilde{v}_g(w_0), w_0) < 0$.

In this section I examine the optimal juvenile behavior in the case where the initial growth rate is negative. This is possible when food density is low, or standard and active metabolism is elevated due to high temperatures. An important result in this case is that the juvenile's weight can never again reach w_0 on $(0, T]$.

C.2.2.1 Result. If $g(\tilde{v}_g(w_0), w_0) < 0$, then the weight path remains below w_0 throughout $(0, T]$.

Proof: Suppose otherwise, so that $g(\tilde{v}_g(w_0), w_0) < 0$ and $w^*(t_1) \geq w_0$ for some t_1 in $(0, T]$. Since the weight path is necessary continuous in time, it is possible to assume that t_1 is the minimum time such that $t_1 > 0$ and $w^*(t_1) = w_0$. At any time $t_1 - \varepsilon$, such that $\varepsilon > 0$ and $t_1 - \varepsilon > 0$, $w^*(t_1 - \varepsilon) < w_0$, and therefore $w^*(t_1) - w^*(t_1 - \varepsilon) > 0$, implying that $\frac{d}{dt}w^*(t_1) \geq 0$. However, by hypothesis, $\frac{d}{dt}w^*(t_1) = g(v^*(t_1), w^*(t_1)) \leq g(\tilde{v}_g(w_0), w_0) < 0$, yielding a contradiction. Hence $w^*(t) < w_0$ on $(0, T]$. ■

C.2.2.2 Switching function initially negative?

Recall that the switching function is a decreasing function of weight. Therefore, if it is initially zero (*i.e.*, $\lambda_1 - \theta_1 k(w_0) < 0$), by result C.2.2.1, it must remain negative throughout $[0, T]$. This is impossible because the juvenile would never migrate to the ocean. It is therefore impossible for the switching function to be initially negative.

C.2.2.3 Switching function initially zero?

By result C.2.0.3, if the switching function is initially zero, then it can remain zero for only an instant of time. Therefore the switching function either becomes initially negative or positive after time $t = 0$. If it becomes negative, then it remains negative so that the fish fails to migrate, which is impossible since by hypothesis, $x^*(T) = a > 0$. Therefore if the switching function is initially zero, it immediately rises to a positive value. This is also impossible since by hypothesis $\frac{d}{dt}\sigma(w_0) = -\theta k_w(w_0)\,\dot{w}^*(0) < 0$. Thus the switching function is not initially zero.

C.2.2.4 Switching function initially positive.

In sections C.2.2.2 and C.2.2.3 I showed that it is impossible for either the switching function to be initially negative or zero, and therefore the switching function is initially positive. This means that the juvenile begins migration immediately at $t = 0$, swimming a rate faster than the optimal growth velocity, and in the swiftest current, and continues this behavior as long as the switching function is positive. Does the switching function remain positive? If it does, then

$$a = x^*(T) = \int_0^T \tilde{v}'(\lambda_1, \lambda_2(t), w^*(t))\,dt + Tu_{max} > \int_0^T \tilde{v}_g(w^*(t))\,dt + Tu_{max}. \quad \text{(C.17)}$$

If (C.17) fails to hold, then at some point in time, say t_1 in the interval $(0, T)$, the switching function must eventually fall to zero (*i.e.*, $\sigma(w^*(t_1)) = 0$) but by result C.2.0.4, remains at zero for only an instant of time. Let t_1 be the minimum time at which this occurs. If the switching function becomes positive immediately after t_1, then $\frac{d}{dt}\sigma(w^*(t_1)) = 0$, and consequently, $\frac{d}{dt}\sigma(w^*(t_1)) = -k_w(w^*(t_1))\,\dot{w}^*(t_1) = 0$,

implying that $\dot{w}^*(t_1) = 0$ since $k(w)$ is strictly decreasing in w. By corollary C.2.0.2, the switching function must then be zero throughout $[0, T]$. This contradicts the hypothesis that the switching function is initially zero, and therefore, at least at the very first time the switching function reaches zero the switching function is negative immediately after t_1. During the time when the switching function is negative, the juvenile holds its station at $x^*(t_1)$, swimming against the current at its optimal growth velocity.

If the juvenile has not reached a at t_1, (*i.e.*, $x^*(t_1) \neq a$), then at some point in time it must begin migrating downstream again, and therefore, once again the switching function becomes positive. This can only occur if at some time after t_1 the juvenile's growth rate is zero and the switching function is negative. However, by result C.2.0.1, this implies that the switching function is a negative constant over $[0, T]$. This contradicts the hypothesis that the switching function is initially positive. Therefore the juvenile must reach position $x = a$ by t_1.

C.2.2.5 Summary of behavior when $g(v_g(w_0), w_0) < 0$.

In summary, it was shown that when the growth function is initially negative at the optimal swimming velocity, then the juvenile begins migration immediately at time zero, and does not cease to migrate until it reaches its final destination at $x = a$. Upon reaching $x = a$, it holds its station, migrating against the current at its optimal growth velocity until time T.

When does the juvenile arrive at $x = a$? Since $\dot{x}^*(t) \leq u_{max} + v_{max}$, there is a lower bound for t_1, namely

$$\frac{a}{(u_{max} + v_{max})} < t_1.$$

Furthermore, if the optimal growth velocity does not vary too much over $[0, t_1]$, then an *approximate* upper bound is given by

$$\frac{a}{u_{max} + v_g(w_0)}.$$

C.2.3 The case where $g(v_g(w_0), w_0) > 0$.

In this case, the juvenile initially is able to grow by swimming at its optimal growth velocity. There is the possibility, however, that in order to achieve its downstream migration target in the allotted time, it will be unable to travel at its optimal growth velocity, and may even have to settle for negative growth. This is one of the several issues examined in this section.

As before, I proceed by considering the initial sign of the switching function.

C.2.3.1 The case where the switching function is initially negative.

At least intuitively, it is not possible to rule out the possibility that the switching function is initially negative when the juvenile has positive initial growth potential. For if time permits, the juvenile could reduce its overall predation risk by initially taking advantage of its growth opportunity and minimizing its predator encounter rate, then running the gauntlet of predators at a larger size.

Assuming that the switching function *is* initially negative, then the juvenile holds its station at $x = 0$, swimming against the current at is optimal growth velocity. Since

growth is then initially positive and the switching function is an increasing function of weight, the switching function is also increasing. The switching function must increase above zero at some time, otherwise, no downstream migration would be possible. Let $t_1 > 0$ be the first time that the switching function reaches zero. By corollary C.2.0.2, the growth function and the switching function cannot be simultaneously zero at t_1. Therefore, either $\dot{w}^*(t_1) > 0$, or $\dot{w}^*(t_1) < 0$. Since t_1 is the first time that the switching function reaches zero, $\frac{d}{dt}\sigma(w^*(t_1)) > 0$, and since the switching function is a strictly increasing function of weight, $\dot{w}^*(t_1) > 0$. Thus immediately after t_1, the switching function increases above zero, and the juvenile begins migrating downstream at a velocity greater that its optimal growth velocity and in the swiftest current.

Does the switching function, once it rises above zero, later turn around and descend to zero? I show that it cannot. Suppose the switching function does display this behavior, so that there exists a minimum time $t_2 > t_1$ such that $\sigma(w^*(t_2)) = \sigma(w^*(t_1)) = 0$. By corollary C.2.0.2, the switching function and the growth function cannot be zero simultaneously, otherwise $\sigma(w^*(t_2)) = \sigma(w_0) < 0$, contradicting the hypothesis that $\sigma(w^*(t_2)) = 0$. Therefore the switching function must be negative immediately after t_1. Consequently, $\frac{d}{dt}\sigma(w^*(t_2)) < 0$ which in turn implies that $\dot{w}^*(t_2) < 0$. Since $w^*(t_1) = w^*(t_2)$,

$$\dot{w}^*(t_1) = g(\tilde{v}_g(w^*(t_1)), w^*{}_1) = g(\tilde{v}_g(w^*(t_2)), w^*(t_2)) = \dot{w}^*(t_2) < 0.$$

This contradicts the early finding that $\dot{w}^*(t_1) > 0$. Therefore it is impossible for the switching function to fall back to zero once it becomes positive.

C.2.3.2 The case where the switching function is initially nonnegative.

If the switching function is initially nonnegative, then the juvenile initially swims downstream at a velocity greater than the optimal growth velocity until the switching function becomes negative or it reaches its destination of $x = a$. Actually, I will show that it is impossible for the switching function to become negative, and the migration will not terminate before at time T.

Suppose that the switching function turns negative, so that there exists a time $t_1 < T$ such that $\sigma(w^*(t_1)) = 0$ and $\sigma(w^*(t_1 + \varepsilon)) < 0$ for any $\varepsilon > 0$ sufficiently small. Once negative, the switching function must remain negative throughout $(t_1, T]$, otherwise it is possible to use corollary C.2.0.2 to show that the switching function is zero and the weight path are constant over $[0, T]$, violating the hypothesis that $g(\tilde{v}_g(w_0), w_0) > 0$. Therefore the juvenile's migration must terminate at t_1, where $x^*(t) = a$. During the time period $[t_1, T]$, the juvenile holds its station, and swims against the current at its optimal growth speed.

I proceed by showing that the above scenario is never optimal, because there exists another strategy which is superior. Let fish 1 follow the velocity trajectories $v_1(t)$ and $u_1(t)$ outlined in the above paragraph, and as usual let $x_1(t)$ and $w_1(t)$ represent the displacement and weight paths. Now consider a juvenile, hereafter referred to as fish 2, adopting velocity curves $v_2(t), u_2(t)$ with corresponding state paths $x_2(t), w_2(t)$, such that its initial weight is w_0, where

$$v_2(t) = v_1(t + t_1),\ u_2(t) = u_1(t + t_1) \text{ when } t < T - t_1, \tag{C.18}$$

$$v_2(t) = v_1(t - (T - t_1)),\ u_2(t) = v_1(t - (T - t_1)) \text{ when } t \geq T - t_1. \tag{C.19}$$

I show that the strategy of fish 2 is superior to that of fish 1. In the first step, I demonstrate that fish 2 satisfies the terminal condition $x_2(T) = a$. This is true because

$$\int_0^T \dot{x}_1(t)\,dt = \int_0^{T-t_1} \dot{x}_1(t)\,dt + \int_{T-t_1}^T \dot{x}_1(t)\,dt$$

$$= 0 + \int_{T-t_1}^T \dot{x}_1(t)\,dt \qquad \text{(Since } \dot{x}_1(t) = 0 \text{ on } (0, T-t_1)\text{)}$$

$$= \int_{T-t_1}^T \dot{x}_2(t-(T-t_1))\,dt \qquad \text{(By (C.19))}$$

$$= \int_0^{t_1} \dot{x}_2(t)\,dt = a. \qquad \text{(Since } x_1(t_1) = a\text{).}$$

Next, I derive a series of results used to show that the strategy of fish 2 is superior to that of fish 1.

Initially, both fish weigh w_0. On the interval $[0, T-t_1]$, fish 2 follows the autonomous differential equation

$$\dot{w} = g(\tilde{v}_g(w), w). \qquad \text{(C.20)}$$

There are two possibilities: $w_2(T-t_1) > w_1(0)$ or $w_2(T-t_1) \le w_1(0)$. Suppose the second of these possibilities prevails. Since $w_1(0) = w_0$ and $g(\tilde{v}_g(w_0), w_0) > 0$, there must exist a time t_2 in $[0, T-t_1]$ such that $\dot{w}_1(t_2) = 0$. But this implies that $w_2(t_2)$ is a stationary point of (C.20). Since it is impossible for a path arising from an autonomous differential equation to reach a stationary point if it begins away from it, $w_2(T-t_1) > w_1(0)$ is the only possibility.

I now compare the weight of fish 2 over $[T - t_1, T]$ to the weight of fish 1 over $[0, t_1]$. Our claim is that $w_2(t) > w_1(t - (T - t_1))$ when $t \geq T - t_1$. For convenience, define $W_1(t) = w_1(t - (T - t_1))$, and $V_1(t) = v_1(t - (T - t_1))$, so that our claim is equivalent to $w_2(t) > W_1(t)$ when $t \geq T - t_1$. Both $W_1(t)$ and $w_2(t)$ follow the differential equation

$$\dot{w} = g(\tilde{v}_1(t), w), \tag{C.21}$$

but $W_1(T - t_1) = w_0$, while $w_2(T - t_1) > w_0$, as demonstrated earlier. If at some time $t_3 > T - t_1$, the weight path W_1 and w_2 coincide, then the uniqueness of solutions of ordinary differential equations is violated, and therefore $w_2(t) > W_1(t)$ as claimed earlier.

Next, I show that the weight of fish 2 over $[0, T - t_1]$ dominates the weight of fish 1 over $[t_1, T]$, (*i.e.*, $w_2(t) > w_1(t + t_1)$ for t in $[0, T - t_1]$). This time define $W_1(t) = w_1(t + t_1)$. Our claim is equivalent to $w_2(t) \geq W_1(t)$ on $[0, T - t_1]$. Both $w_2(t)$ and $W_1(t)$ follow the differential equation

$$\dot{w} = g(v_2(t), w), \tag{C.22}$$

but $w_2(0) = w_0$, while $W(0) \leq w_0$ (this follows since the switching function is zero at t_1 and positive at 0). By uniqueness of solutions to ordinary differential equations, $w_2(t) \geq W_1(t)$ on $[0, T - t_1]$.

I next appeal to the switching function to demonstrate that $w_1(T) \leq w_2(T)$. Suppose otherwise, so that $w_1(T) > w_2(T)$. Since $w_2(t) > w_1(t + t_1)$ for t in $[0, T - t_1]$, $w_1(T) > w_2(T) > w_1(t_1)$. Since the switching function is increasing in weight, $\sigma(w_1(T)) > \sigma(w_1(t_1)) = 0$. This contradicts the earlier finding that the switching

function must remain negative after t_1. Therefore the terminal weight of fish 2 is at least as large as that of fish 1.

Armed with these results, it is now possible to show that fish2 has a greater objective functional value than fish 1. Evaluating the difference in objective functional values for fish 1 and fish 2 gives

$$-\int_0^T (|\dot{x}_2(t)| + \zeta)\,\theta k(w_2(t))\,dt + \Phi(w_2(T)) + \int_0^T (|\dot{x}_1(t)| + \zeta)\,\theta k(w_1(t))\,dt - \Phi(w_1(T))$$

$$> -\int_0^T (\dot{x}_2(t) + \zeta)\,\theta k(w_2(t))\,dt + \int_0^T (\dot{x}_1(t) + \zeta)\,\theta k(w_1(t))\,dt$$

$$> -\int_0^{T-t_1} \zeta\theta k(w_2(t))\,dt - \int_{T-t_1}^{T} (\dot{x}_2 + \zeta)\,\theta k(w_2(t))\,dt$$

$$+\int_{t_1}^{T} \zeta\theta k(w_1(t))\,dt + \int_0^{t_1} (\dot{x}_1(t) + \zeta)\,\theta k(w_1(t))\,dt$$

$$= -\int_0^{T-t_1} \zeta\theta k(w_2(t))\,dt - \int_{T-t_1}^{T} (\dot{x}_2(t) + \zeta)\,\theta k(w_2(t))\,dt$$

$$+\int_0^{T-t_1} \zeta\theta k(w_1(t+t_1))\,dt + \int_{T-t_1}^{T} (\dot{x}_2(t) + \zeta)\,\theta k(w_1(t-(T-t_1)))\,dt$$

$$= \zeta\theta \int_0^{T-t_1} \{k(w_1(t+t_1)) - k(w_2(t))\}\,dt$$

$$+\int_{T-t_1}^{T} \{(\dot{x}_2(t)\,\theta_1 + \theta_2)\,k(w_1(t-(T-t_1))) - (\dot{x}_2(t)\,\theta_1 + \theta_2)\,k(w_2(t))\}\,dt$$

$$> \int_{T-t_1}^{T} \{ (\dot{x}_2(t)\,\theta_1 + \theta_2)\, k(w_1(t-(T-t_1))) - (\dot{x}_2(t)\,\theta_1 + \theta_2)\, k(w_2(t)) \}\, dt$$

$$> 0.$$

Thus the value objective functional of fish 2 exceeds that of fish 1. Therefore it is impossible for the switching function, assumed initially positive, to fall to a negative value in the interval $(0, T)$. Furthermore, if it ever becomes zero, it must do so exactly at T.

C.2.3.3 Varying T.

Now that behavior in the case where the switching function is initially nonnegative has been described, it is useful to know whether it can possibly happen. The answer is yes. For example, if T is chosen such that $(u_{max} + v_{max})\, T = a$, then the migration rate must remain at $u_{max} + v_{max}$ throughout $[0, T]$ in order to achieve the downstream target of $x = a$. This is possible only when the switching function is initially nonnegative. Intuitively, the switching function must be nonnegative initially whenever $(u_{max} + v_{max})\, T$ barely exceeds a. On the other hand, if $(u_{max} + v_{max})\, T$ is much greater than a, then the juvenile can afford to delay migration initially and spend its early days growing at its optimal rate and avoiding predators.

C.3 Summary

The possible behaviors of the maximizing paths are simple to enumerate. One of the following three behaviors is optimal:

S1. Initially, the juvenile holds its station at $x = 0$ swimming against the current at its optimal growth speed. At some critical weight, it begins migrating downstream, swimming in the swiftest current, and actively swimming downstream at a speed greater than its optimal growth speed. The juvenile does not reach $x = a$ until T.

S2. The juvenile begins migrating immediately after emergence swimming at a speed greater than or equal to its optimal growth speed, and in the swiftest current. It ceases migration only when $x = a$. If the juvenile reaches a before T, then it holds its station at a, swimming against the current at its optimal growth speed.

S3. An infinite number of behaviors is optimal. At each instant the juvenile swims downstream at its optimal growth speed, or against the current at its optimal growth speed, and migration upstream is not permitted.

The strategies are exhaustive and the optimal one is determined by examining the sign of the growth function and swimming function (TABLE C.4).

Strategy S1. The strategy is characterized by initial station holding. It occurs only when $g(v_g(w_0), w_0) > 0$, and $T(u_{max} + v_{max})$ is sufficiently larger than a.

Strategy S2. The strategy is characterized by initial migration. It occurs under a variety of conditions:

- When $g(v_g(w_0), w_0) > 0$ and $T(u_{max} + v_{max})$ is not sufficiently greater than a.
- When $g(v_g(w_0), w_0) = 0$ and $T(u_{max} + v_g(w_0))$ does not exceed a.
- When $g(v_g(w_0), w_0) < 0$.

Strategy S3. This is actually a class of strategies—infinitely may strategies are optimal. This occurs when $g(v_g(w_0), w_0) = 0$ and $T(u_{max} + v_g(w_0))$ is greater than a.

TABLE C.4 Optimal strategies based on the initial sign of the growth and switching functions.

	$\sigma(w_0) < 0$	$\sigma(w_0) = 0$	$\sigma(w_0) > 0$
$g(v_g(w_0), w_0) < 0$	Impossible	Impossible	S2
$g(v_g(w_0), w_0) = 0$	Impossible	S3 or S2[a]	S2
$g(v_g(w_0), w_0) > 0$	S1	S2	S2

[a] Strategy S3 applies when $T(u_{max} + v_g(w_0)) > a$, S2 otherwise.

APPENDIX D NUMERICAL METHODS

This appendix outlines the methods used to solve the optimal control problem in the case where the solution does not admit a singular path, when the switching function is always $\sigma = \sigma_1$ (*i.e.*, the co-state variable associated with displacement is positive, the maximum current velocity exceeds the maximum swimming velocity, and the only control parameter is t_f—the time of estuary entry. Under these assumptions, the system of four canonical equations (two state and two co-state equations) are easily specified, along with their boundary conditions. Three of the boundary conditions are specified by end conditions on the state variables: $x(0) = 0$, $w(0) = w_0$, and $x(t_f) = a$. And a fourth condition is supplied by a transversality condition $\lambda_2(t_f) = \Phi_w$. Since the control parameter, t_f, is unknown, it will need to be determined as well. In the standard treatment of optimal control, this control parameter is determined by using a second transversality condition, namely

$$H + \Phi_{t_f} = 0, \tag{D.1}$$

where H and Φ_{t_f} are evaluated at the optimal terminal states and co-states. However, temporal fluctuations in model parameters can make the fitness curve contain multiple maxima and minima, so that solutions of (D.1) can be misleading. Therefore I adopt the more conservative approach broken into three basic steps: First, I of solve the canonical equations for many fixed values of t_f, obtaining a plot of how the value of the fitness

functional varies with t_f; secondly, I bracket the optimal value through visual inspection; lastly, I use a standard one-dimensional numerical function maximizing routine to locate the best value of t_f.

This solution technique requires two types of numerical algorithms—a method for solving a two-point boundary value problem described by the 4 canonical equations along with their four boundary conditions, and a maximizing routine to identify the optimal estuary entry time, and to identify the controls that maximize the values of the controls that maximize the Hamiltonian. To solve the two-point boundary value problem, I use the *shooting method,* a method that is essentially a root finding routine with a built-in integration routine.

D.1 The shooting method

The shooting method starts by solving the canonical equations using the two known initial conditions, $x(0) = 0$ and $w(0) = w_0$, and two guesses for the initial co-state values, say $\hat{\lambda}_1(0)$ and $\hat{\lambda}_2(0)$. The resulting terminal states are then evaluated to see how close they come to satisfying the known terminal constraints: $x(t_f) = a$ and $\lambda_2(t_f) = \Phi_w(w(t_f), t_f)$. The error, represented by the a discrepancy vector, **F**, where

$$\begin{bmatrix} \mathbf{F}_1 \\ \mathbf{F}_2 \end{bmatrix} = \begin{bmatrix} \hat{x}(t_f) - a \\ \hat{\lambda}_2(t_f) - \Phi_w(\hat{w}(t_f), t_f) \end{bmatrix}$$

is then used to construct better estimates of the initial co-state variables (I use Newton-Raphson), and the process repeats. When the terminal constraints are satisfied (to within a specified tolerance), and the solution paths are output (FIGURE D.1). I use the routine

shoot() for the shooting method, along with the numerical integration routine **odeint()** that implements Runge-Kutta with adaptive step size control (Press *et al.*, 1988).

```
procedure shooting method begin t=0
    initialize λ1(0), λ2(0), x(0), w(0)
    initialize Δλ
    do
begin
    λ1(0), λ2(0) <– newton raphson Δλ, λ1(0), λ2(0), x(0), w(0)
end
    while(not terminal condition)
```

FIGURE D.1 Pseudo code for the shooting method.

Each step of the Newton-Raphson algorithm requires building a 2x2 matrix containing partial derivatives of the discrepancies calculated by finite differencing. Finite differencing requires an increment vector $d\lambda$ (see FIGURE D.1), and building the matrix requires three passes of the routine **odeint()**.

D.2 Overcoming difficulties of the shooting method

As mentioned before, this implementation of the shooting method is essentially a Newton-Raphson algorithm that builds a matrix of partial derivatives by finite differencing to update its solution estimate. Choosing good increments $\Delta\lambda = [\Delta\lambda_1(0), \Delta\lambda_2(0)]$ for numerical derivatives is crucial for the success of shooting. If the increments are too large, round-off error can make the solution lose meaning, and if too large, the terminal values of the state and co-state variables may whiplash so that the finite differences do not adequately approximate the partial derivatives.

Another difficulty arises in choosing good estimates of the unknown initial co-state variables. The Newton-Raphson method will work only when the discrepancy vector, **F**, varies smoothly in a neighborhood of the solution, and if the initial guess is close enough to the actual solution. In the vicinity of the root, the method performs well, converging quadratically.

Both of the difficulties mentioned above can be overcome by finding good initial estimates of the initial co-state variables. These estimates would give a good idea of the scale appropriate for choosing the increments $d\lambda$, and put the guesses close enough to the actual solution to allow quadratic convergence of Newton-Raphson. Fortunately, some important qualitative knowledge about the optimal paths of the state variables, and information about the optimal controls assists in choosing these values.

My approach proceeds by solving the canonical equations backward in time to the initial states and co-states, starting with reasonable estimates for the terminal state and co-state variables. Doing this requires good estimates of the terminal weight (weight at estuary entry) and the approximate time that the switching function is zero. A good estimate of terminal weight is obtained by recalling that early juvenile behavior is governed largely by feeding and predator avoidance, with the juvenile optimizing its food intake. This means that its terminal weight is approximated by the weight achieved by maximizing its growth over the time horizon—call it w_{max}. The terminal value of the co-state variable associated with weight can then be approximated using the relationship

$$\lambda_2(t_f) = \Phi_w(w(t_f), t_f) \cong \Phi_w(w_{max}, t_f)$$

Another quantity that can be estimated is the time the switching function is zero. Assuming that migration occurs mainly at the end of the time horizon, and approximating the travel time by assuming that the fish migrates in the swiftest current and at a swimming speed that maximizes its growth, it is then possible to solve the displacement backwards from the terminal conditions $w = w_{max}$ and $x = a$ to the point in time that $x = 0$. This time approximates the time that the switching function is zero. At this time, referred to as the switching time, t_{switch},

$$0 = \sigma = \lambda_1 (t_{switch}) - k (x (t_{switch}), w (t_{switch}), t_{switch}),$$

giving an estimate for $\lambda_1 (t_{switch})$, that I use to estimate $\lambda_1 (t_f)$. I should point out that will not always be a good estimate, especially with a large degree of spatial heterogeneity modelled, but for most of my numerical work the estimate was adequate for convergence.

Given the approximations of the terminal values of the co-state variables, the weight variable, and the known value of the displacement variable, $x = a$, I solve the canonical equations backward in time to estimate the initial values of λ_1 and λ_2. This method of estimation, applied in CHAPTER 6 resulted in convergence usually within 4-6 Newton-Raphson steps. (Note however, that algorithm tolerances also determine the number of necessary steps.)

D.3 Driver for shoot

I have included a documented C program code that drives the function **shoot()**. It is contained in the program file **target.c**. The methods and arguments of **shoot()** are found in FIGURE D.2.

void shoot(nvar, v, delv, n2, x1, x2, eps, h1, hmin, f, dv)
int nvar, n2;
double v[], delv[], x1, x2, eps, h1, hmin, f[], dv[];

Improve the trial solution of a two point boundary value problem for **nvar** coupled ODEs [ordinary differential equations] shooting from **x1** to **x2**. Initial values for the **nvar** ODEs at **x1** are generated from the coefficients **v[1..n2]**, using the user-supplied routine **load**. The routine integrates the ODEs to **x2** using the Runge-Kutta method with tolerance **eps**, initial step size **h1**, and minimum step size **hmin**, At **x2** it calls the user-suppled routine **score** to evaluate the [discrepancy] functions **f[1..n2]** that ought to be zero to satisfy the boundary conditions at **x2**. Multi-dimensional Newton-Raphson is then used to develop a linear matrix equations for the increments **dv[1..n2]** to the adjustable parameters **v**. These increments are solved for and added before return.

FIGURE D.2 Arguments and method of the routine **shoot()** (Press *et al*., 1988).

target.c

```
/* Driver for routine SHOOT */
/* Solve for lambda1(0) and lambda2(0) using */

#include <stdio.h>
#include <math.h>
#include “nr.h”                    /* contains Numerical Recipes declarations */
#include “bio.h”                   /* contains declarations of biological functions */

#define NVAR 4                     /* number of state and co-state variables */
#define N2 2                       /* number of unknown initial conditions */
#define DELTA 1.0e-3               /* used to scale increment for finite differences */
#define EPS1.0e-10                 /* tolerance in Runge-Kutta */
#define DEPS1.0e-7

/* TABLE of global variables
*  T  -       time of estuary entry (final time)
*  a  -       migration distance
*  init_lambda1 - initial lambda1
*  init_labmda2 - initial lambda2
```

```
*/

/*  TABLE of states and co-states
*   y[1] - weight state
*   y[2] - lambda2 co-state
*   y[3] - displacement state
*   y[4] - lambda1 co-state
*/

/* used by shoot set the initial values of the states and co-states */
void load(x1, v, y)
double x1, v[], y[];
{
    y[1] = init_weight;
    y[2]= v[1];
    y[3] = 0.0;
    y[4] = v[2];
}

/* used by shoot to build the discrepancy vector f */
void score(x2,y,f)
double x2,y[],f[];
{
    double dphidw();                    /* partial of phi with respect to w */

    f[1] = y[2] - dphidw(y[1], x2);
    f[2] = y[3] - a;
}

/* the main driver for shoot */
void target()
{
    double   h1,hmin,x1,x2;
    double   delv[3],v[3],dv[7],f[7];
    double   guess_lambda1();
    double   guess_lambda2();
    double   l2_guess;

    v[1] = guess_lambda2();             /* estimate of initial lambda2 */
    v[2] = guess_lambda1();             /* estimate of initial lambda1 */
    l2_guess = v[1];                    /* save for convergence criterion */

    delv[1]=DELTA*v[1];                 /* increment in lambda2 for partial derivs */
    delv[2]=DELTA*v[2];                 /* increment in lambda1 for partial derivs */
    h1=0.1;                             /* initial step size for Runge-Kutta */
    hmin=0.0;                           /* minimum step size for Runge-Kutta */

    x1 = 0.0;                           /* initial time */
    x2= T;                              /* final time (estuary entry time) */

    do {
```

```
        shoot(NVAR,v,delv,N2,x1,x2,EPS,h1,hmin,f,dv);
    } while (fabs(dv[1]) > fabs(DEPS*l2_guess) || fabs(dv[2]) > fabs(DEPS * a));

    init_lambda2 = v[1];            /* set global variable to best est. of lambda2(T) */
    init_lambda1 = v[2];            /* set global variable to best est. of lambda1(T) */

    return;
}
```

D.4 Maximization routines

There are two optimization algorithms incorporated, the first, to solve for the swimming velocity that maximizes the Hamiltonian, and the second to maximize the fitness functional with respect to the estuary entry time. In the former case, I use Brent's method with derivatives, **dbrent()** (Press *et al*., 1988). Maximizing the Hamiltonian with respect to swimming velocity requires simple function evaluations based on the growth function and its derivatives, as well as values and derivatives of the switching function. Recall that when the switching function is negative, we seek to maximize

$$g(v, x, w, t)\text{, with derivative } g_v(v, x, w, t)$$

and when the switching function is positive, we seek to maximize

$$\sigma(\lambda_1, x, w, t)\, v + g(v, x, w, t) \text{ with derivative } \sigma(\lambda_1, x, w, t) + g_v(v, x, w, t)\,.$$

To determine the optimal paths, these maximization problems need to be solved for every step of the numerical integration routine.

I use the routine **brent()** (Press *et al*., 1988), a method based solely on function values, to maximize the objective functional with respect to estuary entry time, t_f. Every function evaluation of the method involves solving the two-point boundary value problem using

the function **target()** described above. Since **target()** itself requires intensive computation, the function evaluations are expensive.

VITA

Richard Allan Hinrichsen was born in Longview, Washington on March 26, 1962, the son of Jeannette B. Wicklund and Harry W. Hinrichsen. He received an A.A.S. from Edmonds Community College, Lynnwood, Washington in 1982; a B.S. degree in Mathematics from Central Washington University, Ellensburg, Washington in 1985; and a M.S. degree in Mathematical Sciences from Clemson University, Clemson, South Carolina in 1987. In 1994 he married Catherine Laura Starrett, the daughter of Norm and Gloria Starrett.